Robust Numerical Methods to Solve Differential Equations Arising in Cancer Modeling

Albert Shikongo

A thesis submitted in partial fulfillment of the requirements for the degree of Doctor of Philosophy in the Department of Mathematics and Applied Mathematics at the Faculty of Natural Sciences, University of the Western Cape

Supervisor: Prof. Kailash C. Patidar

Co-supervisor: Dr. Kolade M. Owolabi

September 2019

KEYWORDS

Tumour Dynamics

Mathematical Biology

Biological Stoichiometry

Cancer Immune Systems

Delay Differential Equations

Partial Differential Equations

Optimal Control

Fitted Operator Finite Difference Methods

Forward-Backward Sweep Method

Theoretical Analysis of the Numerical Methods.

ABSTRACT

Robust Numerical Methods to Solve Differential Equations Arising in Cancer Modeling

by

Albert Shikongo

PhD thesis, Department of Mathematics and Applied Mathematics, Faculty of Natural Sciences, University of the Western Cape

Cancer is a complex disease that involves a sequence of gene-environment interactions in a progressive process that cannot occur without dysfunction in multiple systems. From a mathematical point of view, the sequence of gene-environment interactions often leads to mathematical models which are hard to solve analytically. Therefore, this thesis focuses on the design and implementation of reliable numerical methods for non-linear, first order delay differential equations, second order non-linear time-dependent parabolic partial (integro) differential problems and optimal control problems arising in cancer modeling. The development of cancer modeling is necessitated by the lack of reliable numerical methods, to solve the models arising in the dynamics of this dreadful disease. Our focus is on chemotherapy, biological stoichometry, double infections, micro-environment, vascular and angiogenic signalling dynamics. Therefore, because the existing standard numerical methods fail to capture the solution due to the behaviors of the underlying dynamics. Analysis of the qualitative features of the models with mathematical tools gives clear qualitative descriptions of the dynamics of models which gives a deeper insight of the problems. Hence, enabling us to derive robust numerical methods to solve such models.

September 2019.

DECLARATION

I declare that *Robust Numerical Methods to solve Differential Equations Arising in Cancer Modeling* is my own work, that it has not been submitted before for any degree or examination at any other university, and that all sources I have used or quoted have been indicated and acknowledged by complete references.

Albert Shikongo September 2019

Signed .....

ACKNOWLEDGEMENT

First and foremost, I have to thank my mother and dad (late) for their love and support throughout my life. My sisters, brothers, and cousins deserve my wholehearted thanks as well. I would like to sincerely thank my supervisor, Prof. K.C. Patidar, for his guidance, support throughout this study, especially for his confidence in me. I am also indebted to Prof. Patidar for introducing me to epidemiology, University of Namibia and Namibia Students Financial Assistance Fund for granting me the study leave and the genuine financial support for this studies, respectively. I express my heartfelt gratefulness to my co-supervisor Dr. Kolade M. Owolabi for his support, timely assistance and encouragement. To all my friends, thank you for your understanding and encouragement in my many moments of crisis. Your friendship makes my life a wonderful experience. The space is too little to list your names here but you are always in my mind.

DEDICATION

This thesis is dedicated to the congregation of Oshikuku Roman Catholic Church, which was established in 1924 in Omusati region, Namibia. During the pre-independence period, the church ensured that those who lived in rural villages and subsist by raising cattle, goats, and growing some corn, barley for their own use, education was brought closer. Today many Namibians near and around Oshikuku have graduated from institutions of higher learning through the educational infrastructures availed by this church.

Contents

List of Tables

List of Figures

List of Publications

Part of this thesis has been published/accepted in the form of the following research papers submitted to international journals for publications.

1. Kolade M. Owolabi, Kailash C. Patidar and Albert Shikongo, Mathematical analysis and numerical simulation of a tumor-host model with chemotherapy application, *Communications in Mathematical Biology and Neuroscience* **2018** (2018).

2. Kolade M. Owolabi, Kailash C. Patidar and Albert Shikongo, Efficient numerical method for a model arising in biological stoichiometry of tumour dynamics, *Discrete and Continuous Dynamical Systems Series S* **12(3)** (2019) 591-613.

3. Kolade M. Owolabi, Kailash C. Patidar and Albert Shikongo, A fitted numerical method for a model arising in HIV related cancer-immune system dynamics, *Communications in Mathematical Biology and Neuroscience* **2019** (2019).

4. Kolade M. Owolabi, Kailash C. Patidar and Albert Shikongo, A fitted operator method for tumor cells dynamics in their micro-environment, *Communications in Mathematical Biology and Neuroscience* **2019** (2019).

5. Kolade M. Owolabi, Kailash C. Patidar and Albert Shikongo, A fitted operator method for model arising in vascular tumor dynamics, *Communications in Mathematical Biology and Neuroscience* **2020** (2020) 4.

6. Kolade M. Owolabi, Kailash C. Patidar and Albert Shikongo, Numerical solution for a problem arising in angiogenic signalling, *AIMS Mathematics* **4(1)** (2019) 43-63.

7. Kolade M. Owolabi, Kailash C. Patidar and Albert Shikongo, Robust numerical method for a tumor-host model with chemotherapy application, paper to appear in *Aims: Electronic Research Announcements*.

8. Kolade M. Owolabi, Kailash C. Patidar and Albert Shikongo, A fitted operator method for an extended system of delay model of tumor cells dynamics embedded within their modified micro-environment, paper to appear in *Aims: Electronic Research Announcements*.

Chapter 1

General introduction

All human societies have medical beliefs that provide explanations of birth, death, and diseases. Often illness has been attributed to witchcraft, demons, astral influence, or the will of the gods. These ideas still retain some powers in modern societies. With faith, healing and shrines are still used in some places although the advancement in scientific discoveries on new medications over the past millennium has altered or replaced mysticism in most cases. However, modern medicine requires a better phenomenological description of a disease at hand. In turn the phenomenological description depends on the enlargement of the ideal or real microscopic understanding used by a biologist or by a modeler [50]. This means that, to achieve an optimal success in healing a patient, different methods of different scales could be interlaced to achieve a better understanding of the phenomena. In view of this, in this thesis, our aim is to focus on some key models dealing with cancer dynamics and to look at their robust numerical simulation which may lead to sensible information through mathematical analysis.

1.1 Literature review

When a body develops a disease, the situation can be thought similar to that of predator and prey in ecology. However, some diseases are very much complex in their formation and the manner they reinforce their presence in a body as compare to a situation in

a physical environment. Such diseases are for example HIV and cancer. However, the connection between HIV/AIDS and certain cancers diseases are not completely understood, even though the link is likely to depend on a weakened immune system, see for instance [16, 17, 32, 81, 82, 88, 89, 107]. However, it is understood that most types of cancer begin when healthy cells change and grow out of control, forming a mass called a tumor. Therefore when a host is affected by a tumor, the system requires interaction with its environment. Therefore, it is not strange for the ecological system of cancer cells to interact with surrounding healthy and malignant. This means cancer and healthy cells compete for resources, namely, oxygen, nutrient and space. Thus cancer cells compete against each other and against the healthy cells throughout the body for the same resources. Such studies have led to the development of many cancer models see for instance [45], also an optimal control for mathematical models of cancer therapies in [116], computational modeling of interactions between multiple myeloma and the bone micro-environment in [126], the role of the micro-environment in tumor growth and invasion in [61] and current trends in mathematical modeling of tumor-micro-environment interactions: a survey of tools and applications in [110] in the past few recent years, just to mention a few in this regard.

In our views, we understand that most of the models are developed with one common goal, that is to understand how cancer cells functions. Since a cure to cancerous diseases is still not found, this makes the study of cancer disease an ongoing process. As a result of that, in this thesis, our contribution focuses on the study of chemotherapy, competition among the involved cells, multiple infections, micro-environment, vascular dynamics and optimization of treating cancer in the form of tumor cells.

Therefore, it is imperative to understand that a tumor is scientifically referred to as a neoplasm, or an abnormal tissue area that is either fluid-filled or solid in appearance. A tumor does not necessarily mean cancer, it can be classified into the benign type (which means non-progressive or cannot metastasize, for example, uterine fibroids and moles), pre-malignant (or pre-cancerous growth which include: actinic keratosis, dysplasia of the cervix, metaplasia of the lung and leukoplakia), or malignant (cancerous), and the

malignant tumor which is a cancerous case. Record have shown that there are various types of tumors, which are made up of specific types of cancer cells; these include the carcinoma, sarcoma, lymphoma or leukemia, blastoma and germ cell tumor [90]. Thus, to this end, we also understand that it requires an expert to differentiate between an ordinary tumor and a cancerous type and that tumour treatment can be classified into stages. These stages are from I to IV, where the first two stages is called a low-grade tumor which can be treated by watchful monitoring or surgery. Stage III and IV are malignant spread quickly from the affecting area to other surrounding tissues. In [55], it is stated that tumours' treatment include the use of radiation therapy, chemotherapy, targeted therapy and tumor treating fields.

Based on our understanding, tumor models can either be solved numerically and/or analytically, and such studies are undertaken with the aim of contributing towards understanding the complexity of cancer diseases. These studies include [1, 4, 5, 6, 7, 9, 43, 66, 68, 83, 91, 99, 121, 124] just to mention some of them. However, most of them consider a solution to a cancer model as a cure to a cancer disease, because they are directly compared to experimental data in most cases. Since experimental result is almost surely a case study, therefore it does not capture the mathematical meaning of a model at hand in most cases see for instance [86].

Therefore, our first key model is derived by Hinow et al. [49]. Our second key model focuses on the effects of biological stoichiometry in [37], where we understand that similar considerations can be traced in [24, 28, 127]. At a worse scenario one can be exposed to the issue of immune reaction against tumor and at the same time to HIV dynamics. Thus, our third key model arises from the work of Foryś and Pleszczuk in [41], in vivo. Consequently, we would like to acknowledge the contribution by Nunnari et al. [92], Resclgnow and Delisi [111] and by Rong et al. [113], where a significant increase in the incidence of neoplasms accompany the acquired immunodeficiency syndrome (AIDS), a delay in the formation of killer lymphocytes was introduced to allow tumor development from a single cell, steps between viral infection of CD4+ t-cells and the production of HIV−1 visions have been incorporated by an eclipse phase, an

HIV−1 dynamical model was developed which incorporate AIDS-related cancer cells in which cancer cells, healthy CD4+ t-cells lymphocytes and infected CD4+ t-cells lymphocytes can have six steady states, in that order.

In view of our understanding that cell types such as epithelial cells, fibroblasts, myofibroblasts, endothelial cells, and inflammatory cells form an integral part of a tumor micro-environment [59]. That is, epithelial cells, fibroblasts, myofibroblasts, endothelial cells, and inflammatory cells, communicate with one another and influence each others' behavior by means of the cytokines and growth factors they secrete. Thus, focusing on the role of the composition of the surrounding extra-cellular matrix (ECM), may play an essential role in confining cancer cells. Since, in [59], it is mentioned that confinement of cancer cells, can be achieved by either modulating cell adhesion or blocking Matrix Metalloproteinase (MMP), then, in human Ductal Carcinoma In Situ (DCIS), it is understood that Matrix Metalloproteinase (MMP) material have shown that several classes of MMPs are expressed in periductal fibroblasts and myofibroblasts, indicating an intense stromal involvement during early invasion [59, 60]. Thus, a situation in which a more aggressive carcinoma and tumor cells are degrading the basal membrane and invade into the stroma [3], is therefore considered as our fourth key model.

Further contribution done in the direction of tumor cells embedded in their micro-environments, are for instance the establishment in [27] that as a tumor invades an unsuspecting host and an accumulation of evidence points to the alternative paradigm, where the tumor micro-environment is not an idle bystander, but actively participates in tumor progression and metastasis. In fact, stromal cells and their cytokines coordinate critical pathways that exert important roles in the ability of tumors to invade and metastasize. More information regarding the actively participation of tumor micro-environment in tumor progression and metastasis can also be traced in [20, 80]. Thus understanding the relationship between tumor and its micro-environment may lead to important new therapeutic approaches in controlling the growth and metastasis of cancer. However, tumor micro-environment includes various cell types such as epithelial,

fibroblasts, myofibroblasts, endothelial, and inflammatory cells. These cells communicate with one another and influence each other behavior by means of the cytokines and growth factors they secrete [59].

Since, vascular tumors are a highly diverse group of aberrant growths, our fifth key model is dealing with the inclusion of the study dynamics for the kinetics of a population of cells differentiated by phases of the cell division cycle such as the ones presented by Jackiewicz et al.[51]. The sixth key model deals with the optimal control problems derived by Hahnfeldt et al. [48], where, our sixth key model deals with the case of tumour vasculature which does not exploit tumour cell sensitivities. Thus, among others factors, we understand that developing drug resistance all too often is the limiting factor in conventional chemotherapy treatments as cancers have a formidable capacity to develop resistance to a large and diverse array of chemical, biologic, and physical anti-neoplastic agents. Hence, Kerbel [57], mentioned that it can be largely traced to the instability of the tumour cell genome, and the resultant ability of tumour cell populations to generate phenotypic variants rapidly. Therefore, anti-cancer strategies should be directed at eliminating those genetically stable normal diploid cells that are required for the progressive growth of tumours. Hence tumor anti-angiogenesis has been called a new hope for the treatment of tumors [65]. Although these high hopes have not been realized in practice, there still strong interest and active research on tumor anti-angiogenesis as a method that normalizes the vasculature [53, 54]. Therefore, when combined with traditional treatments like chemotherapy or radiotherapy, enhances the efficiency of these procedures. Hence, more contribution in the direction of anti-cancer strategies as optimal control problems can be traced to the studies [15, 35, 56, 58].

1.2 Outline of the thesis

The rest of the thesis is as follows. Chapter 2 deals with a spatial effects of tumour-host interaction dynamics, whereas in Chapter 3, we consider the biological stoichiometry

of tumour dynamics. Chapter 4 deals with the dynamics of double infection of HIV related cancer-immune system dynamics. In Chapter 5, we deal with tumour cell proliferation and migration under the influence of their micro-environment and we consider a vascular tumour's dynamics in Chapter 6. Chapter 7, deals with the dynamics arising in angiogenic signaling of tumour cells and conclude the thesis with future direction in Chapter 8.

Chapter 2

Mathematical analysis and numerical simulation of a tumor-host model with chemotherapy application

In this chapter, a system of non-linear quasi-parabolic partial differential system, modeling the chemotherapy application in spatial tumor-host interaction is considered. For certain parameters, we derive the anti-angiogenic therapy, the baseline therapy and anti-cytotoxic therapy models as well as their local stability condition. We use the method of upper and lower solutions to show that the equilibria are globally stable. Since the system of non-linear quasi-parabolic partial differential cannot be solved analytically, we formulate a robust numerical scheme based on the semi-fitted finite difference operator. Analysis of the basic properties of the method presents that it is consistent, stable and convergent. Our numerical results are in agreement with the stability conditions.

2.1 The model

Henow et al. in [49] presented that cancer is characterized by abnormal cells growth and division, which eventually metastasize. Furthermore, they mentioned that the

process of metastasizing disrupts the healthy balance between normal and apoptotic cells, thus leading to the new formation of hypoxic cell. Hypoxic cell is capable of sustaining itself with a lower nutrient level than the normal cells. The process of self-sustainability of the hypoxic cell leads to unbiased, biased cell migration and hypoxia-driven angiogenesis. Based on the process of angiogenesis, Hinow et al. regarded the process of hypoxia-driven angiogenesis as the track to deliver anti-cancer drugs in the form of chemotherapy to all regions of a tumor in effective quantities despite the higher metabolic demands of the growing mass of cells. Hence, they were able to derive their model and based on their findings from the dynamics of their model in [49], they were able to deduce that when no and/or treatment is applied to their model;

- the model reproduces a dynamics of early tumor growth.
- through the release of vascular endothelial growth factor (VEGF) secreted by hypoxic cells in the core of the tumor, the VEGF stimulates endothelial cells to migrate towards the tumor and establishes a nutrient supply sufficient for sustained invasion.
- when cytostatic treatment is applied in the form of a VEGF-inhibitor, the treatment has the capability to reduce tumor mass.
- the inhibition of endothelial cell proliferation is more important than the two cellular functions targeted by the drug.
- the application of a cytotoxic drug as a diffusible substance entering the tissue from the blood vessels, can either reduces the tumor mass significantly or in fact accelerates the growth rate of the tumor.

The above facts, motivated us to consider the model derived by Hinow et al. [49]. The model is defined as follows. Let t, x denote time and space, w, n, h, a, m, f, g, c denote oxygen concentration, normoxic cells, hypoxic cells, apoptic cells, endothelial cells, extracellular matrix, angiogenic factor, concentration of a drug, and the density

of all types of cells and matrix combined is

$$v = h + a + n + f + m.$$

For ease of explaining the models, we consider the dependent variables

$$w, n, h, a, m, f, g, c,$$

as components of the vector

$$\mathbf{u} = [w, n, h, a, m, f, g, c]^T,$$

whereas, the diffusion coefficients will be taken as components of the vector

$$\mathbf{D} = [D_w, D_n \max\{n - v_c, 0\} + D_m, 0, 0, D_m, 0, D_g, D_c]^T,$$

respectively. Based on these intepretations, the cytotoxic chemotherapy (the drug that affects cells in the proliferative state) and anti-angiogenic chemotherapy (also considered as cytostatic in the sense that the drugs used are not toxic to the cells, but instead inhibit some mechanism essential for cell division or a specific function) the models in [49] were derived through the baseline model (i.e. the scenario when tumor growth is only limited by intrinsic constraints such as oxygen supply and the surrounding stromal tissue). Using the vectors introduced above, we rewrite these

models in a vector form as

$$\left.\begin{array}{l} \frac{\partial \mathbf{u}}{\partial t}(x,t) - \frac{\partial}{\partial x}\left[\mathbf{D}, F\left(\mathbf{u}, \frac{\partial \mathbf{u}}{\partial x}\right)\right] = F(\mathbf{u}), \text{ with} \\ \\ u_1(x,0) = 1.0, \quad u_2(x,0) = 0.93\exp(-200\xi^2), \quad u_3(x,0) = u_4(x,0) = 0.00, \\ \\ u_5(x,0) = 0.01, \quad u_6(x,0) = 1 - u_2(\xi,0) - u_3(\xi,0) - 0.05, \quad u_7(x,0) = 0.00, \\ \\ u_8(x,0) \in [0,1], \end{array}\right\} \quad (2.1.1)$$

as the initial conditions, $F(\mathbf{u}) = F(w, n, h, a, m, f, g, c)$ and the boundary conditions for the reaction-diffusion system in equation (2.1.1) are the no flux-boundary conditions. Thus, for u_1 in equation (2.1.1), we have

$$\left.\begin{array}{l} \frac{\partial}{\partial x}[D_1, F\left(u_1, \frac{\partial u_1}{\partial x}\right)] = \frac{\partial}{\partial x}\left[D_1, \frac{\partial u_1}{\partial x}\right] \equiv D_w \frac{\partial^2 w}{\partial x^2}, \\ \\ F(u_1) \equiv \alpha_w m(w_{\max} - w) - \beta_w(n + h + m)w - \gamma_w w, \end{array}\right\} \quad (2.1.2)$$

where, $D_w, \alpha_w, w_{\max}, \beta_w, \gamma_w$ denote the coefficient of oxygen diffusion, rate of diffusability of oxygen, maximum oxygen density, uptake rate of oxygen by normoxic, hypoxic, endothelial cells and loss rate of oxygen. The reason for the choice of the source term $\alpha_w m(w_{\max} - w)$ is that, at high environmental levels of oxygen, less oxygen is released through the vessel walls.

For u_2 in equation (2.1.1), we have

$$\left.\begin{array}{l} \frac{\partial}{\partial x}[D_2, F\left(u_2, \frac{\partial u_2}{\partial x}\right)] = \frac{\partial}{\partial x}\left((D_n \max\{n - v_c, 0\} + D_m)\frac{\partial n}{\partial x} - \chi_n n \frac{\partial f}{\partial x}\right), \\ \\ F(u_2) \equiv \alpha_n n(v_{\max} - v) - \alpha_h \mathcal{H}(w_h - w)n + \frac{\alpha_h}{10}\mathcal{H}(w - w_h)h, \end{array}\right\} \quad (2.1.3)$$

where, $v_c, D_n \max\{n - v_c, 0\}n_x, D_m, \chi_n, \alpha_n, v_{\max}, w_h, \alpha_h, \mathcal{H}$ denote a threshold which adds to the dispersion of these cells through crowding-driven motion, nonlinear diffu-

sion, random motility, haptotactic movement, rate of logistic growth, maximal density, critical value, rate of gain or loss, H stands for Heaviside function, a function which is one for positive arguments and zero otherwise. We also see that the growth of normoxic cells levels off in regions where the sum of all cells and matrix approaches the maximal density $v_{\max}$. In the regions where the concentration of oxygen drops below a certain critical value w_h, normoxic cells enter the hypoxic class at a rate α_h and this transition process is reversible, and the reverse transition is denoted by the reduced rate $\alpha_h/10$.

For u_3 in equation (2.1.1) we have

$$\left.\begin{array}{l} \frac{\partial}{\partial x}[D_3, F\left(u_3, \frac{\partial u_3}{\partial x}\right)] = 0, \\ F(u_3) \equiv \alpha_h \mathcal{H}(w_h - w)n - \frac{\alpha_h}{10}\mathcal{H}(w - w_h)h - \beta_h \mathcal{H}(w_a - w)h, \end{array}\right\} \tag{2.1.4}$$

The first and the second terms in equation (2.1.4) are dictated by conservation of mass and correspond to terms in equation (2.1.3). The third term in equation (2.1.4) denotes the transition of hypoxic cells to apoptotic cells at rate β_h as the level of oxygen falls below a second threshold, which is $w_a < w_h$. In [49] it is reported that hypoxic cells are less active in general due to reduced availability of oxygen and other nutrients and thus, the authors assumed that the lack of energy causes them to be immobile.

For u_4 in equation (2.1.1) we have

$$\left.\begin{array}{l} \frac{\partial}{\partial x}[D_4, F\left(u_4, \frac{\partial u_4}{\partial x}\right)] = 0, \\ F(u_4) \equiv \beta_h \mathcal{H}(w_a - w)h, \end{array}\right\} \tag{2.1.5}$$

where, the β_h denotes the transition from hypoxic class to apoptic class.

For u_5 in equation (2.1.1) we have

$$\left.\begin{array}{l} \frac{\partial}{\partial x}[D_5, F\left(u_5, \frac{\partial u_5}{\partial x}\right)] = \frac{\partial}{\partial x}\left(D_m \frac{\partial m}{\partial x} - m\chi_m \frac{\partial g}{\partial x}\right), \\ F(u_5) \equiv \alpha_m m g(v_{\max} - v), \end{array}\right\} \tag{2.1.6}$$

where, D_m denotes the random motility for endothelial cells and endothelial cells respond via chemotaxis to gradients of angiogenic factor and this requires the presence

of angiogenic factor for proliferation. Proliferation is capped by the total density of cells. The proliferation constant for endothelial cells is α_m.

For u_6 in equation (2.1.1) we have

$$\left.\begin{array}{l} \frac{\partial}{\partial x}[D_6, F\left(u_6, \frac{\partial u_6}{\partial x}\right)] = 0, \\ F(u_6) \equiv -\beta_f n f, \end{array}\right\} \tag{2.1.7}$$

where the tissue matrix is degraded by the tumor cells according to a mass-action law with a constant rate β_f.

For u_7 in equation (2.1.1) we have

$$\left.\begin{array}{l} \frac{\partial}{\partial x}[D_7, F\left(u_7, \frac{\partial u_7}{\partial x}\right)] = D_g \frac{\partial^2 g}{\partial x^2}, \\ F(u_7) \equiv \alpha_g h - \beta_g m g, \end{array}\right\} \tag{2.1.8}$$

where, D_g denotes the diffusion coefficient. Cognizance must be taken of the fact that, angiogenic factor is produced by hypoxic cells (alone) at rate α_g and consumed by endothelial cells with a mass-action coefficient of β_g.

To ensure that their model is universal, Hinow et al. dimensionelise the baseline model (see in [49]) and the dimensionless baseline model is

$$\left.\begin{aligned}
&\tfrac{\partial w}{\partial t}(x,t) - D_w \tfrac{\partial^2 w}{\partial x^2} = \alpha_w m(1-w) - \beta_w(n+h+m)w - \gamma_w w,\\
&\tfrac{\partial n}{\partial t}(x,t) - \tfrac{\partial}{\partial x}\left((D_n \max\{n - v_c, 0\} + D_m)\tfrac{\partial n}{\partial x} - \chi_n n \tfrac{\partial f}{\partial x}\right) = \alpha_n n(v_{\max} - v)\\
&-\alpha_h \mathcal{H}(w_h - w)n + \tfrac{\alpha_h}{10}\mathcal{H}(w - w_h)h,\\
&\tfrac{\partial h}{\partial t}(x,t) = \alpha_h \mathcal{H}(w_h - w)n - \tfrac{\alpha_h}{10}\mathcal{H}(w - w_h)h - \beta_h \mathcal{H}(w_a - w)h,\\
&\tfrac{\partial a}{\partial t}(x,t) = \beta_h \mathcal{H}(w_a - w)h,\\
&\tfrac{\partial m}{\partial t}(x,t) - \tfrac{\partial}{\partial x}\left(D_m \tfrac{\partial m}{\partial x} - m\chi_m \tfrac{\partial g}{\partial x}\right) = \alpha_m m g(v_{\max} - v),\\
&\tfrac{\partial f}{\partial t}(x,t) = -\beta_f n f,\\
&\tfrac{\partial g}{\partial t}(x,t) - D_g \tfrac{\partial^2 g}{\partial x^2} = \alpha_g h - \beta_g m g.
\end{aligned}\right\} \quad (2.1.9)$$

When

$$\begin{aligned}
\alpha_m &\rightarrow \frac{\alpha_m}{10},\\
\chi_m &\rightarrow \frac{\chi_m}{10},
\end{aligned}$$

in equation (2.1.9), the baseline model becomes the anti-angiogenic chemotherapy model.

However, when a drug that affects cells in the proliferative state is introduced, then the normoxic cells are driven into apoptosis at a rate proportional to the drug concentration, in which case the baseline becomes the cytotoxic chemotherapy model. This implies that the reaction function equation in (2.1.3) becomes

$$F(u_2) \equiv \alpha_n n(v_{\max} - v) - \alpha_h \mathcal{H}(w_h - w)n + \frac{\alpha_h}{10}\mathcal{H}(w - w_h)h - \gamma_n nc, \qquad (2.1.10)$$

with a constant rate $\gamma > 0$, whereas, in order to balance the loss of normoxic cells, the reaction function for apoptotic cells in equation (2.1.5) is amended accordingly to

$$F(u_4) \equiv \beta_h \mathcal{H}(w_a - w)h + \gamma_n nc, \qquad (2.1.11)$$

and whenever, the concentration of the drug, denoted by $c \in [0, 1]$, which is assumed to be delivered through blood infusion and thus enters the tissue from the blood stream. The production rate of the drug is therefore proportional to the density of endothelial cells, which implies that regions with higher vascular density will experience a higher concentration of the drug. Hence, it is described by a reaction-diffusion equation similar to that of oxygen as

$$\left.\begin{aligned} &\tfrac{\partial}{\partial x}[D_8, F\left(u_8, \tfrac{\partial u_8}{\partial x}\right)] = \tfrac{\partial}{\partial x}\left[D_8, \tfrac{\partial u_8}{\partial x}\right] \equiv D_c \tfrac{\partial^2 c}{\partial x^2}, \\ &F(u_8) \equiv \alpha_c(t)m(1 - c) - \gamma_c c - k\gamma_n nc, \end{aligned}\right\} \qquad (2.1.12)$$

where, the drug diffuses at a constant rate D_c in the tissue and decays at a constant rate γ, it also affects the normoxic cells in such a way that it is consumed at a rate $k\gamma_n$ when it kills normoxic cells. Instead of looking at a constant drug supply, Hinow et al. in [49] included a scheduling of the drug by letting the production rate $\alpha_c(t) > 0$ be a time-dependent function

$$\alpha_c(t) = 100 \sum_{k=0}^{5} \exp(-4(t - (200 + 2k))^2),$$

corresponding to the drug being delivered to the tissue.

Further detailed information on these models can be found in [49, 94] and the references therein.

Apart from the contribution by Cristini et al. [31] reported that a thermodynamic consistent mixture model for avascular solid tumor growth, takes into account the effects of cell to cell adhesion, and taxis inducing chemical and molecular species, we also would like to mentioned that Tuan et al. [122] studied the identification of the population density of a logistic equation backwards in time associated with non-local diffusion and nonlinear reaction.

In some cases, most of the solution for a dynamic models is considered as a cure to a tumor disease, because they are compared to experimental data in most cases, see for instance [29, 125], without their extensive mathematical dispensations.

Thus, [49] presented their results without presenting the stability analysis of the models [49]. Therefore, we believe that they were not able to explain their results by referring to direct mathematical analysis. This, we believe has undermined the qualitative features of the underlying mathematical models. In this chapter, our focus is mainly on mathematical analysis of the models. Due to the non-linearities of terms in the models we construct a reliable numerical method capable of capturing the qualitative features of the models.

Solving the problems like (2.1.1) using the standard finite difference (SFDMs) has limitations. That is, explicit methods finite difference (EFDMs), can solve such differential equations with low computational cost, but with very small stability regions, which in turn implies severe restrictions on the meshes sizes, which are required in order to achieve the desired results. Then, one is of a view of considering the implicit finite difference (IFDMs) to solve such differential equations, because they possess wider stability regions as compared to the EFDMs. However, their associated computational complexity can achieve only one order of convergence as compared to EFDMs that use the same number of stages [22].

The rest of the chapter is organized as follows. Mathematical analysis of the models is presented in Section 2.2 and a robust numerical scheme based on the semi-fitted finite difference technique is formulated in Section 2.3, whereas, analysis of the basic properties of this scheme is also examined for convergence. To show the effectiveness of the proposed schemes, we present some numerical results in Section 2.4. We conclude the chapter with Section 2.5.

2.2 Mathematical analysis of the models

In this work, our major attention is on the baseline, anti-angiogenic and cytotoxic chemotherapy models. We use linear stability analysis method to discuss the general dynamics of each model. At the steady state, the cytotoxic chemotherapy model in equation (2.1.1), becomes

$$\left.\begin{aligned}
&\alpha_w m(1-w) - \beta_w(n+h+m)w - \gamma_w w = 0,\\
&\alpha_n n(v_{\max} - v) - \alpha_h \mathcal{H}(w_h - w)n + \tfrac{1}{10}\alpha_h \mathcal{H}(w - w_h)h - \gamma_n nc = 0,\\
&\alpha_h \mathcal{H}(w_h - w)n - \tfrac{1}{10}\alpha_h \mathcal{H}(w - w_h)h - \beta_h \mathcal{H}(w_a - w)h = 0,\\
&\beta_h \mathcal{H}(w_a - w)h + \gamma_n nc = 0,\\
&\alpha_m mg(v_{\max} - v) = 0,\\
&-\beta_f nf = 0,\\
&\alpha_g h - \beta_g mg = 0,\\
&\gamma_c c - k\gamma_n nc = 0,
\end{aligned}\right\} \tag{2.2.1}$$

as $\alpha_c(t) \to 0$ as $t \to \infty$. Solving the system of nonlinear equations in equation (2.2.1), we obtain

$$w^* = \frac{\alpha_w m^*}{\alpha_w + \beta_w m^* + \gamma_w},\ m^* = v_{\max},\ n^* = h^* = a^* = f^* = g^* = 0,\ c^* > 0. \quad (2.2.2)$$

We see that the oxygen and endothelial cells equilibria (w^* and m^*) are positive for the baseline, anti-angiogenic and cytotoxic chemotherapy models. Consequently, the hypoxic, apoptic cells', angiogenic factor (VEGF) and the extra-cellular matrix equilibria are zero. On the other hand, when a host is tumor free, we find that

$$\underline{w} = 0,\ \underline{f} = v_{max}, \quad (2.2.3)$$

which implies that the extra-cellular matrix ($\underline{f}$) in all three models is well and healthy. We also see that the oxygen cells' steady state is zero, rendering the tumor free case unworthy for further investigation.

Therefore, for the baseline, anti-angiogenic and cytotoxic chemotherapy models, we have the uniform equilibria as

$$\begin{bmatrix} w^* \\ n^* \\ h^* \\ a^* \\ m^* \\ f^* \\ g^* \\ c^* \end{bmatrix} = \begin{bmatrix} \frac{\alpha_w v_{\max}}{\alpha_w+\beta_w v_{\max}+\gamma_w} \\ 0 \\ 0 \\ 0 \\ v_{\max} \\ 0 \\ 0 \\ 0 \end{bmatrix}, \begin{bmatrix} \frac{\alpha_w m^*}{\alpha_w+\beta_w v_{\max}+\gamma_w} \\ 0 \\ 0 \\ 0 \\ v_{\max} \\ 0 \\ 0 \\ 0 \end{bmatrix}, \begin{bmatrix} \frac{\alpha_w v_{\max}}{\alpha_w+\beta_w v_{\max}+\gamma_w} \\ 0 \\ 0 \\ 0 \\ v_{\max} \\ 0 \\ 0 \\ c^* > 0 \end{bmatrix}. \quad (2.2.4)$$

Stability of the equilibria in equation (2.2.4) can be investigated from the corresponding homogeneous baseline, anti-angiogenic and cytotoxic chemotherapy models, (the investigation which includes spatial distribution of cells is dealt with elsewhere). Thus,

extracting the Jacobian matrix from the system in equation (2.2.1), we find the non-zero entries of the Jacobian matrix evaluated at the critical points as

$$\begin{aligned}
J_{1,1} &= -\alpha_w m^* - \beta_w m^* - \gamma_w,\ J_{1,2} = J_{1,3} = -\beta_w w^*,\ J_{1,5} = \alpha_w(1-w^*) - \beta_w w^*,\\
J_{2,2} &= \alpha_n v_{\max} - \alpha_h \mathcal{H}(w_h - w) - \gamma_n c^*,\ J_{2,3} = \frac{\alpha_h}{10}\mathcal{H}(w - w_h),\ J_{3,2} = \alpha_h \mathcal{H}(w_h - \bar{w}),\\
J_{3,3} &= -\frac{\alpha_h}{10}\mathcal{H}(w - w_h) - \beta_h \mathcal{H}(w_a - w),\ J_{4,2} = \gamma_n c^*,\ J_{4,3} = \beta_h \mathcal{H}(w_a - w),\\
J_{7,3} &= \alpha_g,\ J_{7,5} = -\beta_g m^*,\ J_{8,2} = -k\gamma_n c^*,\ J_{8,8} = -\gamma_c,
\end{aligned} \tag{2.2.5}$$

which leads to characteristic equation of the form

$$\lambda^2 - \mathrm{tr}(J)\lambda + \det(J) = 0, \tag{2.2.6}$$

where,

$$\left.\begin{aligned}
&\mathrm{tr}(J) = \alpha_n v_{\max} - \alpha_h \mathcal{H}(w_h - w) - \gamma_n c^* - \tfrac{\alpha_h}{10}\mathcal{H}(w - w_h) - \beta_h \mathcal{H}(w_a - w),\\
&\det(J) = -\left(\alpha_n v_{\max} - \alpha_h \mathcal{H}(w_h - w) - \gamma_n c^*\right)\left(\tfrac{1}{10}\alpha_h \mathcal{H}(w - w_h) + \beta_h \mathcal{H}(w_a - w)\right)\\
&-\tfrac{\alpha_h^2}{10}\mathcal{H}(w_h - \bar{w})\mathcal{H}(w - w_h).
\end{aligned}\right\}$$

Hence, the equilibria in equation (2.2.4) are stable if

$$(\alpha_n v_{\max} - \alpha_h \mathcal{H}(w_h - \bar{w}) - \gamma_n c^*) < \frac{\alpha_h}{10}\mathcal{H}(\bar{w} - w_h) + \beta_h \mathcal{H}(w_a - \bar{w}), \tag{2.2.7}$$

and

$$\begin{aligned}
-\left(\alpha_n v_{max} - \alpha_h \mathcal{H}(w_h - w) - \gamma_n c^*\right)&\left(\frac{\alpha_h}{10}\mathcal{H}(w - w_h) + \beta_h \mathcal{H}(w_a - w)\right)\\
&-\frac{\alpha_h^2}{10}\mathcal{H}(w_h - \bar{w})\mathcal{H}(w - w_h) > 0,\\
\Rightarrow (\alpha_n v_{\max} - \alpha_h \mathcal{H}(w_h - w) - \gamma_n c^*) &< \frac{-\frac{\alpha_h^2}{10}\mathcal{H}(w_h - \bar{w})\mathcal{H}(w - w_h)}{\left(\frac{\alpha_h}{10}\mathcal{H}(w - w_h) + \beta_h \mathcal{H}(w_a - w)\right)}.
\end{aligned} \tag{2.2.8}$$

The stability conditions in equation (2.2.7)-(2.2.8) are in agreement with the core

transitions of tumor cells [49], because the condition in equation (2.2.7) implies that $\alpha_n v_{max} > \alpha_h \mathcal{H}(w_h - \bar{w}) + \gamma_n c^*$, whereas the condition in equation (2.2.8) implies that $\alpha_n v_{\max} < \alpha_h \mathcal{H}(w_h - w) + \gamma_n c^*$.

2.2.1 Global stability of the equilibria

In this section, we mainly prove that the equilibrium points in equation (2.2.4) are globally asymptotically stable with the upper and lower solution method in [101, 102]. Denoting the reaction functions in equation (2.1.1) by $l_j(w, n, h, a, m, f, g, c)$ for $j = 1, 2, 3, 4, 5, 6, 7, 8$, then from equation (2.1.1) we let

$$\left.\begin{aligned}
l_1 &= \alpha_w m(1-w) - \beta_w(n+h+m)w - \gamma_w w,\\
l_2 &= \alpha_n n(v_{max} - v) - \alpha_h \mathcal{H}(w_h - w)n + \tfrac{1}{10}\alpha_h \mathcal{H}(w - w_h)h - \gamma_n nc,\\
l_3 &= \alpha_h \mathcal{H}(w_h - w)n - \tfrac{1}{10}\alpha_h \mathcal{H}(w - w_h)h - \beta_h \mathcal{H}(w_a - w)h,\\
l_4 &= \beta_h \mathcal{H}(w_a - w)h + \gamma_n nc,\\
l_5 &= \alpha_m mg(v_{\max} - v),\\
l_6 &= -\beta_f nf,\\
l_7 &= \alpha_g h - \beta_g mg,\\
l_8 &= 100\sum_{k=0}^{5}\exp(-4(t-(200+2k))^2)m(1-c) - \gamma_c c - k\gamma_n nc,
\end{aligned}\right\} \quad (2.2.9)$$

and let $U \subset \mathbb{R}^8_+$ such that $U = \{\mathbf{u} \in \mathbb{R}^8_+ : \underline{\mathbf{u}} \leq 0 \leq \bar{\mathbf{u}}\}$ and K_j be any positive constant satisfying

$$\begin{aligned} K &\geq \max\{K_w, K_n, K_h, K_a, K_m, K_f, K_g, , K_c\}, \\ &\geq \max\left\{\frac{-\partial l_j}{\partial u_j} : \mathbf{u} = (w, n, h, a, m, f, g, c) \in S\right\}, j = 1, 2, 3, 4, 5, 6, 7, 8, \end{aligned}$$

then, we have the following results.

Lemma 2.2.1. *Let*

$$\left.\begin{array}{l} \frac{\partial w}{\partial t}(x,t) - D_w \frac{\partial^2 w}{\partial x^2} \leq K_w, \\ \frac{\partial n}{\partial t}(x,t) - \frac{\partial}{\partial x}\left((D_n \max\{n - v_c, 0\} + D_m)\frac{\partial n}{\partial x} - \chi_n n \frac{\partial f}{\partial x}\right) \leq K_n, \\ \frac{\partial h}{\partial t}(x,t) \leq K_h, \\ \frac{\partial a}{\partial t}(x,t) \leq K_a, \\ \frac{\partial m}{\partial t}(x,t) - \frac{\partial}{\partial x}\left(D_m \frac{\partial m}{\partial x} - m\chi_m \frac{\partial g}{\partial x}\right) \leq K_m, \\ \frac{\partial f}{\partial t}(x,t) \leq K_f, \\ \frac{\partial g}{\partial t}(x,t) - D_g \frac{\partial^2 g}{\partial x^2} \leq K_g, \\ \frac{\partial c}{\partial t}(x,t) - D_c \frac{\partial^2 c}{\partial x^2} \leq K_c, \end{array}\right\} \quad (2.2.10)$$

then,

$$\lim_{t\to\infty} w(x,t) = K_w,\ \lim_{t\to\infty} n(x,t) = K_n,\ \lim_{t\to\infty} h(x,t) = K_h,\ \lim_{t\to\infty} a(x,t) = K_a,$$

$$\lim_{t\to\infty} m(x,t) = K_m,\ \lim_{t\to\infty} f(x,t) = K_f,\ \lim_{t\to\infty} g(x,t) = K_g,\ \lim_{t\to\infty} c(x,t) = K_c.$$

Theorem 2.2.2. *The equilibrium points in equation (2.2.4) are globally asymptotically stable.*

Proof: From the maximum principle of parabolic equations, it is known that for any initial value

$$(w_0(t,x), n_0(t,x), h_0(t,x), a_0(t,x), m_0(t,x), f_0(t,x), g_0(t,x), c_0(t,x)) > (0,0,0,0,0)$$

the corresponding non-negative solution

$$(w(t,x), n(t,x), h(t,x), a(t,x), m(t,x), f(t,x), g(t,x), c(t,x)),$$

is strictly positive for $t > 0$. Since the equilibrium points in equation (2.2.4) are non-negative, then let $\varepsilon_0 \in (0,1)$. Then according to Lemma (2.2.1) and the comparison

principle of parabolic equations, there exists $t_1 > t_0 > 0$ such that, for any $t > t_1$,

$$\left.\begin{aligned} w(x,t) &\leq K_w + \varepsilon_0 := \bar{w}(x,t), \\ n(x,t) &\leq K_n + \varepsilon_0 := \bar{n}(x,t), \\ h(x,t) &\leq K_h + \varepsilon_0 := \bar{h}(x,t), \\ a(x,t) &\leq K_a + \varepsilon_0 := \bar{a}(x,t), \\ m(x,t) &\leq K_m + \varepsilon_0 := \bar{m}(x,t), \\ f(x,t) &\leq K_f + \varepsilon_0 := \bar{f}(x,t), \\ g(x,t) &\leq K_g + \varepsilon_0 := \bar{g}(x,t), \\ c(x,t) &\leq K_c + \varepsilon_0 := \bar{c}(x,t), \end{aligned}\right\} \tag{2.2.11}$$

and

$$\left.\begin{array}{l} w(x,t) \geq K_w - \varepsilon_0 := \underline{w}(x,t), \\ n(x,t) \geq K_n - \varepsilon_0 := \underline{n}(x,t), \\ h(x,t) \geq K_m - \varepsilon_0 := \underline{m}(x,t), \\ a(x,t) \geq K_a - \varepsilon_0 := \underline{a}(x,t), \\ m(x,t) \geq K_m - \varepsilon_0 := \underline{m}(x,t), \\ f(x,t) \geq K_f - \varepsilon_0 := \underline{f}(x,t), \\ g(x,t) \geq K_g - \varepsilon_0 := \underline{g}(x,t), \\ c(x,t) \geq K_c - \varepsilon_0 := \underline{c}(x,t). \end{array}\right\} \tag{2.2.12}$$

Thus, for $t > t_0$, it is possible to obtain

$$\begin{aligned} \underline{w}(x,t) &\leq w(x,t) \leq \bar{w}(x,t), \underline{n}(x,t) \leq n(x,t) \leq \bar{n}(x,t), \\ \underline{h}(x,t) &\leq h(x,t) \leq \bar{h}(x,t),\ \underline{a}(x,t) \leq a(x,t) \leq \bar{a}(x,t), \\ \underline{m}(x,t) &\leq m(x,t) \leq \bar{m}(x,t),\ \underline{f}(x,t) \leq f(x,t) \leq \bar{f}(x,t), \\ \underline{g}(x,t) &\leq g(x,t) \leq \bar{g}(x,t),\ \underline{c}(x,t) \leq c(x,t) \leq \bar{c}(x,t). \end{aligned} \tag{2.2.13}$$

Since $l_j(w, n, h, a, m, f, g, c)$ in equation (2.2.9) is a C^1 function of w, n, h, a, m, f, g, c, where l_1 is quasi-monotone non-increasing in n, h, a, m, f, g, c, l_2 is mixed quasi-monotone in w, h, a, m, f, g, c, l_3 is quasi-monotone non-decreasing in w, n, a, m, f, g, c, l_4 is mixed quasi-monotone in w, n, h, m, f, g, c, h_5 is mixed quasi-monotone in w, n, h, a, f, g, c, l_6 is quasi-monotone non-decreasing in w, n, h, a, m, g, c, l_7 is mixed quasi-monotone in w, n, h, a, m, f, c and l_8 is mixed quasi-monotone in w, n, h, a, m, f, g, then by the method of upper and lower solutions we know that the system in (2.1.1) has a unique global non-negative solution w, n, h, a, m, f, g, c, [101]. Thus,

$$\underline{w}, \bar{w}, \underline{n}, \bar{n}, \underline{h}, \bar{h}, \underline{a}, \bar{a}, \underline{m}, \bar{m}, \underline{f}, \bar{f}, \underline{g}, \bar{g}, \underline{c}, \bar{c}, \tag{2.2.14}$$

satisfy

$$\left.\begin{array}{l}
\alpha_w \underline{m}(1-\bar{w}) - \beta_w(\underline{n}+\underline{h}+\underline{m})\bar{w} - \gamma_w\bar{w} \geq 0 \geq \alpha_w\bar{m}(1-\underline{w}) \\
-\beta_w(\bar{n}+\bar{h}+\bar{m})\underline{w} - \gamma_w\underline{w}, \\
\\
\alpha_n\bar{n}(v_{max} - (\underline{h}+\underline{a}+\bar{n}+\underline{f}+\underline{m})) - \alpha_h\mathcal{H}(w_h-\underline{w})\bar{n} \\
+\frac{\alpha_h}{10}\mathcal{H}(\underline{w}-w_h)h - \gamma_n\bar{n}\underline{c} \geq 0 \geq \alpha_n\underline{n}(v_{max} - (\bar{h}+\bar{a}+\underline{n}+\bar{f}+\bar{m})) \\
-\alpha_h\mathcal{H}(w_h-\bar{w})\underline{n} + \frac{\alpha_h}{10}\mathcal{H}(\bar{w}-w_h)h - \gamma_n\underline{n}\bar{c}, \\
\\
\alpha_h\mathcal{H}(w_h-\bar{w})\bar{n} - \frac{\alpha_h}{10}\mathcal{H}(\bar{w}-w_h)\bar{h} - \beta_h\mathcal{H}(w_a-\bar{w})\bar{h} \geq 0 \geq \\
\alpha_h\mathcal{H}(w_h-\underline{w})\underline{n} - \frac{\alpha_h}{10}\mathcal{H}(\underline{w}-w_h)\underline{h} - \beta_h\mathcal{H}(w_a-\underline{w})\underline{h}, \\
\\
\beta_h\mathcal{H}(w_a-\underline{w})\underline{h} + \gamma_n\underline{n}\underline{c} \geq 0 \geq \beta_h\mathcal{H}(w_a-\bar{w})\bar{h} + \gamma_n\bar{n}\bar{c}, \\
\\
\alpha_m\bar{m}\underline{g}(v_{\max} - (\underline{h}+\underline{a}+\underline{n}+\underline{f}+\bar{m})) \geq 0 \geq \\
\alpha_m\underline{m}\bar{g}(v_{\max} - (\bar{h}+\bar{a}+\bar{n}+\bar{f}+\underline{m})), \\
\\
-\beta_f\bar{n}\bar{f} \geq 0 \geq -\beta_f\underline{n}\underline{f}, \\
\\
\alpha_g\underline{h} - \beta_g\underline{m}\bar{g} \geq 0 \geq \alpha_g\bar{h} - \beta_g\bar{m}\underline{g}, \\
\\
100\sum_{k=0}^{5}\exp(-4(t-(200+2k))^2)\underline{m}(1-\bar{c}) - \gamma_c\bar{c} - k\gamma_n\underline{n}\bar{c} \geq 0 \geq \\
100\sum_{k=0}^{5}\exp(-4(t-(200+2k))^2)\bar{m}(1-\underline{c}) - \gamma_c\underline{c} - k\gamma_n\bar{n}\underline{c}.
\end{array}\right\} \quad (2.2.15)$$

Therefore, $(\bar{w},\bar{n},\bar{h},\bar{a},\bar{m},\bar{f},\bar{g},\bar{c})$ and $(\underline{w},\underline{n},\underline{h},\underline{a},\underline{m},\underline{f},\underline{g},\underline{c})$,
are a pair of coupled upper and lower solutions of system (2.1.1), [130], respectively.

Thus, for any

$$(\underline{w},\underline{n},\underline{h},\underline{a},\underline{m},\underline{f},\underline{g},\underline{c}) \leq (w_1,n_1,h_1,a_1,m_1,g_1,c_1),$$
$$\text{and } (w_2,n_2,h_2,a_2,m_2,f_2,g_2,c_2) \leq (\bar{w},\bar{n},\bar{h},\bar{a},\bar{m},\bar{f},\bar{g},\bar{c})$$

we have

$$\left.\begin{aligned}
&|\alpha_w m_1(1-w_1) - \beta_w(n_1+h_1+m_1)w_1 - \gamma_w w_1 \\
&-(\alpha_w m_2(1-w_2) - \beta_w(n_2+h_2+m_2)w_2 - \gamma_w w_2)| \\
&\leq K(|w_1-w_2| + |n_1-n_2| + |h_1-h_2| + |a_1-a_2|), \\
&|\alpha_n n_1(v_{max}-v_1) - \alpha_h\mathcal{H}(w_h-w_1)n_1 + \tfrac{\alpha_h}{10}\mathcal{H}(w_1-w_h)h_1 - \gamma_n n_1 c_1 \\
&-(\alpha_n n_2(v_{max}-v_2) - \alpha_h\mathcal{H}(w_h-w_2)n_2 + \tfrac{\alpha_h}{10}\mathcal{H}(w_2-w_h)h_2 - \gamma_n n_2 c_2)| \\
&\leq K(|n_1-n_2| + |h_1-h_2| + |a_1-a_2| + |v_1-v_2|), \\
&|\alpha_h\mathcal{H}(w_h-w_1)n_1 - \tfrac{\alpha_h}{10}\mathcal{H}(w_1-w_h)h_1 - \beta_h\mathcal{H}(w_a-w_1)h_1 \\
&-(\alpha_h\mathcal{H}(w_h-w_2)n_2 - \tfrac{\alpha_h}{10}\mathcal{H}(w_2-w_h)h_2 - \beta_h\mathcal{H}(w_a-w_2)h_2)| \\
&\leq K(|n_1-n_2| + |h_1-h_2|), \\
&|\beta_h\mathcal{H}(w_a-w_1)h_1 + \gamma_n n_1 c_1 - (\beta_h\mathcal{H}(w_a-w_2)h_2 + \gamma_n n_2 c_2)| \\
&\leq K(|n_1-n_2| + |h_1-h_2+|c_1-c_2|), \\
&|\alpha_m m_1 g_1(v_{\max}-v_1) - (\alpha_m m_2 g_2(v_{\max}-v_2))| \\
&\leq K(|m_1-m_2| + |g_1-g_2+|v_1-v_2|), \\
&|-\beta_f n_1 f_1 - (-\beta_f n_2 f_2)| \leq K(|n_1-n_2| + |f_1-f_2), \\
&|\alpha_g h_1 - \beta_g m_1 g_1 - (\alpha_g h_2 - \beta_g m_2 g_2)| \leq \\
&K(|h_1-h_2| + |m_1-m_2| + |g_1-g_2|), \\
&|100\textstyle\sum_{k=0}^{5}\exp(-4(t-(200+2k))^2)m_1(1-c_1) - \gamma_c c_1 - k\gamma_n n_1 c_1 \\
&-(100\textstyle\sum_{k=0}^{5}\exp(-4(t-(200+2k))^2)m_2(1-c_2) - \gamma_c c_2 - k\gamma_n n_2 c_2)| \\
&\leq K(|n_1-n_2| + |m_1-m_2| + |c_1-c_2|).
\end{aligned}\right\} \quad (2.2.16)$$

Defining two iteration sequences $(\bar{w}, \bar{n}, \bar{h}, \bar{a}, \bar{m}, \bar{f}, \bar{g}, \bar{c})$ and $(\underline{w}, \underline{n}, \underline{h}, \underline{a}, \underline{m}, \underline{f}, \underline{g}, \underline{c})$ for $i \geq 1$,

$$
\left.
\begin{aligned}
&\bar{w}^{(i)} = \bar{w}^{(i-1)} + (\alpha_w \underline{m}^{(i-1)}(1 - \bar{w}^{(i-1)}) - \beta_w(\underline{n}^{(i-1)} + \underline{h}^{(i-1)} \\
&+\underline{m}^{(i-1)})\bar{w}^{(i-1)} - \gamma_w \bar{w}^{(i-1)})/K, \\
&\bar{n}^{(i)} = \bar{n}^{(i-1)} + (\alpha_n \bar{n}(v_{max} - (\underline{h} + \underline{a} + \bar{n} + \underline{f} + \underline{m})) - \alpha_h \mathcal{H}(w_h - \underline{w})\bar{n} \\
&\quad +\tfrac{\alpha_h}{10}\mathcal{H}(\underline{w} - w_h)h - \gamma_n \bar{n}\underline{c})/K, \\
&\bar{h}^{(i)} = \bar{h}^{(i-1)} + (\alpha_h \mathcal{H}(w_h - \bar{w}^{(i-1)})\bar{n}^{(i-1)} - \tfrac{\alpha_h}{10}\mathcal{H}(\bar{w}^{(i-1)} - w_h)\bar{h}^{(i-1)} \\
&-\beta_h \mathcal{H}(w_a - \bar{w}^{(i-1)})\bar{h}^{(i-1)})/K, \\
&\bar{a}^{(i)} = \bar{a}^{(i-1)} + (\beta_h \mathcal{H}(w_a - \underline{w}^{(i-1)})\underline{h}^{(i-1)} + \gamma_n \underline{n}^{(i-1)}\underline{c}^{(i-1)})/K, \\
&\bar{m}^{(i)} = \bar{m}^{(i-1)} + (\alpha_m \bar{m}^{(i-1)}\underline{g}^{(i-1)}(v_{\max} - (\underline{v}^{(i-1)})))/K, \\
&\bar{f}^{(i)} = \bar{f}^{(i-1)} + (-\beta_f \bar{n}^{(i-1)}\bar{f}^{(i-1)})/K, \\
&\bar{g}^{(i)} = \bar{g}^{(i-1)} + (\alpha_g \underline{h}^{(i-1)} - \beta_g \underline{m}^{(i-1)}\bar{g}^{(i-1)})/K, \\
&\bar{c}^{(i)} = \bar{c}^{(i-1)} + ((100\textstyle\sum_{k=0}^{5}\exp(-4(t - (200 + 2k))^2)\underline{m}^{(i-1)}(1 - \bar{c}^{(i-1)}) \\
&-\gamma_c \bar{c}^{(i-1)} - k\gamma_n \underline{n}^{(i-1)}\bar{c}^{(i-1)})/K, \\
&\underline{w}^{(i)} = \underline{w}^{(i-1)} + (\alpha_w \bar{m}(1 - \underline{w}) - \beta_w(\bar{n} + \bar{h} + \bar{m})\underline{w} - \gamma_w \underline{w})/K, \\
&\underline{n}^{(i)} = \underline{n}^{(i-1)} \\
&+(\alpha_n \underline{n}^{(i-1)}(v_{max} - (\bar{h}^{(i-1)} + \bar{a}^{(i-1)} + \underline{n}^{(i-1)} + \bar{f}^{(i-1)} + \bar{m}^{(i-1)})) \\
&-\alpha_h \mathcal{H}(w_h - \bar{w}^{(i-1)})\underline{n}^{(i-1)} + \tfrac{\alpha_h}{10}\mathcal{H}(\bar{w}^{(i-1)} - w_h)h - \gamma_n \underline{n}^{(i-1)}\bar{c}^{(i-1)})/K, \\
&\underline{h}^{(i)} = \underline{h}^{(i-1)} + (\alpha_h \mathcal{H}(w_h - \underline{w}^{(i-1)})\underline{n}^{(i-1)} \\
&\quad -\tfrac{\alpha_h}{10}\mathcal{H}(\underline{w}^{(i-1)} - w_h)\underline{h}^{(i-1)} - \beta_h \mathcal{H}(w_a - \underline{w}^{(i-1)})\underline{h}^{(i-1)})/K, \\
&\underline{a}^{(i)} = \underline{a}^{(i-1)} + (\beta_h \mathcal{H}(w_a - \bar{w}^{(i-1)})\bar{h}^{(i-1)} + \gamma_n \bar{n}^{(i-1)}\bar{c}^{(i-1)})/K, \\
&\underline{m}^{(i)} = \underline{m}^{(i-1)} \\
&+(\alpha_m \underline{m}^{(i-1)}\bar{g}^{(i-1)}(v_{\max} - (\bar{h}^{(i-1)} + \bar{a}^{(i-1)} + \bar{n}^{(i-1)} + \bar{f}^{(i-1)} + \underline{m}^{(i-1)})), \\
&\underline{f}^{(i)} = \underline{f}^{(i-1)} + (-\beta_f \underline{n}^{(i-1)}\underline{f}^{(i-1)})/K, \\
&\underline{g}^{(i)} = \underline{g}^{(i-1)} + (\alpha_g \bar{h}^{(i-1)} - \beta_g \bar{m}^{(i-1)}\underline{g}^{(i-1)})/K, \\
&\underline{c}^{(i)} = \underline{c}^{(i-1)} + (100\textstyle\sum_{k=0}^{5}\exp(-4(t - (200 + 2k))^2)\bar{m}^{(i-1)}(1 - \underline{c}^{(i-1)}) \\
&\qquad -\gamma_c \underline{c}^{(i-1)} - k\gamma_n \bar{n}^{(i-1)}\underline{c}^{(i-1)})/K,
\end{aligned}
\right\} \quad (2.2.17)
$$

where, $(\bar{w}^{(0)}, \bar{n}^{(0)}, \bar{h}^{(0)}, \bar{a}^{(0)}, \bar{m}^{(0)}, \bar{f}^{(0)}, \bar{g}^{(0)}, \bar{c}^{(0)}) = (\bar{w}, \bar{n}, \bar{h}, \bar{a}, \bar{m}, \bar{f}, \bar{g}, \bar{c})$
and $(\underline{w}^{(0)}, \underline{n}^{(0)}, \underline{h}^{(0)}, \underline{a}^{(0)}, \underline{m}^{(0)}, \underline{f}^{(0)}, \underline{g}^{(0)}, \underline{c}^{(0)}) = (\underline{w}, \underline{n}, \underline{h}, \underline{a}, \underline{m}, \underline{f}, \underline{g}, \underline{c})$. Thus, for $i \geq 1$

$$\begin{aligned}
(\underline{w}, \underline{n}, \underline{h}, \underline{a}, \underline{m}, \underline{f}, \underline{g}, \underline{c}) &\leq (\underline{w}^{(i)}, \underline{n}^{(i)}, \underline{h}^{(i)}, \underline{a}^{(i)}, \underline{m}^{(i)}, \underline{f}^{(i)}, \underline{g}^{(i)}, \underline{c}^{(i)}) \\
&\leq (\underline{w}^{(i+1)}, \underline{n}^{(i+1)}, \underline{h}^{(i+1)}, \underline{a}^{(i+1)}, \underline{m}^{(i+1)}, \underline{f}^{(i+1)}, \underline{g}^{(i+1)}, \underline{c}^{(i+1)}) \\
&\leq (\bar{w}^{(i+1)}, \bar{n}^{(i+1)}, \bar{h}^{(i+1)}, \bar{a}^{(i+1)}, \bar{m}^{(i+1)}, \bar{f}^{(i+1)}, \bar{g}^{(i+1)}, \bar{c}^{(i+1)}) \\
&\leq (\bar{w}^{(i)}, \bar{n}^{(i)}, \bar{h}^{(i)}, \bar{a}^{(i)}, \bar{m}^{(i)}, \bar{f}^{(i)}, \bar{g}^{(i)}, \bar{c}^{(i)}) \\
&\leq (\bar{w}, \bar{n}, \bar{h}, \bar{a}, \bar{m}, \bar{f}, \bar{g}, \bar{c}),
\end{aligned}$$

and there exist $(\tilde{w}^{(0)}, \tilde{n}^{(0)}, \tilde{h}^{(0)}, \tilde{a}^{(0)}, \tilde{m}^{(0)}, \tilde{f}^{(0)}, \tilde{g}^{(0)}, \tilde{c}^{(0)}) > (0,0,0,0,0)$,
and $(\hat{w}^{(0)}, \hat{n}^{(0)}, \hat{h}^{(0)}, , \hat{a}^{(0)}, \hat{m}^{(0)}, \hat{f}^{(0)}, \hat{g}^{(0)}, \hat{c}^{(0)}) > (0,0,0,0,0)$ such that

$$\begin{aligned}
\lim_{i\to\infty} \bar{w} &= \tilde{w}, \lim_{i\to\infty} \bar{n} = \tilde{n}, \lim_{i\to\infty} \bar{h} = \tilde{h}, \lim_{i\to\infty} \bar{a} = \tilde{a}, \lim_{i\to\infty} \bar{m} = \tilde{m}, \lim_{i\to\infty} \bar{f} = \tilde{f}, \\
\lim_{i\to\infty} \bar{g} &= \tilde{g}, \lim_{i\to\infty} \bar{c} = \tilde{c},
\end{aligned}$$

and

$$\begin{aligned}
\lim_{i\to\infty} \underline{w} &= \hat{w}, \lim_{i\to\infty} \underline{n} = \hat{n}, \lim_{i\to\infty} \underline{h} = \hat{h}, \lim_{i\to\infty} \underline{a} = \hat{a}, \lim_{i\to\infty} \underline{m} = \hat{m}, \lim_{i\to\infty} \underline{f} = \hat{f}, \\
\lim_{i\to\infty} \underline{g} &= \hat{g}, \lim_{i\to\infty} \underline{c} = \hat{c},
\end{aligned}$$

and

$$
\left.
\begin{aligned}
&\alpha_w \hat{m}(1-\tilde{w}) - \beta_w(\hat{n}+\hat{h}+\hat{m})\bar{w} - \gamma_w \tilde{w} = 0,\\
&\alpha_w \tilde{m}(1-\hat{w}) - \beta_w(\tilde{n}+\tilde{h}+\tilde{m})\hat{w} - \gamma_w \hat{w} = 0,\\
&\\
&\alpha_n \tilde{n}(v_{max} - (\hat{h}+\hat{a}+\tilde{n}+\hat{f}+\hat{m}))\\
&-\alpha_h \mathcal{H}(w_h - \hat{w})\tilde{n} + \tfrac{\alpha_h}{10}\mathcal{H}(\hat{w}-w_h)\hat{h} - \gamma_n \tilde{n}\hat{c} = 0,\\
&\alpha_n \hat{n}(v_{max} - (\tilde{h}+\tilde{a}+\tilde{n}+\tilde{f}+\tilde{m}))\\
&-\alpha_h \mathcal{H}(w_h - \tilde{w})\hat{n} + \tfrac{\alpha_h}{10}\mathcal{H}(\tilde{w}-w_h)\tilde{h} - \gamma_n \hat{n}\tilde{c} = 0,\\
&\\
&\alpha_h \mathcal{H}(w_h - \tilde{w})\tilde{n} - \tfrac{\alpha_h}{10}\mathcal{H}(\tilde{w}-w_h)\tilde{h} - \beta_h \mathcal{H}(w_a - \tilde{w})\tilde{h} = 0\\
&\alpha_h \mathcal{H}(w_h - \hat{w})\hat{n} - \tfrac{\alpha_h}{10}\mathcal{H}(\hat{w}-w_h)\hat{h} - \beta_h \mathcal{H}(w_a - \hat{w})\hat{h} = 0,\\
&\\
&\beta_h \mathcal{H}(w_a - \hat{w})\hat{h} + \gamma_n \hat{n}\hat{c} = 0,\\
&\beta_h \mathcal{H}(w_a - \tilde{w})\tilde{h} + \gamma_n \tilde{n}\tilde{c} = 0,\\
&\\
&\alpha_m \tilde{m}\hat{g}(v_{\max} - (\hat{h}+\hat{a}+\hat{n}+\hat{f}+\tilde{m})) = 0,\\
&\alpha_m \hat{m}\tilde{g}(v_{\max} - (\tilde{h}+\tilde{a}+\tilde{n}+\tilde{f}+\hat{m})),\\
&\\
&-\beta_f \tilde{n}\tilde{f} = 0,\\
&-\beta_f \hat{n}\hat{f} = 0,\\
&\\
&\alpha_g \hat{h} - \beta_g \hat{m}\tilde{g} = 0,\\
&\alpha_g \tilde{h} - \beta_g \tilde{m}\hat{g} = 0,\\
&\\
&100\sum_{k=0}^{5}\exp(-4(t-(200+2k))^2)\hat{m}(1-\tilde{c}) - \gamma_c \tilde{c} - k\gamma_n \hat{n}\tilde{c} = 0,\\
&100\sum_{k=0}^{5}\exp(-4(t-(200+2k))^2)\tilde{m}(1-\hat{c}) - \gamma_c \hat{c} - k\gamma_n \tilde{n}\hat{c} = 0.
\end{aligned}
\right\} \quad (2.2.18)
$$

Since, the equilibrium points in equation (2.2.4) are the unique semi-positive constant equilibrium of system (2.1.1), it must hold for

$$\begin{aligned}(\tilde{w},\tilde{n},\tilde{h},\tilde{a},\tilde{m},\tilde{f},\tilde{g},\tilde{c}) &= (\hat{w},\hat{n},\hat{h},\hat{a},\hat{m},\hat{f},\hat{g},\hat{c}) \\ &= (\frac{\alpha_w v_{\max}}{\alpha_w+\beta_w v_{\max}+\gamma_w},0,0,0,v_{\max},0,0,c^*>0). \quad (2.2.19)\end{aligned}$$

Thus, by [101, 102], the solution $(\frac{\alpha_w v_{\max}}{\alpha_w+\beta_w v_{\max}+\gamma_w},0,0,0,v_{\max},0,0,c^*>0)$ of system (2.1.1) satisfies

$$\begin{aligned}\lim_{t\to\infty} w(x,t) &= w^*,\ \lim_{t\to\infty} n(x,t)=n^*,\ \lim_{t\to\infty} h(x,t)=h^*,\ \lim_{t\to\infty} a(x,t)=a^*,\\ \lim_{t\to\infty} m(x,t) &= m^*,\ \lim_{t\to\infty} f(x,t)=f^*,\ \lim_{t\to\infty} g(x,t)=g^*,\ \lim_{t\to\infty} c(x,t)=c^*.\end{aligned}$$

Hence, the constant equilibrium point $(\frac{\alpha_w v_{\max}}{\alpha_w+\beta_w v_{\max}+\gamma_w},0,0,0,v_{\max},0,0,c^*>0)$ is globally asymptotically stable.

2.3 Construction and analysis of the numerical method

In this section, we describe the derivation of the fitted numerical method for solving the system in equation (2.1.1). We determine an approximation to the derivatives of the functions

$w(t,x), n(x,t), h(x,t), a(x,t), m(x,t), f(x,t), g(x,t), c(x,t),$

with respect to the spatial variable x as follow.

Let S_x be a positive integer. Discretize the interval $[0,x_f], x_f \in \mathbb{Z}^+$ through the points

$$0 = x_0 < x_1 < x_2 < \cdots < x_{S_x} = x_f,$$

where the step-size $\Delta x = x_{j+1} - x_j = x_f/S_x$, $j = 0,1,\ldots,S_x$. Let

$$W_j(t), N_j(t), H_j(t), A_j(t), M_j(t), F_j(t), G_j(t), C_j(t), \quad (2.3.1)$$

denote the numerical approximations of
$w(t,x), n(x,t), h(x,t), a(x,t), m(x,t), f(x,t), g(x,t), c(x,t)$. Then we approximate the second order spatial derivative in the system in (2.1.1) by

$$\left.\begin{aligned}
&\tfrac{\partial w}{\partial x^2}(t,x_j) \approx \tfrac{W_{j+1}-2W_j+W_{j-1}}{\phi_w^2},\\
&\tfrac{\partial}{\partial x}\left([D_n \max\{N_j - v_c, 0\} + D_m]\tfrac{\partial n}{\partial x} - \chi_n n \tfrac{\partial f}{\partial x}\right)(t,x_j)\\
&\qquad \approx [D_n \max\{N_j - v_c, 0\} + D_m]\tfrac{N_{j+1}-2N_j+N_{j-1}}{\phi_n^2} - D_x^+\left(\chi_n N_j D_x^- F_j\right),\\
&\tfrac{\partial}{\partial x}\left(D_m \tfrac{\partial m}{\partial x} - m\chi_m \tfrac{\partial g}{\partial x}\right)(t,x_j) \approx \tfrac{M_{j+1}-2M_j+M_{j-1}}{\phi_m^2} - D^+(M_j \chi_m D^- G_j),\\
&\tfrac{\partial^2 g}{\partial x^2}(t,x_j) \approx D_x^+(D^- G_j),\ \tfrac{\partial^2 c}{\partial x^2}(t,x_j) \approx \tfrac{C_{j+1}-2C_j+C_{j+1}}{\phi_c^2},
\end{aligned}\right\} \quad (2.3.2)$$

where,

$$D^+(\cdot)_j = \frac{(\cdot)_{i+1} - (\cdot)_i}{\Delta x} \text{ and } D^-(\cdot)_i = \frac{(\cdot)_i - (\cdot)_{i-1}}{\Delta x},$$

and the denominator functions

$$\phi_w^2 := \frac{4}{\varrho_w^2}\sinh^2\left(\frac{\varrho_w \Delta x}{2}\right), \quad \varrho_w := \sqrt{\frac{\gamma_w}{D_w}},\ \phi_n^2 := \frac{\tilde{D}_n \Delta x}{\chi_n}\left[\exp(\frac{\chi_n \Delta x}{\tilde{D}_n}) - 1\right],$$

$$\phi_m^2 := \frac{D_m \Delta x}{\chi_m}\left[\exp(\frac{\chi_m \Delta x}{D_m}) - 1\right],\ \phi_c^2 := \frac{4}{\varrho_c^2}\sinh^2\left(\frac{\varrho_c \Delta x}{2}\right),\ \varrho_c := \sqrt{\frac{\gamma_c}{D_c}},$$

where we see that $\phi_w \to \Delta x, \phi_n \to \Delta x, \phi_m \to \Delta x, \phi_c \to \Delta x$, as $\Delta x \to 0$. Let S_t be a positive integer and $\Delta t = T/S_t$ where $0 < t < T$. Discretizing the time interval $[0, t_{S_t}]$ through the points

$$0 = t_0 < t_1 < \cdots < t_{S_t} = T,$$

where

$$t_{i+1} - t_i = \Delta t,\ i = 0, 1, \ldots, (t_{S_t} - 1).$$

We approximate the time derivative at t_i by

$$\left.\begin{array}{l} \frac{\partial w}{\partial t}(x,t_i) \approx \frac{W_{j+1}^{i+1} - W_j^i}{\psi_w},\ \frac{\partial n}{\partial t}(x,t_i) \approx \frac{N_{j+1}^{i+1} - N_j^i}{\Delta t},\ \frac{\partial h}{\partial t}(x,t_i) \approx \frac{H_{j+1}^{i+1} - H_j^i}{\Delta t}, \\ \frac{\partial a}{\partial t}(x,t_i) \approx \frac{A_{j+1}^{i+1} - A_j^i}{\Delta t},\ \frac{\partial m}{\partial t}(x,t_i) \approx \frac{M_{j+1}^{i+1} - M_j^i}{\Delta t},\ \frac{\partial f}{\partial t}(x,t_i) \approx \frac{F_{j+1}^{i+1} - F_j^i}{\Delta t}, \\ \frac{\partial g}{\partial t}(x,t_i) \approx \frac{G_{j+1}^{i+1} - G_j^i}{\Delta t},\ \frac{\partial c}{\partial t}(x,t_i) \approx \frac{C_{j+1}^{i+1} - C_j^i}{\psi_c}, \end{array}\right\} \quad (2.3.3)$$

where,

$$\psi_w = \psi_w(\Delta t) = (1 - \exp(-\gamma_w \Delta t))/\gamma_w,\ \psi_c = (1 - \exp(-\gamma_c \Delta t))/\gamma_c,$$

where we see that $\psi_w \to \Delta t, \psi_c \to \Delta t$ as $\Delta t \to 0$. The denominator functions in equations (2.3.2) and (2.3.3) are used explicitly to remove the inherent stiffness in the central finite derivatives parts and can be derived by using the theory of nonstandard finite difference methods, see, e.g., [84, 103, 104] and references therein.

Combining the equation (2.3.2) for the spatial with equation (2.3.3) for time deriva-

tives, we obtain

$$
\left.
\begin{aligned}
&\tfrac{W_{j+1}^{i+1}-W_j^i}{\psi_w} - D_w \tfrac{W_{j-1}^{i+1}-2W_j^{i+1}+W_{j+1}^{i+1}}{\phi_w^2} = \alpha_w M_j^i(1-W_j^i)\\
&-\beta_w(N_j^i+H_j^i+M_j^i)W_j^i - \gamma_w W_j^i,\\[2ex]
&\tfrac{N_{j+1}^{i+1}-N_j^i}{\Delta t} - [D_n \max\{N_j - v_c, 0\} + D_m]\tfrac{N_{j-1}^{i+1}-2N_j^{i+1}+N_{j+1}^{i+1}}{\phi_n^2} =\\
&D_x^+\left(\chi_n N_j^i D_x^- F_j^i\right) + \alpha_n N_j^i(v_{max}-V_j^i) - \alpha_h \mathcal{H}(w_h - W_j^i)N_j^i\\
&+\tfrac{\alpha_h}{10}\mathcal{H}(W_j^i - w_h)H_j^i - \gamma_n N_j^i C_j^i,\\[2ex]
&\tfrac{H_{j+1}^{i+1}-H_j^i}{\Delta t} = \alpha_h \mathcal{H}(w_h - W_j^i)N_j^i - \tfrac{\alpha_h}{10}\mathcal{H}(W_i^i - w_h)H_j^i - \beta_h \mathcal{H}(w_a - W_j^i)H_j^i,\\[2ex]
&\tfrac{A_j^{i+1}-A_j^i}{\Delta t} = \beta_h \mathcal{H}(w_a - W_j^i)H_j^i + \gamma_n N_j^i C_j^i,\\[2ex]
&\tfrac{M_{j+1}^{i+1}-M_j^i}{\Delta t} - D_m \tfrac{M_{j-1}^{i+1}-2M_j^{i+1}+M_{j+1}^{i+1}}{\phi_m^2} = D_x^+(M_j^i \chi_m D_x^- G_j^i)\\
&+\alpha_m M_j^i G_j^i(v_{\max}-V_j^i),\\[2ex]
&\tfrac{F_{j+1}^{i+1}-F_j^i}{\Delta t} = -\beta_f N_j^i F_j^i,\\
&\tfrac{G_{j+1}^{i+1}-G_j^i}{\Delta t} - D_g \tfrac{G_{j-1}^{i+1}-2G_j^{i+1}+G_{j+1}^{i+1}}{(\Delta x)^2} = \alpha_g H_j^i - \beta_g M_j^i G_j^i,\\[2ex]
&\tfrac{C_{j+1}^{i+1}-C_j^i}{\psi_c} - D_c \tfrac{C_{j-1}^{i+1}-2C_j^{i+1}+C_{j+1}^{i+1}}{\phi_c^2} =\\
&100\sum_{k=0}^{5}\exp(-4(t_k-(200+2k))^2)M_j^i(1-C_j^i) - \gamma_c C_j^i - k\gamma_n N_j^i C_j^i,\\[2ex]
&W_1^i = W_{-1}^n,\ N_1^i = N_{-1}^i,\ H_1^i = H_{-1}^i,\ A_1^i = A_{-1}^i,\ M_1^i = M_{-1}^i,\ F_1^i = F_{-1}^i,\\
&G_1^i = G_{-1}^i, C_1^i = C_{-1}^i,\ W_{x_{S_x}}^i = W_{x_{S_x}-1}^i,\ N_{x_{S_x}}^i = N_{x_{S_x}-1}^i,\ H_{x_{S_x}}^i = H_{x_{S_x}-1}^i,\\
&A_{x_{S_x}}^i = A_{x_{S_x}-1}^i,\ M_{x_{S_x}}^i = M_{x_{S_x}-1}^i,\ F_{x_{S_x}}^i = F_{x_{S_x}-1}^i,\ G_{x_{S_x}}^i = G_{x_{S_x}-1}^i,\\
&C_{x_{S_x}}^i = C_{x_{S_x}-1}^i,\ W_j^0 = 1.0,\ N_j^0 = 0.93\exp(-200x_j^2),\ H_j^0 = A_j^0 = 0.0,\\
&M_j^0 = 0.01,\ F_j^0 = 1 - N_j^0 - M_j^0 - 0.05,\ G_j^0 = 0.0,\ C_j^0 \in [0,1].
\end{aligned}
\right\} \quad (2.3.4)
$$

We refer to the scheme in (2.3.4) as a semi-fitted operator finite difference numerical

method (FOFDM), whereas when all the denominator functions in (2.3.2) and (2.3.3) are replaced with the uniform step sizes, the scheme becomes standard finite difference method (SFDM).

Let the functions

$$w(x,t), n(x,t), h(x,t), a(x,t), m(x,t), f(x,t), g(x,t), c(x,t),$$

and their partial derivatives with respect to both t and x be smooth such that they satisfy

$$\begin{aligned}
\left|\frac{\partial^{i+j} w(t,x)}{\partial t^i x^j}\right| &\leq \Upsilon_w, \left|\frac{\partial^{i+j} n(t,x)}{\partial t^i x^j}\right| \leq \Upsilon_n, \left|\frac{\partial^{i+j} h(t,x)}{\partial t^i x^j}\right| \leq \Upsilon_h, \\
\left|\frac{\partial^{i+j} a(t,x)}{\partial t^i x^j}\right| &\leq \Upsilon_a, \left|\frac{\partial^{i+j} m(t,x)}{\partial t^i x^j}\right| \leq \Upsilon_m, \left|\frac{\partial^{i+j} f(t,x)}{\partial t^i x^j}\right| \leq \Upsilon_f, \\
\left|\frac{\partial^{i+j} g(t,x)}{\partial t^i x^j}\right| &\leq \Upsilon_g, \left|\frac{\partial^{i+j} c(t,x)}{\partial t^i x^j}\right| \leq \Upsilon_c, \ \forall i,j \geq 0,
\end{aligned} \tag{2.3.5}$$

where,

$$\Upsilon_w, \Upsilon_n, \Upsilon_h, \Upsilon_a, \Upsilon_m, \Upsilon_f, \Upsilon_g, \Upsilon_c,$$

are constant that are independent of the time and space step-sizes. Therefore, in view of the FOFDM, we see that the local truncation errors

$$\varsigma_w, \varsigma_n, \varsigma_h, \varsigma_a, \varsigma_m, \varsigma_f, \varsigma_g, \varsigma_c,$$

are given by

$$\left.\begin{aligned}
(\varsigma_w)^i_j &= (\mathcal{L}_w w)^i_j - (\mathcal{F}_w)^i_j = (\mathcal{A}_w(w-W))^i_j,\\
(\varsigma_n)^i_j &= (\mathcal{L}_n)^i_j - (\mathcal{F}_n)^i_j = (\mathcal{A}_n(n-N))^i_j,\\
(\varsigma_h)^i_j &= (\mathcal{L}_h)^i_j - (\mathcal{F}_h)^i_j = (h-H)^i_j,\\
(\varsigma_a)^i_j &= (\mathcal{L}_a a)^i_j - (\mathcal{F}_a)^i_j = (a-A)^i_j,\\
(\varsigma_m)^i_j &= (\mathcal{L}_m)^i_j - (\mathcal{F}_m)^i_j = (\mathcal{A}_m(m-M))^i_j,\\
(\varsigma_g)^i_j &= (\mathcal{L}_g)^i_j - (\mathcal{F}_g)^i_j = (\mathcal{A}_g(g-G))^i_j,\\
(\varsigma_c)^i_j &= (\mathcal{L}_c)^i_j - (\mathcal{F}_c)^i_j = (\mathcal{A}_c(c-C))^i_j,
\end{aligned}\right\} \tag{2.3.6}$$

where,

$$\begin{aligned}
\mathcal{A}_w &= \text{Tri}\left(-\frac{D_w}{\phi_w^2}, \frac{1}{\psi_w}+\frac{D_w}{\phi_w^2}, -\frac{D_w}{\phi_w^2}\right),\ \mathcal{A}_n = \text{Tri}\left(-\frac{\tilde{D}_n}{\phi_n^2}, \frac{1}{\Delta t}+\frac{\tilde{D}_n}{\phi_n^2}, -\frac{\tilde{D}_n}{\phi_n^2}\right),\\
\mathcal{A}_m &= \text{Tri}\left(-\frac{D_m}{\phi_n^2}, \frac{1}{\Delta t}+\frac{D_m}{\phi_m^2}, -\frac{D_m}{\phi_m^2}\right), \mathcal{A}_c = \text{Tri}\left(-\frac{D_c}{\phi_c^2}, \frac{1}{\psi_c}+\frac{D_c}{\phi_c^2}, -\frac{D_c}{\phi_c^2}\right)\\
\mathcal{A}_g &= \text{Tri}\left(-\frac{D_g}{(\Delta x)^2}, \frac{1}{\Delta t}+\frac{D_g}{(\Delta x)^2}, -\frac{D_g}{(\Delta x)^2}\right).
\end{aligned}$$

Thus,

$$\left.\begin{array}{l}
\max_{1\le i\le t_{S_t},1\le j\le x_{S_x}} |w_j^i - W_j^i| \le ||(\mathcal{A}_w)^{-1}||\max_{1\le i\le t_{S_t},1\le j\le x_{S_x}} |(\varsigma_w)_j^i|,\\
\max_{1\le i\le t_{S_t},1\le j\le x_{S_x}} |n_j^i - N_j^i| \le ||(\mathcal{A}_n)^{-1}||\max_{1\le i\le t_{S_t},1\le j\le x_{S_x}} |(\varsigma_n)_j^i|,\\
\max_{1\le i\le t_{S_t},1\le j\le x_{S_x}} |h_j^i - H_j^i| \le \max_{1\le i\le t_{S_t},1\le j\le x_{S_x}} |(\varsigma_h)_j^i|,\\
\max_{1\le i\le t_{S_t},1\le j\le x_{S_x}} |a_j^i - A_j^i| \le \max_{1\le i\le t_{S_t},1\le j\le x_{S_x}} |(\varsigma_a)_j^i|,\\
\max_{1\le i\le t_{S_t},1\le j\le x_{S_x}} |m_j^i - M_j^i| \le ||(\mathcal{A}_m)^{-1}||\max_{1\le i\le t_{S_t},1\le j\le x_{S_x}} |(\varsigma_m)_j^i|,\\
\max_{1\le i\le t_{S_t},1\le j\le x_{S_x}} |f_j^i - F_j^i| \le \max_{1\le i\le t_{S_t},1\le j\le x_{S_x}} |(\varsigma_f)_j^i|,\\
\max_{1\le i\le t_{S_t},1\le j\le x_{S_x}} |g_j^i - G_j^i| \le ||(\mathcal{A}_g)^{-1}||\max_{1\le i\le t_{S_t},1\le j\le x_{S_x}} |(\varsigma_g)_j^i|,\\
\max_{1\le i\le t_{S_t},1\le j\le x_{S_x}} |c_j^i - C_j^i| \le ||(\mathcal{A}_c)^{-1}||\max_{1\le i\le t_{S_t},1\le j\le x_{S_x}} |(\varsigma_c)_j^i|,
\end{array}\right\} \quad (2.3.7)$$

where

$$\left.\begin{array}{l}
\max_{1\le i-1\le t_{S_t},1\le j\le x_{S_x}-1} |(\varsigma_w)_j^i| \le \frac{\Delta t}{2}|w_{tt}(\zeta)| + D_w\frac{(\Delta x)^2}{12}|w_{xxxx}(\xi)|,\\
\max_{1\le i-1\le t_{S_t},1\le j\le x_{S_x}-1} |(\varsigma_n)_j^i| \le \frac{\Delta t}{2}|n_{tt}(\zeta)|\\
\qquad\qquad +[D_n\max\{N_j - v_c, 0\} + D_m]\frac{(\Delta x)^2}{12}|n_{xxxx}(\xi)|,\\
\max_{1\le i-1\le t_{S_t},1\le j\le x_{S_x}-1} |(\varsigma_h)_j^i| \le \frac{\Delta t}{2}|h_{tt}(\zeta)|,\\
\max_{1\le i-1\le t_{S_t},1\le j\le x_{S_x}-1} |(\varsigma_a)_j^i| \le \frac{\Delta t}{2}|a_{tt}(\zeta)|,\\
\max_{1\le i-1\le t_{S_t},1\le j\le x_{S_x}-1} |(\varsigma_m)_j^i| \le \frac{\Delta t}{2}|m_{tt}(\zeta)| + D_m\frac{(\Delta x)^2}{12}|m_{xxxx}(\xi)|,\\
\max_{1\le i-1\le t_{S_t},1\le j\le x_{S_x}-1} |(\varsigma_f)_j^i| \le \frac{\Delta t}{2}|f_{tt}(\zeta)|,\\
\max_{1\le i-1\le t_{S_t},1\le j\le x_{S_x}-1} |(\varsigma_g)_j^i| \le \frac{\Delta t}{2}|g_{tt}(\zeta)| + D_g\frac{(\Delta x)^2}{12}|g_{xxxx}(\xi)|,\\
\max_{1\le i-1\le t_{S_t},1\le j\le x_{S_x}-1} |(\varsigma_c)_j^i| \le \frac{\Delta t}{2}|c_{tt}(\zeta)| + D_c\frac{(\Delta x)^2}{12}|c_{xxxx}(\xi)|,
\end{array}\right\} \quad (2.3.8)$$

for $t_{i-1} \leq \zeta \leq t_{i+1}$, $x_{j-1} \leq \xi \leq x_{j+1}$. In view of inequalities in (2.3.5), then (2.3.8) becomes

$$\left.\begin{array}{l}
\max_{1\leq i-1\leq t_{S_t},1\leq j\leq x_{S_x}-1} |(\varsigma_w)_j^i| \leq \left(\frac{\Delta t}{2} + D_w\frac{(\Delta x)^2}{12}\right)\Upsilon_w,\\
\max_{1\leq i-1\leq t_{S_t},1\leq j\leq x_{S_x}-1} |(\varsigma_n)_j^i| \leq \left(\frac{\Delta t}{2} + \varpi\frac{(\Delta x)^2}{12}\right)\Upsilon_n,\\
\max_{1\leq i-1\leq t_{S_t},1\leq j\leq x_{S_x}-1} |(\varsigma_h)_j^i| \leq \frac{\Delta t}{2}\Upsilon_h,\\
\max_{1\leq i-1\leq t_{S_t},1\leq j\leq x_{S_x}-1} |(\varsigma_a)_j^i| \leq \frac{\Delta t}{2}\Upsilon_a,\\
\max_{1\leq i-1\leq t_{S_t},1\leq j\leq x_{S_x}-1} |(\varsigma_m)_j^i| \leq \left(\frac{\Delta t}{2} + D_m\frac{(\Delta x)^2}{12}\right)\Upsilon_m,\\
\max_{1\leq i-1\leq t_{S_t},1\leq j\leq x_{S_x}-1} |(\varsigma_f)_j^i| \leq \frac{\Delta t}{2}\Upsilon_f,\\
\max_{1\leq i-1\leq t_{S_t},1\leq j\leq x_{S_x}-1} |(\varsigma_g)_j^i| \leq \left(\frac{\Delta t}{2} + D_g\frac{(\Delta x)^2}{12}\right)\Upsilon_g,\\
\max_{1\leq i-1\leq t_{S_t},1\leq j\leq x_{S_x}-1} |(\varsigma_c)_j^i| \leq \left(\frac{\Delta t}{2} + D_c\frac{(\Delta x)^2}{12}\right)\Upsilon_c,
\end{array}\right\} \tag{2.3.9}$$

for $t_{i-1} \leq \zeta \leq t_{i+1}$, $x_{j-1} \leq \xi \leq x_{j+1}$, $\varpi = [D_n \max\{N_j - v_c, 0\} + D_m]$, and by [117] we have

$$\begin{array}{rcl}
||(\mathcal{A}_w)^{-1}|| & \leq & \Xi_w,\ ||(\mathcal{A}_n)^{-1}|| \leq \Xi_n,\ ||(\mathcal{A}_m)^{-1}|| \leq \Xi_m,\\
||(\mathcal{A}_g)^{-1}|| & \leq & \Xi_g.\ ||(\mathcal{A}_c)^{-1}|| \leq \Xi_c.
\end{array} \tag{2.3.10}$$

Using (2.3.9) and (2.3.10) in (2.3.7), we obtain

$$\left.\begin{array}{l}
\max_{1\leq i-1\leq t_{S_t},1\leq j\leq x_{S_x}-1} |(\varsigma_w)_j^i| \leq \left(\frac{\Delta t}{2} + D_w\frac{(\Delta x)^2}{12}\right)\Upsilon_w,\\
\max_{1\leq i-1\leq t_{S_t},1\leq j\leq x_{S_x}-1} |(\varsigma_n)_j^i| \leq \left(\frac{\Delta t}{2} + \varpi\frac{(\Delta x)^2}{12}\right)\Upsilon_n,\\
\max_{1\leq i-1\leq t_{S_t},1\leq j\leq x_{S_x}-1} |(\varsigma_h)_j^i| \leq \frac{\Delta t}{2}\Upsilon_h,\\
\max_{1\leq i-1\leq t_{S_t},1\leq j\leq x_{S_x}-1} |(\varsigma_a)_j^i| \leq \frac{\Delta t}{2}\Upsilon_a,\\
\max_{1\leq i-1\leq t_{S_t},1\leq j\leq x_{S_x}-1} |(\varsigma_m)_j^i| \leq \left(\frac{\Delta t}{2} + D_m\frac{(\Delta x)^2}{12}\right)\Upsilon_m,\\
\max_{1\leq i-1\leq t_{S_t},1\leq j\leq x_{S_x}-1} |(\varsigma_f)_j^i| \leq \frac{\Delta t}{2}\Upsilon_f,\\
\max_{1\leq i-1\leq t_{S_t},1\leq j\leq x_{S_x}-1} |(\varsigma_g)_j^i| \leq \left(\frac{\Delta t}{2} + D_g\frac{(\Delta x)^2}{12}\right)\Upsilon_g,\\
\max_{1\leq i-1\leq t_{S_t},1\leq j\leq x_{S_x}-1} |(\varsigma_c)_j^i| \leq \left(\frac{\Delta t}{2} + D_c\frac{(\Delta x)^2}{12}\right)\Upsilon_c.
\end{array}\right\} \tag{2.3.11}$$

Hence, we obtain the following results.

Theorem 2.3.1. *Let*

$$\mathcal{F}_w(x,t), \mathcal{F}_n(x,t), \mathcal{F}_h(x,t), \mathcal{F}_a(x,t), \mathcal{F}_m(x,t), \mathcal{F}_f(x,t), \mathcal{F}_g(x,t), \mathcal{F}_c(x,t),$$

be sufficiently smooth functions so that
$w(x,t), n(x,t), h(x,t), a(x,t), m(x,t), f(x,t), g(x,t), c(x,t) \in C^{\infty}([0, x_{S_x}] \times [0, t_{S_t}])$. *Let* $(W_j^i, N_j^i, H_j^i, A_j^i, M_j^i, F_j^i, G_j^i, C_j^i)$, $j = 1, 2, \ldots x_{S_x}, i = 1, 2, \ldots t_{S_t}$ *be the approximate solutions to (2.1.1), obtained using the semi-FOFDM with* $W_j^0 = w_j^0, N_j^0 = n_j^0, H_j^0 = h_j^0, A_j^0 = a_j^0, M_j^0 = m_j^0, F_j^0 = f_j^0, G_j^0 = g_j^0, C_j^0 = c_j^0$. *Then there exists*
$\Xi_w, \Xi_n, \Xi_h, \Xi_a, \Xi_m, \Xi_f, \Xi_g, \Xi_c$ *independent of the step sizes* Δt *and* Δx *such that*

$$\left.\begin{array}{l}
\max_{1\le i-1\le t_{S_t}, 1\le j\le x_{S_x}-1} |(\varsigma_w)_j^i| \le \left(\frac{\Delta t}{2} + D_w \frac{(\Delta x)^2}{12}\right) \Upsilon_w, \\
\max_{1\le i-1\le t_{S_t}, 1\le j\le x_{S_x}-1} |(\varsigma_n)_j^i| \le \left(\frac{\Delta t}{2} + \varpi \frac{(\Delta x)^2}{12}\right) \Upsilon_n, \\
\max_{1\le i-1\le t_{S_t}, 1\le j\le x_{S_x}-1} |(\varsigma_h)_j^i| \le \frac{\Delta t}{2} \Upsilon_h, \\
\max_{1\le i-1\le t_{S_t}, 1\le j\le x_{S_x}-1} |(\varsigma_a)_j^i| \le \frac{\Delta t}{2} \Upsilon_a, \\
\max_{1\le i-1\le t_{S_t}, 1\le j\le x_{S_x}-1} |(\varsigma_m)_j^i| \le \left(\frac{\Delta t}{2} + D_m \frac{(\Delta x)^2}{12}\right) \Upsilon_m, \\
\max_{1\le i-1\le t_{S_t}, 1\le j\le x_{S_x}-1} |(\varsigma_f)_j^i| \le \frac{\Delta t}{2} \Upsilon_f, \\
\max_{1\le i-1\le t_{S_t}, 1\le j\le x_{S_x}-1} |(\varsigma_g)_j^i| \le \left(\frac{\Delta t}{2} + D_g \frac{(\Delta x)^2}{12}\right) \Upsilon_g, \\
\max_{1\le i-1\le t_{S_t}, 1\le j\le x_{S_x}-1} |(\varsigma_c)_j^i| \le \left(\frac{\Delta t}{2} + D_c \frac{(\Delta x)^2}{12}\right) \Upsilon_c,
\end{array}\right\} \tag{2.3.12}$$

and conclude our analysis with the following result.

Theorem 2.3.2. (Fatunla [39], Trefethen [123]) *A difference scheme is said to be convergent if and only if it is consistent and stable.*

2.4 Numerical results and discusions

The stability conditions in equations (2.2.7) and (2.2.8) present the core behaviors of tumor cells. That is the transitions of the normoxic cells into the hypoxic class and vice-versa. Thus, to demonstrate the robustness of our numerical method we present

our numerical results for both stability conditions which underpin the core behaviors of tumor cells represented by the models in equation (2.1.1). Therefore, for that reason we adjusted the biological feasible parameter values as presented in Table 2.5.1. We present the numerical results at times $t = 5$ and $t = 15$. Thus, for condition in equation (2.2.7), (we let $v_{\max} = 10^{-1}$) and present the baseline model's numerical results in Figure 2.5.1 - Figure 2.5.2, anti-angiogenic chemotherapy the numerical results are presented in Figure 2.5.3 - Figure 2.5.4 and numerical results for anti-cytotoxic chemotherapy are presented in Figure 2.5.5 - Figure 2.5.6, whereas for condition in equation (2.2.8) (we let $v_{\max} = 10$), then we present the baseline model's numerical results in Figure 2.5.7 - Figure 2.5.8, for anti-angiogenic chemotherapy the numerical results are presented in Figure 2.5.9 - Figure 2.5.10 and numerical results for anti-cytotoxic chemotherapy are presented in Figure 2.5.11 - Figure 2.5.12. Below we discuss the numerical results for each model.

Baseline model for stability condition in equation (2.2.7): We see the oxygen concentration (w) is decreasing to its low steady state. This fact is traceable from the behavior of the normoxic cells (n) which is due to the increasing level of hypoxic cells (h), the apoptic cells (a) and angiogenic growth factor (VEGF) (g). However, when oxygen cells (w) are at a high level, we see that the behavior of the endothelial cells (m) are higher too, which in turn degrades the extra-cellular matrix (f). This implies that tumor cells are well supported during this phase. This can be seen on the behaviors of hypoxic, the apoptic cells and angiogenic growth factor (VEGF) (g), at early stages of the infection. At $t = 15$, we see that the above-mentioned behaviors are taking place at a later stage than at $t = 5$. This implies that a host is infected at $t = 15$, because at this time level the same behaviors as mentioned above start to take place.

Baseline model for stability condition in equation (2.2.8): We again see similar behaviors as for stability condition in equation (2.2.7), which is in agreement with the fact that the transitions are reversible.

Anti-angiogenic chemotherapy for stability condition in equations (2.2.7): This model represents a therapeutically intervention after the tumor infection is detected in

a host. Thus, we see that oxygen cells (w) decrease for some time before it increases slightly to its steady growth. This behavior can be vividly explained by the behavior of the normoxic cells (n) and behavior of endothelial cells (m). However, the angiogenic growth factor (VEGF) (g) degrades the extra-cellular matrix to the extends that it restores the survival of the tumor cells. This implies that the process of transformation of hypoxic cells into apoptic cells is again restored to ensure that tumor cells thrives forward in the host if therapeutically intervention is delayed or stopped and/or neglected. At $t = 15$, we see that the above-mentioned behaviors are taking place at a later stage than at $t = 5$. This implies that tumour cells resurrect themselves once more at $t = 15$, because at this time level the same behaviors as mentioned above start to take place.

Anti-angiogenic chemotherapy for stability condition in equations (2.2.8): We again see similar behaviors as for stability condition in equation (2.2.7), which is in agreement with the fact that the transitions are reversible.

Cytotoxic chemotherapy for stability conditions in equations (2.2.7): The application of a diffusible substance entering a tissue from the blood vessels presents slightly different results as compare to the anti-angiogenic chemotherapy. This is presented by the slight decrease in the behavior of the apoptic cells. The diffusible substance has indeed affected the endothelial cells to decrease sharply as its presence continue to treat a host. However, the slight change in the apoptic behavior is not enough to completely destroy the tumor cells. As results the core behavior of a tumor cells are not completely derailed. This, we clearly see it from the behaviour of hypoxic cells and that of the extra-cellular matrix. At $t = 15$, we see that the above-mentioned behaviors are taking place at a later stage than at $t = 5$. This implies that a host is infected at $t = 15$ and then treated immediately, because at this time level the same behaviors as mentioned above start to take place.

Cytotoxic chemotherapy for stability conditions in equations (2.2.8): We again see similar behaviors as for stability condition in equation (2.1.10), which is in agreement with the fact that the transitions are reversible.

2.5 Conclusion

In this chapter, we examined the cytotoxic chemotherapy model mathematically, and our numerical findings could serve as a template to examine the efficacy of low-and high-grade tumors via drugs administering. Studies have revealed that when no treatment is applied, the model which represents a tumor tissue reproduces the typical dynamics of early growth, that is, a cytostatic treatment is administered in the form of a VEGF-inhibitor. An experimental result of a diffusive cytotoxic drug was presented in [49] to treat a tumor by entering the tissue via blood vessels. It was shown that the drug can either significantly reduce the mass tumor or rather aid its growth. In the present work, through mathematical analysis and numerical results showing the spatial distribution of oxygen, normoxic, hypoxic, apoptic, endothelial and angiogenic cells are presented for the baseline model, anti-angiogenic chemotherapy model and anti-cytotoxic chemotherapy model at different time levels. We were able to determine directly that both anti-angiogenic and cytotoxic chemotherapy can result in the reduction of the tumor cells. Though the models considered are not solvable analytically, but our numerical findings are in good agreement with the hypotheses and what has been reported in the literature. Hence, this should be seen as the first attempt to bring forth some of the essential features of the application of chemotherapy to treat a tumor that is clearly missing in the work reported by Hinow et al. [49].

Table 2.5.1: Values of the parameters used in the model (2.3.4) [49]

$D_w = 0.58$	$\alpha_w = 0.001$	$\beta_w = 0.57$	$\gamma_w = 0.25$
$\beta_h = 0.32$	$w_h = 0.05$	$w_a = 0.03$	$\beta_f = 0.50$
$D_n = 5.7600 \times 10^{-3}$	$v_c = 0.8$	$\chi_n = 1.4 \times 10^{-4}$	$D_m = 5.7600 \times 10^{-05}$
$D_g = 0.02$	$\chi_m = 2.1 \times 10^{-6}$	$\alpha_m = 0.99$	$\alpha_g = 0.1$
$\beta_g = 10.00$	$D_c = 0.5$		$\alpha_h = 0.160$
$\alpha_n = \log(2)$	$\gamma_c = 0.21$	$k = 10.5$	$\gamma_n = 0.7$

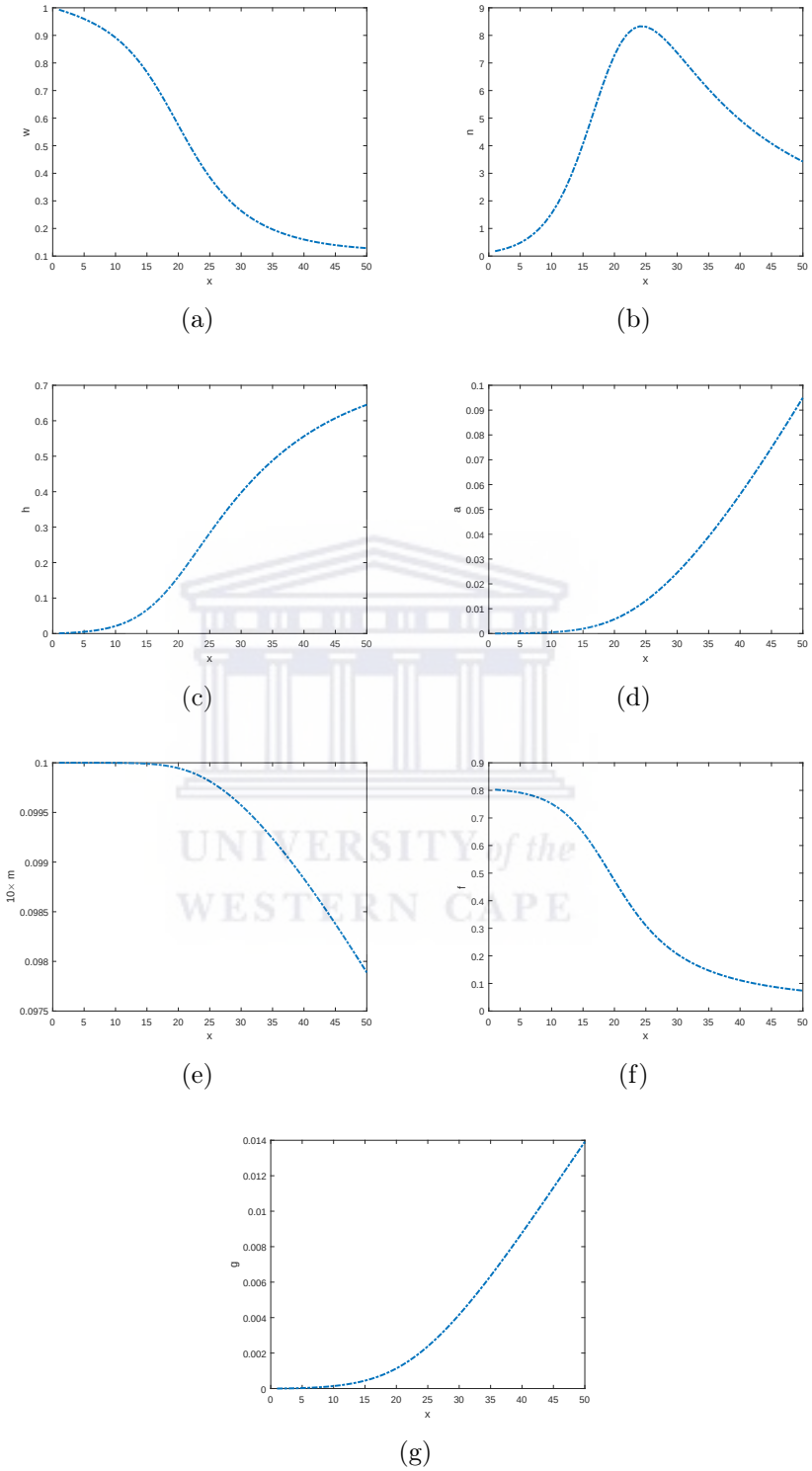

Figure 2.5.1: Numerical solution of the baseline model at $t = 5$ and $v_{\max} = 10^{-1}$, showing the spatial distributions of: (a) oxygen, (b) normoxic, (c) hypoxic, (d) apoptic, (e) endothelial, (f) extracellular matrix and (g) angiogenic cells, for parameter values as in Table 2.5.1.

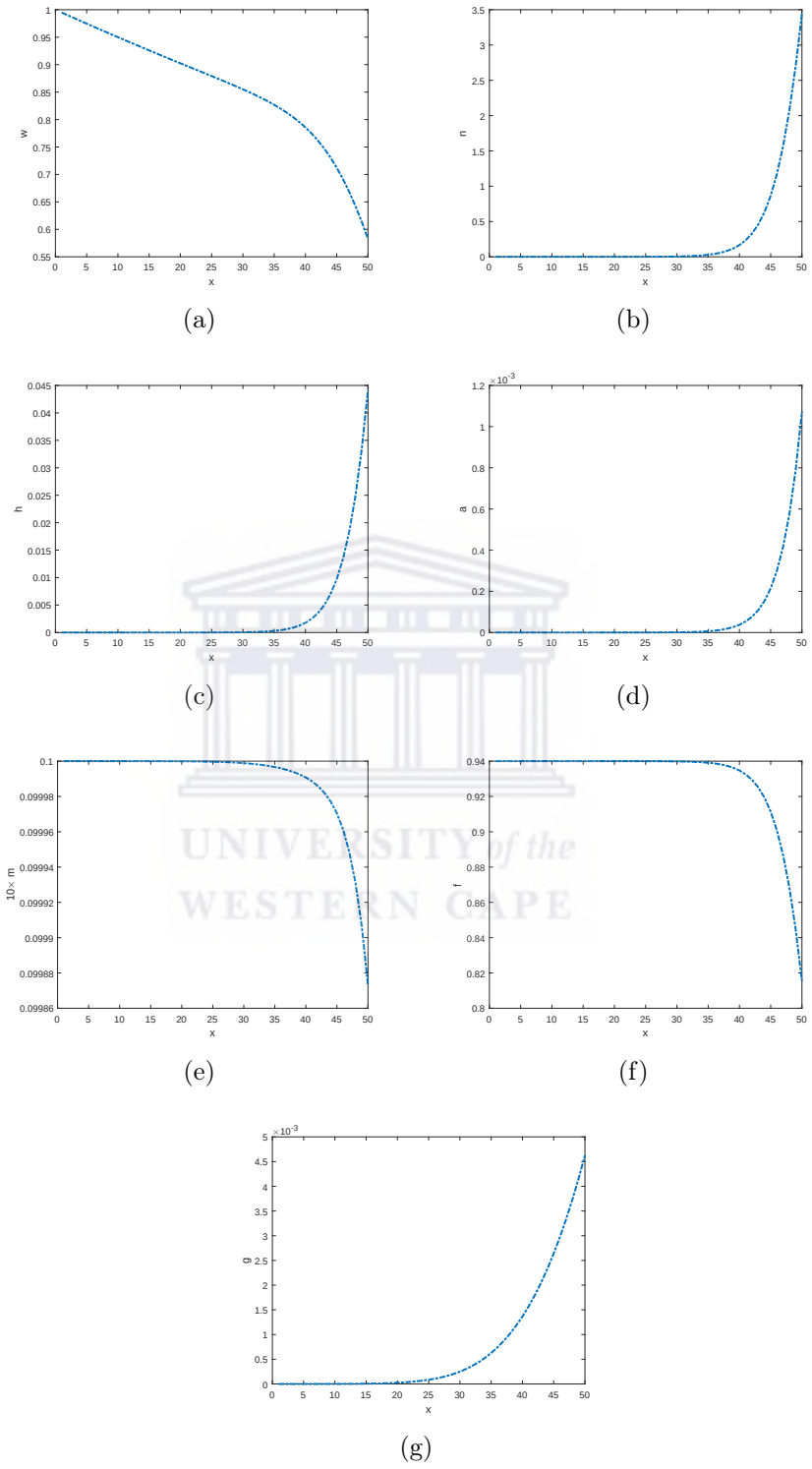

Figure 2.5.2: Numerical solution of the baseline model at $t = 15$ and $v_{\max} = 10^{-1}$, showing the spatial distributions of: (a) oxygen, (b) normoxic, (c) hypoxic, (d) apoptic, (e) endothelial, (f) extracellular matrix and (g) angiogenic cells, for parameter values as in Table 2.5.1.

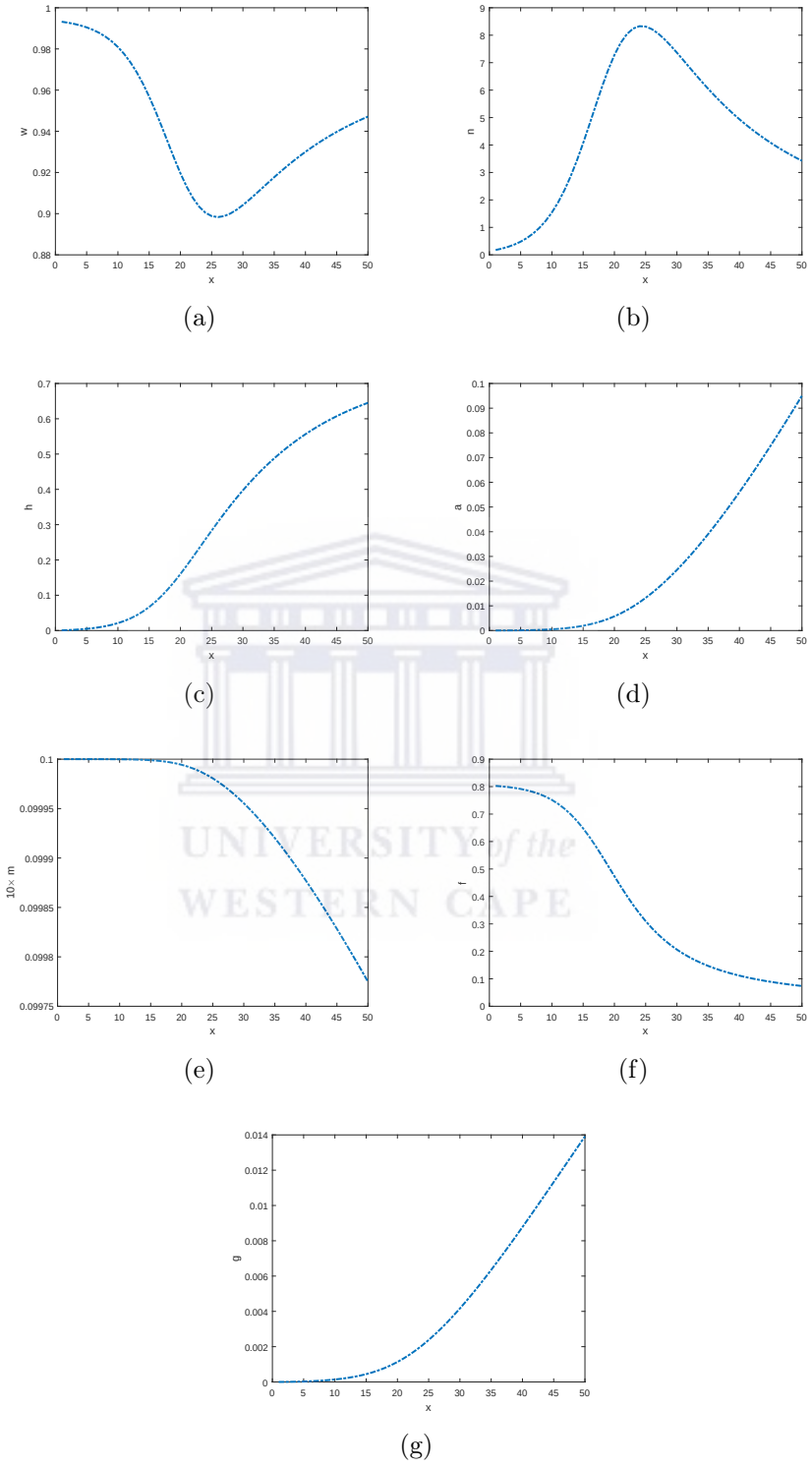

(a) (b) (c) (d) (e) (f) (g)

Figure 2.5.3: Numerical solution of anti-angiogenic chemotherapy model at $t = 5$ and $v_{\max} = 10^{-1}$, showing the spatial distributions of: (a) oxygen, (b) normoxic, (c) hypoxic, (d) apoptic, (e) endothelial, (f) extracellular matrix and (g) angiogenic cells, for parameter values as in Table 2.5.1.

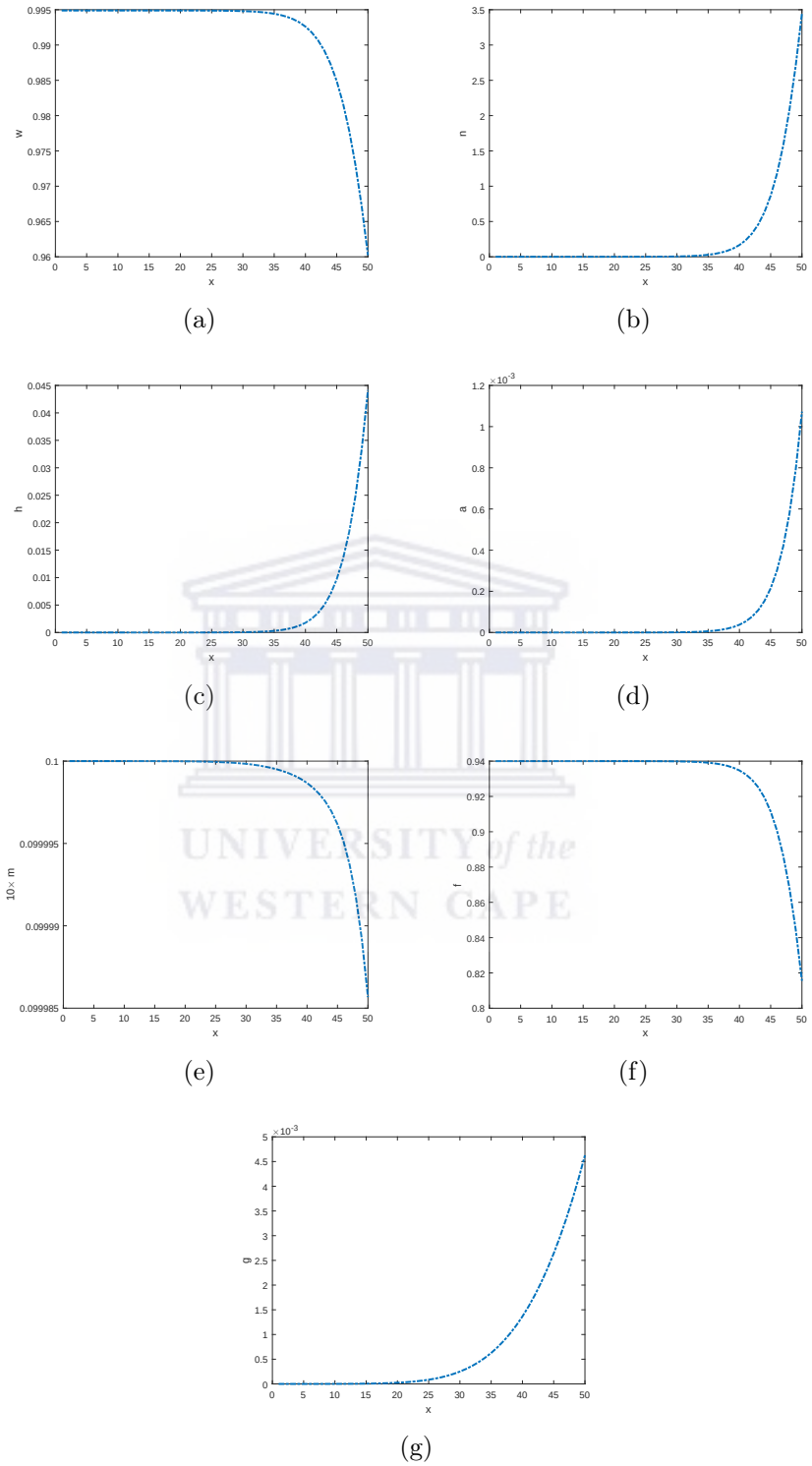

Figure 2.5.4: Numerical solution of anti-angiogenic chemotherapy model at $t = 15$ and $v_{\max} = 10^{-1}$, showing the spatial distributions of: (a) oxygen, (b) normoxic, (c) hypoxic, (d) apoptic, (e) endothelial, (f) extracellular matrix and (g) angiogenic cells, for parameter values as in Table 2.5.1.

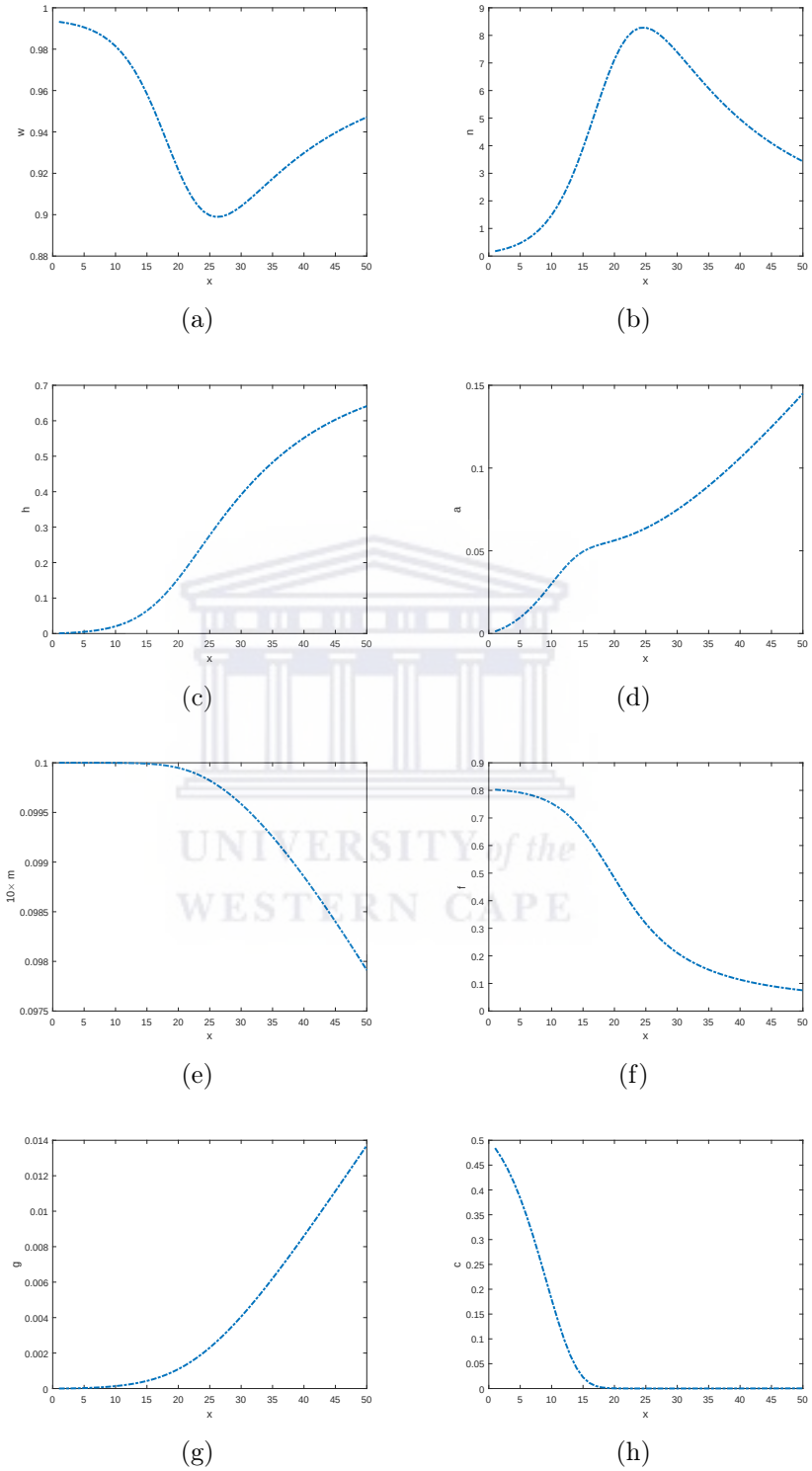

(a) (b) (c) (d) (e) (f) (g) (h)

Figure 2.5.5: Numerical solution of anti-cytotoxic chemotherapy model at $t = 5$ and $v_{\max} = 10^{-1}$, showing the spatial distributions of: (a) oxygen, (b) normoxic, (c) hypoxic, (d) apoptic, (e) endothelial, (f) extracellular matrix, (g) agiogenic and (h) cytotoxic cells, for parameter values as in Table 2.5.1.

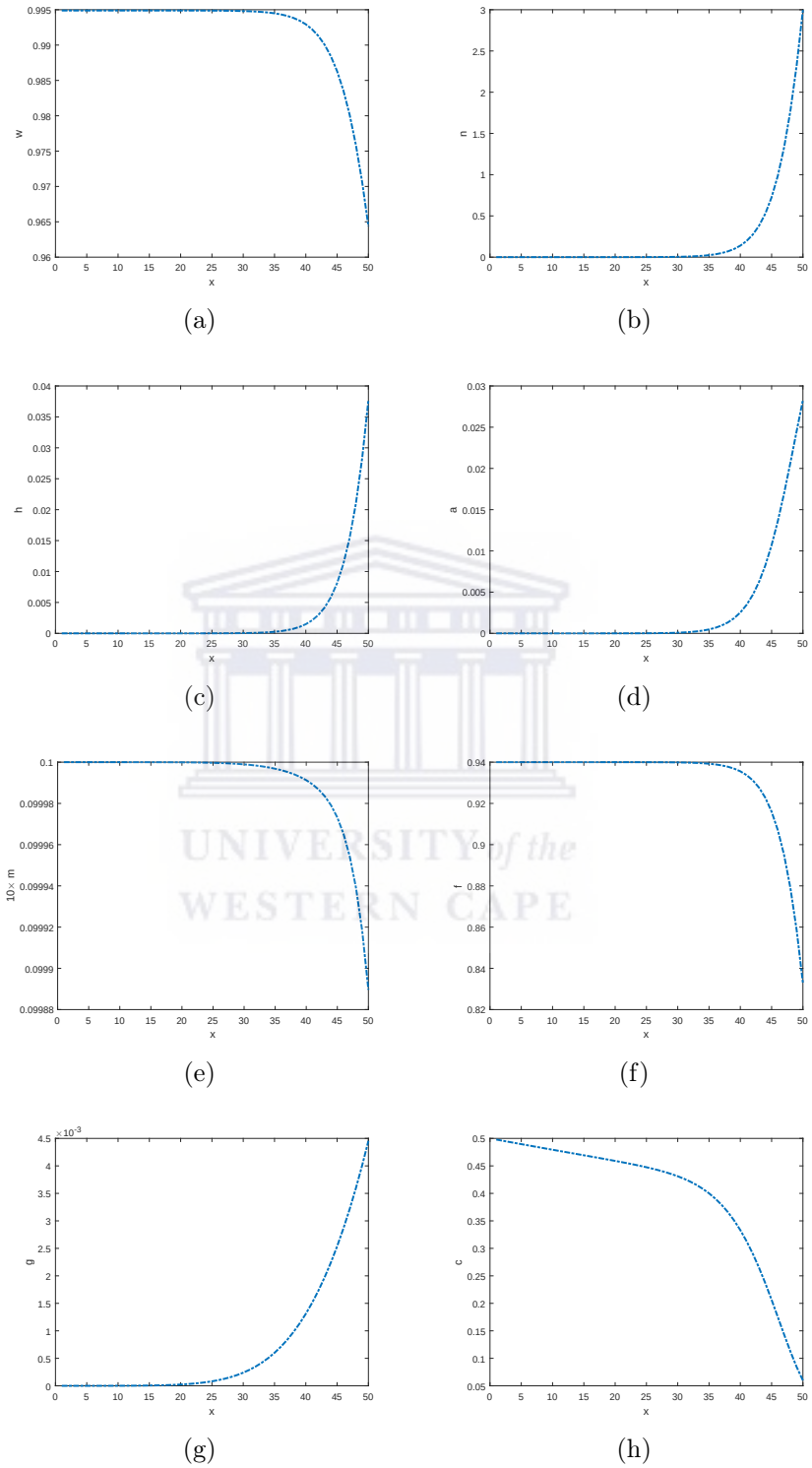

Figure 2.5.6: Numerical solution of anti-cytotoxic chemotherapy model at $t = 15$ and $v_{\max} = 10^{-1}$, showing the spatial distributions of: (a) oxygen, (b) normoxic, (c) hypoxic, (d) apoptic, (e) endothelial, (f) extracellular matrix, (g) agiogenic and (h) cytotoxic cells, for parameter values as in Table 2.5.1.

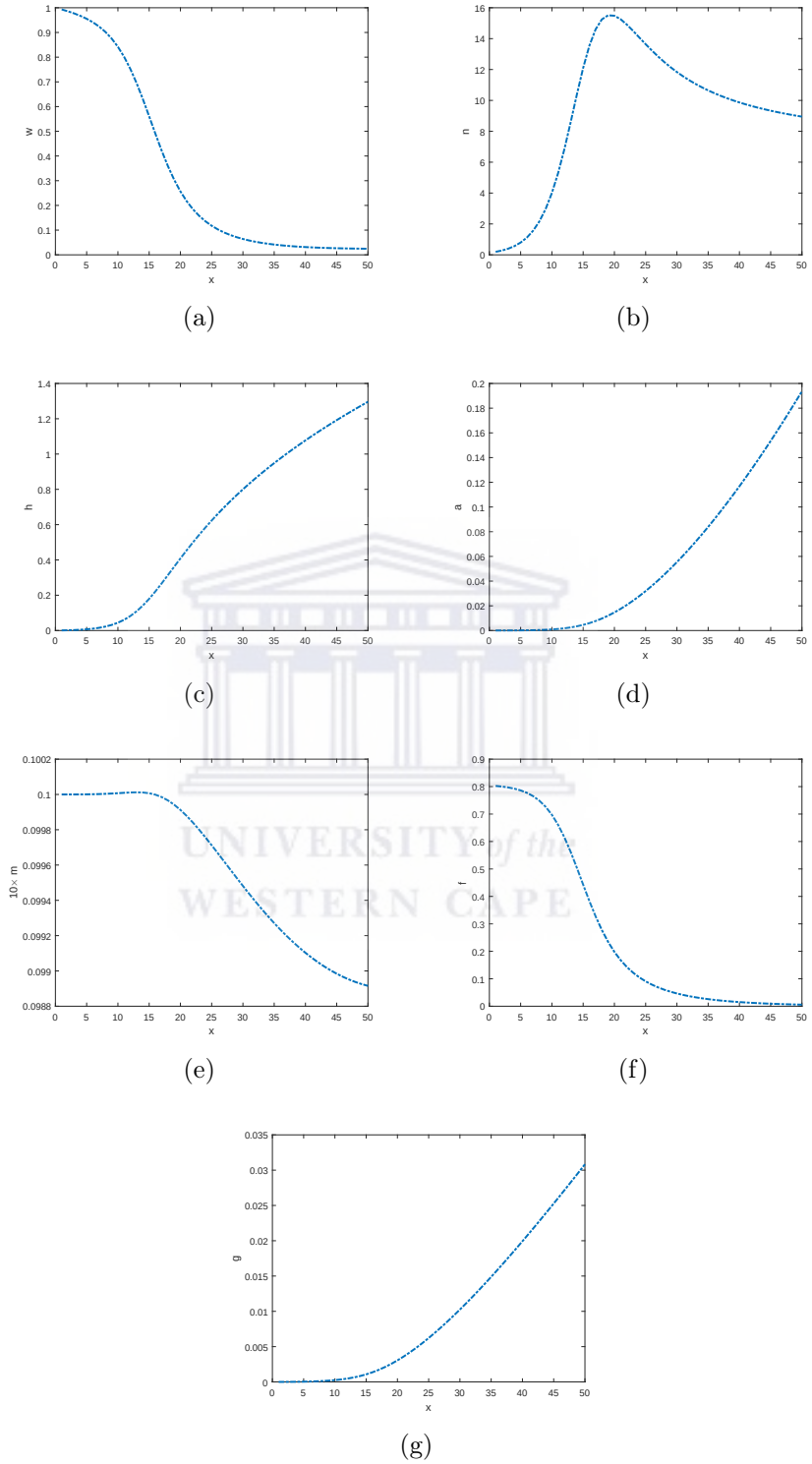

Figure 2.5.7: Numerical solution of the baseline model at $t = 5$ and $v_{\max} = 10$, showing the spatial distributions of: (a) oxygen, (b) normoxic, (c) hypoxic, (d) apoptic, (e) endothelial, (f) extracellular matrix and (g) angiogenic cells, for parameter values as in Table 2.5.1.

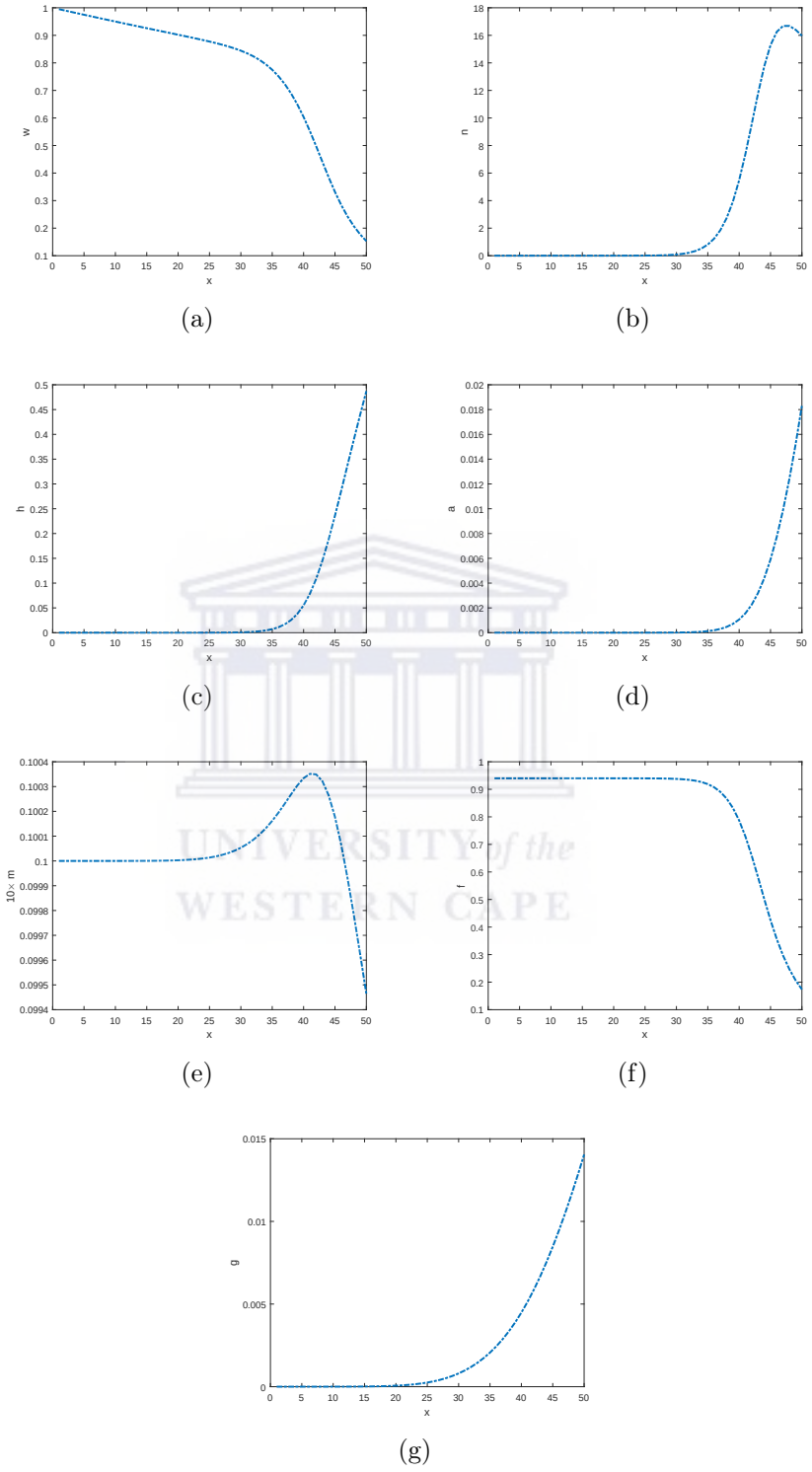

Figure 2.5.8: Numerical solution of the baseline model at $t = 15$ and $v_{\max} = 10$, showing the spatial distributions of: (a) oxygen, (b) normoxic, (c) hypoxic, (d) apoptic, (e) endothelial, (f) extracellular matrix and (g) angiogenic cells, for parameter values as in Table 2.5.1.

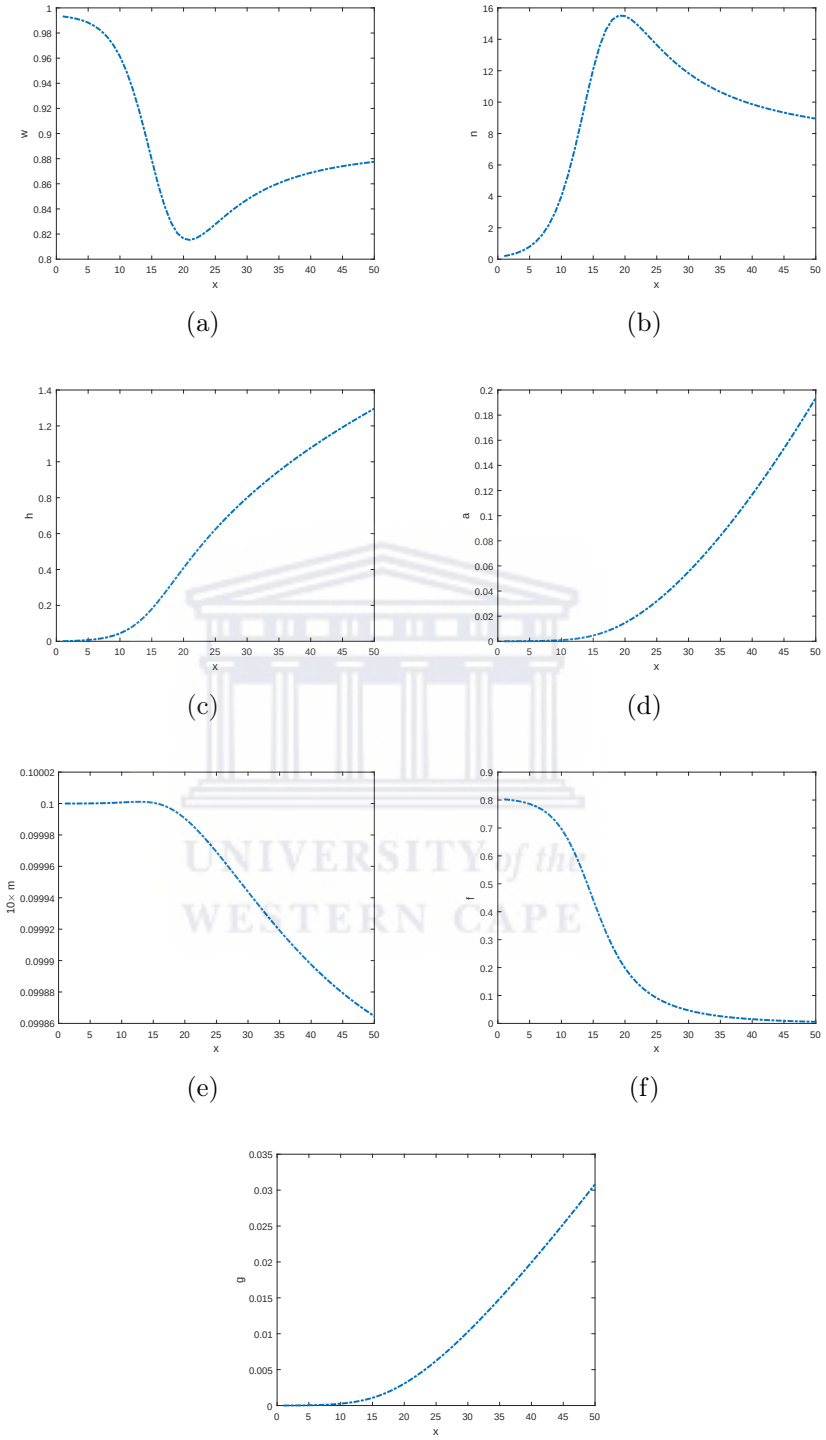

Figure 2.5.9: Numerical solution of anti-angiogenic chemotherapy model at $t = 5$ and $v_{\max} = 10$, showing the spatial distributions of: (a) oxygen, (b) normoxic, (c) hypoxic, (d) apoptic, (e) endothelial, (f) extracellular matrix and (g) angiogenic cells, for parameter values as in Table 2.5.1.

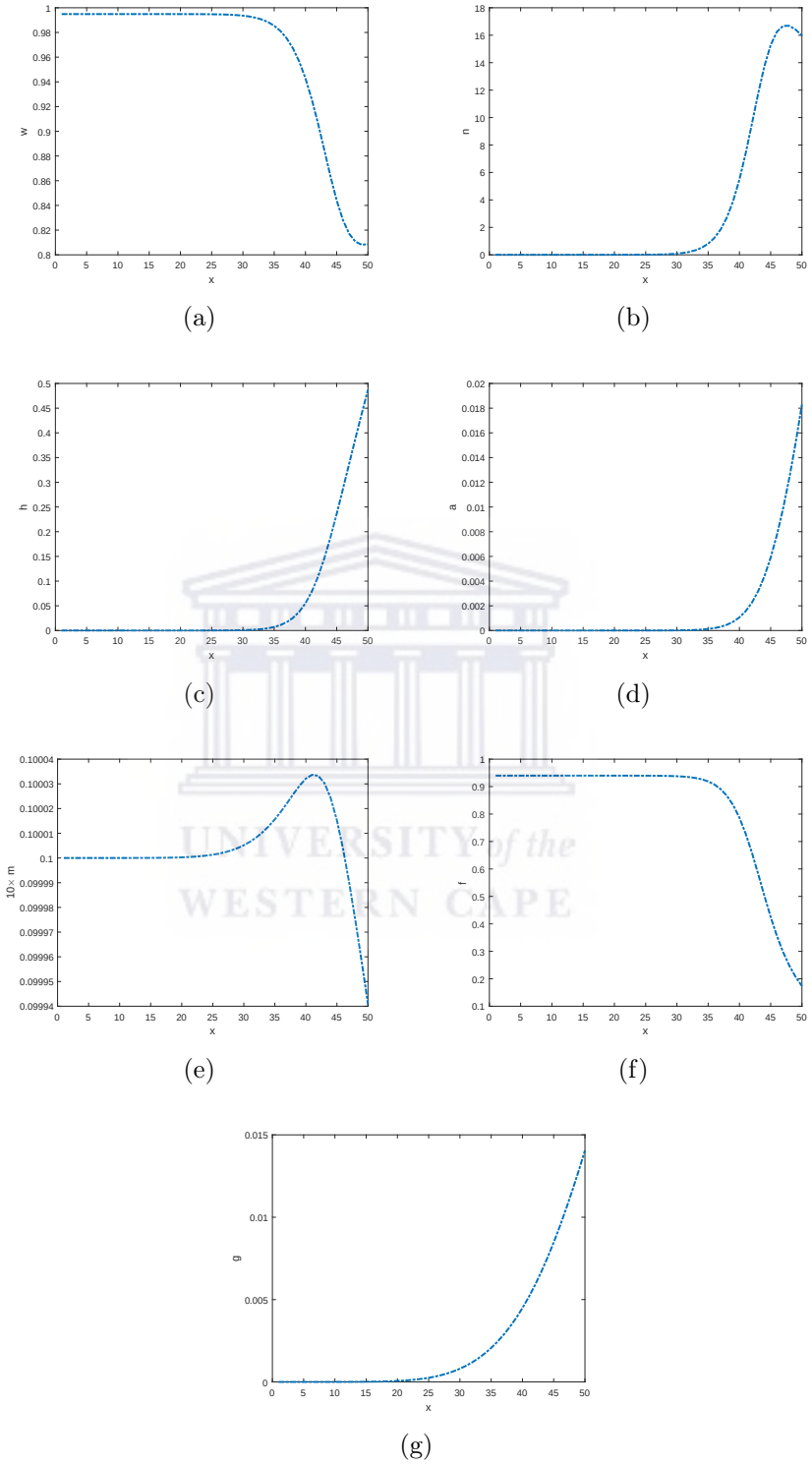

Figure 2.5.10: Numerical solution of anti-angiogenic chemotherapy model at $t = 15$ and $v_{\max} = 10$, showing the spatial distributions of: (a) oxygen, (b) normoxic, (c) hypoxic, (d) apoptic, (e) endothelial, (f) extracellular matrix and (g) angiogenic cells, for parameter values as in Table 2.5.1.

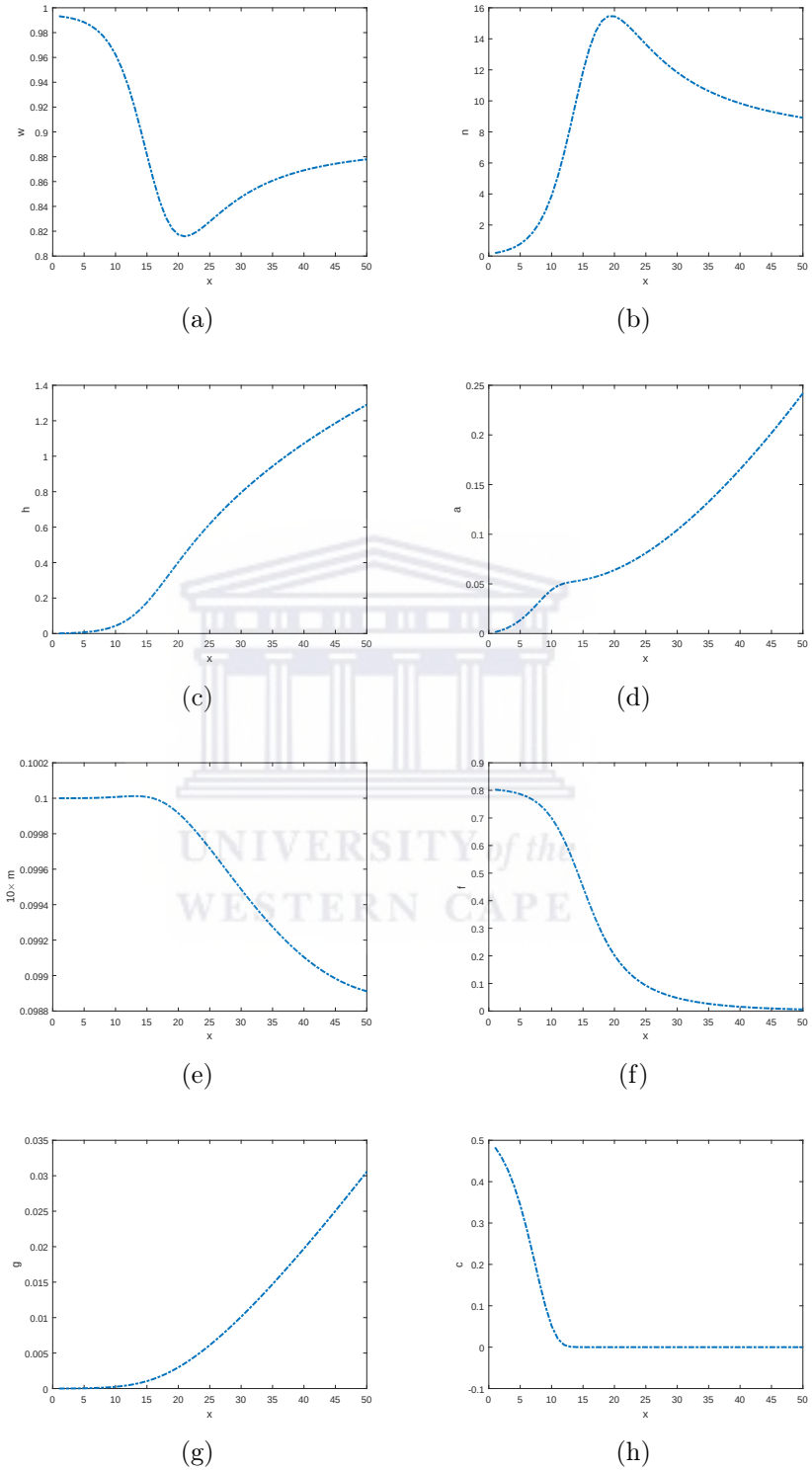

Figure 2.5.11: Numerical solution of anti-cytotoxic chemotherapy model at $t = 5$ and $v_{\max} = 10$, showing the spatial distributions of: (a) oxygen, (b) normoxic, (c) hypoxic, (d) apoptic, (e) endothelial, (f) extracellular matrix, (g) agiogenic and (h) cytotoxic cells, for parameter values as in Table 2.5.1.

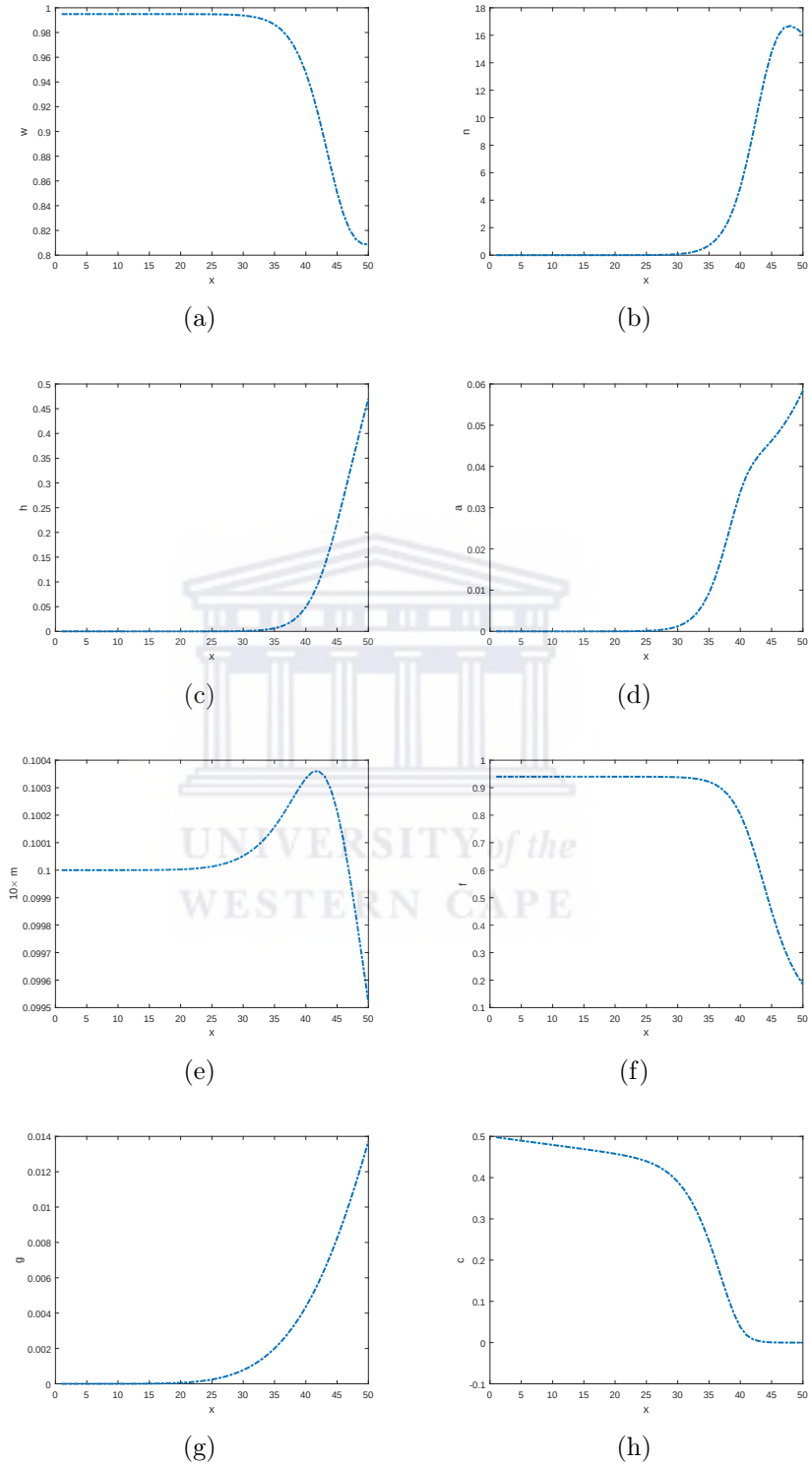

Figure 2.5.12: Numerical solution of anti-cytotoxic chemotherapy model at $t = 15$ and $v_{\max} = 10$, showing the spatial distributions of: (a) oxygen, (b) normoxic, (c) hypoxic, (d) apoptic, (e) endothelial, (f) extracellular matrix, (g) agiogenic and (h) cytotoxic cells, for parameter values as in Table 2.5.1.

In view of our consideration of the chemotherapy in this chapter, in the next chapter we focus on the biological stoichoimetry for tumour cells arising from biological stoichoimetry dynamics.

Chapter 3

Efficient numerical method for a mathematical model arising in biological stoichiometry of tumour dynamics

We extend a system of coupled first order non-linear systems of delay differential equations (DDEs) arising in modeling of stoichiometry of tumour dynamics, to a system of diffusion-reaction system of partial delay differential equations (PDDEs). Since tumor cells are further modified by blood supply through the vascularization process, we determine the local uniform equilibria of the homogeneous tumour growth model with respect to the vascularization process. We show that the equilibria are globally stable, determine the existence of Hopf bifurcation of the homogeneous tumour growth model with respect to the vascularization process. We derive, analyse and implement a fitted operator finite difference method (FOFDM) to solve the extended model. This FOFDM is analyzed for convergence and it is seen that it has second-order accuracy. Some numerical results confirming theoretical observations are also presented. These results are comparable with those obtained in the literature.

3.1 The model

In [37], it is established that the qualitative dynamics of the models are essentially unchanged whether phosphorus limits blood vessel construction or not. Thus, Elser et al. [37] claimed that varying the supply of phosphorus continuously seems to create no new dynamical behavior. Therefore, this motivated us to investigate the extended homogeneous tumor growth model directly.

Therefore, when a single solid tumour is growing within an organ Elser et al. [37] mentioned that the initial mass starts near some genetically determined carrying capacity (k_h) and its vascularization process takes place at approximately 0.01kg. Since the parenchyma cells may contain distinct cell types that differ in their nutrient use and growth rates, then Elser et al. [37] developed the heterogeneous tumor model with dietary regulation as

$$\left.\begin{aligned}
\frac{dx}{dt} &= x\left(a\min\left(1,\frac{P_e}{fnk_h}\right) - d_x - (a-d_x)\,\frac{x+y_1+y_2+z}{k_h}\right),\\
\frac{dy_1}{dt} &= y_1\left(b_1\min\left(1,\beta\frac{P_e}{fmk_h}\right)\min(1,L) - d_1 - (b_1-d_1)\,\frac{y_1+y_2+z}{k_t}\right),\\
\frac{dy_2}{dt} &= y\left(b_2\min\left(1,\beta\frac{P_e}{fmk_h}\right)\min(1,L) - d_2 - (b_2-d_2)\,\frac{y_1+y_2+z}{k_t}\right),\\
\frac{dz}{dt} &= c\min\left(1,\frac{P_e}{fnk_h}\right)(y_1(t-\tau)+y_2(t-\tau)) - d_z z,\\
\frac{dP}{dt} &= r - \gamma\left(n(d_x x + d_z z) + (a-d_x)nx\frac{x+y_1+y_2+z}{k_h}\right)\\
&\quad -\gamma\left(\sum_{i=1}^{2} m_i d_i y_i + \frac{y_1+y_2+z}{k_t}\sum_{i=1}^{2} m_i(b_i-d_i)\right),\\
L &= g^{\frac{z-\alpha(y_1+y_2)}{y_1+y_2}},\\
P_e &\equiv P(t) - nx - m_1y_1 - m_2y_2 - nz,
\end{aligned}\right\} \tag{3.1.1}$$

where, x, y_i ($i = 1, 2$ in this case), z, f, β, P_e, P, L, n and m_i denote mass of healthy cells, tumor mass contributed by the i^{th} parenchyma cell type, mass of tumor micro-vessels, fraction of the total fluid within an organ, therapeutic intervention, extracellular phosphorus within the organ, the homeostatic regulation of the total amount of phosphorus, maximum proliferation rate of tumor cells, the mean amount of phosphorus in healthy cells and mean amount of phosphorus in parenchyma cells in that order. The cells proliferation and death at maximum per capita rates are denoted by a, b_i and d_x, d_i, respectively, whereas α and g denote mass of cancer cells of which one unit of blood vessels can barely maintain and measurements of sensitivity of tumour tissue due to lack blood.

The model in equation (3.1.1) is a system of first order delay differential equations (DDEs), therefore initial values are required by the system. Elser et al. [37] provided the initial conditions as $(x(0), y_1(0), y_2(0), z(0)) = (9.00, 0.01, 0.01, 0.001)$, and did not give the initial condition for $P(0)$.

When a tumor has only one parenchyma cell type then the system of first order delay differential equations in equations (DDE) (3.1.1) is known as homogeneous tumor growth model and heterogeneous tumor growth model when a tumor has more than one parenchyma cell type.

As we see, all of the models in equation (3.1.1) did not take spatial effects into account. In fact, cells can move around subject to many factors including diffusion. Thus, instead of depicting the models with purely time dependent ordinary differential equations (ODEs) with delay, it is more realistic to introduce the diffusion of the cells into the system, and the simplest way to reach this goal is to use the concept of reaction-diffusion equations [87, 93]. Elser et al. [37] showed that at a equilibrium, tumor growth is no longer limited by its blood vessel infrastructure. For that reason, they also found out that when the tumor is viewed as a single entity, the homogeneous and heterogeneous models essentially generate the same dynamics. Thus, in this chapter we consider the homogeneous tumor growth model. Therefore, incorporating spatial

effects into equation (3.1.1), the homogeneous tumor growth model in (3.1.1) becomes

$$\left.\begin{aligned}
&\tfrac{\partial X}{\partial t} - \mathcal{D}_x \Delta X = X\left(a\min\left(1, \tfrac{P_e}{fnk_h}\right) - d_x - (a-d_x)\tfrac{X+Y_1+Z}{k_h}\right),\\
&\tfrac{\partial Y_1}{\partial t} - \mathcal{D}_{y_1} \Delta Y_1 = Y_1\left(b_1\min\left(1, \beta\tfrac{P_e}{fmk_h}\right)\min(1,L) - d_1 - (b_1-d_1)\tfrac{Y_1+Z}{k_t}\right),\\
&\tfrac{\partial Z}{\partial t} - \mathcal{D}_z \Delta Z = c\min\left(1, \tfrac{P_e}{fnk_h}\right) Y_1(t-\tau) - d_z Z,\ L = g\tfrac{Z-\alpha Y_1}{Y_1},\\
&P_e \equiv P - nX - m_1 Y_1 - nZ,\ \text{on } (x,t) \in \Omega \times (0,\infty),\\
&\tfrac{\partial X}{\partial \nu}(0,t) = \tfrac{\partial Y_1}{\partial \nu}(0,t) = \tfrac{\partial Z}{\partial \nu}(0,t) = 0,\ \text{on } (x,t) \in \Omega \times (0,\infty),\\
&\tfrac{\partial X}{\partial \nu}(x_f,t) = \tfrac{\partial Y_1}{\partial \nu}(x_f,t) = \tfrac{\partial Z}{\partial \nu}(x_f,t) = 0,\ \text{on } (x,t) \in \Omega \times (0,\infty),\\
&\mathcal{X}_j(x,0) = \eta_j(x),\ \text{on } (x,t) \in \bar{\Omega} \times [-\tau,0],\ j = 1,2,3,
\end{aligned}\right\} \quad (3.1.2)$$

where, Δ denotes the Laplace operator, $\mathcal{X}_j(x,t) = [X, Y_1, Z]$, $\Omega \in \mathbb{R}^3$ denotes a bounded domain with smooth boundary $\partial\Omega$ and ν denotes the outward unit normal on $\partial\Omega$. The initial function $\eta_j(x,t)$ is Holder continuous on $[-\tau, 0]$ [106]. We imposed the no flux-boundary conditions in order to ensure that we exclude the external effects.

Our first aim in this chapter is to investigate the qualitative features of the model with regard to blood vessel construction and determine the possibility of the time delay τ on the dynamics of the homogeneous tumour growth model. By applying the Poincaré normal form and center manifold theorem [79, 128], we determine conditions on the functions and derive formulas which determine the properties of Hopf bifurcation [118] such as the direction of bifurcation, the period of periodic solutions and the stability of solutions. More specifically, we show that the positive equilibrium point losses its stability and the system exhibits Hopf bifurcation under certain conditions. Our second aim is to solve the extended model in equation (3.1.2). Thus, to do so, we

develop an efficient numerical method for solving the extended model with respect to the qualitative features of the extended model. To this end, we highlight our motivation for our numerical method. The deficiencies of the standard finite difference methods in solving the problems like the one in equation (3.1.2) are well-known. While explicit methods can solve such differential equations with low computational cost, they have the drawback that their stability regions are very small. This implies severe restrictions on the time and space step-sizes will be required in order to achieve satisfactorily converging results. On the other hand, an implicit schemes do have wider stability regions but the associated computational complexity is very high and they cannot achieve more than one order as compared to explicit methods that use the same number of stages [22].

The rest of the chapter is as follows. In Section 3.2, we analyse the equilibrium and existence of Hopf bifurcation for two possible blood limiting cases. We derive, analyse our numerical method in Section 3.3 and present our numerical results in Section 3.4 and conclude the chapter with Section 3.5.

3.2 Mathematical analysis of the homogeneous tumour growth model

To proceed, we recall from Elser et al. [37], that in a phosphorus-rich environment, healthy cells and tumor cells can proliferate, however, if the extracellular phosphorus concentration drops below a threshold value, then the growth rates of both healthy and tumor cells are impaired. Therefore, in such case we let

$$\varphi_{P_x} := \min\left(1, \frac{P_e}{fnk_h}\right), \varphi_{P_{y_1}} := \min\left(1, \beta\frac{P_e}{fm_1k_h}\right),$$
$$\varphi_{P_z} := \min\left(1, \frac{P_e}{fnk_h}\right), \tag{3.2.1}$$

to denote such possibilities of limitations. Since maximum proliferation rate of tumor cells is dictated by the value of $\min\left(1, g\frac{Z-\alpha Y_1}{Y_1}\right)$ [37], then, at the equilibrium, the homogeneous tumour growth model in equation (3.1.2) becomes

$$\left.\begin{aligned} &X\left(a\varphi_{P_x} - d_x - (a-d_x)\,\tfrac{X+Y_1+Z}{k_h}\right) = 0,\\ &Y_1\left(b_1\varphi_{P_{y_1}}\min\left(1, g\tfrac{Z-\alpha Y_1}{Y_1}\right) - d_1 - (b_1-d_1)\,\tfrac{Y_1+Z}{k_t}\right) = 0,\\ &c\varphi_{P_z}Y_1 - d_z Z = 0, \end{aligned}\right\} \tag{3.2.2}$$

which gives the trivial equilibrium point $(0,0,0)$, and the system

$$\left.\begin{aligned} &\tfrac{(a-d_x)}{k_h}(X+Y_1+Z) = a\varphi_{P_x} - d_x,\\ &\tfrac{(b_1-d_1)}{k_t}(Y_1+Z) = b_1\varphi_{P_{y1}} - d_1,\\ &c\varphi_{P_z}Y_1 - d_z Z = 0, \end{aligned}\right\} \tag{3.2.3}$$

if $\min\left(1, g\frac{Z-\alpha Y_1}{Y_1}\right) = 1$ and

$$\left.\begin{aligned} &\tfrac{(a-d_x)}{k_h}(X+Y_1+Z) = a\varphi_{P_x} - d_x,\\ &\tfrac{(b_1-d_1)}{k_t}(Y_1+Z) - b_1\varphi_{P_{y_1}} g\tfrac{Z-\alpha Y_1}{Y_1} = -d_1,\\ &c\varphi_{P_z}Y_1 - d_z Z = 0, \end{aligned}\right\} \tag{3.2.4}$$

if $\min\left(1, g\frac{Z-\alpha Y_1}{Y_1}\right) \neq 1$. Thus, we consider both cases in the next two sections.

3.2.1 Local stability for $\min\left(1, g\frac{Z-\alpha Y_1}{Y_1}\right) = 1$

When $\min\left(1, g\frac{z-\alpha Y_1}{Y_1}\right) = 1$ equation (3.2.3) is equivalent to

$$\begin{pmatrix} \frac{(a-d_x)}{k_h} & \frac{(a-d_x)}{k_h} & \frac{(a-d_x)}{k_h} \\ 0 & \frac{(b_1-d_1)}{k_t} & \frac{(b_1-d_1)}{k_t} \\ 0 & c\varphi_{P_z} & -d_z \end{pmatrix} \begin{pmatrix} X \\ Y_1 \\ Z \end{pmatrix} = \begin{pmatrix} a\varphi_{P_x} - d_x \\ b_1\varphi_{P_{y_1}} - d_1 \\ 0 \end{pmatrix}, \tag{3.2.5}$$

and the determinant of the matrix in equation (3.2.5) is

$$\frac{(a-d_x)}{k_h} \begin{vmatrix} \frac{(b_1-d_1)}{k_t} & \frac{(b_1-d_1)}{k_t} \\ c\varphi_{P_z} & -d_z \end{vmatrix} = -\frac{(a-d_x)}{k_h}\frac{(b_1-d_1)}{k_t}\left(d_z + c\varphi_{P_z}\right), \tag{3.2.6}$$

provided that $a > d_x$, $a\varphi_{P_x} > d_x$ and $b_1 \neq d_1$. Thus,

$$X^* = \frac{\begin{vmatrix} a\varphi_{P_x} - d_x & \frac{(a-d_x)}{k_h} & \frac{(a-d_x)}{k_h} \\ b_1\varphi_{P_{y_1}} - d_1 & \frac{(b_1-d_1)}{k_t} & \frac{(b_1-d_1)}{k_t} \\ 0 & c\varphi_{P_z} & -d_z \end{vmatrix}}{-\frac{(a-d_x)}{k_h}\frac{(b_1-d_1)}{k_t}\left(d_z + c\varphi_{P_z}\right)}, \tag{3.2.7}$$

where the determinant of the numerator in equation (3.2.7) is

$$\begin{aligned}
\begin{vmatrix} a\varphi_{P_x}-d_x & \frac{(a-d_x)}{k_h} & \frac{(a-d_x)}{k_h} \\ b_1\varphi_{P_{y_1}}-d_1 & \frac{(b_1-d_1)}{k_t} & \frac{(b_1-d_1)}{k_t} \\ 0 & c\varphi_{P_z} & -d_z \end{vmatrix} &= (a\varphi_{P_x}-d_x)\begin{vmatrix} \frac{(b_1-d_1)}{k_t} & \frac{(b_1-d_1)}{k_t} \\ c\varphi_{P_z} & -d_z \end{vmatrix} \\
&\quad -\frac{(a-d_x)}{k_h}\begin{vmatrix} b_1\varphi_{P_{y_1}}-d_1 & \frac{(b_1-d_1)}{k_t} \\ 0 & -d_z \end{vmatrix} \\
&\quad +\frac{(a-d_x)}{k_h}\begin{vmatrix} b_1\varphi_{P_{y_1}}-d_1 & \frac{(b_1-d_1)}{k_t} \\ 0 & c\varphi_{P_z} \end{vmatrix}, \\
&= -\frac{(b_1-d_1)}{k_t}(a\varphi_{P_x}-d_x)[d_z+c\varphi_{P_z}] \\
&\quad +\frac{(a-d_x)}{k_h}(b_1\varphi_{P_{y_1}}-d_1)\left[d_z+c\varphi_{P_z}\right], \\
&= (d_z+c\varphi_{P_z})\left(\frac{(a-d_x)(b_1\varphi_{P_{y_1}}-d_1)}{k_h}\right) \\
&\quad -(d_z+c\varphi_{P_z})\left(\frac{(b_1-d_1)(a\varphi_{P_x}-d_x)}{k_t}\right).
\end{aligned}$$

Therefore, equation (3.2.7) becomes

$$\begin{aligned}
X^* &= \frac{(d_z+c\varphi_{P_z})\left(\frac{(a-d_x)(b_1\varphi_{P_{y_1}}-d_1)}{k_h}-\frac{(b_1-d_1)(a\varphi_{P_x}-d_x)}{k_t}\right)}{-\frac{(a-d_x)}{k_h}\frac{(b_1-d_1)}{k_t}(d_z+c\varphi_{P_z})}, \\
&= \frac{\left(\frac{(a-d_x)(b_1\varphi_{P_{y_1}}-d_1)}{k_h}-\frac{(b_1-d_1)(a\varphi_{P_x}-d_x)}{k_t}\right)}{-\frac{(a-d_x)}{k_h}\frac{(b_1-d_1)}{k_t}}, \\
&= \frac{k_h(a\varphi_{P_x}-d_x)}{(a-d_x)}-\frac{k_t(b_1\varphi_{P_{y_1}}-d_1)}{(b_1-d_1)},
\end{aligned}$$

provided that $\frac{k_h(a\varphi_{P_x}-d_x)}{(a-d_x)} > \frac{k_t(b_1\varphi_{P_{y_1}}-d_1)}{(b_1-d_1)}$. For Y_1^*, we then have from equations in (3.2.5)-(3.2.6) that

$$\begin{aligned} Y_1^* &= \frac{\begin{vmatrix} \frac{(a-d_x)}{k_h} & a\varphi_{P_x}-d_x & \frac{(a-d_x)}{k_h} \\ 0 & b_1\varphi_{P_{y_1}}-d_1 & \frac{(b_1-d_1)}{k_t} \\ 0 & 0 & -d_z \end{vmatrix}}{-\frac{(a-d_x)}{k_h}\frac{(b_1-d_1)}{k_t}(d_z+c\varphi_{P_z})} = \frac{-d_z\frac{(a-d_x)(b_1\varphi_{P_{y_1}}-d_1)}{k_h}}{-\frac{(a-d_x)}{k_h}\frac{(b_1-d_1)}{k_t}(d_z+c\varphi_{P_z})}, \\ &= \frac{k_t d_z(b_1\varphi_{P_{y_1}}-d_1)}{(b_1-d_1)(d_z+c\varphi_{P_z})}, \end{aligned}$$

provided that $b_1 > d_1$ and $b_1\varphi_{P_{y_1}} > d_1$. Similarly for Z^*, from equations in (3.2.5)-(3.2.6) we have

$$Z^* = \frac{\begin{vmatrix} \frac{(a-d_x)}{k_h} & \frac{(a-d_x)}{k_h} & a\varphi_{P_x}-d_x \\ 0 & \frac{(b_1-d_1)}{k_t} & b_1\varphi_{P_{y_1}}-d_1 \\ 0 & c\varphi_{P_z} & 0 \end{vmatrix}}{-\frac{(a-d_x)}{k_h}\frac{(b_1-d_1)}{k_t}(d_z+c\varphi_{P_z})} = \frac{ck_t\varphi_{P_z}(b_1\varphi_{P_{y_1}}-d_1)}{(b_1-d_1)(d_z+c\varphi_{P_z})}, \tag{3.2.8}$$

which requires $b_1 > d_1$ and $b_1\varphi_{P_{y_1}} > d_1$, as anticipated. Therefore, we have two positive equilibrium points and they are

$$\mathcal{E}_1 := \begin{pmatrix} k_h\frac{a\varphi_{P_x}-d_x}{(a-d_x)} \\ 0 \\ 0 \end{pmatrix} \text{ and } \mathcal{E}_2 := \begin{pmatrix} \frac{k_h(a\varphi_{P_x}-d_x)}{(a-d_x)} - \frac{k_t(b_1\varphi_{P_{y_1}}-d_1)}{(b_1-d_1)} \\ \frac{k_t d_z(b_1\varphi_{P_{y_1}}-d_1)}{(b_1-d_1)(d_z+c\varphi_{P_z})} \\ \frac{ck_t\varphi_{P_z}(b_1\varphi_{P_{y_1}}-d_1)}{(b_1-d_1)(d_z+c\varphi_{P_z})} \end{pmatrix}. \tag{3.2.9}$$

This gives us the following results.

Theorem 3.2.1. *When* $\min\left(1, g\frac{Z-\alpha Y_1}{Y_1}\right) = 1$ *and the following conditions hold*

(i) $a > d_x$,

(ii) $a\varphi_{P_x} > d_x$,

(iii) $\frac{k_h(a\varphi_{P_x}-d_x)}{(a-d_x)} > \frac{k_t(b_1\varphi_{P_{y_1}}-d_1)}{(b_1-d_1)}$,

(iv) $b_1\varphi_{P_{y_1}} > d_1$,

the homogeneous tumor growth model in equation (3.1.2) possess the unique semi-trivial non-negative constant solution $(X^*, Y_1^*, Z^*) = (k_h\frac{a\varphi_{P_x}-d_x}{(a-d_x)}, 0, 0)$ *and a unique positive constant solution*

$$(X^*, Y_1^*, Z^*) = \begin{pmatrix} \frac{k_h(a\varphi_{P_x}-d_x)}{(a-d_x)} - \frac{k_t(b_1\varphi_{P_{y_1}}-d_1)}{(b_1-d_1)} \\ \frac{k_t d_z(b_1\varphi_{P_{y_1}}-d_1)}{(b_1-d_1)(d_z+c\varphi_{P_z})} \\ \frac{ck_t\varphi_{P_z}(b_1\varphi_{P_{y_1}}-d_1)}{(b_1-d_1)(d_z+c\varphi_{P_z})} \end{pmatrix}. \tag{3.2.10}$$

Therefore, when the maximum proliferation rate of tumor cells greater than unity, then the equilibria are positive as long as the genetically determined, carrying capacity for healthy cells is bigger than that of the tumor cells.

3.2.2 Local stability for $\min\left(1, g\frac{Z-\alpha Y_1}{Y_1}\right) \neq 1$

From equation (3.2.4) we have a system of non-linear equations

$$\left.\begin{aligned} &\tfrac{(a-d_x)}{k_h}(X+Y_1+Z) = a\varphi_{P_x} - d_x, \\ &b_1\varphi_{P_{y_1}} gZ - (g\alpha - d_1)Y_1 - (b_1-d_1)\tfrac{Y_1^2+Y_1Z}{k_t} = 0, \\ &c\varphi_{P_z}Y_1 - d_zZ = 0. \end{aligned}\right\} \tag{3.2.11}$$

From the last equation in (3.2.11), we have $Z = \frac{c\varphi_{P_z}}{d_z}Y_1$. Substituting $Z = \frac{c\varphi_{P_z}}{d_z}Y_1$ into the first and second equation in (3.2.11), we obtain

$$\left.\begin{aligned} &\tfrac{(a-d_x)}{k_h}X + (\tfrac{(a-d_x)}{k_h} + \tfrac{c\varphi_{P_z}}{d_z})Y_1 = a\varphi_{P_x} - d_x, \\ &\left(b_1\varphi_{P_{y_1}} g\tfrac{c\varphi_{P_z}}{d_z} - (g\alpha - d_1)\right)Y_1 - (b_1-d_1)\tfrac{(1+c\varphi_{P_z})}{d_zk_t}Y_1^2 = 0, \end{aligned}\right\} \tag{3.2.12}$$

from which we obtain $Y_1^* = 0$ and $Y_1^* = \frac{\left(b_1\varphi_{P_{y_1}} g\frac{c\varphi_{P_z}}{d_z} - (g\alpha - d_1)\right)}{(b_1-d_1)\frac{(1+c\varphi_{P_z})}{d_z k_t}}$. When $Y_1^* = 0$, we obtain a trivial equilibrium solution $(X^*, Y_1^*, Z^*) = (0, 0, 0)$. However, for non-zero Y_1^*, we find

$$\left.\begin{aligned} X^* &= \frac{k_h(a\varphi_{P_x} - d_x)}{(a-d_x)} - (1 + \frac{c\varphi_{P_z}}{d_z})\frac{\left(b_1\varphi_{P_{y_1}} g\frac{c\varphi_{P_z}}{d_z} - (g\alpha - d_1)\right)}{(b_1-d_1)\frac{(1+c\varphi_{P_z})}{d_z k_t}}, \\ Z^* &= \frac{c\varphi_{P_z}}{d_z} Y_1^*. \end{aligned}\right\} \tag{3.2.13}$$

Thus, we see that if $b_1\varphi_{P_{y_1}} g\frac{c\varphi_{P_z}}{d_z} > (g\alpha - d_1)$ then Y_1^* is positive as $b_1 > d_1$. This implies that $Z^* = \frac{c\varphi_{P_z}}{d_z} Y_1^*$ is positive too. We also see that $X^* > 0$ whenever $\frac{k_h(a\varphi_{P_x} - d_x)}{(a-d_x)} > (1 + \frac{c\varphi_{P_z}}{d_z})\frac{\left(b_1\varphi_{P_{y_1}} g\frac{c\varphi_{P_z}}{d_z} - (g\alpha - d_1)\right)}{(b_1-d_1)\frac{(1+c\varphi_{P_z})}{d_z k_t}}$. Hence the following results.

Theorem 3.2.2. *When* $\min\left(1, g\frac{Z-\alpha Y_1}{Y_1}\right) \neq 1$ *and the following conditions hold*

(i) $a > d_x$,

(ii) $b_1 > d_1$,

(ii) $b_1\varphi_{P_{y_1}} g\frac{c\varphi_{P_z}}{d_z} > (g\alpha - d_1)$,

(iv) $\frac{k_h(a\varphi_{P_x} - d_x)}{(a-d_x)} > (1 + \frac{c\varphi_{P_z}}{d_z})\frac{\left(b_1\varphi_{P_{y_1}} g\frac{c\varphi_{P_z}}{d_z} - (g\alpha - d_1)\right)}{(b_1-d_1)\frac{(1+c\varphi_{P_z})}{d_z k_t}}$,

then the homogeneous tumor growth model has a unique positive constant solution

$$(X^*, Y_1^*, Z^*) = \begin{pmatrix} \frac{k_h(a\varphi_{P_x} - d_x)}{(a-d_x)} - (1 + \frac{c\varphi_{P_z}}{d_z})\frac{\left(b_1\varphi_{P_{y_1}} g\frac{c\varphi_{P_z}}{d_z} - (\alpha - d_1)\right)}{(b_1-d_1)\frac{(1+c\varphi_{P_z})}{d_z k_t}} \\ \frac{\left(b_1\varphi_{P_{y_1}} g\frac{c\varphi_{P_z}}{d_z} - (\alpha - d_1)\right)}{(b_1-d_1)\frac{(1+c\varphi_{P_z})}{d_z k_t}} \\ \frac{c\varphi_{P_z}}{d_z} Y_1^* \end{pmatrix}. \tag{3.2.14}$$

Similarly, when the maximum proliferation rate of tumor cells drops below unity, then the equilibria are positive as long as the genetically determined, carrying capacity for healthy cells is bigger than that of the tumor cells.

3.2.3 Global stability of the uniform equilibria

In this section, we show that the uniform positive equilibria are globally uniform. Since the homogeneous tumor growth model is of quasi-Lotka-Vorterra type [36], we let $V : \mathbb{R}^3_{\geq 0} \to \mathbb{R}$ defined by

$$\begin{aligned} V(X, Y_1, Z) &= \left(X - X^* - X^* \log\left(\frac{X}{X^*}\right)\right) + \left(Y_1 - Y_1^* - Y_1^* \log\left(\frac{Y_1}{Y_1^*}\right)\right) \\ &\quad + \left(Z - Z^* - Z^* \log\left(\frac{Z}{Z^*}\right)\right), \end{aligned}$$

then we see that $V(X^*, Y_1^*, Z^*) = 0$ and $V(X, Y_1, Z) > 0$ for all $(X, Y_1, Z) \neq (X^*, Y_1^*, Z^*)$. Moreover, on $\mathbb{R}^3_{\geq 0}$, we have

$$\begin{aligned} \frac{dV(X, Y_1, Z)}{dt} &= V_x \dot{X} + V_{y_1} \dot{Y}_1 + V_z \dot{Z}, \\ &= \left(1 - \frac{X^*}{X}\right) X \left(a\varphi_{P_x} - d_x - (a - d_x)\frac{X + Y_1 + Z}{k_h}\right) \\ &\quad + \left(1 - \frac{Y_1^*}{Y_1}\right) Y_1 \left(b_1 \varphi_{P_{y_1}} \min\left(1, g\frac{Z - \alpha Y_1}{Y_1}\right) - d_1 - (b_1 - d_1)\frac{Y_1 + Z}{k_t}\right) \\ &\quad + \left(1 - \frac{Z^*}{Z}\right) c \min \varphi_{P_z} Y_1 - d_z Z, \\ &= (X - X^*)\left(a\varphi_{P_x} - d_x - (a - d_x)\frac{X + Y_1 + Z}{k_h}\right) \\ &\quad + (Y_1 - Y_1^*)\left(b_1 \varphi_{P_{y_1}} \min\left(1, g\frac{Z - \alpha Y_1}{Y_1}\right) - d_1 - (b_1 - d_1)\frac{Y_1 + Z}{k_t}\right) \\ &\quad + (Z - Z^*)\left(c\varphi_{P_z} Y_1 - d_z (Z - Z^*)\right), \end{aligned} \tag{3.2.15}$$

upon multiplying the last equation with Z. When $\min\left(1, g\frac{Z - \alpha Y_1}{Y_1}\right) \equiv 1$, then equation in (3.2.15) becomes

$$\begin{aligned} \frac{dV(X, Y_1, Z)}{dt} &= (X - X^*)\left(-(a - d_x)\frac{(X - X^*) + (Y_1 - Y_1^*) + (Z - Z^*)}{k_h}\right) \\ &\quad + (Y_1 - Y_1^*)\left(-(b_1 - d_1)\frac{(Y_1 - Y_1^*) + (Z - Z^*)}{k_t}\right) \\ &\quad + (Z - Z^*)\left(c\varphi_{P_z}(Y_1 - Y_1^*) - d_z (Z - Z^*)\right). \end{aligned} \tag{3.2.16}$$

Let $\bar{X} = X - X^*, \bar{Y}_1 = Y_1 - Y_1^*, \bar{Z} = Z - Z^*$, then the equation in (3.2.16) becomes

$$\begin{aligned}\frac{dV(X,Y_1,Z)}{dt} &= -(a-d_x)\,X\left(\frac{X+Y_1+Z}{k_h}\right)\\ &\quad -(b_1-d_1)\,Y_1\left(\frac{Y_1+Z}{k_t}\right)+Z\left(c\varphi_{P_z}Y-d_zZ\right)\leq 0, \quad (3.2.17)\end{aligned}$$

after dropping the bar signs. Similarly, $\min\left(1, g\frac{Z-\alpha Y_1}{Y_1}\right) \neq 1$, then equation in (3.2.15) becomes

$$\begin{aligned}\frac{dV(X,Y_1,Z)}{dt} &= -(a-d_x)\,(X-X^*)\left(\frac{X+Y_1+Z}{k_h}\right)\\ &\quad -\frac{(b_1-d_1)}{k_t}\,(Y_1-Y_1^*)\left((Y_1-Y_1^*)+(b_1\varphi_{P_{y_1}}g-1)(Z-Z^*)\right)\\ &\quad +(Z-Z^*)\left(c\varphi_{P_z}Y_1-d_z\,(Z-Z^*)\right)\leq 0. \quad (3.2.18)\end{aligned}$$

Thus, we have the following results.

Theorem 3.2.3. *The positive equilibria in equation (3.2.10) and (3.2.14) are globally stable.*

Thus, in this section we determine the positive solutions of both cases and found out that similar conditions hold for the survival of tumor cells which play an integral part in this stoichometric dynamics.

In the next sections we consider the existence of Hopf bifurcation.

3.2.4 Stability of the equilibrium points and existence of Hopf bifurcation for $\min\left(1, g\frac{Z-\alpha Y_1}{Y_1}\right) = 1$ and $\min\left(1, g\frac{Z-\alpha Y_1}{Y_1}\right) \neq 1$

In this section, we concentrate on the dynamical behavior of equation (3.1.2). Our goal is to investigate the stability of the equilibrium points of (3.1.2) and also the existence of Hopf bifurcation. This is achieved by taking the delay time τ as a bifurcation parameter. Thus, we study effects of the time delay on the dynamics of (3.1.2) as follows.

Stability of positive equilibrium points and the existence of Hopf bifurcation for $\min\left(1, g\frac{Z-\alpha Y_1}{Y_1}\right) = 1$

Let (X^*, Y_1^*, Z^*) be an equilibrium point for the system in equation (3.1.2) and

$$(\bar{X}, \bar{Y}_1, \bar{Z}) = (X - X^*, Y_1 - Y_1^*, Z - Z^*).$$

Linearizing the system in equation (3.1.2) around (X^*, Y_1^*, Z^*), and drop bars again, we obtain

$$\left.\begin{aligned}
X_t - \mathcal{D}_x \Delta X &= \left(a\varphi_{P_x} - d_x - (a - d_x)\,\tfrac{2X^* + Y_1^* + Z^*}{k_h}\right) X - (a - d_x)\,\tfrac{X^*}{k_h} Y_1 \\
&\quad - (a - d_x)\,\tfrac{X^*}{k_h} Z, \\
(Y_1)_t - \mathcal{D}_{y_1} \Delta Y_1 &= \left(\varphi_{P_{y_1}} - d_1 - (b_1 - d_1)\,\tfrac{2Y_1^* + Z^*}{k_t}\right) Y_1 - \tfrac{Y_1^*(b_1 - d_1)}{k_t} Z, \\
Z_t - \mathcal{D}_z \Delta Z &= c\varphi_{P_z} Y_1(t - \tau) - d_z Z, \\
\tfrac{\partial X}{\partial \nu} &= \tfrac{\partial Y_1}{\partial \nu} = \tfrac{\partial Y_2}{\partial \nu} = \tfrac{\partial Z}{\partial \nu} = 0, \text{ on } (x,t) \in \partial\Omega \times (0, \infty), \\
\mathcal{X}_j(x,t) &= \eta_j(x,t) \geq 0 (x,t) \in \Omega \times (0, \infty), \\
\mathcal{X}_j(x,t) &= \eta_j(x,t) - \mathcal{X}_j^*, \ (x,t) \in \bar{\Omega} \times [-\tau, 0], \ j = 1, 2, 3.
\end{aligned}\right\} \quad (3.2.19)$$

Let $0 = \mu_0 < \mu_1 < \cdots$ be the eigenvalues of the operator Δ on Ω with the homogeneous Neumann boundary condition, then the characteristic equation for equation in (3.2.19) is given by

$$\left.\begin{aligned}
\lambda + \mathcal{D}_x \mu_k + a\varphi_{P_x} - d_x - \tfrac{(a - d_x)}{k_h}\,(2\,X^* + Y^* + Z^*) = 0, \\
\lambda^2 k_t + \mathcal{K}_1 \lambda + Y_1^* c\,(b_1 - d_1)\,\varsigma_{P_z} \exp(-\lambda\tau) + \mathcal{K}_2 = 0,
\end{aligned}\right\} \quad (3.2.20)$$

where,

$$\mathcal{K}_1 = k_t(\mathcal{D}_z + \mathcal{D}_{y_1})\mu_k + (\varphi_{P_{y_1}} - (d_1 + d_z))k_t - (2Y_1^* + Z^*)(\,d_1 - \,b_1),$$
$$\mathcal{K}_2 = \mathcal{D}_{y_1}\mathcal{D}_z k_t {\mu_k}^2 + k_t(\varphi_{P_{y_1}}\mathcal{D}_z - \mathcal{D}_{y_1}d_z)\mu_k + \mathcal{D}_z((\,d_1 - \,b_1)(2Y_1^* + Z^*) - d_1 k_t))\mu_k$$
$$+ d_z(2Y_1^* + Z^*)(b_1 - d_1) + k_t(d_1 - \varphi_{P_{y_1}})d_z.$$

Negative real parts for the first equation in (3.2.20) requires that

$$k_h d_x > -(a - d_x), \tag{3.2.21}$$

whereas in the second equation in (3.2.20), when $\tau = 0$, Routh-Hurwitz criteria requires that

$$(\varphi_{P_{y_1}} - (d_1 + d_z))k_t > (2Y_1^* + Z^*)(d_1 - b_1),\ \varphi_{P_{y_1}}\mathcal{D}_z > \mathcal{D}_{y_1}d_z,\ d_1 > \varphi_{P_{y_1}}. \tag{3.2.22}$$

Therefore, we have the following result.

Lemma 3.2.4. *Assume that the conditions in equation (3.2.21)-(3.2.22) holds. Then the positive constant solution (X^*, Y_1^*, Z^*) of system in (3.1.2) is locally asymptotically stable when $\tau = 0$.*

Next, we examine when equation in (3.2.20) has pure imaginary roots $\lambda = \pm i\omega$ with ω real number and $\omega > 0$. This is given by the following lemma.

Lemma 3.2.5. *The characteristic equation associated to equation in (3.2.20) has pure imaginary roots.*

Proof: If $\lambda = i\omega$ be a root of the characteristic equation (3.2.20) where $\omega > 0$, then we have

$$-\omega^2 k_t + \mathcal{K}_1 i\omega + Y_1^* c\,(b_1 - d_1)\,\varsigma_{P_z}(\cos(\omega\tau) + i\sin(\omega\tau)) + \mathcal{K}_2 = 0. \tag{3.2.23}$$

Separating real and imaginary parts, we have the following two equations

$$\begin{aligned} -\omega^2 k_t + Y_1^* c\,(b_1 - d_1)\,\varsigma_{P_z}\cos(\omega\tau) + \mathcal{K}_2 = 0, \\ \mathcal{K}_1\omega + Y_1^* c\,(b_1 - d_1)\,\varsigma_{P_z}\sin(\omega\tau)) = 0. \end{aligned} \tag{3.2.24}$$

Equations in (3.2.24) give possible values of τ and ω for which the characteristic equation in (3.2.20) can have pure imaginary roots. To see it we square each equation and we obtain

$$\begin{aligned} (Y_1^* c(b_1 - d_1)\varsigma_{P_z})^2\cos^2(\omega\tau) = (\omega^2 k_t - \mathcal{K}_2)^2, \\ (Y_1^* c\,(b_1 - d_1)\,\varsigma_{P_z})^2\sin^2(\omega\tau) = (\mathcal{K}_1\omega)^2. \end{aligned} \tag{3.2.25}$$

Adding the two equations, we obtain

$$2(Y_1^* c(b_1 - d_1)\varsigma_{P_z})^2 = (\omega^2 k_t - \mathcal{K}_2)^2 + (\mathcal{K}_1\omega)^2, \tag{3.2.26}$$

which implies that

$$\omega^4 + \frac{(\mathcal{K}_1^2 - 2k_t\mathcal{K}_2)}{k_t}\omega^2 + \frac{\mathcal{K}_2^2 - 2(Y_1^* c(b_1 - d_1)\varsigma_{P_z})^2}{k_t} = 0. \tag{3.2.27}$$

Hence,

$$\omega^2 = \frac{-\frac{(\mathcal{K}_1^2 - 2k_t\mathcal{K}_2)}{k_t} \pm \sqrt{\left(\frac{(\mathcal{K}_1^2 - 2k_t\mathcal{K}_2)}{k_t}\right)^2 - 4\frac{\mathcal{K}_2^2 - 2(Y_1^* c(b_1 - d_1)\varsigma_{P_z})^2}{k_t}}}{2}. \tag{3.2.28}$$

Thus, in view of the first equation in (3.2.24) and the first equation in (3.2.25), we obtain

$$\tau_j^* = \frac{1}{\omega}\cos^{-1}\left(\left(\frac{(\omega^2 k_t - \mathcal{K}_2)}{Y_1^* c\,(b_1 - d_1)\,\varsigma_{P_z}}\right) + 2j\pi\right), \tag{3.2.29}$$

as the critical values of τ, for $j = 0, 1, 2, \ldots$, and this complete the proves. This gives

us the following lemma.

Lemma 3.2.6. *Assume that the conditions in equation (3.2.21) and (3.2.22) hold. Then for $j \in \mathbb{N}_0$ the following statements are true.*

(i) Equation in (3.2.25) has a pair of purely imaginary roots $\pm i\omega$ when $\tau = \tau_j^*$ and there are no other roots of equation in (3.2.25) with zero real parts.

(ii) All the roots of equation in (3.2.25) have negative real parts when $\tau \in [0, \tau^*)$, where $\tau^* = \tau_0^*$.

We have verified the hypotheses for Hopf bifurcation to occur at $\tau^* = \tau_0^*$ except for the transversality condition. Differentiate the second equation in (3.2.20) with respect to τ, we have

$$\begin{aligned}\mathrm{Re}\left(\frac{\partial \lambda_2{}^2 k_t + \mathcal{K}_1\lambda_2 + Y_1^* c\,(b_1 - d_1)\,\varsigma_{P_z}\exp(-\lambda_2\tau) + \mathcal{K}_2}{\partial\tau}\right)\Bigg|_{\lambda=i\omega,\tau=\tau_0^*} \\ = \mathrm{Re}\left(\omega Y_1^* c\,(b_1 - d_1)\,\varsigma_{P_z}\sin(\omega\tau_0^*)\right) > 0. \qquad (3.2.30)\end{aligned}$$

Thus, the following results.

Lemma 3.2.7. *The transversality condition*

$$Re\left(\frac{\partial \lambda_2{}^2 k_t + \mathcal{K}_1\lambda_2 + Y_1^* c\,(b_1 - d_1)\,\varsigma_{P_z}\exp(-\lambda_2\tau) + \mathcal{K}_2}{\partial\tau}\right)\Bigg|_{\lambda=i\omega,\tau=\tau_0^*} > 0,$$

is satisfied.

Stability of positive equilibrium points and the existence of Hopf bifurcation for $\min\left(1, g\frac{Z-\alpha Y_1}{Y_1}\right) \neq 1$

Similarly, after linearizing the system in equation (3.1.2) around (X^*, Y_1^*, Z^*), we obtain the characteristic equation as

$$\left.\begin{aligned}&\lambda + \mathcal{D}_x\mu_k + a\varphi_{P_x} - d_x - \tfrac{(a-d_x)}{k_h}\,(2\,X^* + Y^* + Z^*) = 0,\\ &\lambda^2 k_t + \mathcal{K}_1\lambda + c\mathcal{D}_z(b_1 - d_1)Y_1^*\exp(-\lambda\tau) + \mathcal{K}_2 = 0,\end{aligned}\right\} \qquad (3.2.31)$$

where,

$$\begin{aligned}\mathcal{K}_1 &= (\varphi_{P_{y_1}} - d_z - d_1)k_t + (d_1 - b_1)(Z^* + 2Y_1^*) + k_t(\mathcal{D}_{y_1} + \mathcal{D}_z)\mu_k,\\ \mathcal{K}_2 &= d_z((d_1 - \varphi_{P_{y_1}})k_t + (b_1 - d_1)(2Y_1^* + Z^*)) + k_t\mathcal{D}_{y_1}\mu_k{}^2\mathcal{D}_z\\ &\quad + k_t(\varphi_{P_{y_1}}\mathcal{D}_z - \mathcal{D}_{Y_1}d_z - d_1\mathcal{D}_z)\mu_k) + \mathcal{D}_z(d_1 - b_1)(2Y_1^* + Z^*)\mu_k.\end{aligned}$$

Negative real parts for the first equation in (3.2.31) requires that

$$k_h d_x > -(a - d_x), \tag{3.2.32}$$

whereas, in the second equation in (3.2.31), when $\tau = 0$, Routh-Hurwitz criteria requires that

$$\begin{aligned}(\varphi_{P_{y_1}} - (d_1 + d_z))k_t &> (2Y_1^* + Z^*)(d_1 - b_1),\ \varphi_{P_{y_1}}\mathcal{D}_z > \mathcal{D}_{y_1}d_z + d_1\mathcal{D}_z,\\ d_1 &> \varphi_{P_{y_1}}.\end{aligned} \tag{3.2.33}$$

Therefore, we have the following result.

Lemma 3.2.8. *Assume that the conditions in equation (3.2.32)-(3.2.33) holds. Then the positive constant solution (X^*, Y_1^*, Z^*) of system (3.1.2) is locally asymptotically stable when $\tau = 0$.*

Next, we examine when equation in (3.2.31) has pure imaginary roots $\lambda = \pm i\omega$ with ω real number and $\omega > 0$. This is given by the following lemma.

Lemma 3.2.9. *The characteristic equation associated to equation in (3.2.31) has pure imaginary roots.*

Proof: If $\lambda = i\omega$ be a root of the characteristic equation (3.2.31) where $\omega > 0$, then we have

$$-\omega^2 k_t + \mathcal{K}_1 i\omega + Y_1^* c\,(b_1 - d_1)\,\mathcal{D}_z(\cos(\omega\tau) + i\sin(\omega\tau)) + \mathcal{K}_2 = 0. \tag{3.2.34}$$

Separating real and imaginary parts, we have the following two equations

$$\begin{aligned} -\omega^2 k_t + Y_1^* c\,(b_1 - d_1)\,\mathcal{D}_z \cos(\omega\tau) + \mathcal{K}_2 = 0, \\ \mathcal{K}_1\omega + Y_1^* c\,(b_1 - d_1)\,\mathcal{D}_z \sin(\omega\tau)) = 0. \end{aligned} \tag{3.2.35}$$

Equations in (3.2.35) give possible values of τ and ω for which the characteristic equation in (3.2.31) can have pure imaginary roots. To see it, we square each equation and we obtain

$$\begin{aligned} (Y_1^* c(b_1 - d_1)\mathcal{D}_z)^2 \cos^2(\omega\tau) = (\omega^2 k_t - \mathcal{K}_2)^2, \\ (Y_1^* c\,(b_1 - d_1)\,\mathcal{D}_z)^2 \sin^2(\omega\tau)) = (\mathcal{K}_1\omega)^2. \end{aligned} \tag{3.2.36}$$

Adding the two equations, we obtain

$$2(Y_1^* c(b_1 - d_1)\mathcal{D}_z)^2 = (\omega^2 k_t - \mathcal{K}_2)^2 + (\mathcal{K}_1\omega)^2, \tag{3.2.37}$$

which implies that

$$\omega^4 + \frac{(\mathcal{K}_1^2 - 2k_t\mathcal{K}_2)}{k_t}\omega^2 + \frac{\mathcal{K}_2^2 - 2(Y_1^* c(b_1 - d_1)\mathcal{D}_z)^2}{k_t} = 0. \tag{3.2.38}$$

Hence,

$$\omega^2 = \frac{-\frac{(\mathcal{K}_1^2 - 2k_t\mathcal{K}_2)}{k_t} \pm \sqrt{\left(\frac{(\mathcal{K}_1^2 - 2k_t\mathcal{K}_2)}{k_t}\right)^2 - 4\frac{\mathcal{K}_2^2 - 2(Y_1^* c(b_1 - d_1)\mathcal{D}_z)^2}{k_t}}}{2}. \tag{3.2.39}$$

Thus, in view of the first equation in (3.2.36) and equation in (3.2.39), we obtain

$$\tau_j^* = \frac{1}{\omega}\cos^{-1}\left(\left(\frac{(\omega^2 k_t - \mathcal{K}_2)}{Y_1^* c\,(b_1 - d_1)\,\mathcal{D}_z}\right) + 2j\pi\right), \tag{3.2.40}$$

as the critical values of τ, for $j = 0, 1, 2, \ldots$, and this complete the proves. This gives us the following lemma.

Lemma 3.2.10. *Assume that the conditions in equation (3.2.32) and (3.2.33) hold. Then for $j \in \mathbb{N}_0$ the following statements are true.*

(i) Equation in (3.2.31) has a pair of purely imaginary roots $\pm i\omega$ when $\tau = \tau_j^*$ and there are no other roots of equation in (3.2.31) with zero real parts.

(ii) All the roots of equation in (3.2.31) have negative real parts when $\tau \in [0, \tau^*)$, where $\tau^* = \tau_0^*$.

We have verified the hypotheses for Hopf bifurcation to occur at $\tau^* = \tau_0^*$ except for the transversality condition. Differentiate the second equation in (3.2.31) with respect to τ, we have

$$\operatorname{Re}\left(\frac{\partial \lambda_2{}^2 k_t + \mathcal{K}_1\lambda_2 + Y_1^* c\,(b_1 - d_1)\,\mathcal{D}_z \exp(-\lambda_2\tau) + \mathcal{K}_2}{\partial\tau}\right)\Bigg|_{\lambda=i\omega,\tau=\tau_0^*}$$
$$= \operatorname{Re}\left(\omega Y_1^* c\,(b_1 - d_1)\,\mathcal{D}_z \sin(\omega\tau_0^*)\right) > 0. \qquad (3.2.41)$$

Thus, the following results.

Lemma 3.2.11. *The transversality condition*

$$Re\left(\frac{\partial \lambda_2{}^2 k_t + \mathcal{K}_1\lambda_2 + Y_1^* c\,(b_1 - d_1)\,\varsigma_{P_z} \exp(-\lambda_2\tau) + \mathcal{K}_2}{\partial\tau}\right)\Bigg|_{\lambda=i\omega,\tau=\tau_0^*} > 0,$$

is satisfied.

In the next section, we derive our efficient numerical method.

3.3 Construction and analysis of the numerical method

In this section, we describe the derivation of the fitted numerical method for solving the system in equation (3.1.2). We determine an approximation to the derivatives of the functions $X(t,x), Y_1(x,t)$ and $Z(t,x)$ with respect to the spatial variable x.

Let N_x be a positive integer. Discretize the interval $[0, x_f]$ through the points

$$0 = x_0 < x_1 < x_2 < \cdots < x_{N_x} = x_f,$$

where the step-size $\Delta x = x_{j+1} - x_j = x_f/N_x$, $j = 0, 1, \ldots, x_{N_x}$. Let $\mathcal{X}_j(t), (\mathcal{Y}_1)_j(t), \mathcal{Z}_j(t)$ denote the numerical approximations of $X(t, j), Y_1(t, j), Z(t, j)$, then we approximate the second order spatial derivatives by

$$\begin{aligned} \Delta X(t, x_j) &\approx \frac{\mathcal{X}_{j+1} - 2\mathcal{X}_j + \mathcal{X}_{j-1}}{(\phi_X)^2},\ \Delta Y_1(t, x_j) \approx \frac{(\mathcal{Y}_1)_{j+1} - 2(\mathcal{Y}_1)_j + (\mathcal{Y}_1)_{j-1}}{(\phi_{Y_1})^2}, \\ \Delta Z(t, x_j) &\approx \frac{\mathcal{Z}_{j+1} - 2\mathcal{Z}_j + \mathcal{Z}_{j-1}}{(\phi_Z)^2}, \end{aligned} \tag{3.3.1}$$

where,

$$\begin{aligned} (\phi_X)^2 &= \frac{4}{(\sigma_X)} \sin^2\left(\frac{(\sigma_X)_j \Delta x}{4}\right),\ (\phi_{Y_1})^2 = \frac{(1 - \exp((\sigma_{Y_1})\Delta x)}{(\sigma_{Y_1})}, \\ (\phi_Z)^2 &= \frac{(1 - \exp((\sigma_Z)\Delta x)}{(\sigma_Z)}, \end{aligned}$$

and

$$(\sigma_X) = \sqrt{\frac{(d_x - a\varphi_{P_x})}{\mathcal{D}_x}},\ (\sigma_{Y_1}) = \sqrt{\frac{d_1}{\mathcal{D}_{y_1}}},\ (\sigma_Z) = \sqrt{\frac{d_z}{\mathcal{D}_z}}. \tag{3.3.2}$$

It is obvious that all the $\phi_X \to \Delta x, \phi_{Y_1} \to \Delta x, \phi_Z \to \Delta x$ as $\Delta x \to 0$.

Let N_t be a positive integer and $\Delta t = T/N_t$ where $0 < t < T$. Discretizing the time interval $[0, T]$ through the points

$$0 = t_0 < t_1 < \cdots < t_{N_t} = T,$$

where,

$$t_{n+1} - t_n = \Delta t,\ n = 0, 1, \ldots, (t_{N_t} - 1).$$

We approximate the time derivatives at t_n by

$$\frac{d\mathcal{X}_j(t_n)}{dt} \approx \frac{\mathcal{X}_j^{n+1}-\mathcal{X}_j^n}{\psi_X},\ \frac{d(\mathcal{Y}_1)_j(t_n)}{dt} \approx \frac{(\mathcal{Y}_1)_j^{n+1}-(\mathcal{Y}_1)_j^n}{\psi_{Y_1}},$$
$$\frac{d\mathcal{Z}_j(t_n)}{dt} \approx \frac{\mathcal{Z}_j^{n+1}-\mathcal{Z}_j^n}{\psi_Z}, \tag{3.3.3}$$

where,

$$\begin{aligned}\psi_X &= (\exp((d_x-a\varphi_{P_x})\Delta t)-1)/(d_x-a\varphi_{P_x}),\ \psi_{Y_1}=(1-\exp(-d_1\Delta t))/d_1,\\ \psi_Z &= (1-\exp(-d_z\Delta t))/d_z,\end{aligned} \tag{3.3.4}$$

where we see that all the $\psi_X \to \Delta t, \psi_{Y_1} \to \Delta t, \psi_Z \to \Delta t$ as $\Delta t \to 0$.

The denominator functions in (3.3.1) and (3.3.3) are used explicitly to remove the inherent stiffness in the central finite derivatives parts and are derived by using the theory of nonstandard finite difference methods, see, e.g., [84, 103, 104] and references therein.

Combining the equation (3.3.1) with equation (3.3.3) for time derivatives, we obtain

$$\left.\begin{aligned}
&\tfrac{\mathcal{X}_j^{n+1}-\mathcal{X}_j^n}{\psi_X} = \mathcal{D}_x \tfrac{\mathcal{X}_{j+1}^{n+1}-2\mathcal{X}_j^{n+1}+\mathcal{X}_{j-1}^{n+1}}{(\phi_X)^2} + \mathcal{X}_j^n\left(a\varphi_{P_x}-d_x-(a-d_x)\tfrac{\mathcal{X}_j^n+(\mathcal{Y}_1)_j^n+\mathcal{Z}_j^n}{k_h}\right),\\
&\tfrac{(\mathcal{Y}_1)_j^{n+1}-(\mathcal{Y}_1)_j^n}{\psi_{Y_1}} = \mathcal{D}_{y_1}\tfrac{(\mathcal{Y}_1)_{j+1}^{n+1}-2(\mathcal{Y}_1)_j^{n+1}+(\mathcal{Y}_1)_{j-1}^{n+1}}{(\phi_{Y_1})^2}\\
&+(\mathcal{Y}_1)_1^n\left(b_1\varphi_{P_{y_1}}\min\left(1,g\tfrac{\mathcal{Z}_j^n-\alpha(\mathcal{Y}_1)_j^n}{(\mathcal{Y}_1)_j^n}\right)-d_1-(b_1-d_1)\tfrac{(\mathcal{Y}_1)_j^n+\mathcal{Z}_j^n}{k_t}\right),\\
&\tfrac{\mathcal{Z}_j^{n+1}-\mathcal{Z}_j^n}{\psi_Z} = \mathcal{D}_z\tfrac{\mathcal{Z}_{j+1}^{n+1}-2\mathcal{Z}_j^{n+1}+\mathcal{Z}_{j-1}^{n+1}}{(\phi_Z)^2}+c\varphi_{P_z}(\mathcal{H}_{Y_1})_j^n-d_z\mathcal{Z}_j^n,\\
&\mathcal{X}_1^n=\mathcal{X}_{-1}^n,\ (\mathcal{Y}_1)_1^n=(\mathcal{Y}_1)_{-1}^n,\ \mathcal{Z}_1^n=\mathcal{Z}_{-1}^n,\\
&\mathcal{X}_{x_{N_x}}^n=\mathcal{X}_{x_{N_x}-1}^n,\ (\mathcal{Y}_1)_{x_{N_x}}^n=(\mathcal{Y}_1)_{x_{N_x}-1}^n,\ \mathcal{Z}_{x_{N_x}}^n=\mathcal{Z}_{x_{N_x}-1}^n,\\
&\mathcal{X}_j^0=9.00,\ (\mathcal{Y}_1)_j^0=0.01,\ \mathcal{Z}_j^0=0.001,
\end{aligned}\right\} \tag{3.3.5}$$

where, the no-flux boundary conditions are discretised by means of the central finite difference [21], $j = 1, 2, \ldots, x_{N_x} - 1$, $n = 0, 1, \ldots, t_{N_t} - 1$ and

$$(\mathcal{H}_{Y_1})_j^n \approx Y_1(t_n - \tau, x_j), \tag{3.3.6}$$

is denoting the history functions corresponding to the equation in Y_1.

The system in equation (3.3.5) can further be simplified as

$$\left.\begin{aligned}
&-\tfrac{\mathcal{D}_x}{(\phi_X)^2}\mathcal{X}_{j-1}^{n+1} + \left(\tfrac{1}{\psi_X} + \tfrac{2\mathcal{D}_x}{(\phi_X)^2}\right)\mathcal{X}_j^{n+1} - \tfrac{\mathcal{D}_x}{(\phi_X)^2}\mathcal{X}_{j+1}^{n+1} \\
&= \mathcal{X}_j^n\left(\tfrac{1}{\psi_X} + a\varphi_{P_x} - d_x - (a - d_x)\,\tfrac{\mathcal{X}_j^n + (\mathcal{Y}_1)_j^n + \mathcal{Z}_j^n}{k_h}\right), \\
&-\tfrac{\mathcal{D}_{y_1}}{(\phi_{Y_1})^2}(\mathcal{Y}_1)_{j-1}^{n+1} + \left(\tfrac{1}{\psi_{Y_1}} + \tfrac{2\mathcal{D}_{y_1}}{(\phi_{Y_1})^2}\right)(\mathcal{Y}_1)_j^{n+1} - \tfrac{\mathcal{D}_{y_1}}{(\phi_{Y_1})^2}(\mathcal{Y}_1)_{j+1}^{n+1} \\
&= (\mathcal{Y}_1)_1^n\left(\tfrac{1}{\psi_{Y_1}} + b_1\varphi_{P_{y_1}}\min\left(1, g\tfrac{\mathcal{Z}_j^n - \alpha(\mathcal{Y}_1)_j^n}{\mathcal{Y}_1)_j^n}\right) - d_1 - (b_1 - d_1)\,\tfrac{(\mathcal{Y}_1)_j^n + \mathcal{Z}_j^n}{k_t}\right), \\
&-\tfrac{\mathcal{D}_z}{(\phi_Z)^2}\mathcal{Z}_{j-1}^{n+1} + \left(\tfrac{1}{\psi_Z} + \tfrac{2\mathcal{D}_z}{(\phi_Z)^2}\right)\mathcal{Z}_j^{n+1} - \tfrac{\mathcal{D}_z}{(\phi_Z)^2}\mathcal{Z}_{j+1}^{n+1} \\
&= c\varphi_{P_z}(\mathcal{H}_{Y_1})_j^n + \left(\tfrac{1}{\psi_Z} - d_z\right)\mathcal{Z}_j^n,
\end{aligned}\right\} \tag{3.3.7}$$

which can be written as a tridiagonal system given by

$$\left.\begin{aligned}
&(\mathcal{A})_x\mathcal{X}_j^{n+1} = \mathcal{X}_j^n\left(\tfrac{1}{\psi_X} + a\varphi_{P_x} - d_x - (a - d_x)\,\tfrac{\mathcal{X}_j^n + (\mathcal{Y}_1)_j^n + \mathcal{Z}_j^n}{k_h}\right), \\
&(\mathcal{A})_{y_1}(\mathcal{Y}_1)_j^{n+1} \\
&= (\mathcal{Y}_1)_j^n\left(\tfrac{1}{\psi_{Y_1}} + b_1\varphi_{P_{y_1}}\min\left(1, g\tfrac{\mathcal{Z}_j^n - \alpha(\mathcal{Y}_1)_j^n}{\mathcal{Y}_1)_j^n}\right) - d_1 - (b_1 - d_1)\,\tfrac{(\mathcal{Y}_1)_j^n + \mathcal{Z}_j^n}{k_t}\right), \\
&(\mathcal{A})_z\mathcal{Z}_j^{n+1} = c\varphi_{P_z}(\mathcal{H}_{Y_1})_j^n + \left(\tfrac{1}{\psi_Z} - d_z\right)\mathcal{Z}_j^n,
\end{aligned}\right\} \tag{3.3.8}$$

where, $j = 1, \ldots, x_{N_x} - 1$, $n = 0, \ldots, t_{N_t} - 1$ and

$$\left.\begin{aligned}(\mathcal{A})_x &= \text{Tri}\left(-\tfrac{\mathcal{D}_x}{(\phi_X)^2}, \tfrac{1}{\psi_X} + \tfrac{2\mathcal{D}_x}{(\phi_X)^2}, -\tfrac{\mathcal{D}_x}{(\phi_X)^2}\right),\\ (\mathcal{A})_{y_1} &= \text{Tri}\left(-\tfrac{\mathcal{D}_{y_1}}{(\phi_{Y_1})^2}, \tfrac{1}{\psi_{Y_1}} + \tfrac{2\mathcal{D}_{y_1}}{(\phi_{Y_1})^2}, -\tfrac{\mathcal{D}_{y_1}}{(\phi_{Y_1})^2}\right),\\ (\mathcal{A})_z &= \text{Tri}\left(-\tfrac{\mathcal{D}_z}{(\phi_Z)^2}, \tfrac{1}{\psi_Z} + \tfrac{2\mathcal{D}_z}{(\phi_Z)^2}, -\tfrac{\mathcal{D}_z}{(\phi_Z)^2}\right).\end{aligned}\right\}$$

On the interval $[0, \tau]$, the delayed arguments $t_n - \tau$ belong to $[-\tau, 0]$, and therefore the delayed variables in equation (3.3.5) are evaluated directly from the history functions $Y_1^0(t, x)$ as

$$(\mathcal{H}_{Y_1})_j^n \approx Y_1^0(t_n - \tau, x_j), \tag{3.3.9}$$

and equation (3.3.8) becomes

$$\left.\begin{aligned}&(\mathcal{A})_x \mathcal{X}_j^{n+1} = \mathcal{X}_j^n \left(\tfrac{1}{\psi_X} + a\varphi_{P_x} - d_x - (a - d_x)\tfrac{\mathcal{X}_j^n + (\mathcal{Y}_1)_j^n + \mathcal{Z}_j^n}{k_h}\right),\\ &(\mathcal{A})_{y_1}(\mathcal{Y}_1)_j^{n+1}\\ &= (\mathcal{Y}_1)_j^n \left(\tfrac{1}{\psi_{Y_1}} + b_1\varphi_{P_{y_1}} \min\left(1, g\tfrac{\mathcal{Z}_j^n - \alpha(\mathcal{Y}_1)_j^n}{\mathcal{Y}_1)_j^n}\right) - d_1 - (b_1 - d_1)\tfrac{(\mathcal{Y}_1)_j^n + \mathcal{Z}_j^n}{k_t}\right),\\ &(\mathcal{A})_z \mathcal{Z}_j^{n+1} = c\varphi_{P_z}(\mathcal{Y})_1^0(t_n - \tau, x_j) + \left(\tfrac{1}{\psi_Z} - d_z\right)\mathcal{Z}_j^n.\end{aligned}\right\} \tag{3.3.10}$$

Let s be the largest integer such that $\tau_s \leq \tau$. By using the system equation (3.3.10) we can compute $\mathcal{X}_j^n, (\mathcal{Y}_1)_j^n, \mathcal{Z}_j^n$ for $1 \leq n \leq s$. Up to this stage, we interpolate the data

$$(t_0, (\mathcal{Y}_1)_j^0),\ (t_1, (\mathcal{Y}_1)_j^1), \ldots, (t_s, (\mathcal{Y}_1)_j^s),$$

using an interpolating cubic Hermite spline $\iota_j(t)$. Then

$$(\mathcal{Y}_1)_j^n = \iota_{Y_1}(t_n, x_j),$$

for all $n = 0, 1, \ldots, s$ and $j = 1, 2, \ldots, x_{N_x} - 1$.

For $n = s+1, s+2, \ldots, t_{N_t} - 1$, when we move from level n to level $n+1$, we extend the definitions of the cubic Hermite spline $\iota_j(t)$ to the point $(t_n + k, (\mathcal{Y}_1)_j^n)$. Then the history term $(\mathcal{H}_{Y_1})_j^n$ can be approximated by the functions $\iota_j(t_n - \tau)$ for $n \geq s$. This implies that,

$$(\mathcal{H}_{Y_1})_j^n \approx (\iota_{Y_1})_j(t_n - \tau), \tag{3.3.11}$$

and equation (3.3.10) becomes

$$\left.\begin{aligned}
(\mathcal{A})_x \mathcal{X}_j^{n+1} &= \mathcal{X}_j^n \left(\tfrac{1}{\psi_X} + a\varphi_{P_x} - d_x - (a - d_x) \tfrac{\mathcal{X}_j^n + (\mathcal{Y}_1)_j^n + \mathcal{Z}_j^n}{k_h} \right), \\
(\mathcal{A})_{y_1} (\mathcal{Y}_1)_j^{n+1} &= (\mathcal{Y}_1)_j^n \left(\tfrac{1}{\psi_{Y_1}} + b_1 \varphi_{P_{y_1}} \min\left(1, g \tfrac{\mathcal{Z}_j^n - \alpha(\mathcal{Y}_1)_j^n}{(\mathcal{Y}_1)_j^n}\right) - d_1 \right) \\
&\quad - (\mathcal{Y}_1)_1^n \left((b_1 - d_1) \tfrac{(\mathcal{Y}_1)_j^n + \mathcal{Z}_j^n}{k_t} \right), \\
(\mathcal{A})_z \mathcal{Z}_j^{n+1} &= c\varphi_{P_z} (\iota_{Y_1})_j (t_n - \tau) + \left(\tfrac{1}{\psi_Z} - d_z \right) \mathcal{Z}_j^n,
\end{aligned}\right\} \tag{3.3.12}$$

where,

$$\iota_{Y_1}(t_n - \tau) = [(\mathcal{H}_{Y_1})_1^n, (\mathcal{H}_{Y_1})_2^n \ldots, (\mathcal{H}_{Y_1})_{N_x - 1}^n]'.$$

Our FOFDM is then consists of equations (3.3.5)-(3.3.12). Rewriting the scheme in (3.3.12) in the form of the system of equations, we obtain

$$\left.\begin{aligned}
\mathcal{A}_x \mathcal{X} &= F_x, \\
\mathcal{A}_{y_1} \mathcal{Y}_1 &= F_{y_1}, \\
\mathcal{A}_z \mathcal{Z} &= F_z,
\end{aligned}\right\} \tag{3.3.13}$$

where,

$$\left.\begin{aligned} F_x &= \mathcal{X}_j^n \left(\tfrac{1}{\psi_X} + a\varphi_{P_x} - d_x - (a - d_x) \tfrac{\mathcal{X}_j^n + (\mathcal{Y}_1)_j^n + \mathcal{Z}_j^n}{k_h} \right), \\ F_{y_1} &= (\mathcal{Y}_1)_j^n \left(\tfrac{1}{\psi_{Y_1}} + b_1\varphi_{P_{y_1}} \min\left(1, g\tfrac{\mathcal{Z}_j^n - \alpha(\mathcal{Y}_1)_j^n}{\mathcal{Y}_1)_j^n}\right) - d_1 - (b_1 - d_1) \tfrac{(\mathcal{Y}_1)_j^n + \mathcal{Z}_j^n}{k_t} \right), \\ F_z &= c\varphi_{P_z}(\iota_{Y_1})_j(t_n - \tau) + \left(\tfrac{1}{\psi_Z} - d_z \right) \mathcal{Z}_j^n. \end{aligned}\right\}$$

Let the functions

$$X(x,t), Y_1(x,t), Z(x,t),$$

and their partial derivatives with respect to both t and x be smooth such that they satisfy

$$\begin{aligned} \left| \frac{\partial^{i+j} X(t,x)}{\partial t^i x^j} \right| &\leq \Upsilon_X, \left| \frac{\partial^{i+j} Y_1(t,x)}{\partial t^i x^j} \right| \leq \Upsilon_Y, \\ \left| \frac{\partial^{i+j} Z(t,x)}{\partial t^i x^j} \right| &\leq \Upsilon_Z, \forall i,j \geq 0, \end{aligned} \tag{3.3.14}$$

where,

$$\Upsilon_X, \Upsilon_Y, \Upsilon_Z,$$

are constant that are independent of the time and space step-sizes. Then we see that the truncation errors are $(\varsigma_x)_j^n, (\varsigma_{y_1})_j^n, (\varsigma_z)_j^n$ are given by

$$\left.\begin{aligned} (\varsigma_x)_j^n &= (\mathcal{A})_x X - F_x = (\mathcal{A}_x(X - \mathcal{X}))_j^n, \\ (\varsigma_{y_1})_j^n &= (\mathcal{A})_{y_1} Y_1 - F_{y_1} = (\mathcal{A}_{y_1}(Y_1 - \mathcal{Y}_1))_j^n, \\ (\varsigma_z)_j^n &= (\mathcal{A})_z Z - F_z = (\mathcal{A}_z(Z - \mathcal{Z}))_j^n. \end{aligned}\right\} \tag{3.3.15}$$

Therefore,

$$\left.\begin{array}{l} \max_{j,n}|(X_j^n - \mathcal{X}_j^n| \leq ||(\mathcal{A})_x^{-1}||\max_{j,n}|(\varsigma_x)_j^n|, \\ \max_{j,n}|(Y_1)_j^n - (\mathcal{Y}_1)_j^n| \leq ||(\mathcal{A})_{y_1}^{-1}||\max_{j,n}|(\varsigma_{y_1})_j^n|, \\ \max_{j,n}|(Z_j^n - \mathcal{Z}_j^n| \leq ||(\mathcal{A})_z^{-1}||\max_{j,n}|(\varsigma_z)_j^n|, \end{array}\right\} \tag{3.3.16}$$

where,

$$\left.\begin{array}{l} \max_{j,n}|(\varsigma_x)_j^n| \leq \frac{\Delta t}{2}|X_{tt}(\xi, x_j)| + \frac{(\Delta x)^2}{12}|X_{xxxx}(t_n, \zeta)|, \\ \max_{j,n}|(\varsigma_{y_1})_j^n| \leq \frac{\Delta t}{2}|(Y_1)_{tt}(\xi, x_j)| + \frac{(\Delta x)^2}{12}|(Y_1)_{xxxx}(t_n, \zeta)|, \\ \max_{j,n}|(\varsigma_z)_j^n| \leq \frac{\Delta t}{2}|Z_{tt}(\xi, x_j)| + \frac{(\Delta x)^2}{12}|Z_{xxxx}(t_n, \zeta)|, \end{array}\right\} \tag{3.3.17}$$

for $t_{n-1} \leq \xi \leq t_{n+1}, x_{j-1} \leq \zeta \leq x_{j+1}$. Then by (3.3.14), inequalities in (3.3.17) implies that

$$\left.\begin{array}{l} \max_{j,n}|(\varsigma_x)_j^n| \leq \left(\frac{\Delta t}{2} + \frac{(\Delta x)^2}{12}\right)\Upsilon_X, \\ \max_{j,n}|(\varsigma_{y_1})_j^n| \leq \left(\frac{\Delta t}{2} + \frac{(\Delta x)^2}{12}\right)\Upsilon_Y, \\ \max_{j,n}|(\varsigma_z)_j^n| \leq \left(\frac{\Delta t}{2} + \frac{(\Delta x)^2}{12}\right)\Upsilon_Z, \end{array}\right\} \tag{3.3.18}$$

for $t_{n-1} \leq \xi \leq t_{n+1}, x_{j-1} \leq \zeta \leq x_{j+1}$, and by [117], we have

$$||(\mathcal{A})_x^{-1}|| \leq \Xi_x, \ ||(\mathcal{A})_{y_1}^{-1}|| \leq \Xi_{y_1}, \ ||(\mathcal{A})_z^{-1}|| \leq \Xi_z. \tag{3.3.19}$$

Therefore, using (3.3.17) and (3.3.18) into (3.3.16) we obtain the following results.

Theorem 3.3.1. *Let*

$$F_x(x,t), F_{y_1}(x,t), F_z(x,t),$$

be sufficiently smooth functions so that $X(x,t), Y_1(x,t), Z(x,t) \in C^{\infty}([0,t_{N_t}]\times[0,x_{N_x}])$. *Let* $(\mathcal{X}_j^n, (\mathcal{Y}_1)_j^n, \mathcal{Z}_j^n)$, $j = 1,2,\ldots x_{N_x}, n = 1,2,\ldots t_{N_t}$ *be the approximate solutions to (3.1.2), obtained using the FOFDM with* $\mathcal{X}_j^0 = X_j^0, (\mathcal{X}_1)_j^0 = (Y_1)_j^0, \mathcal{Z}_j^0 = Z_j^0,$. *Then there exists* Ξ_x, Ξ_{y_1}, Ξ_z *independent of the step sizes* Δt *and* Δx *such that*

$$\left.\begin{array}{l} \max_{j,n} |(\varsigma_x)_j^n| \leq \left(\frac{\Delta t}{2} + \frac{(\Delta x)^2}{12}\right) \Upsilon_X, \\ \max_{j,n} |(\varsigma_{y_1})_j^n| \leq \left(\frac{\Delta t}{2} + \frac{(\Delta x)^2}{12}\right) \Upsilon_Y, \\ \max_{j,n} |(\varsigma_z)_j^n| \leq \left(\frac{\Delta t}{2} + \frac{(\Delta x)^2}{12}\right) \Upsilon_Z. \end{array}\right\} \tag{3.3.20}$$

This, concludes the analysis of our numerical method.

3.4 Numerical results and discussions

In this section, we present our numerical results with respect to the maximum proliferation rate of tumor cells and blood supply limitation indicator to help visualize when there are indeed limiting healthy and tumor cells growth. In order to investigate it, we implement our numerical method such that the stability conditions given in Theorems 3.2.1-3.2.2 are satisfied. Due to the unavailability of diffusion values, we set the diffusion constants $\mathcal{D}_x = 10^{-3}, \mathcal{D}_{y_1} = 20^{-4}, \mathcal{D}_x = 30^{-5}$. Following Elser et al. [37], we present our numerical results as follows.

In Figure 3.5.1, we present the case when the birth rate of healthy cell are decreased than that of parenchyma cell ($a < b_1$) and death rate of healthy cell is increased than that of parenchyma cell ($d_x > d_1$) for (a) no treatment blocking phosphorus uptake by tumor cells, (b) lowered phosphorus P by 20%, (c) increased the time delay τ from 7

to 11 days and in (d) blocked tumor cell uptake of phosphorus by half.

In Figure 3.5.2, we present the case when the birth and death rates of healthy and parenchyma cells are equal ($a = b_1$ and $d_x = d_1$) for (a) no treatment blocking phosphorus uptake by tumor cells, (b) lowered phosphorus P by 20%, (c) increased the time delay τ from 7 to 11 days and in (d) blocked tumor cell uptake of phosphorus by half.

In Figure 3.5.3, we present the case when the birth of healthy cells are increased than that of a parenchyma cell ($a > b_1$) and increased death rate of healthy cells than that of a parenchyma cell ($d_x < d_1$) for (a) no treatment blocking phosphorus uptake by tumor cells, (b) lowered phosphorus P by 20%, (c) increased the time delay τ from 7 to 11 days and in (d) blocked tumor cells uptake of phosphorus by half.

The numerical solutions in Figure 3.5.1 presents a slight growth of healthy cells and fast growth of tumor cell during the first 40 days from the infection date. We also see that after 40 days of infection, both cells converges to their equilibria, with a slight decrease in their growth. This is due to the competition for resources among cells, presented by this case. After 40 days the process of vascularization starts to grow because the tumor cell has reached some genetically size. We also see that lowered phosphorus and blocked tumor cell uptake of phosphorus do not differ from the no treatment blocking phosphorus uptake by tumor cells, whereas the above features are postponed when we increased the time delay τ from 7 to 11 days.

The numerical solutions in Figure 3.5.2 presents an increase growth of healthy cells and tumor cell during the first 40 days from the infection date. We also see that after 40 days of infection, both cells converges to their equilibria, with a slight increase for healthy cells and a decrease growth of tumor cells. This is due to the competition for resources among cells presented by this case. After 40 days the process of vascularization starts to grow because the tumor cell has reached some genetically size. We note that lowered phosphorus and blocked tumor cell uptake of phosphorus do not differ from the no treatment blocking phosphorus uptake by tumor cells, whereas the above features are postponed when we increased the time delay τ from 7 to 11

days.

The numerical solutions in Figure 3.5.3 presents an increase growth of healthy cells as compare to the previous cases and a drastic decrease for tumor cell during the first 40 days from the infection date. After 40 days of infection, both cells converges to their respective equilibria, with an increase of healthy cells and a decrease growth of tumor cell. This is due to the competition for resources among cells presented by this case. After 40 days the process of vascularization starts to grow, thus causing tumor cell to grow gradually. We note that lowered phosphorus and blocked tumor cell uptake of phosphorus do not differ from the no treatment blocking phosphorus uptake by tumor cell, whereas the above features are postponed when we increased the time delay τ from 7 to 11 days.

3.5 Conclusion

In this chapter, we have considered the biological stoichiometry of tumor dynamics, vascularized by a single solid tumor growing within the confinement of an organ and the environment provided by an organ. We examined the presence of positive equilibrium solutions for all the possible limiting cases with respect to proliferation rate of tumor cell and determine the existence of Hopf bifurcation. Thus, our numerical solutions clearly present that the biological stoichiometry of tumor dynamics is real and can contribute a great deal toward the development of therapeutically drugs which can contribute toward healing tumor and tumor related diseases. Thus, our approach in this work should serve as a first numerical attempt to incorporate the detailed effects of healthy and tumor cells competing for both space and essentials, but limiting nutrients within a host.

Table 3.5.1: Values of the parameters used in the model (3.3.5) [37]

$m = 20.00$	$n = 10.00$	$k_h = 10.00$
$k_t = 3.00$	$f = 0.6667$	$P = 150.00$
$m_1 = 20.00$	$\beta_1 = 1.00$	$c = 0.005$
$dz = 0.20$	$g = 100.00$	$\alpha = 0.05$

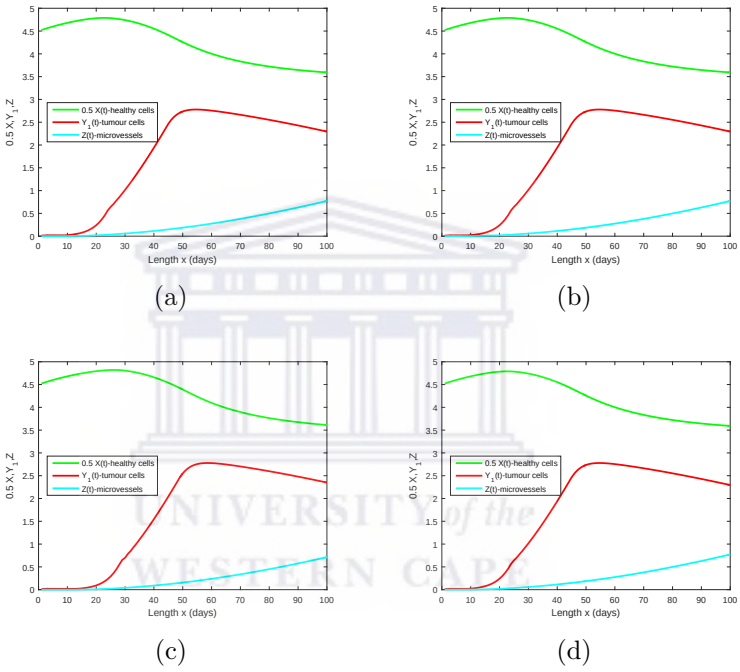

Figure 3.5.1: Numerical solution for the dynamics of homogeneous tumor growth model, when $a = 3, d_x = 2, b_1 = 6, d_1 = 0.5$.

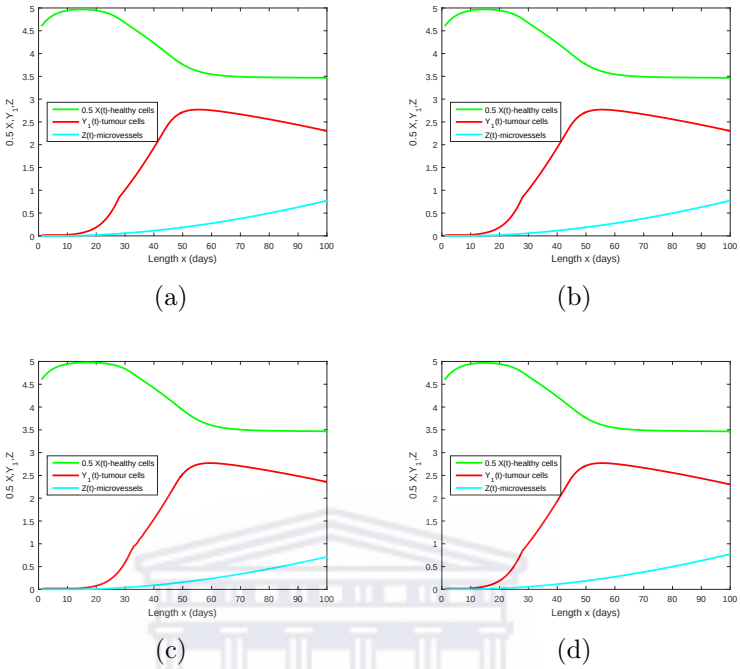

Figure 3.5.2: Numerical solution for the dynamics of homogeneous tumor growth model, when $a = b_1 = 6, d_x = d_1 = 1$.

We believe that we have gathered essential facts concerning the basic understanding of tumour cells with regard to the models considered in Chapter 1. Thus, Chapter 4, we consider the dynamics when a host has a double infection.

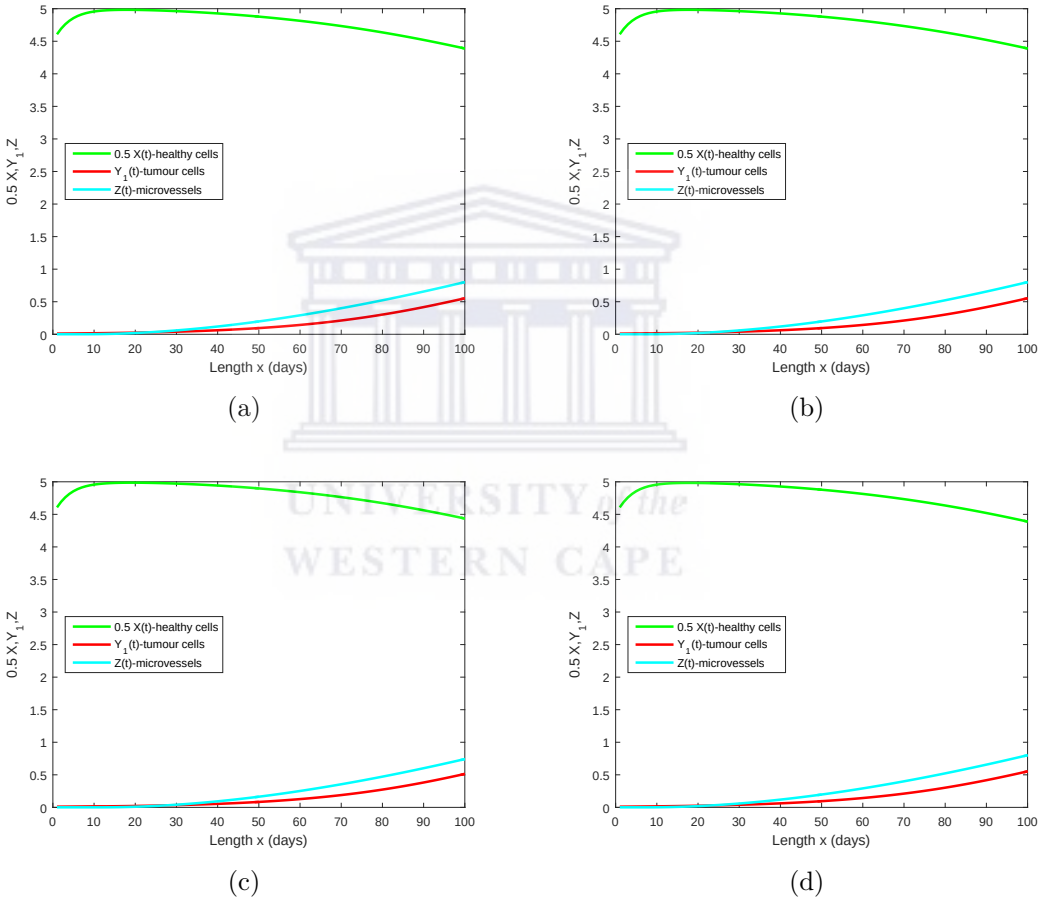

Figure 3.5.3: Numerical solution for the dynamics of homogeneous tumor growth model, when $a = 6, d_x = 0.5, b_1 = 3, d_1 = 2$.

Chapter 4

A fitted operator for a mathematical model arising in HIV related cancer-immune system dynamics

The effect of disease and virus such as cancer and HIV among our societies is evident. Thus, from the mathematical point of view many models have been developed with the aim to contribute towards understanding the dynamics of diseases. In this chapter, we begin by extending a system of delay differential equations (DDEs) model of HIV related cancer-immune system to a system of delay partial differential equations (DPDEs) model of HIV related cancer-immune dynamics, we are contributing toward the understanding of the dynamics more clearly. Thus, we analyse the DPDEs and use the qualitative features of the extended model to derive, analyse and implement a fitted operator finite difference method (FOFDM) and present our results. This FOFDM is analyzed for convergence and it is seen that it has has second-order accuracy. We present some numerical results for some cases of the the model to illustrate the reliability of our numerical method.

4.1 The model

Assuming that the cancer-immune system interactions is governed by cancer cells proliferation and their interaction with the immune system, our first aim in this chapter is to present the fact that in the absence of the cancer and HIV infections, the governing dynamics of the extended model tends to the expected physiological level and derive the corresponding stability conditions of the extended model. Our second aim is to develop a fitted operator numerical method, analyse, implement and present our numerical results with regard to the governing dynamics.

Thus, as a way forward, toward understanding the connection between HIV/AIDS and certain cancers diseases, Forys̀ and Poleszczuk in [41] derived a system of nonlinear delay-differential equations (DDEs) model of HIV related cancer-immune system dynamics as

$$\left.\begin{aligned} T_t &= r_1 T(t) - k_1 T(t)E(t), \\ E_t &= r_2 T(t) + \alpha - \mu_1 E(t) - k_1 T(t)E(t) + (1-\varepsilon)k_1 T(t-\tau)E(t-\tau) \\ &\quad -k_2' E(t)I(t) - k_3 E(t)V(t), \\ I_t &= k_2' E(t)I(t) + k_3 E(t)V(t) - \mu_2 I(t), \\ V_t &= N\delta I(t) - cV(t), \end{aligned}\right\} \tag{4.1.1}$$

where, the subscript t denotes the partial derivative with respect to time t, $T(t)$, $E(t)$, $I(t)$, $V(t)$ denote concentration of cancer cells, healthy effector cells (mainly CD4+ t-cells), effector cells infected by the HIV virus, and free HIV viral particles in that order. Since the dynamics of cancer cells are assumed to be governed by cancer cells proliferation, their interactions with the immune system, then the term describing the influence of effector cells on cancer cells is taken proportional to the product of both concentrations [64, 81]. Thus, the parameters r_2, α, μ_1 denote the

antigenicity (difference between tumor and normal tissue) of the tumor, normal rate of the flow of mature effector cells into the region of cancer cells localization [67], rate of elimination of effector cells, in that order. It is understood that the process of effector cells regeneration after the injection of lytic granules into the target cells causes the cytotoxic T-cells to kill target cells mainly using lytic granules containing perforin, granzymes and TNF, by binding to the surface of the target cell. This trigger the extracellular release of perforin molecules from the granules. Thus, polymerize to form trans-membrane channels which may facilitate lysis of the target by permitting entry of granzymes which induce apoptotic cell death through activation of the caspase protease cascade and ultimate fragmentation of nuclear DNA [34]. As a result, effector cells should regenerate lytic granules to this effect. Thus, the term τ denotes the time needed by effector cells to regenerate lytic granules and the time required for some small percentage (ε) to breach into the target T-cells.

The term describing the release of the new free viral particles by the infected cells is multiplied by the additional parameter N to represent the number of those particles released by the single infected cell. Furthermore, Fory$\acute{s}$ and Poleszczuk in [41] assumed that the rate of change of the free HIV viral particles is high relative to the rate of change of the concentration of considered cellular populations. Hence, Fory$\acute{s}$ and Poleszczuk in [41] assumed that the rate of change of the free HIV viral particles is high relative to the rate of change of the concentration of considered cellular populations. Therefore, during the whole process $dV/dt \equiv 0$, that is $V(t) \equiv N\delta/cI(t)$. This implies that the system of non-linear delay differential equations (DDEs) in equation (4.1.1)

reduces to the following system of three non-linear delay differential equations (DDEs)

$$\left.\begin{aligned} T_t &= r_1 T(t) - k_1 T(t)E(t), \\ E_t &= r_2 T(t) + \alpha - \mu_1 E(t) - k_1 T(t)E(t) + (1-\varepsilon)k_1 T(t-\tau)E(t-\tau) \\ &\quad -k_2' E(t)I(t), \\ I_t &= k_2 E(t)I(t) - \mu_2 I(t), \end{aligned}\right\} \tag{4.1.2}$$

where,

$$k_2 = k_2' + k_3 \frac{N\delta}{c}.$$

Since their model take no spacial effects, then in this chapter we extend the system of DDEs in equation (4.1.2) to a system of delayed partial differential equations (DPDEs) as

$$\left.\begin{aligned} &T_t - d_1 \Delta T = r_1 T(t) - k_1 T(t)E(t), \\ &E_t - d_2 \Delta E = r_2 T(t) + \alpha - \mu_1 E(t) - k_1 T(t)E(t) \\ &\quad +(1-\varepsilon)k_1 T(t-\tau)E(t-\tau) - k_2' E(t)I(t), \\ &I_t - d_3 \Delta I = k_2 E(t)I(t) - \mu_2 I(t), \\ &\tfrac{\partial T}{\partial \nu}(0,t) = \tfrac{\partial E}{\partial \nu}(0,t) = \tfrac{\partial I}{\partial \nu}(0,t) = 0, \\ &\tfrac{\partial T}{\partial \nu}(x_f,t) = \tfrac{\partial E}{\partial \nu}(x_f,t) = \tfrac{\partial I}{\partial \nu}(x_f,t) = 0, \text{ on } (x,t) \in \Omega \times (0,\infty), \\ &\mathcal{X}_j(x,0) = \eta_j(x), \text{ on } (x,t) \in \bar{\Omega} \times [-\tau, 0], \ j = 1,2,3, \end{aligned}\right\} \tag{4.1.3}$$

where d_1, d_2, d_3 denote the cancer cells, healthy effector cells, HIV-infected cells constant diffusion coefficients, Δ denotes the Laplace operator, $\mathcal{X}_j(x,t) = [T, E, I], j = 1, 2, 3$, $\Omega \in \mathbb{R}^3$ denotes a bounded domain with smooth boundary $\partial\Omega$ and ν denotes the outward unit normal on $\partial\Omega$. The initial function $\eta_j(x,t)$ is Holder continuous on $[-\tau, 0]$ and the no-flux boundary conditions are imposed to ensure the exclusion of external effects. More details on reaction rates can be found in [41].

Many mathematical models such as those in [16, 17, 32, 81, 82, 88, 89, 107] has been derived in order to shed more light as to how the dynamics of such virus takes place. While the authors made the utmost efforts to include whatever we could, we would like to apologize if there are any omissions which are totally unintentional.

In this chapter, our focus is on the model in which the issue of immune reaction against tumor and HIV dissemination arising from the work of Foryś and Pleszczuk in [41], in vivo. We also would like to note the work done by Nunnari et al. [92], Resclgnow and Delisi [111] and by Rong et al. [113], where a significant increase in the incidence of neoplasms accompany the acquired immunodeficiency syndrome (AIDS), a delay in the formation of killer lymphocytes was introduced to allow tumor development from a single cell, steps between viral infection of CD4+ t-cells and the production of HIV−1 visions have been incorporated by an eclipse phase, an HIV−1 dynamical model was developed which incorporate AIDS-related cancer cells in which cancer cells, healthy CD4+ t-cells lymphocytes and infected CD4+ t-cells lymphocytes can have six equilibria, in that order.

Assuming that the cancer-immune system interactions dynamics is governed by cancer cells proliferation and their interaction with the immune system, thus our first aim in this chapter is to present the fact that in the absence of the cancer and HIV infections, the governing dynamics of the extended model tends to the expected physiological level and derive the corresponding stability conditions of the extended model. Our second aim is to develop a fitted operator numerical method, analyse, implement and present our numerical results with regard to the governing dynamics.

The rest of chapter is organized in the following way. In Section 4.2, we analyse

the extended model, whereas in Section 4.3 we derive, analyse our numerical method. We present our numerical results in Section 4.4 and conclude the chapter with Section 4.5.

4.2 Mathematical analysis of the model

First and foremost, we verify that the extended model in equation (4.1.3) reflects the normal physiological level (α/μ_1) of the healthy effector cells E, as it is determined by Fory$\acute{s}$ and Poleszczuk in [41]. To do that, we solve equation (4.1.3) in the absence of the cancer cells ($T \equiv 0$) and HIV-infected effector cells ($I \equiv 0$). Thus, in such absence the system of DPDEs in equation (4.1.3) reduces to,

$$\frac{dE}{dt} - d_2 \Delta E + \mu_1 E = \alpha. \tag{4.2.1}$$

Following the techniques in [23], we have

$$E(x,t) = u(x) + w(x,t), \tag{4.2.2}$$

where, $u := f(x)$ is independent of the time t and satisfies the boundary value problem (BVP)

$$-d_2 u_{xx} + \mu_1 u = \alpha, \text{ with } u'(0) = u'(x_f) = 0, \tag{4.2.3}$$

and $w := f(x,t)$, which satisfies the BVP

$$w_t = d_2 w_{xx} - \mu_1 w, \text{ with } w'(0) = w'(x_f) = 0 \text{ and } w(x,0) = -u(x). \tag{4.2.4}$$

Since the solution for the homogeneous ordinary differential equation (ODE) in equation (4.2.3) is

$$u_c(x) = c_1 \exp\left(-\sqrt{\frac{\mu_1}{d_2}}x\right) + c_2 \exp\left(\sqrt{\frac{\mu_1}{d_2}}x\right), \tag{4.2.5}$$

then we let the corresponding particular solution to the ODE in equation (4.2.3) to be

$$u_p(x) = c_3 x + c_4, \tag{4.2.6}$$

where, c_1, c_2, c_3, c_4, are constants to be determined. Thus,

$$\mu_1(c_3 x + c_4) = \alpha, \Rightarrow \mu_1 c_3 x + \mu_1 c_4 = \alpha. \tag{4.2.7}$$

Equating terms of same coefficients in equation (4.2.7), we find $c_3 = 0$ and $c_4 = \frac{\alpha}{\mu_1}$, which implies that the solution to the BVP in equation (4.2.3) becomes

$$u(x) = c_1 \exp\left(-\sqrt{\frac{\mu_1}{d_2}}x\right) + c_2 \exp\left(\sqrt{\frac{\mu_1}{d_2}}x\right) + \frac{\alpha}{\mu_1}. \tag{4.2.8}$$

Using the boundary conditions in equation (4.2.3) we find

$$u'(x) = -c_1\sqrt{\frac{\mu_1}{d_2}} \exp\left(-\sqrt{\frac{\mu_1}{d_2}}x\right) + c_2\sqrt{\frac{\mu_1}{d_2}} \exp\left(\sqrt{\frac{\mu_1}{d_2}}x\right), \tag{4.2.9}$$

so that at $x = 0$, we have

$$u'(0) = -c_1\sqrt{\frac{\mu_1}{d_2}} + c_2\sqrt{\frac{\mu_1}{d_2}} = 0, \tag{4.2.10}$$

which implies that

$$c_1 = c_2. \tag{4.2.11}$$

Similarly, At $x = x_f$, we find

$$u'(x_f) = -c_1\sqrt{\frac{\mu_1}{d_2}}\exp\left(-\sqrt{\frac{\mu_1}{d_2}}x_f\right) + c_2\sqrt{\frac{\mu_1}{d_2}}\exp\left(\sqrt{\frac{\mu_1}{d_2}}x_f\right) = 0, \tag{4.2.12}$$

which is equivalent to

$$c_2\sqrt{\frac{\mu_1}{d_2}}\exp\left(2\sqrt{\frac{\mu_1}{d_2}}x_f\right) = c_1\sqrt{\frac{\mu_1}{d_2}}. \tag{4.2.13}$$

In view of equation (4.2.11), equation (4.2.13) becomes

$$c_2\exp\left(2\sqrt{\frac{\mu_1}{d_2}}x_f\right) = c_2, \Rightarrow c_2 = 0. \tag{4.2.14}$$

Hence, the solution in equation (4.2.8) becomes,

$$u(x) = \frac{\alpha}{\mu_1}. \tag{4.2.15}$$

Let $w(x,t) = X(x)T(t)$, then applying the method of separation of variables [23] to the BVP in (4.2.3), we have

$$X(x)T'(t) = T(t)\left(d_2X''(x) - \mu_1X(x)\right),$$

$$\Rightarrow \frac{T'(t)}{T(t)} = \frac{d_2X''(x) - \mu_1X(x)}{X(x)} = -\varrho^2, \tag{4.2.16}$$

where ϱ is an arbitrary separation constant. Solving for $T(t)$ we have

$$\frac{d}{dt}\left(T(t)\exp(\varrho^2t)\right) = 0, \tag{4.2.17}$$

which is equivalent to

$$T(t)\exp(\varrho^2t) = c_5, \tag{4.2.18}$$

where c_5 is a constant of integration. Hence,

$$T(t) = c_5 \exp(-\varrho^2 t). \tag{4.2.19}$$

Solving for $X(x)$ in equation (4.2.16), we have

$$\begin{aligned} X''(x) + \frac{(\varrho^2 - \mu_1)}{d_2} X(x) = 0, \\ \Rightarrow X(x) = c_6 \cos\left(\sqrt{\frac{(\varrho^2 - \mu_1)}{d_2}} x\right) \\ + c_7 \sin\left(\sqrt{\frac{(\varrho^2 - \mu_1)}{d_2}} x\right). \end{aligned} \tag{4.2.20}$$

Thus,

$$w(x,t) = c_5 \exp(-\varrho^2 t)\left(c_6 \cos\left(\sqrt{\frac{(\varrho^2 - \mu_1)}{d_2}} x\right) + c_7 \sin\left(\sqrt{\frac{(\varrho^2 - \mu_1)}{d_2}} x\right)\right). \tag{4.2.21}$$

Applying the boundary conditions in equation (4.2.3) to the equation in (4.2.21), we have

$$\begin{aligned} w'(x,t) &= -c_5 c_6 \sqrt{\frac{(\varrho^2 - \mu_1)}{d_2}} \exp(-\varrho^2 t) \sin\left(\sqrt{\frac{(\varrho^2 - \mu_1)}{d_2}} x\right) \\ &\quad + c_7 c_5 \sqrt{\frac{(\varrho^2 - \mu_1)}{d_2}} \exp(-\varrho^2 t) \cos\left(\sqrt{\frac{(\varrho^2 - \mu_1)}{d_2}} x\right). \end{aligned} \tag{4.2.22}$$

Assuming that $c_5 \neq 0$, then at $x = 0$, equation (4.2.22) becomes

$$0 = c_7 c_5 \sqrt{\frac{(\varrho^2 - \mu_1)}{d_2}} \exp(-\varrho^2 t), \Rightarrow c_7 = 0. \tag{4.2.23}$$

Thus, at $x = x_f$, we see that $c_6 \neq 0$, so that

$$\begin{aligned} 0 &= -c_5 c_6 \sqrt{\frac{(\varrho^2 - \mu_1)}{d_2}} \exp(-\varrho^2 t) \sin\left(\sqrt{\frac{(\varrho^2 - \mu_1)}{d_2}} x\right) \\ &= \sin\left(\sqrt{\frac{(\varrho^2 - \mu_1)}{d_2}} x_f\right) = 0. \end{aligned} \tag{4.2.24}$$

Hence, for $j = 1, 2, 3, \ldots$, we have from equation (4.2.24) that

$$\sqrt{\frac{(\varrho^2 - \mu_1)}{d_2}} x_f = \pm j\pi. \tag{4.2.25}$$

This implies that

$$w(x,t) = c_j \exp(-\varrho^2 t) \sin(j\pi x), \quad \text{for } j = 1, 2, 3, \ldots. \tag{4.2.26}$$

Thus, in view of the solutions in (4.2.15) and (4.2.26) the equation in (4.2.2) clearly present the fact that in the absence of the tumor and HIV-infected effector cells, the solution $E(t)$ in equation (4.2.2) of the extended model in equation (4.1.3) converges to the normal physiological level α/μ_1 as $t \to \infty$. This implies that our extended model in equation (4.1.3) reflects the normal physiological level (α/μ_1) of the healthy effector cells E, as reported by Fory$\acute{s}$ and Poleszczuk in [41] for the model in equation (4.1.1).

4.2.1 Stability analysis of the equilibria when $\tau = 0$

When the regeneration of lytic granules by the effector cells and breaching of some effector cells into T-cells happens instantaneously, Fory$\acute{s}$ and Poleszczuk in [41] established that when there is no HIV-infected cells, the set $\mathcal{D} = \mathbb{R}^2_+$ is invariant for system (4.1.3) at the unique strictly positive steady state $(\bar{T}, \bar{E}) = (\frac{\mu_1 r_1 - \alpha k_1}{k_1(r_2 - \varepsilon r_1)}, \frac{r_1}{k_1})$, which implies that the immune system is capable to successfully prevent further cancer development. Therefore, for every solution in $\mathcal{D}$ there is $E(t) \leq \max\{E(0), \frac{r_2}{\varepsilon k_1}, \frac{r_1}{k_1}\}$,

such that, if $r_1 > \frac{\alpha k_1}{\mu_1}$,

- for $\varepsilon < \frac{r_2}{r_1}$, then the unique positive steady state $(\bar{T}, \bar{E})$ is globally stable in $\mathcal{D}$,
- for $\varepsilon > \frac{r_2}{r_1}$ there is no positive steady state as $T(t) \to \infty$, $\forall\, t \to \infty$.

Thus, the rate of tumor growth reflected by the parameter r_1 and rate of cancer elimination by the immune system, reflected by the parameter value k_1, plays an integral part in the investigation of the governing dynamics of our model. When the concentration of HIV-infected effector cells is present, Fory$\acute{s}$ and Poleszczuk in [41] showed that the set $\mathcal{D} = \mathbb{R}^3_+$ is invariant for system (4.1.3) at the unique strictly positive steady state $(\bar{T}, \bar{E}, \bar{I}) = (\frac{\mu_1 r_1 - \alpha k_1}{k_1(r_2 - \varepsilon r_1)}, \frac{r_1}{k_1}, 0)$. That is, if $r_1 > \frac{\alpha k_1}{\mu_1}$, then $(0, \frac{\alpha k_1}{\mu_1}, 0)$ is unstable. In addition if $r_1 < \frac{\mu_2 k_1}{k_2}$,

- if $\varepsilon < \frac{r_2}{r_1}$ then $(\frac{\mu_1 - \alpha k_1}{k_1(r_2 - \varepsilon r_1)}, \frac{r_1}{k_1}, 0)$ is locally asymptotic stable,
- if $\alpha > \frac{\mu_1 \mu_2}{k_2}$, then $(0, \frac{\mu_2}{k_2}, \frac{\alpha k_2 - \mu_1 \mu_2}{\mu_2 k_2})$ is locally asymptotic stable.

Thus, the above facts suggest that there is no steady state describing the coexistence of the concentration of cancer and HIV-infected effector cells in vivo, even at the instantaneous pace.

4.2.2 Stability analysis of the equilibria when $\tau > 0$

In this section, we examine the case for the regeneration of lytic granules by the effector cells and breaching of some effector cells into t-cells that require sometimes to take place, with respect to the governing dynamics in the previous section. In view of the governing dynamics mentioned in the previous section, we see that the equilibria for the system in (4.1.3) is same as the equilibria of the corresponding reduced system in equation (4.1.3). Therefore, it suffices to consider the stability for the positive equilibria in equation (4.1.3). Thus, for the extended model in equation (4.1.3), the jacobian matrix is

$$\Delta(\lambda, \tau) = \mathcal{M} + \mathcal{N},$$

where

$$\mathcal{M} = \begin{pmatrix} d_1 & 0 & 0 \\ 0 & d_2 & 0 \\ 0 & 0 & d_3 \end{pmatrix},$$

$$\mathcal{N} = \begin{pmatrix} 0 & -k_1\bar{T} & 0 \\ r_2 - r_1 + (1-\epsilon)r_1\exp(-\lambda\tau) & -\mu_1 - k_1\bar{T} + (1-\varepsilon)k_1\bar{T}\exp(-\lambda\tau) & -k_2\bar{E} \\ 0 & 0 & k_2\bar{E} - \mu_2 \end{pmatrix}.$$

Hence, the characteristic matrix for the steady state for cancer-immune system interactions with the concentration of HIV-infected effector cells is

$$\begin{aligned} \det(\Delta(\lambda,\tau)) &= (d_1-\lambda)[(d_2 - (\mu_1 + k_1\bar{T} - (1-\varepsilon)k_1\bar{T}\exp(-\lambda\tau)) - \lambda](d_3 - (\mu_2 - k_2\bar{E})) - \lambda) \\ &\quad + k_1\bar{T}[(r_2 - r_1 + (1-\varepsilon)r_1\exp(-\lambda\tau)](d_3 - (\mu_2 - k_2\bar{E})) - \lambda), \end{aligned}$$

in which we let

$$\begin{aligned} W(\lambda,\tau) &= \det(\Delta(\lambda,\tau)) = (d_3 - (\mu_2 - k_2\bar{E})) - \lambda)W_2(\lambda,\tau), \\ W_2(\lambda,\tau) &= P(\lambda) + Q(\lambda)\exp(-\lambda\tau), \end{aligned} \tag{4.2.27}$$

where, W_2 denotes the characteristic quasi-polynomial for the reduced two-variable system in (4.1.3) with $I \equiv 0$,

$$\begin{aligned} P(\lambda) &= (d_1-\lambda)(d_2 - (\mu_1 + k_1\bar{T}) - \lambda) + (r_2 - r_1)k_1\bar{T}, \\ &= \lambda^2 + (\mu_1 + k_1\bar{T} - (d_1+d_2))\lambda + (r_2 - r_1)k_1\bar{T} + d_1d_2, \end{aligned}$$

and

$$\begin{aligned} Q(\lambda) &= k_1\bar{T}(1-\varepsilon)(-\lambda + r_1), \\ &= -k_1\bar{T}\lambda + \varepsilon k_1\bar{T}\lambda + r_1k_1\bar{T} - \varepsilon r_1k_1\bar{T}. \end{aligned}$$

Since $\exp(-\lambda\tau) > 0$ for all values of λ and τ, then we have

$$P(\lambda) + Q(\lambda) = \lambda^2 + (\mu_1 + \varepsilon k_1\bar{T} - (d_1 + d_2))\lambda + r_2k_1\bar{T} - \varepsilon r_1k_1\bar{T} + d_1d_2.$$

However, the Routh-Hurwitz criteria requires that, all the roots of (4.2.27) have negative real parts. This implies that

$$(d_3 - (\mu_2 - k_2\bar{E})) > 0,\ (\mu_1 + \varepsilon k_1\bar{T} - (d_1 + d_2)) > 0 \text{ and } r_2k_1\bar{T} - \varepsilon r_1k_1\bar{T} + d_1d_2 > 0,$$

which is equivalent to

$$\mu_2 < k_2\bar{E} - d_3,\ (\mu_1 + \varepsilon k_1\bar{T}) > d_1 + d_2,\ r_2k_1\bar{T} + d_1d_2 > \varepsilon r_1k_1\bar{T}.$$

This enable us to obtain the following results.

Corollary 4.2.1. *If $r_2k_1\bar{T} + d_1d_2 > \varepsilon r_1k_1\bar{T}$ and*

- *$\mu_2 < k_2\bar{E} - d_3$, then if $(\frac{\mu_1 - \alpha k_1}{k_1(r_2 - \varepsilon r_1)}, \frac{r_1}{k_1})$ is stable as a steady state in the two-variable system, then $(\frac{\mu_1 - \alpha k_1}{k_1(r_2 - \varepsilon r_1)}, \frac{r_1}{k_1}, 0)$ is stable as a steady state for system in equation (4.1.3),*
- *$\mu_2 > k_2\bar{E} - d_3$, then $(\frac{\mu_1 - \alpha k_1}{k_1(r_2 - \varepsilon r_1)}, \frac{r_1}{k_1}, 0)$ is unstable.*

Since there is no steady state describing the coexistence of the tumor cells with the HIV infection in vivo and in view of the results in Corollary (4.2.1), we see that the equilibria for the system in (4.1.3) under the governing dynamics are the same as for the governing dynamics without the infection. Then in the next section it suffices to examine the existence of Hopf bifurcation for the reduced (two-variable) system in equation (4.1.3).

4.2.3 Existence of Hopf bifurcation

If $r_2k_1\bar{T}_3 + d_1d_2 > \varepsilon r_1k_1\bar{T}_3$, then $(\frac{\mu_1 - \alpha k_1}{k_1(r_2 - \varepsilon r_1)}, \frac{r_1}{k_1})$ is stable for $\tau = 0$. Therefore, for stability switches, we follow the ideas from Cooke and Driessche in [30], which state

that the necessary condition for stability switches is the existence of purely imaginary eigenvalue

$$\lambda = i\omega,\ \omega > 0 \text{ for some threshold value } \tau_{th}.$$

If $i\omega$ is an eigenvalue for τ_{th}, then

$$W_2(i\omega, \tau_{th}) = 0 \Rightarrow P(i\omega) = -Q(i\omega)\exp(i\omega\tau_{th}),$$

which implies

$$\|P(i\omega)\| = \|Q(i\omega)\|.$$

Defining

$$F(\omega) = \|P(i\omega)\|^2 - \|Q(i\omega)\|^2,$$

where

$$F(y) = y^2 + Ay + B,\ y = \omega^2,$$

$$\begin{aligned} A &= \varepsilon(2-\varepsilon)k_1^2\bar{T}^2 + 2(\mu_1 - r_2 + r_1)k_1\bar{T} + \mu_1^2 - 2(\mu_1 + k_1\bar{T})d_1d_2 + d_1^2d_2^2 > 0, \\ B &= (r_2 - r_1(2-\varepsilon))(r_2 - r_1\varepsilon)k_1^2\bar{T}^2 > 0, \end{aligned}$$

if $r_2 - r_1\varepsilon > 0$, $\varepsilon < 1$, and if

- $r_2 - r_1(2-\varepsilon) > 0$, then there is no positive roots of F.
- $r_2 - r_1(2-\varepsilon) < 0$, then F has exactly one positive root $\bar{y}$.

The above two facts enable us to state the following results.

Theorem 4.2.2. *Assume that the steady state* $(\frac{\mu_1 - \alpha k_1}{k_1(r_2 - \varepsilon r_1)}, \frac{r_1}{k_1})$ *exists. Then if*

- $r_2 - r_1(2-\epsilon) > 0$, *then* $(\bar{T}, \bar{E})$ *is stable for any positive delay* $\tau > 0$.
- $r_2 - r_1(2-\varepsilon) < 0$, *then there exists the threshold delay* $\tau_{th} > 0$ *such that* $(\bar{T}, \bar{E})$ *is stable for* $\tau < \tau_{th}$, *loses stability at* $\tau = \tau_{th}$ *in which Hopf bifurcation occurs.*

Remark 4.2.3. *From the analysis presented above it is obvious that the state*

$$(\frac{\mu_1 - \alpha k_1}{k_1(r_2 - \varepsilon r_1)}, \frac{r_1}{k_1}, 0),$$

cannot recover stability for larger values of τ.

4.3 Derivation and analysis of the numerical method

In this section, we describe the derivation of the fitted numerical method for solving the system in equation (4.1.3). We determine an approximation to the derivatives of the functions $T(t,x), E(t,x)$ and $I(t,x)$ with respect to the spatial variable x.

Let N_x be a positive integer. Discretize the interval $[0, x_f]$ through the points

$$x_0 = 0 < x_1 < x_2 < \cdots < x_{N_x} = x_f,$$

where the step-size $\Delta x = x_{j+1} - x_j = x_f/N_x,\ j = 0, 1, \ldots, x_f$. Let $\mathcal{T}_j(t), \mathcal{E}_j(t), \mathcal{I}_j(t)$ denote the numerical approximations of $T(t,j), E(t,j), I(t,j)$, then we approximate the second order spatial derivative terms by

$$\Delta T(t,x_j) \approx \frac{\mathcal{T}_{j+1} - 2\mathcal{T}_j + \mathcal{T}_{j-1}}{\phi_T^2},\ \Delta E(t,x_j) \approx \frac{\mathcal{E}_{j+1} - 2\mathcal{E}_j + \mathcal{E}_{j-1}}{\phi_E^2},$$
$$\Delta I(t,x_j) \approx \frac{\mathcal{I}_{j+1} - 2\mathcal{I}_j + \mathcal{I}_{j-1}}{\phi_j^2}, \tag{4.3.1}$$

where

$$\phi_T^2 = \frac{(\exp(\sigma_T \Delta x) - 1)}{\sigma_T},\ (\phi_E)_j = \frac{4}{\sigma_E^2}\sinh^2\left(\frac{\sigma_E \Delta x}{2}\right),\ \phi_I = \frac{4}{\sigma_I^2}\sinh^2\left(\frac{\sigma_I \Delta x}{2}\right),$$

and

$$\sigma_T = \sqrt{\frac{r_1}{d_1}},\ \sigma_E = \sqrt{\frac{\mu_1}{d_2}},\ \sigma_I = \sqrt{\frac{\mu_2}{d_3}}.$$

It is not that difficult to see that $\phi_T \to \Delta x$, $\phi_E \to \Delta x$ and $\phi_I \to \Delta x$, as $\Delta x \to 0$.

Let N_t be a positive integer and $\Delta t = t_f/N_t$ where $0 < t < t_f$. Discretizing the time interval $[0, t_f]$ through the points

$$0 = t_0 < t_1 < \cdots < t_{N_t} = t_f,$$

where

$$t_{n+1} - t_n = \Delta t,\ n = 0, 1, \ldots, (t_f - 1).$$

We approximate the time derivative at t_n by

$$\frac{d\mathcal{T}_j(t_n)}{dt} \approx \frac{\mathcal{T}_j^{n+1} - \mathcal{T}_j^n}{\psi_T}, \frac{d\mathcal{E}_j(t_n)}{dt} \approx \frac{\mathcal{E}_j^{n+1} - \mathcal{E}_j^n}{\psi_E}, \frac{d\mathcal{I}_j(t_n)}{dt} \approx \frac{\mathcal{I}_j^{n+1} - \mathcal{I}_j^n}{\psi_I}, \tag{4.3.2}$$

where

$$\psi_T = (1 - \exp(-r_1\Delta t) - 1)/r_1,\ \psi_E = (\exp(\mu_1\Delta t) - 1)/\mu_1,\ \psi_I = (\exp(\mu_2\Delta t) - 1)/\mu_2,$$

where we see that $\psi_T \to \Delta t$, $\psi_E \to \Delta t$ and $\psi_I \to \Delta t$ as $\Delta t \to 0$.

The denominator functions in (4.3.1) and (4.3.2) are used explicitly to remove the inherent stiffness in the central finite derivatives parts and are derived by using the theory of nonstandard finite difference methods, see, e.g., [84, 103, 104] and references therein.

Combining the equation (4.3.1) for the spatial derivatives with equation (4.3.2) for

time derivatives, we obtain

$$\left.\begin{aligned}
&\tfrac{\mathcal{T}_j^{n+1}-\mathcal{T}_j^n}{\psi_T} = d_1\tfrac{\mathcal{T}_{j+1}^{n+1}-2\mathcal{T}_j^{n+1}+\mathcal{T}_{j-1}^{n+1}}{\phi_T^2} + r_1\mathcal{T}_j^n - k_1\mathcal{T}_j^n\mathcal{E}_j^n,\\
&\tfrac{\mathcal{E}_j^{n+1}-\mathcal{E}_j^n}{\psi_E} = d_2\tfrac{\mathcal{E}_{j+1}^{n+1}-2\mathcal{E}_j^{n+1}+\mathcal{E}_{j-1}^{n+1}}{\phi_E^2} + r_2\mathcal{T}_j^n - \mu_1\mathcal{E}_j^n - k_1\mathcal{T}_j^n\mathcal{E}_j^n\\
&\qquad\qquad +(1-\varepsilon)k_1(\mathcal{H}_T)_j^n(\mathcal{H}_E)_j^n - k_2'\mathcal{E}_j^n\mathcal{I}_j^n + \alpha,\\
&\tfrac{\mathcal{I}_j^{n+1}-\mathcal{I}_j^n}{\psi_I} = d_3\tfrac{\mathcal{I}_{j+1}^{n+1}-2\mathcal{I}_j^{n+1}+\mathcal{I}_{j-1}^{n+1}}{\phi_I^2} + k_2\mathcal{E}_j^n\mathcal{I}_j^n - \mu_2\mathcal{I}_j^n,\\
&\mathcal{T}_1^n = \mathcal{T}_{-1}^n,\ \mathcal{E}_1^n = \mathcal{E}_{-1}^n,\ \mathcal{I}_1^n = \mathcal{I}_{-1}^n,\\
&\mathcal{T}_{x_f}^n = \mathcal{T}_{x_f-1}^n,\ \mathcal{E}_{x_f}^n = \mathcal{E}_{x_f-1}^n,\ \mathcal{I}_{x_f}^n = \mathcal{I}_{x_f-1}^n,\\
&\mathcal{E}_j^0 = 780,\ \mathcal{T}_j^0 = 10,\ \mathcal{I}_j^0 = 10.
\end{aligned}\right\} \tag{4.3.3}$$

where

$$(\mathcal{H}_T)_j^n \approx T(t_n-\tau, x_j) \text{ and } (\mathcal{H}_E)_j^n \approx E(t_n-\tau, x_j), \tag{4.3.4}$$

are the history functions corresponding to the equations in T and E for $j = 1, 2, \ldots, x_f - 1$, $n = 0, 1, \ldots, t_f - 1$.

The system in equation (4.3.3) can be further be simplified as

$$\left.\begin{aligned}
&-\tfrac{d_1}{\phi_T^2}\mathcal{T}_{j-1}^{n+1} + \left(\tfrac{1}{\psi_T} + \tfrac{2d_1}{\phi_T^2}\right)\mathcal{T}_j^{n+1} - \tfrac{d_1}{\phi_T^2}\mathcal{T}_{j+1}^{n+1} = \left(\tfrac{1}{\psi_T} + r_1\right)\mathcal{T}_j^n - k_1\mathcal{T}_j^n\mathcal{E}_j^n,\\
&-\tfrac{d_2}{\phi_E^2}\mathcal{E}_{j-1}^{n+1} + \left(\tfrac{1}{\psi_E} + \tfrac{2d_2}{\phi_E^2}\right)\mathcal{E}_j^{n+1} - \tfrac{d_2}{\phi_E^2}\mathcal{E}_{j+1}^{n+1} = r_2\mathcal{T}_j^n\\
&+\left(\tfrac{1}{\psi_E} - \mu_1\right)\mathcal{E}_j^n - k_1\mathcal{T}_j^n\mathcal{E}_j^n + (1-\varepsilon)k_1(\mathcal{H}_T)_j^n(\mathcal{H}_E)_j^n - k_2'\mathcal{E}_j^n\mathcal{I}_j^n + \alpha,\\
&-\tfrac{d_3}{\phi_I^2}\mathcal{I}_{j-1}^{n+1} + \left(\tfrac{1}{\psi_I} + \tfrac{2d_3}{\phi_I^2}\right)\mathcal{I}_j^n - \tfrac{d_3}{\phi_I^2}\mathcal{I}_{j+1}^{n+1} = k_2\mathcal{E}_j^n\mathcal{I}_j^n + \left(\tfrac{1}{\psi_I} - \mu_2\right)\mathcal{I}_j^n.
\end{aligned}\right\} \tag{4.3.5}$$

Consequently, the system in equation (4.3.5) can be written as a tridiagonal system

given by

$$\left.\begin{aligned} A_T\mathcal{T}_j^{n+1} &= \left(\tfrac{1}{\psi_T}+r_1\right)\mathcal{T}_j^n - k_1\mathcal{T}_j^n\mathcal{E}_j^n, \\ A_E\mathcal{E}_j^{n+1} &= r_2\mathcal{T}_j^n + \left(\tfrac{1}{\psi_E}-\mu_1\right)\mathcal{E}_j^n - k_1\mathcal{T}_j^n\mathcal{E}_j^n + (1-\varepsilon)k_1(\mathcal{H}_T)_j^n(\mathcal{H}_E)_j^n \\ &\quad -k_2'\mathcal{E}_j^n\mathcal{I}_j^n + \alpha, \\ A_I\mathcal{I}_j^{n+1} &= k_2\mathcal{E}_j^n\mathcal{I}_j^n + \left(\tfrac{1}{\psi_I}-\mu_2\right)\mathcal{I}_j^n, \end{aligned}\right\} \tag{4.3.6}$$

where $j = 1, \ldots, x_f - 1$, $n = 0, \ldots, t_f - 1$ and

$$\left.\begin{aligned} A_T &= \text{Tri}\left(-\tfrac{d_1}{\phi_T)^2}, \tfrac{1}{\psi_T}+\tfrac{2d_1}{\phi_T^2}, -\tfrac{d_1}{\phi_T^2}\right),\ A_E = \text{Tri}\left(\tfrac{d_2}{\phi_E^2}, \tfrac{1}{\psi_E}+\tfrac{2d_2}{\phi_E^2}, \tfrac{d_2}{\phi_E^2}\right), \\ A_I &= \text{Tri}\left(-\tfrac{d_3}{\phi_I^2}, \tfrac{1}{\psi_I}+\tfrac{2d_3}{\phi_I^2}, -\tfrac{d_3}{\phi_I^2}\right). \end{aligned}\right\}$$

On the interval $[0, \tau]$ the delayed arguments $t_n - \tau$ belong to $[-\tau, 0]$, and therefore the delayed variables in equation (4.3.6) are evaluated directly from the history functions $T^0(t,x), E^0(t,x)$ as

$$(\mathcal{H}_T)_j^n \approx T^0(t_n - \tau, x_j) \text{ and } (\mathcal{H}_E)_j^n \approx E^0(t_n - \tau, x_j), \tag{4.3.7}$$

and equation (4.3.6) becomes

$$\left.\begin{aligned} A_T\mathcal{T}_j^{n+1} &= \left(\tfrac{1}{\psi_T}+r_1\right)\mathcal{T}_j^n - k_1\mathcal{T}_j^n\mathcal{E}_j^n, \\ A_E\mathcal{E}_j^{n+1} &= r_2\mathcal{T}_j^n + \left(\tfrac{1}{\psi_E}-\mu_1\right)\mathcal{E}_j^n - k_1\mathcal{T}_j^n\mathcal{E}_j^n \\ &\quad +(1-\varepsilon)k_1T^0(t_n-\tau,x_j)E^0(t_n-\tau,x_j) - k_2'\mathcal{E}_j^n\mathcal{I}_j^n + \alpha, \\ A_I\mathcal{I}_j^{n+1} &= k_2\mathcal{E}_j^n\mathcal{I}_j^n + \left(\tfrac{1}{\psi_I}-\mu_2\right)\mathcal{I}_j^n. \end{aligned}\right\} \tag{4.3.8}$$

Let s be the largest integer such that $\tau_s \leq \tau$. By using the system equation (4.3.8) we

can compute $\mathcal{T}_j^n, \mathcal{E}_j^n, \mathcal{I}_j^n$ for $1 \leq n \leq s$. Up to this stage, we interpolate the data

$$(t_0, \mathcal{T}_j^0),\ (t_1, \mathcal{T}_j^1), \ldots, (t_s, \mathcal{T}_j^s) \text{ and } (t_0, \mathcal{E}_j^0),\ (t_1, \mathcal{E}_j^1), \ldots, (t_s, \mathcal{E}_j^s),$$

using an interpolating cubic Hermite spline $\varphi_j(t)$. Then

$$\mathcal{T}_j^n = \varphi_T(t_n, x_j) \text{ and } \mathcal{E}_j^n = \varphi_E(t_n, x_j),$$

for all $n = 0, 1, \ldots, s$ and $j = 1, 2, \ldots, x_f - 1$.

For $n = s+1, s+2, \ldots, t_f - 1$, when we move from level n to level $n+1$ we extend the definitions of the cubic Hermite spline $\varphi_j(t)$ to the point $(t_n + \Delta t, \mathcal{T}_j^n, \mathcal{E}_j^n)$. Then the history terms $(\mathcal{H}_T)_j^n$ and $(\mathcal{H}_E)_j^n$ can be approximated by the functions $\varphi_j(t_n - \tau)$ for $n \geq s$. This implies that,

$$(\mathcal{H}_T)_j^n \approx (\varphi_T)_j(t_n - \tau) \text{ and } (\mathcal{H}_E)_j^n \approx (\varphi_E)_j(t_n - \tau), \tag{4.3.9}$$

and equation (4.3.3) becomes

$$\left.\begin{aligned} A_T\mathcal{T}_j^{n+1} &= \left(\tfrac{1}{\psi_T} + r_1\right)\mathcal{T}_j^n - k_1\mathcal{T}_j^n\mathcal{E}_j^n, \\ A_E\mathcal{E}_j^{n+1} &= r_2\mathcal{T}_j^n + \left(\tfrac{1}{\psi_E} - \mu_1\right)\mathcal{E}_j^n - k_1\mathcal{T}_j^n\mathcal{E}_j^n \\ &\quad +(1-\varepsilon)k_1\varphi_T(t_n-\tau)\varphi_E(t_n-\tau) - k_2'\mathcal{E}_j^n\mathcal{I}_j^n + \alpha, \\ A_I\mathcal{I}_j^{n+1} &= k_2\mathcal{E}_j^n\mathcal{I}_j^n + \left(\tfrac{1}{\psi_I} - \mu_2\right)\mathcal{I}_j^n, \end{aligned}\right\} \tag{4.3.10}$$

where

$$\varphi_T(t_n - \tau) = [(\mathcal{H}_T)_1^n, (\mathcal{H}_T)_2^n \ldots, (\mathcal{H}_T)_{N_x-1}^n]',\ \varphi_E(t_n - \tau) = [(\mathcal{H}_E)_1^n, (\mathcal{H}_E)_2^n \ldots, (\mathcal{H}_E)_{N_x-1}^n]'.$$

Our FOFDM is then consists of equations (4.3.3)-(4.3.10). Re-writing the scheme in

(4.3.10) in a form of a system of equations

$$\left.\begin{aligned} A_T\mathcal{T} &= F_T, \\ A_E\mathcal{E} &= F_E, \\ A_I\mathcal{I} &= F_I. \end{aligned}\right\} \tag{4.3.11}$$

Let the functions

$$T(x,t), E(x,t), I(x,t),$$

and their partial derivatives with respect to both t and x be smooth such that they satisfy

$$\begin{aligned} \left|\frac{\partial^{i+j}T(t,x)}{\partial t^i x^j}\right| &\leq \Upsilon_T, \left|\frac{\partial^{i+j}E(t,x)}{\partial t^i x^j}\right| \leq \Upsilon_E, \\ \left|\frac{\partial^{i+j}I(t,x)}{\partial t^i x^j}\right| &\leq \Upsilon_I, \forall n, j \geq 0, \end{aligned} \tag{4.3.12}$$

where,

$$\Upsilon_T, \Upsilon_E, \Upsilon_I,$$

are constant that are independent of the time and space step-sizes. Then we see that the local truncation errors $(\varsigma_T)_j^n, (\varsigma_E)_j^n, (\varsigma_I)_j^n$ are given by

$$\left.\begin{aligned} (\varsigma_T)_j^n &= (A_T T)_j^n - (F_T)_j^n = (A_T(T-\mathcal{T}))_j^n, \\ (\varsigma_E)_j^n &= (A_E)_j^n - (F_E)_j^n = (A_E(E-\mathcal{E}))_j^n, \\ (\varsigma_I)_j^n &= (A_I I)_j^n - (F_I)_j^n = (A_I(I-\mathcal{I}))_j^n, \end{aligned}\right\} \tag{4.3.13}$$

Thus,

$$\left.\begin{array}{l} \max_{n,j} |T_j^n - \mathcal{T}_j^n| \leq ||A_T^{-1}|| \max_{n,j} |\varsigma_T|, \\ \max_{n,j} |E_j^n - \mathcal{E}_j^n| \leq ||A_E^{-1}|| \max_{n,j} |\varsigma_E|, \\ \max_{n,j} |I_j^n - \mathcal{I}_j^n| \leq ||A_I^{-1}|| \max_{n,j} |\varsigma_I|, \end{array}\right\} \tag{4.3.14}$$

where

$$\left.\begin{array}{l} \max_{n,j} |\varsigma_T| \leq \frac{\Delta t}{2} |T_{tt}(\xi, x_j)| + \frac{(\Delta x)^2}{12} |T_{xxxx}(t_n, \zeta)|, \\ \max_{n,j} |\varsigma_E| \leq \frac{\Delta t}{2} |E_{tt}(\xi, x_j)| + \frac{(\Delta x)^2}{12} |E_{xxxx}(t_n, \zeta)|, \\ \max_{n,j} |\varsigma_I| \leq \frac{\Delta t}{2} |I_{tt}(\xi, x_j)| + \frac{(\Delta x)^2}{12} |I_{xxxx}(t_n, \zeta)|. \end{array}\right\} \tag{4.3.15}$$

In view of the inequalities in (4.3.12), we see that inequalities in (4.3.15) are equivalent to

$$\left.\begin{array}{l} \max_{n,j} |\varsigma_T| \leq \left(\frac{\Delta t}{2} + \frac{(\Delta x)^2}{12}\right) \Upsilon_T, \\ \max_{n,j} |\varsigma_E| \leq \left(\frac{\Delta t}{2} + \frac{(\Delta x)^2}{12}\right) \Upsilon_E, \\ \max_{n,j} |\varsigma_I| \leq \left(\frac{\Delta t}{2} + \frac{(\Delta x)^2}{12}\right) \Upsilon_I. \end{array}\right\} \tag{4.3.16}$$

$t_{n-1} \leq \xi \leq t_{n+1}, x_{j-1} \leq \zeta \leq x_{j+1}$ and by the result in [117], we obtain

$$\left.\begin{aligned} ||A_T^{-1}|| &\leq \Xi_T, \\ ||A_E^{-1}|| &\leq \Xi_E, \\ ||A_I^{-1}|| &\leq \Xi_I. \end{aligned}\right\} \tag{4.3.17}$$

Using (4.3.16) and (4.3.17) into (4.3.14), we obtain the following results.

Theorem 4.3.1. *Let*

$$F_T(x,t), F_E(x,t), F_I(x,t),$$

be sufficiently smooth functions so that $T(x,t), E(x,t), I(x,t) \in C^{\infty}([0,t_f] \times [0,x_f])$. *Let* $(\mathcal{T}_j^n, \mathcal{E}_j^n, \mathcal{I}_j^n)$, $j = 1, 2, \ldots x_f, n = 1, 2, \ldots t_f$ *be the approximate solutions to (4.1.3), obtained using the FOFDM with* $\mathcal{T}_j^0 = T_j^0, \mathcal{E}_j^0 = E_j^0, \mathcal{I}_j^0 = I_j^0,$. *Then there exists* Ξ_T, Ξ_E, Ξ_I *independent of the step sizes* Δt *and* Δx *such that*

$$\left.\begin{aligned} \max_{n,j} |T_j^n - \mathcal{T}_j^n| &\leq \Xi_T[\tfrac{\Delta t}{2} + \tfrac{(\Delta x)^2}{12}]\Upsilon_T, \\ \max_{n,j} |E_j^n - \mathcal{E}_j^n| &\leq \Xi_E[\tfrac{\Delta t}{2} + \tfrac{(\Delta x)^2}{12}]\Upsilon_E, \\ \max_{n,j} |I_j^n - \mathcal{I}_j^n| &\leq \Xi_I[\tfrac{\Delta t}{2} + \tfrac{(\Delta x)^2}{12}]\Upsilon_I. \end{aligned}\right\} \tag{4.3.18}$$

Hence, we conclude our analysis with the following result.

Theorem 4.3.2. (Fatunla [39], Trefethen [123]) *A difference scheme is convergent if and only if it is consistent and stable.*

4.4 Numerical results and discussions

Taking the diffusion constants d_1, d_2, d_3 in $[10^{-1}, 10^{-20}]$, using the parameter values in Table 4.5.1, and the fact that the regeneration of lytic granules by the effector cells and the breaching of some effector cells into T-cells requires some time τ to happened, then we present our numerical solutions for the case when $\tau \neq 0$ and $\tau = 0$ as follows. In (a) and (b), we have the situation when a host is infected by the concentration of cancer cells only, (c) and (d), the situation when a host is infected by the concentrations of cancer cells, then becomes infected with HIV at a later stage, whereas in (e) and (f) we have the case when a host is infected with HIV then at a later stage becomes infected with cancer too.

In (a), we see the immune cells raising to their equilibrium, whereas the cancer cells drastically being reduced to nothing. We also see similar interactions in (b) even though the immune healthy effector healthy cells start with a slow decrease due to the infection inflicted by the cancer cells, before it converges to its steady state.

In (c) and (d), the situation which is depicted in (a) and (b) changes, due to the introduction of the HIV-infected effector cells. In (c), we see healthy effector cells raises before the introduction of the HIV-infected effector cells. We also see that HIV-infected cells raised to some magnitude which causes the healthy cells to drop drastically to a low steady state. As soon as the healthy effector cells drops low so does the HIV-infected cells. This, we see that it paves the way for cancer cells to raise. In (d,) we see similar behaviors to the behaviors in (c) at a magnified pace.

In (e), we see HIV-infected cells raising causing the healthy immune cells to fluctuate towards their equilibria. Such fluctuations can be seen in the behaviour of the HIV-infected cells due to the strength of the immune healthy cells. However, the introduction of cancer cells weakened the immune healthy cells which in turn subject the HIV-infected cells to raise to a high level. The dynamics in (f) are straight forward except that the HIV-infected cells eventual converge to their low equilibrium. This is due to the impaired healthy immune healthy cells by both infections.

4.5 Conclusion

In this chapter, we investigated the extended model arising in HIV related cancer-immune system dynamics and we were able to show that the physiological level of our extended model coincides with the original model in equation (4.1.1). Our numerical results present a clear fact played by the inclusion of a delay term (τ) in the dynamics of our extended model. We also see the crucial agreement of our results that the healthy immune system is able to successfully prevent the development of the cancer infection in a host and unable to do so when a host is infected by an additional infection, such as HIV. However, when a host is infected with HIV our results clearly shows that the healthy immune system is unable to prevent further development of the HIV-infected cells. Consequently, our results also present the fact that the weakened immune system cannot prevent the growth of the cancerous cells. Thus, our contribution in this chapter, should be seen as the first attempt to provide an in depth information about the growth rate of tumor cells which is relatively larger than the rate of elimination of cancerous cells by the healthy immune system.

Table 4.5.1: Values of the parameters used in the model (4.3.3) [41]

r_1[81]	k_1[81]	r_2	α/μ_1[46]	k_2'[81]	k_3[32]
$0.05 \sim 0.5$	$10^{-5} \sim 10^{-3}$	$0 \sim 0.05$	$800 \sim 1200$	$10^{-5} \sim 5 \times 10^{-4}$	2.4×10^{-5}
μ_2[81]	δ[107]	c[107]	μ_1	ε[17]	N[32]
0.3	$0.3 \sim 0.7$	$2.1 \sim 3.8$	0.03	0.1	$100 \sim 2000$
r_1	k_1	r_2[64]	α/μ_1	k_2'	k_3
0.1	10^{-4}	0.03	800	5×10^{-5}	2.4×10^{-5}
μ_2	δ	c	μ_1[64]	ϵ	N
0.3	0.3	3.8	0.03	0.1	275

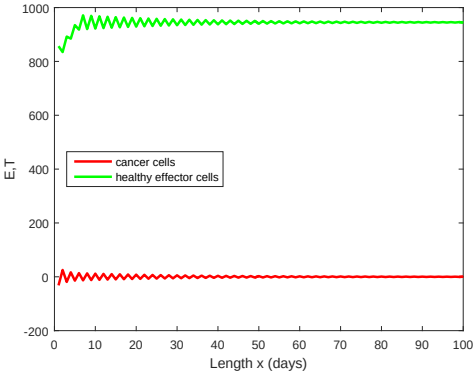

(a) Behavior of the concentrations of cancer and healthy effector cells with delay = 5days.

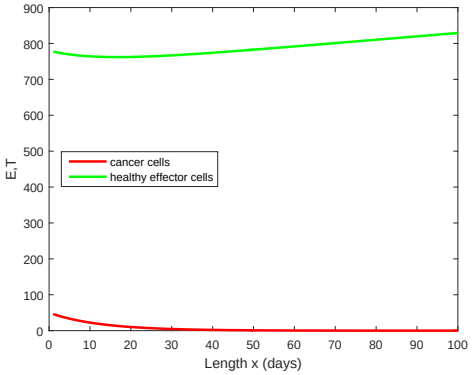

(b) Behavior of the concentrations of cancer and healthy effector cells without delay.

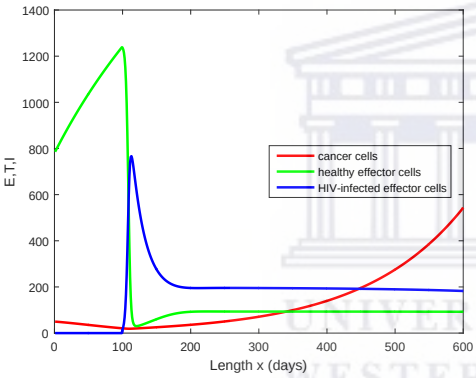

(c) Behavior of the concentration of cancer and healthy effector cells with the introduction of HIV-infected effector cells with delay = 5 days.

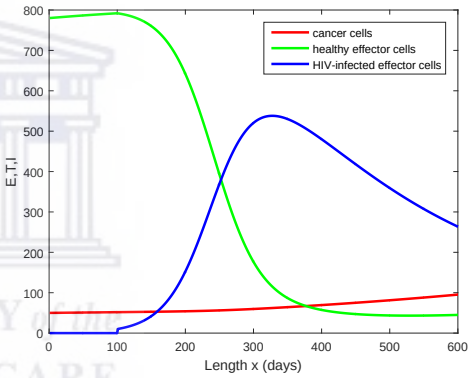

(d) Behavior of the concentrations of cancer and healthy effector cells with the introduction of HIV-infected effector cells without delay.

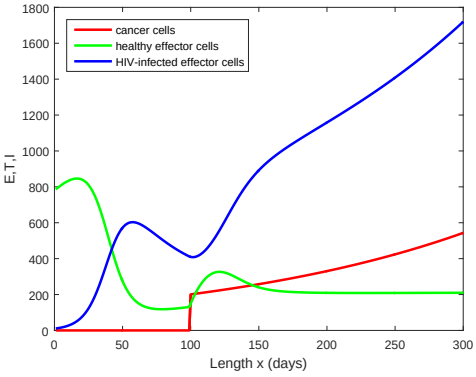

(e) Behavior of the concentrations of healthy and HIV-infected effector cells with the introduction of the concentration of cancer cells with delay = 5 days.

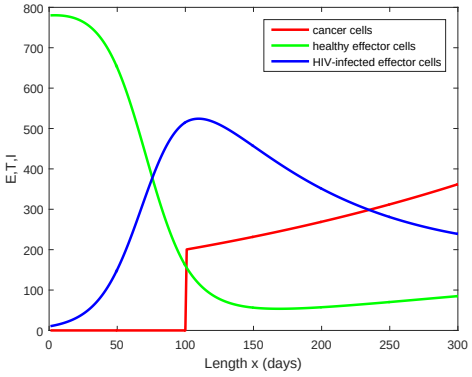

(f) Behavior of the concentration of healthy and HIV-infected effector cells with the introduction of the concentration of cancer cells without delay

Figure 4.5.1: Numerical solution of the concentrations of cancer, HIV-infected and healthy effector cells interaction model.

Having considered the dynamics of the double infection, we are intensifying our consideration in the Chapter 5 by considering the dynamics of tumour cells within their micro-environment.

Chapter 5

A fitted operator method for solving a mathematical model describing tumor cells dynamics in their micro-environment

We consider a quasi non-linear reaction-diffusion model designed to mimic tumor cells' proliferation and migration under the influence of their micro-environment in vitro. Since the model can be used to generate hypotheses regarding the development of drugs which confine tumor growth, then considering the composition of the model, we modify the model by incorporating realistic effects which we believe can shed more light into the original model. We do this by extending the quasi non-linear reaction-diffusion model to a system of discrete delay quasi non-linear reaction-diffusion model. Thus, we determine the equilibria, provide the conditions for global stability of the equilibria by using the method of upper and lower solutions and analyze the extended model for the existence of Hopf bifurcation and present the conditions for Hopf bifurcation to occur. Since it is not possible to solve the models analytically, we derive, analyze, implement a fitted operator method and present our results for the extended model. Our numerical

method is analyzed for convergence and we find that is of second order accuracy. We present our numerical results for both of the models for comparison purposes.

5.1 The model

Before highlighting the system of non linear reaction-diffusion models modeling an in-vitro situation of tumor cells in their micro-environment with regard to its growth, metastasis derived and experimented in [63] and simulated in [42], we would like to mention that Friedman and Kim in [42] mentioned that tumor cells proliferate at different rates and migrate in different patterns depending on the micro-environment in which they are embedded.

Tumor micro-environment includes various cell types such as epithelial cells, fibroblasts, myofibroblasts, endothelial cells, and inflammatory cells. These cells communicate with one another and influence each other behavior by means of the cytokines and growth factors they secrete. Thus, in an effort to understand the interaction between tumor cells, fibroblasts and/or myofibroblasts at an early stage of cancer, Friedman

and Kim in [42] simulated the model derived in [63] an in-vitro model as

$$\left.\begin{aligned}
\tfrac{\partial n}{\partial t} &= \underbrace{\frac{\partial}{\partial x}\left(D_n \frac{\partial n}{\partial x}\right)}_{\text{Random walk}} - \tfrac{\partial}{\partial x}\left(\underbrace{\chi_n n \frac{\frac{\partial E}{\partial x}}{\sqrt{1+(\frac{\partial E}{\partial x}/\lambda_E)^2}}}_{\text{Chemotaxis}}\right) \\
&+ \underbrace{a_{11}\frac{E^4}{k_E^4+E^4} n(1-n/\kappa)}_{\text{Proliferation}}, \quad 0<x<L/2, \\
\tfrac{\partial f}{\partial t} &= \underbrace{\frac{\partial}{\partial x}\left(D_f \frac{\partial f}{\partial x}\right)}_{\text{Random walk}} - \underbrace{a_{21}Gf}_{f\to m} + \underbrace{a_{22}f}_{\text{Proliferation}}, \quad -L/2<x<0, \\
\tfrac{\partial m}{\partial t} &= \underbrace{\frac{\partial}{\partial x}\left(D_m \frac{\partial m}{\partial x}\right)}_{\text{Random walk}} - \underbrace{\frac{\partial}{\partial x}\left(\chi_m m \frac{\frac{\partial G}{\partial x}}{\sqrt{1+(\frac{\partial G}{\partial x}/\lambda_G)^2}}\right)}_{\text{Chemotaxis}} + \underbrace{a_{21}Gf}_{f\to m} \\
&+ \underbrace{a_{31}m}_{\text{Proliferation}}, \quad -L/2<x<0, \\
\tfrac{\partial E}{\partial t} &= \underbrace{\frac{\partial}{\partial x}\left(D_E \frac{\partial E}{\partial x}\right)}_{\text{Diffusion}} + \underbrace{a_{41}f + Ba_{41}m)}_{\text{Production}} - \underbrace{a_{43}E}_{\text{Decay}}, \quad -L/2<x<L/2, \\
\tfrac{\partial G}{\partial t} &= \underbrace{\frac{\partial}{\partial x}\left(D_G \frac{\partial G}{\partial x}\right)}_{\text{Diffusion}} + \underbrace{a_{51}n}_{\text{Production}} - \underbrace{a_{52}G}_{\text{Decay}}, \quad -L/2<x<L/2,
\end{aligned}\right\} \tag{5.1.1}$$

where, transformed epithelial cells (TECs), fibroblasts and myfibroblasts are denoted by n, f and m respectively, in equation (5.1.1), are placed in a trans-well, separated by a semi-permeable membrane. The membrane has small micro-holes ($\approx 0.4\mu m$ diameter) to allow the epidermal growth factor (EGF) and transformed growth factor (TGF-β))

to pass through the membrane from one compartment to another. These molecules are denoted by E and G, respectively, and the length of the compartment is denoted by L in equation (5.1.1). Friedman and Kim [42] main conclusions' are

- fibroblasts enhance proliferation of breast cancer cell lines,
- transformed epithelial cells (TECs) population is sensitive to membrane permeability and to the transformation rate from fibroblasts to myofibroblasts,
- interaction between transformed epithelial cells (TECs) and fibroblasts promotes not only transformed epithelial cells (TECs) proliferation but also the proliferation of fibroblasts and/or myofibroblasts and the transformation from fibroblasts into myofibroblasts.

Eventhough Friedman and Kim [42], did not present their simulation results explicitly, we realised that their findings are in agreement with assertion in [33, 62], that when epithelial cells are in the breast duct, they are transformed by genetic mutations, from which they begin to form aggregates that secrete higher concentrations of transformed growth factor (TGF-β) and this results into transformation of fibroblasts into myofibroblasts. Consequently, the increased concentration of transformed growth factor (TGF-β) also triggers the fibroblasts and myofibroblasts to secrete higher concentrations of epidermal growth factor (EGF) than in a healthy tissue.

Thus, to capture the higher concentrations of epidermal growth factor (EGF), we believe one has to consider the time required for a complete aggregation of the epithelial cells through the secretion of higher concentrations of epidermal growth factor (EGF) than in a healthy tissue. Denoting the required time by τ, this implies that we extend the quasi non-linear reaction-diffusion model simulated in [42] to mimic tumor cells' proliferation and migration under the influence the micro-environment in vitro in

equation (5.1.1), to a discrete delay quasi non-linear reaction-diffusion model

$$\left.\begin{aligned}
\frac{\partial n}{\partial t} &= \frac{\partial}{\partial x}\left(D_n \frac{\partial n}{\partial x}\right) - \frac{\partial}{\partial x}\left(\chi_n n \frac{\frac{\partial E}{\partial x}}{\sqrt{1+(\frac{\partial E}{\partial x}/\lambda_E)^2}}\right) \\
&\quad + a_{11}\frac{E^4}{k_E^4+E^4} n(1-n/\kappa),\ x \in (0, L/2), \\
\frac{\partial f}{\partial t} &= \frac{\partial}{\partial x}\left(D_f \frac{\partial f}{\partial x}\right) - a_{21} G(x, t-\tau) f(x, t-\tau) \\
&\quad + a_{22} f(x, t-\tau),\ x \in (-L/2, 0), \\
\frac{\partial m}{\partial t} &= \frac{\partial}{\partial x}\left(D_m \frac{\partial m}{\partial x}\right) - \frac{\partial}{\partial x}\left(\chi_m m \frac{\frac{\partial G}{\partial x}}{\sqrt{1+(\frac{\partial G}{\partial x}/\lambda_G)^2}}\right) \\
&\quad + a_{21} G(x, t-\tau) f(x, t-\tau) + a_{31} m,\ x \in (-L/2; 0), \\
\frac{\partial E}{\partial t} &= \frac{\partial}{\partial x}\left(D_E \frac{\partial E}{\partial x}\right) + a_{41} f(x, t-\tau) \\
&\quad + B a_{41} m(x, t-\tau) - a_{43} E,\ x \in (-L/2, L/2), \\
\frac{\partial G}{\partial t} &= \frac{\partial}{\partial x}\left(D_G \frac{\partial G}{\partial x}\right) + a_{51} n(x, t-\tau) - a_{52} G,\ x \in (-L/2, L/2),
\end{aligned}\right\} \tag{5.1.2}$$

with uniform delay τ. We do not include a delay term τ, in the first equation in equation (5.1.2) because we would like to show the sensitivity of TECs to membrane permeability and the attraction of TECs in the direction of the concentration gradient of the epidermal growth factor (EGF) directly. Thus, the time τ is required for the proliferation of fibroblasts into myfibroblasts, which in turn requires some time τ for an increased concentration of transformed growth factor (TGF-β) to triggers the fibroblasts and myofibroblasts to secrete higher concentrations of epidermal growth factor (EGF) should reflects its effects in the growth of the transformed epithelial cells, than in a healthy tissue.

Delay differential equations (DDEs) are widely used for analysis and predictions in various areas of life sciences, see for instance [10], epidemiology see for instance [47], immunology see for instance [112], physiology see for instance [115], and neural

networks see for instance [40, 52]. Since time-delays and/or time-lags, can be related to the duration of certain hidden processes like the stages of the life cycle, the time between infection of a cell and the production of new viruses, the duration of the infectious period, the immune period, then introduction of such time-delays in a differential model significantly increases the complexity of the model. Therefore, our first aim in this chapter is to investigate how the uniform time delay τ affects the dynamics of the models in equation (5.1.2). By applying the Poincaré normal form and the center manifold theorem as in [79, 128] we find conditions on the functions and derive formulas which determine the properties of Hopf bifurcation [118]. More specifically, we show that the semi-positive equilibrium point losses its stability and the system exhibits Hopf bifurcation under certain conditions. Considering the stiffness of system of equations in equation (5.1.2), our second aim is therefore, to develop a fitted operator numerical method based on the qualitative features of the models in equation (5.1.2), in such a way that the numerical method has wider stability region despite the computational complexities associated with it.

Therefore, the boundary conditions for the original model remain unchanged as provided in [42]. That is the fact that the semi-permeable membrane allows concentrations of epidermal growth factor (EGF) and transformed growth factor (TGF-β) to cross over, is represented by the following boundary conditions at the membrane $x = 0$ as

$$\left.\begin{array}{l} \left(D_n\Delta_n - \chi_n n\frac{\Delta E}{\sqrt{1+(|\Delta E|/\lambda_E)^2}}\right)\cdot \upsilon = 0 \quad \text{at} \quad x = 0+, \\ D_f\Delta f\cdot \upsilon = 0 \quad \left(D_m\Delta_m - \chi_m m\frac{\Delta G}{\sqrt{1+(|\Delta G|/\lambda_G)^2}}\right)\cdot \upsilon = 0 \quad \text{at} \quad x = 0-, \end{array}\right\} \tag{5.1.3}$$

and

$$\left.\begin{array}{l} \frac{\partial E^+}{\partial x} = \frac{\partial E^-}{\partial x}, \ -\frac{\partial E^+}{\partial x} + \gamma(E^+ - E^-) = 0, \\ \\ \frac{\partial G^+}{\partial x} = \frac{\partial G^-}{\partial x}, \ -\frac{\partial G^+}{\partial x} + \gamma(g^+ - g^-) = 0, \end{array}\right\} \tag{5.1.4}$$

where,

$$E(x) = \begin{cases} E^+(x) & \text{if} \quad x > 0, \\ \\ E^-(x) & \text{if} \quad x < 0, \end{cases} \qquad G(x) = \begin{cases} G^+(x) & \text{if} \quad x > 0, \\ \\ G^-(x) & \text{if} \quad x < 0, \end{cases}$$

υ is the outward normal, and γ is a positive parameter which is determined by the size and density of the holes in the membrane. The initial conditions [63] become

$$\left.\begin{array}{l} n(x,0) = 1.0\exp(-40(x-1.0)^2), \text{ on } [0, L/2] \times [-\tau, 0], \\ \\ f(x,0) = 1.0\exp(-40x^2)r_f, \text{ on } [-L/2, 0]] \times [-\tau, 0], \\ \\ m(x,0) = 0.00, \text{ on } [-L/2, 0] \times [-\tau, 0], \\ \\ E(x,0) = 1.0, \text{ on } [-L/2, L/2] \times [-\tau, 0], \\ \\ G(x,0) = 1.0, \text{ on } [-L/2, L/2] \times [-\tau, 0]. \end{array}\right\} \tag{5.1.5}$$

The rest of the chapter is organized as follow. Mathematical analysis of the main model is presented in Section 5.2. A robust numerical scheme based on the fitted finite difference technique is formulated in Section 5.3, analysis of the basic properties of this scheme is also examined for convergence. To justify the effectiveness of the proposed schemes, we present some numerical results in Section 5.4. Section 5.5 concludes the

chapter.

5.2 Mathematical analysis of the model

In this section, we carry out the local stability and Hopf Bifurcation analysis and global stability analysis of the equilibria.

5.2.1 Local stability and Hopf Bifurcation analysis

At the equilibria the in-vitro trans-well model in equation (5.1.2) becomes

$$\left.\begin{array}{l} a_{11}\frac{E^4}{k_E^4+E^4}n(1-n/\kappa)=0,\ \ 0<x<L/2, \\ -a_{21}Gf+a_{22}f=0,\quad -L/2<x<0, \\ a_{21}Gf+a_{31}m=0,\ \ -L/2<x<0, \\ a_{41}f+Ba_{41}m-a_{43}E=0,\quad -L<x<L, \\ a_{51}n-a_{52}G=0,\quad -L<x<L. \end{array}\right\} \tag{5.2.1}$$

which implies that

$$\left.\begin{array}{l} n^*=0,\ n^*=\kappa \text{ and } G^*=\frac{a_{51}}{a_{52}}\begin{cases} 0 \text{ if } n^*=0, & \\ \frac{a_{51}}{a_{52}}\kappa, \text{ if } n^*=\kappa, & \end{cases} \text{on } 0<x<L/2, \\ f^*=m^*=0, \text{ on } -L/2<x<0, E^*=0, \text{ on } -L/2<x<L/2. \end{array}\right\} \tag{5.2.2}$$

Therefore, the transwell model in equation (5.1.2) has a trivial equilibrium $(0,0,0,0,0)$ and a semi-positive equilibrium $(\kappa,0,0,0,\frac{a_{51}}{a_{52}}\kappa)$. To analyze the stability of the semi-positive equilibrium $(\kappa,0,0,0,\frac{a_{51}}{a_{52}}\kappa)$, the first step is to linearize the in-vitro trans-well

model in equation (5.1.2) at the equilibria $(n^*, f^*, m^*, E^*, G^*)$ as follow:

$$\frac{\partial U(t)}{\partial t} = d\Delta U(t) + L(U_t), \tag{5.2.3}$$

where,

$$\begin{aligned} d\Delta &= \begin{bmatrix} \frac{\partial}{\partial x}\left(D_n \frac{\partial n}{\partial x}\right) - \frac{\partial}{\partial x}\left(\chi_n n \frac{\frac{\partial E}{\partial x}}{\sqrt{1+(\frac{\partial E}{\partial x}/\lambda_E)^2}}\right), \frac{\partial}{\partial x}\left(D_f \frac{\partial f}{\partial x}\right), \\ \frac{\partial}{\partial x}\left(D_m \frac{\partial m}{\partial x}\right) - \frac{\partial}{\partial x}\left(\chi_m m \frac{\frac{\partial G}{\partial x}}{\sqrt{1+(\frac{\partial G}{\partial x}/\lambda_G)^2}}\right), \frac{\partial}{\partial x}\left(D_E \frac{\partial E}{\partial x}\right), \frac{\partial}{\partial x}\left(D_G \frac{\partial G}{\partial x}\right) \end{bmatrix}, \\ \mathrm{dom}(d\Delta) &= \left\{(n, f, m, E, G)^T : (n, f, m, E, G) \in C([-L/2, L/2]), \mathbb{R}\right\}, \end{aligned}$$

such that the given boundary conditions are satisfied in $[-L/2, L/2]$ and $L : C([-\tau, 0], X) \to X$ is defined as

$$L(\phi) = \begin{pmatrix} 0\phi_1(0) \\ a_{22}\phi_2(0) - a_{21}G^*\phi_2(-\tau) - a_{21}f^*\phi_5(-\tau) \\ a_{31}\phi_3(0) + a_{21}G^*\phi_2(-\tau) + a_{21}f^*\phi_5(-\tau) \\ -a_{43}\phi_3(0) + a_{41}\phi_2(-\tau) + Ba_{41}\phi_3(-\tau) \\ -a_{52}\phi_5(0) + a_{51}\phi_5(-\tau) \end{pmatrix}, \tag{5.2.4}$$

for $\phi = (\phi_1, \phi_2, \phi_3, \phi_4, \phi_5)^T \in C([-\tau, 0], X)$. The characteristic equation of equation in (5.2.3) is

$$\lambda y - d\Delta - L(\exp(\lambda y)) = 0, \text{ where } y \in \mathrm{dom}(d\Delta),\ y \neq 0. \tag{5.2.5}$$

Since the boundary conditions in equation (5.1.3-5.1.4) are of Nuemann type, then the operator $-\Delta$ has eigenvalues $0 = \mu_1 \leq \mu_2 \leq \mu_3 \leq \mu_4 \ldots \mu_i \leq \mu_{i+1} \leq \ldots$ and

$\lim_{i\to\infty}\mu_i = \infty$, with the corresponding eigenfunctions $\Phi(x)$. Substituting

$$y = \sum_{i=0}^{\infty} \Phi(x) \begin{pmatrix} y_{1i} \\ y_{2i} \\ y_{3i} \\ y_{4i} \\ y_{5i} \end{pmatrix}, \tag{5.2.6}$$

into equation (5.2.5) we obtain

$$\begin{pmatrix} 0\phi_1(0) - D_n\mu_i \\ a_{22} - D_f\mu_i - a_{21}G^*\exp(-\lambda\tau) - a_{21}f^*\exp(-\lambda\tau) \\ a_{31} - D_m\mu_i + a_{21}G^*\exp(-\lambda\tau) + a_{21}f^*\exp(-\lambda\tau) \\ -a_{43} - D_E\mu_i + a_{41}\exp(-\lambda\tau) + Ba_{41}\exp(-\lambda\tau) \\ -a_{52} - D_G\mu_i + a_{51}\exp(-\lambda\tau) \end{pmatrix} \begin{pmatrix} y_{1i} \\ y_{2i} \\ y_{3i} \\ y_{4i} \\ y_{5i} \end{pmatrix} = \lambda \begin{pmatrix} y_{1i} \\ y_{2i} \\ y_{3i} \\ y_{4i} \\ y_{5i} \end{pmatrix} \tag{5.2.7}$$

The stability of the positive equilibrium can be determined by the distribution of the roots of (5.2.7). It is locally asymptotically stable if all the roots of equation (5.2.7) have negative real parts for all $i = 0, 1, 2, 3, \ldots$. Obviously, zero is not a root of (5.2.7) for all $i = 0, 1, 2, 3, \ldots$. When $\tau = 0$, we obtain the eigenvalues as

$$\lambda = -D_n\mu_i,\ -D_f\mu_i - a_{21}G^* + a_{22},\ -D_m\mu_i + a_{31},\ -D_e\mu_i,\ -D_g\mu_i. \tag{5.2.8}$$

The eigenvalues in equation (5.2.8) are unconditionally asymptotic stable for the equilibrium point $(0, 0, 0, 0, 0)$ and conditionally asymptotic stable for the equilibrium point $(\kappa, 0, 0, 0, \frac{a_{51}}{a_{52}}\kappa)$ when $a_{22} < \frac{a_{21}a_{51}}{a_{52}}\kappa$. Thus, the following results.

Theorem 5.2.1.

(i) The trivial $(0, 0, 0, 0, 0)$ *equilibrium is unconditional asymptotic stable.*

(ii) If $a_{22} < \frac{a_{21}a_{51}}{a_{52}}\kappa$ *holds, the interior equilibrium* $(\kappa, 0, 0, 0, \frac{a_{51}}{a_{52}}\kappa)$ *of the transwell model in equation (5.1.2) is asymptotically stable.*

When $\tau \neq 0$, we assume that $\lambda = i\omega, (\omega > 0)$. In view of equation (5.2.8), we have

$$i\omega + D_f\mu_k + a_{21}G^*(\cos(\omega\tau) + i\sin(\omega\tau)) - a_{22} = 0, \tag{5.2.9}$$

Separating the real and imaginary parts in equation (5.2.9), we have

$$i\omega + ia_{21}G^*\sin(\omega\tau) = 0,\ D_f\mu_k + a_{21}G^*\cos(\omega\tau) - a_{22} = 0, \tag{5.2.10}$$

which implies that

$$\tau_i = \frac{1}{\omega}\cos^{-1}\left(\frac{a_{22} - D_f\mu_k}{a_{21}G^*} + 2i\pi\right),\ \forall i = 0, 1, 2, 3, \ldots, \tag{5.2.11}$$

and we can show that

$$\text{Sign}\left[\text{Re}\left(\frac{\partial\lambda}{\partial\tau}\right)\right] = \text{Sign}\left[\text{Re}\left(\frac{\partial\lambda}{\partial\tau}\right)^{-1}\right]. \tag{5.2.12}$$

Squaring on both sides of equation (5.2.10), we have

$$\begin{aligned} \omega^2 + 2\omega a_{21}G^*\sin(\omega\tau) + (a_{21}G^*)^2\sin^2(\omega\tau) = 0, \\ (D_f\mu_k - a_{22})^2 + 2(D_f\mu_k - a_{22})(a_{21}G^*\cos(\omega\tau)) + (a_{21}G^*)^2\cos^2(\omega\tau) = 0. \end{aligned} \tag{5.2.13}$$

Adding the two equations in (5.2.13) and simplify we obtain

$$\omega = \sqrt{3(D_f\mu_k - a_{22})^2 + (a_{21}G^*)}. \tag{5.2.14}$$

Let $\tau_0 = \min\{\tau_i\}$, the we are able to state the following results.

Lemma 5.2.2.

(i) If $a_{22} < \frac{a_{21}a_{51}}{a_{52}}\kappa$ hold for $i = 0, 1, 2, \ldots$, then the equilibrium point $(\kappa, 0, 0, 0, \frac{a_{51}}{a_{52}}\kappa)$ of the transwell model in equation (5.1.2) is asymptotically stable for all $\tau \geq 0$.

(ii) If $0 \leq \tau_0$, then the equilibrium point $(\kappa, 0, 0, 0, \frac{a_{51}}{a_{52}}\kappa)$ of the transwell model in

equation (5.1.2) is asymptotically stable.

(iii) If $\tau > \tau_0$, then the equilibrium point $(\kappa, 0, 0, 0, \frac{a_{51}}{a_{52}}\kappa)$ of the transwell model in equation (5.1.2) is unstable.

(iv) The transwell model in equation (5.1.2) undergoes a Hopf bifurcation at the equilibrium point $(\kappa, 0, 0, 0, \frac{a_{51}}{a_{52}}\kappa)$ for $\tau = \tau_i$, where $i = 0, 1, 2, \ldots$.

5.2.2 Global stability analysis

In this section, we mainly prove that the equilibrium point $(\kappa, 0, 0, 0, \frac{a_{51}}{a_{52}}\kappa)$ is globally asymptotically stable with the upper and lower solution method in [101, 102]. Let $\vartheta_E = \frac{E^4}{k_E^4+E^4}$, then denoting the reaction functions in equation (5.1.2) by $h_j(n, f, m, E, G)$ for $j = 1, 2, 3, 4, 5$, then from equation (5.2.1) we have

$$\left.\begin{aligned} h_1 &= a_{11}\vartheta_E n(1 - n/\kappa) = 0, \;\; 0 < x < L/2, \\ h_2 &= -a_{21}Gf + a_{22}f = 0, \;\; -L/2 < x < 0, \\ h_3 &= a_{21}Gf + a_{31}m = 0, \;\; -L/2 < x < 0, \\ h_4 &= a_{41}f + Ba_{41}m - a_{43}E = 0, \;\; -L/2 < x < L/2, \\ h_5 &= a_{51}n - a_{52}G = 0, \;\; -L/2 < x < L/2, \end{aligned}\right\} \tag{5.2.15}$$

and let $S \subset \mathbb{R}^5_+$ such that $S = \{\mathbf{u} \in \mathbb{R}^5_+ : \underline{\mathbf{u}} \leq 0 \leq \bar{\mathbf{u}}\}$ and K_j be any positive constant satisfying

$$K \geq \max\{K_j\} \geq \max\left\{\frac{-\partial h_j}{\partial u_j} : \mathbf{u} = (n, f, m, E, G) \in S\right\}, \; j = 1, 2, 3, 4, 5,$$

then we have the following results.

Lemma 5.2.3. *Let*

$$\left.\begin{array}{l} \frac{\partial n}{\partial t} - \frac{\partial}{\partial x}\left(D_n \frac{\partial n}{\partial x}\right) + \frac{\partial}{\partial x}\left(\chi_n n \frac{\frac{\partial E}{\partial x}}{\sqrt{1+(\frac{\partial E}{\partial x}/\lambda_E)^2}}\right) \leq K_1, \;\; 0 < x < L/2, \\ \\ \frac{\partial f}{\partial t} - \frac{\partial}{\partial x}\left(D_f \frac{\partial f}{\partial x}\right) \leq K_2, \;\; -L/2 < x < 0, \\ \\ \frac{\partial m}{\partial t} - \frac{\partial}{\partial x}\left(D_m \frac{\partial m}{\partial x}\right) + \frac{\partial}{\partial x}\left(\chi_m m \frac{\frac{\partial G}{\partial x}}{\sqrt{1+(\frac{\partial G}{\partial x}/\lambda_G)^2}}\right) \leq K_3, \;\; -L/2 < x < 0, \\ \\ \frac{\partial E}{\partial t} - \frac{\partial}{\partial x}\left(D_E \frac{\partial E}{\partial x}\right) \leq K_4, \;\; -L/2 < x < L/2, \\ \\ \frac{\partial G}{\partial t} - \frac{\partial}{\partial x}\left(D_G \frac{\partial G}{\partial x}\right) \leq K_5, \;\; -L/2 < x < L/2, \end{array}\right\} \quad (5.2.16)$$

then

$$\lim_{t\to\infty} n(x,t) = K_1, \lim_{t\to\infty} f(x,t) = K_2, \lim_{t\to\infty} m(x,t) = K_3,$$

$$\lim_{t\to\infty} E(x,t) = K_4, \lim_{t\to\infty} G(x,t) = K_5.$$

Theorem 5.2.4. *If $a_{22} < \frac{a_{21}a_{51}}{a_{52}}\kappa$ for the transwell model in equation (5.1.2) implies that the equilibrium $(\kappa, 0, 0, 0, \frac{a_{51}}{a_{52}}\kappa)$ is globally asymptotically stable.*

Proof: From the maximum principle of parabolic equations, it is known that for any initial value $(n_0(t,x), f_0(t,x), m_0(t,x), E_0(t,x), G_0(t,x)) > (0,0,0,0,0)$ the corresponding non-negative solution $(n(t,x), f(t,x), m(t,x), E(t,x), G(t,x))$ is strictly positive for $t > 0$. Since $a_{22} < \frac{a_{21}a_{51}}{a_{52}}\kappa$, then we choose $\varepsilon_0 \in (0,1)$. Then, according to Lemma (5.2.3) and the comparison principle of parabolic equations, there exists $t_1 > 0$ such

that, for any $t > t_1$,

$$\left.\begin{array}{ll} n(x,t) \leq K_1 + \varepsilon_0 := \bar{n}(x,t), & 0 < x < L/2, \\ f(x,t) \leq K_2 + \varepsilon := \bar{f}(x,t), & -L/2 < x < 0, \\ m(x,t) \leq K_3 + \varepsilon := \bar{m}(x,t), & -L/2 < x < 0, \\ E(x,t) \leq K_4 + \varepsilon := \bar{E}(x,t), & -L/2 < x < L/2, \\ G(x,t) \leq K_5 + \varepsilon := \bar{G}(x,t), & -L/2 < x < L/2, \end{array}\right\} \tag{5.2.17}$$

and

$$\left.\begin{array}{ll} n(x,t) \geq K_1 - \varepsilon_0 := \underline{n}(x,t), & 0 < x < L/2, \\ f(x,t) \geq K_2 - \varepsilon := \underline{f}(x,t), & -L/2 < x < 0, \\ m(x,t) \geq K_3 - \varepsilon := \underline{m}(x,t), & -L/2 < x < 0, \\ E(x,t) \geq K_4 - \varepsilon := \underline{E}(x,t), & -L/2 < x < L/2, \\ G(x,t) \geq K_5 - \varepsilon := \underline{G}(x,t), & -L/2 < x < L/2. \end{array}\right\} \tag{5.2.18}$$

Thus, for $t > t_0$, it is possible to obtain

$$\begin{aligned}
\underline{n}(x,t) &\leq n(x,t) \leq \bar{n}(x,t),\ 0 < x < L/2,\\
\underline{f}(x,t) &\leq f(x,t) \leq \bar{f}(x,t),\ \ -L/2 < x < 0,\\
\underline{m}(x,t) &\leq m(x,t) \leq \bar{m}(x,t),\ -L/2 < x < 0,\\
\underline{E}(x,t) &\leq E(x,t) \leq \bar{E}(x,t),\ \ -L/2 < x < L/2,\\
\underline{G}(x,t) &\leq G(x,t) \leq \bar{G}(x,t),\ -L/2 < x < L/2.
\end{aligned} \tag{5.2.19}$$

Since $h_j(n,f,m,E,G)$ in equation (5.2.15) is a C^1 function of n,f,m,E,G, where h_1 is quasi-monotone non-decreasing in f,m,E,G, h_2 is quasi-monotone non-increasing in n,m,E,G, h_3 is quasi-monotone non-increasing in n,f,E,G, h_4 is quasi-monotone non-decreasing in n,f,m,G and h_5 is quasi-monotone non-decreasing in n,f,m,E, then by the method of upper and lower solutions we know that the system in (5.1.2) has a unique global non-negative solution n,f,m,E,G, [101]. Thus,

$$\underline{n},\bar{n},\underline{f},\bar{f},\underline{m},\bar{m},\underline{E},\bar{E},\underline{G},\bar{G}, \tag{5.2.20}$$

satisfy

$$\left.\begin{aligned}
&\tfrac{a_{11}}{\kappa}\bar{E}_4\bar{n}(1-\bar{n}) \leq 0 \leq \tfrac{a_{11}}{\kappa}\underline{E}\underline{n}(1-\underline{n}),\ \ 0 < x < L/2,\\
&-a_{21}\underline{G}\bar{f} + a_{22}\bar{f} \leq 0 \leq -a_{21}\bar{G}\underline{f} + a_{22}\underline{f},\ \ -L/2 < x < 0,\\
&a_{21}\underline{G}\underline{f} + a_{31}\bar{m} \leq 0 \leq a_{21}\bar{G}\bar{f} + a_{31}\underline{m},\ \ -L/2 < x < 0,\\
&a_{41}\bar{f} + Ba_{41}\bar{m} - a_{43}\bar{E} \leq 0 \leq a_{41}\underline{f} + Ba_{41}\underline{m} - a_{43}\underline{E},\ \ -L < x < L,\\
&a_{51}\bar{n} - a_{52}\bar{G} \leq 0 \leq a_{51}\underline{n} - a_{52}\underline{G},\ \ -L < x < L.
\end{aligned}\right\} \tag{5.2.21}$$

Therefore, $(\bar{n}, \bar{f}, \bar{m}, \bar{E}, \bar{G})$ and $(\underline{n}, \underline{f}, \underline{m}, \underline{E}, \underline{G})$, are a pair of coupled upper and lower solutions of system (5.1.2),[130], respectively. Thus, for any

$$(\underline{n}, \underline{f}, \underline{m}, \underline{E}, \underline{G}) \leq (n_1, f_1, m_1, E_1, G_1),$$

and

$$(n_2, f_2, m_2, E_2, G_2) \leq (\bar{n}, \bar{f}, \bar{m}, \bar{E}, \bar{G}),$$

we have

$$\left.\begin{array}{l} \left|\frac{a_{11}E_1^4 n_1}{k_E^4+E_1^4}(1-\frac{n_1}{\kappa}) - (\frac{a_{11}E_2^4 n_2}{k_E^4+E_2^4}(1-\frac{n_2}{\kappa}))\right| \\ \leq K(|E_1-E_2|+|n_1-n_2|), 0<x<L/2, \\ \\ |-a_{21}G_1f_1 + a_{22}f_1 - (-a_{21}G_2f_2 + a_{22}f_2)| \\ \leq K(|G_1-G_2|+|f_1-f_2|), -L/2<x<0, \\ \\ |a_{21}G_1f_1 + a_{31}m_1 - (a_{21}G_2f_2 + a_{31}m_2)| \\ \leq K(G_1-G_2|+|m_1-m_2|)=0, -L/2<x<0, \\ \\ |a_{41}f_1 + Ba_{41}m_1 - a_{43}E_1 - (a_{41}f_2 + Ba_{41}m_2 - a_{43}E_2)) \\ \leq K(f_1-f_2|+|m_1-m_2|), -L<x<L, \\ \\ |a_{51}n_1 - a_{52}G_1 - (a_{51}n_2 - a_{52}G_2)| \leq K(|n_1-n_2|+|G_2-G_2|), -L<x<L. \end{array}\right\}$$

Defining two iteration sequences $(\bar{n}, \bar{f}, \bar{m}, \bar{E}, \bar{G})$ and $(\underline{n}, \underline{f}, \underline{m}, \underline{E}, \underline{G})$ for $i \geq 1$,

$$\left.\begin{aligned}
&\bar{n}^{(i)} = \bar{n}^{(i-1)} + (\tfrac{a_{11}}{\kappa}\bar{E}^{(i-1)}\bar{n}^{(i-1)}(1-\bar{n}^{(i-1)}))/K, \;\; 0 < x < L/2,\\
&\bar{f}^{(i)} = \bar{f}^{(i-1)} + (-a_{21}\underline{G}^{(i-1)}\bar{f}^{(i-1)} + a_{22}\bar{f}^{(i-1)})/K,\\
&\\
&\bar{m}^{(i)} = \bar{m}^{(i-1)} + (a_{21}\underline{G}^{(i-1)}\underline{f}^{(i-1)} + a_{31}\bar{m}^{(i-1)})/K, \;\; -L/2 < x < 0,\\
&\bar{E}^{(i)} = \bar{E}^{(i-1)} + (a_{41}\bar{f}^{(i-1)} + Ba_{41}\bar{m}^{(i-1)} - a_{43}\bar{E}^{(i-1)})/K, \;\; -L < x < L,\\
&\bar{G}^{(i)} = \bar{G}^{(i-1)} + (a_{51}\bar{n}^{(i-1)} - a_{52}\bar{G}^{(i-1)})/K, \;\; -L < x < L,\\
&\underline{n}^{(i)} = \underline{n}^{(i-1)} + (\tfrac{a_{11}}{\kappa}\underline{E}^{(i-1)}\underline{n}_1^{(i-1)}(1-\underline{n}_1^{(i-1)}))/K, \;\; 0 < x < L/2,\\
&\underline{f}^{(i)} = \underline{f}^{(i-1)} + (-a_{21}\bar{G}^{(i-1)}\underline{f}^{(i-1)} + a_{22}\underline{f}^{(i-1)})/K, \;\; -L/2 < x < 0,\\
&\underline{m}^{(i)} = \underline{m}^{(i-1)} + (a_{21}\bar{G}^{(i-1)}\bar{f}^{(i-1)} + a_{31}\underline{m}^{(i-1)})/K, \;\; -L/2 < x < 0,\\
&\underline{E}^{(i)} = \underline{E}^{(i-1)} + (a_{41}\underline{f}^{(i-1)} + Ba_{41}\underline{m}^{(i-1)} - a_{43}\underline{E}^{(i-1)})/K, \;\; -L < x < L,\\
&\underline{G}^{(i)} = \underline{G}^{(i-1)} + (a_{51}\underline{n}^{(i-1)} - a_{52}\underline{G}^{(i-1)})/K, \;\; -L < x < L,
\end{aligned}\right\} \quad (5.2.22)$$

where, $(\bar{n}^{(0)}, \bar{f}^{(0)}, \bar{m}^{(0)}, \bar{E}^{(0)}, \bar{G}^{(0)}) = (\bar{n}, \bar{f}, \bar{m}, \bar{E}, \bar{G})$
and $(\underline{n}^{(0)}, \underline{f}^{(0)}, \underline{m}^{(0)}, \underline{E}^{(0)}, \underline{G}^{(0)}) = (\underline{n}, \underline{f}, \underline{m}, \underline{E}, \underline{G})$. Thus, for $i \geq 1$,

$$(\underline{n}, \underline{f}, \underline{m}, \underline{E}, \underline{G}) \leq (\underline{n}^{(i)}, \underline{f}^{(i)}, \underline{m}^{(i)}, \underline{E}^{(i)}, \underline{G}^{(i)}) \leq (\underline{n}^{(i+1)}, \underline{f}^{(i+1)}, \underline{m}^{(i+1)}, \underline{E}^{(i+1)}, \underline{G}^{(i+1)})$$
$$\leq (\bar{n}^{(i+1)}, \bar{f}^{(i+1)}, \bar{m}^{(i+1)}, \bar{E}^{(i+1)}, \bar{G}^{(i+1)} \leq (\bar{n}^{(i)}, \bar{f}^{(i)}, \bar{m}^{(i)}, \bar{E}^{(i)}, \bar{G}^{(i)}) \leq (\bar{n}, \bar{f}, \bar{m}, \bar{E}, \bar{G}),$$

and there exist $(\tilde{n}^{(0)}, \tilde{f}^{(0)}, \tilde{m}^{(0)}, \tilde{E}^{(0)}, \tilde{G}^{(0)}) > (0,0,0,0,0)$,
and $(\hat{n}^{(0)}, \hat{f}^{(0)}, \hat{m}^{(0)}, \hat{E}^{(0)}, \hat{G}^{(0)}) > (0,0,0,0,0)$ such that

$$\lim_{i\to\infty} \bar{n} = \tilde{n}, \; \lim_{i\to\infty} \bar{f} = \tilde{f}, \; \lim_{i\to\infty} \bar{m} = \tilde{m}, \; \lim_{i\to\infty} \bar{E} = \tilde{E}, \; \lim_{i\to\infty} \bar{G} = \tilde{G},$$

and

$$\lim_{i\to\infty} \underline{n} = \hat{n}, \; \lim_{i\to\infty} \underline{f} = \hat{f}, \; \lim_{i\to\infty} \underline{m} = \hat{m}, \; \lim_{i\to\infty} \underline{E} = \hat{E}, \; \lim_{i\to\infty} \underline{G} = \hat{G},$$

and

$$\left.\begin{array}{l} \frac{a_{11}}{\kappa}\tilde{E}\tilde{n}(1-\tilde{n})=0,\ \frac{a_{11}}{\kappa}\hat{E}\hat{n}(1-\hat{n})=0,\ 0<x<L/2, \\ -a_{21}\hat{E}\tilde{f}+a_{22}\tilde{f}=0,\ -a_{21}\tilde{G}\hat{f}+a_{22}\hat{f}=0,\ -L/2<x<0, \\ a_{21}\hat{G}\hat{f}+a_{31}\tilde{m}=0,\ a_{21}\tilde{G}\tilde{f}+a_{31}\hat{m}=0,\ -L/2<x<0, \\ a_{41}\tilde{f}+Ba_{41}\tilde{m}-a_{43}\tilde{E}=0,\ a_{41}\hat{f}+Ba_{41}\hat{m}-a_{43}\hat{E}=0,\ -L<x<L, \\ a_{51}\tilde{n}-a_{52}\tilde{G}=0,\ a_{51}\hat{n}-a_{52}\hat{G}=0,\ -L<x<L. \end{array}\right\} \quad (5.2.23)$$

Since, $(\kappa,0,0,0,\frac{a_{51}}{a_{52}}\kappa)$ is the unique positive constant equilibrium of system (5.1.2), it must hold for

$$(\tilde{n},\tilde{f},\tilde{m},\tilde{E},\tilde{G})=(\hat{n},\hat{f},\hat{m},\hat{E},\hat{G})=(\kappa,0,0,0,\frac{a_{51}}{a_{52}}\kappa). \quad (5.2.24)$$

Thus, by [101, 102], the solution $(n(x,t),f(x,t),m(x,t),E(x,t),G(x,t))$ of system (5.1.2) satisfies

$$\begin{aligned} \lim_{t\to\infty} n(x,t) &= n^*,\ \lim_{t\to\infty} f(x,t)=f^*,\ \lim_{t\to\infty} m(x,t)=m^*,\ \lim_{t\to\infty} E(x,t)=E^*, \\ \lim_{t\to\infty} G(x,t) &= G^*. \end{aligned} \quad (5.2.25)$$

Hence, the constant equilibrium point $(\kappa,0,0,0,\frac{a_{51}}{a_{52}}\kappa)$ is globally asymptotically stable.

5.3 Derivation and analysis of the numerical method

In this section, we describe the derivation of the fitted operator method for solving the system in equation (5.1.2). We determine an approximation to the derivatives of the functions $n(t,x),f(x,t),m(x,t),E(x,t),G(x,t)$, with respect to the spatial variable x.

Let S_x be a positive integer. Discretize the interval $[-L/2,L/2]$ through the points

$$-L/2=x_0<x_1<x_2<\cdots<x_{s-1}<x_s<x_{s+1}\cdots<x_{S_x-2}<x_{S_x-1}<x_{S_x}=L/2,$$

where, the step-size $\Delta x = x_{j+1} - x_j = (L/2 + L/2)/S_x$, $j = 0, 1, \ldots, x_{S_x}$. Let

$$\mathcal{N}_j(t), \mathcal{F}_j(t), \mathcal{M}_j(t), \mathcal{E}_j(t), \mathcal{G}_j(t), \tag{5.3.1}$$

denote the numerical approximations of $n(t,x), f(x,t), m(x,t), E(x,t), G(x,t)$. Then we approximate the spatial derivative of the system in equation (5.1.2) by

$$\left.\begin{aligned}
\frac{\partial}{\partial x}\left(D_n\frac{\partial n}{\partial x} - \chi_n n\frac{\frac{\partial E}{\partial x}}{\sqrt{1+(\frac{\partial E}{\partial x}/\lambda_E)^2}}\right)(t,x_j) &\approx D_n\frac{\mathcal{N}_{j+1}-2\mathcal{N}_j+\mathcal{N}_{j-1}}{\phi_n^2} \\
&\quad -\chi_n(D_x^-\mathcal{N}_j)\frac{(D_x^-\mathcal{E}_j)}{\sqrt{1+\left(\frac{D_x^-\mathcal{E}_j}{\lambda_E}\right)^2}} \\
&\quad -\chi_n\mathcal{N}_j\frac{D_x^+(D_x^-\mathcal{E}_j)}{\left(1+\left(\frac{D_x^-\mathcal{E}_j}{\lambda_E}\right)^2\right)^{3/2}}, \\
\frac{\partial}{\partial x}\left(D_f\frac{\partial f}{\partial x}\right)(t,x_j) &\approx D_f\frac{\mathcal{F}_{j+1}-2\mathcal{F}_j+\mathcal{F}_{j-1}}{\phi_f^2}, \\
\frac{\partial}{\partial x}\left(D_m\frac{\partial m}{\partial x} - \chi_m m\frac{\frac{\partial G}{\partial x}}{\sqrt{1+(\frac{\partial G}{\partial x}/\lambda_G)^2}}\right) &\approx D_m\frac{\mathcal{M}_{j+1}-2\mathcal{M}_j+\mathcal{M}_{j-1}}{\phi_m^2} \\
&\quad -\chi_m(D_x^-\mathcal{M}_j)\frac{(D_x^-\mathcal{G}_j)}{\sqrt{1+\left(\frac{D_x^-\mathcal{G}_j}{\lambda_G}\right)^2}} \\
&\quad -\chi_m\mathcal{M}_j\frac{D_x^+(D_x^-\mathcal{G}_j)}{\left(1+\left(\frac{D_x^-\mathcal{G}_j}{\lambda_G}\right)^2\right)^{3/2}}, \\
\frac{\partial}{\partial x}\left(D_E\frac{\partial E}{\partial x}\right)(t,x_j) &\approx D_E\frac{\mathcal{E}_{j+1}-2\mathcal{E}_j+\mathcal{E}_{j-1}}{\phi_E^2}, \\
\frac{\partial}{\partial x}\left(D_G\frac{\partial G}{\partial x}\right)(t,x_j) &\approx D_G\frac{\mathcal{G}_{j+1}-2\mathcal{G}_j+\mathcal{G}_{j-1}}{\phi_G^2},
\end{aligned}\right\} \tag{5.3.2}$$

where,

$$D^+(\cdot)_j = \frac{(\cdot)_{j+1} - (\cdot)_j}{\Delta x},\ D^-(\cdot)_j = \frac{(\cdot)_j - (\cdot)_{j-1}}{\Delta x},$$

and the denominator functions

$$\begin{aligned}
\phi_n^2 &:= \frac{D_n\Delta x}{\chi_n}\left[\exp(\frac{\chi_n\Delta x}{D_n})-1\right],\ \phi_f^2 := \frac{4}{\varrho_f^2}\sin\left(\frac{\varrho_f\Delta x}{2}\right)^2,\ \ \varrho_f := \sqrt{\frac{a_{22}}{D_f}},\\
\phi_m^2 &:= \frac{D_m\Delta x}{\chi_m}\left[\exp(\frac{\chi_m\Delta x}{D_m})-1\right],\ \phi_E^2 := \frac{4}{\varrho_e^2}\sinh\left(\frac{\varrho_e\Delta x}{2}\right)^2,\ \ \varrho_e := \sqrt{\frac{a_{43}}{D_e}},\\
\phi_G^2 &:= \frac{4}{\varrho_g^2}\sinh\left(\frac{\varrho_g\Delta x}{2}\right)^2,\ \ \varrho_g := \sqrt{\frac{a_{52}}{Dg}}.
\end{aligned}$$

Let S_t be a positive integer and $\Delta t = T/S_t$ where $0 < t < T$. Discretizing the time interval $[0,T], T \in \mathbb{N}^+$ through the points

$$0 = t_0 < t_1 < \cdots < t_{S_t} = T,$$

where,

$$t_{i+1} - t_i = \Delta t,\ i = 0, 1, \ldots, (t_{S_t} - 1).$$

We approximate the time derivative at t_i by

$$\left.\begin{aligned}
&\tfrac{\partial n}{\partial t}(x,t_i) \approx \tfrac{\mathcal{N}_{j+1}^{i+1}-\mathcal{N}_j^i}{\Delta t},\ \tfrac{\partial f}{\partial t}(x,t_i) \approx \tfrac{\mathcal{F}_{j+1}^{i+1}-\mathcal{F}_j^i}{\psi_f},\ \tfrac{\partial m}{\partial t}(x,t_i) \approx \tfrac{\mathcal{M}_{j+1}^{i+1}-\mathcal{M}_j^i}{\psi_m},\\
&\tfrac{\partial E}{\partial t}(x,t_i) \approx \tfrac{\mathcal{E}_{j+1}^{i+1}-\mathcal{E}_j^i}{\psi_E},\ \tfrac{\partial G}{\partial t}(x,t_i) \approx \tfrac{\mathcal{G}_{j+1}^{i+1}-\mathcal{G}_j^i}{\psi_G},
\end{aligned}\right\} \qquad (5.3.3)$$

where,

$$\begin{aligned}
\psi_f = (1-\exp(-a_{22}\Delta t))/a_{22},\ \psi_E = (1-\exp(-a_{43}\Delta t))/a_{43},\\
\psi_G = (1-\exp(-a_{52}\Delta t))/a_{52}, \psi_m = (1-\exp(-a_{31}\Delta t))/a_{31},
\end{aligned}$$

where we see that $\psi_f \to \Delta t, \psi_E \to \Delta t, \psi_G \to \Delta t,\ \psi_m \to \Delta t$ as $\Delta t \to 0$. The denominator functions in equations (5.3.2) and (5.3.3) are used explicitly to remove the inherent stiffness in the central finite derivatives parts and can be derived by using the

theory of nonstandard finite difference methods, see, e.g., [84, 103, 104] and references therein.

Combining the equation (5.3.2) for the spatial derivatives with equation (5.3.3) for

time derivatives, we obtain

$$
\left.
\begin{aligned}
&\frac{\mathcal{N}_j^{i+1}-\mathcal{N}_j^i}{\Delta t} - D_n\frac{\mathcal{N}_{j+1}^{i+1}-2\mathcal{N}_j^{i+1}+\mathcal{N}_{j-1}^{i+1}}{\phi_n^2} = -\chi_n(D_x^+ n_j^i)\frac{(D_x^-\mathcal{E}_j^i)}{\sqrt{1+\left(\frac{D_x^-\mathcal{E}_j^i}{\lambda_E}\right)^2}}\\
&\qquad -\chi_n\mathcal{N}_j^i\frac{D_x^+(D_x^-\mathcal{E}_j^i)}{\left(1+\left(\frac{D_x^-\mathcal{E}_j^i}{\lambda_E}\right)^2\right)^{3/2}}\\
&\qquad +\frac{a_{11}(\mathcal{E}^4)_j^i\mathcal{N}_j^i}{k_E^4+(\mathcal{E}^4)_j^i}(1-\frac{\mathcal{N}_j^i}{\kappa}),\ x\in[x_s,L/2],\\
&\frac{\mathcal{F}_j^{i+1}-\mathcal{F}_j^i}{\psi_f} - D_f\frac{\mathcal{F}_{j+1}^{i+1}-2\mathcal{F}_j^{i+1}+\mathcal{F}_{j-1}^{i+1}}{\phi_f^2} = -a_{21}(\mathcal{H}_G)_j^i(\mathcal{H}_f)_j^i\\
&\qquad +a_{22}(\mathcal{H}_f)_j^i,\ x\in[-\tfrac{L}{2},x_s],\\
&\frac{\mathcal{M}_j^{i+1}-\mathcal{M}_j^i}{\psi_m} - D_m\frac{\mathcal{M}_{j+1}^{i+1}-2\mathcal{M}_j^{i+1}+\mathcal{M}_{j-1}^{i+1}}{\phi_m^2} = -\chi_m(D_x^+\mathcal{M}_j^i)\frac{(D_x^-\mathcal{G}_j^i)}{\sqrt{1+\left(\frac{D_x^-\mathcal{G}_j^i}{\lambda_G}\right)^2}}\\
&\qquad -\chi_m\mathcal{M}_j^i\frac{D_x^+(D_x^-\mathcal{G}_j^i)}{\left(1+\left(\frac{D_x^-\mathcal{G}_j^i}{\lambda_G}\right)^2\right)^{3/2}}\\
&\qquad +a_{21}(\mathcal{H}_G)_j^i(\mathcal{H}_f)_j^i+a_{31}\mathcal{M}_j^i,\ x\in[-\tfrac{L}{2},x_s],\\
&\frac{\mathcal{E}_j^{i+1}-\mathcal{E}_j^i}{\psi_E} - D_E\frac{\mathcal{E}_{j+1}^{i+1}-2\mathcal{E}_j^{i+1}+\mathcal{E}_{j-1}^{i+1}}{\phi_E^2} = a_{41}(\mathcal{H}_f)_j^i+Ba_{41}(\mathcal{H}_m)_j^i-a_{43}\mathcal{E}_j^i,\ x\in[-\tfrac{L}{2},\tfrac{L}{2}],\\
&\frac{\mathcal{G}_j^{i+1}-\mathcal{G}_j^i}{\psi_G} - D_G\frac{\mathcal{G}_{j+1}^{i+1}-2\mathcal{G}_j^{i+1}+\mathcal{G}_{j-1}^{i+1}}{\phi_G^2} = a_{51}(\mathcal{H}_n)_j^i-a_{52}\mathcal{G}_j^i, x\in[-\tfrac{L}{2},\tfrac{L}{2}],\\
&\mathcal{F}_{\frac{-L}{2}+1}^i=\mathcal{F}_{\frac{-L}{2}-1}^i,\ \mathcal{G}_{\frac{L}{2}+1}^i=\mathcal{G}_{\frac{L}{2}-1}^i+2\gamma\Delta x\left((\mathcal{G}^+)_{\frac{L}{2}}-(\mathcal{G}^-)_{\frac{L}{2}}\right),\\
&\mathcal{G}_{\frac{-L}{2}-1}^i=(\mathcal{G}^-)^i_{\frac{-L}{2}+1}(1+2\Delta x\gamma),\\
&\mathcal{M}_{\frac{-L}{2}+1}^i=\mathcal{M}_{\frac{-L}{2}-1}^i+2\Delta x\chi_m\mathcal{M}_{\frac{-L}{2}}^i\left(\frac{\mathcal{G}^i_{\frac{-L}{2}+1}-\mathcal{G}^i_{\frac{-L}{2}-1}}{2\Delta x\sqrt{1+\left(\frac{\mathcal{G}^i_{\frac{-L}{2}+1}-\mathcal{G}^i_{\frac{-L}{2}-1}}{2\Delta x\lambda_G}\right)^2}}\right),\\
&\mathcal{E}_{\frac{-L}{2}-1}^i=(\mathcal{E}^-)^i_{\frac{-L}{2}+1}(1+2\Delta x\gamma),\ \mathcal{E}_{\frac{L}{2}+1}^i=\mathcal{E}_{\frac{L}{2}-1}^i+2\gamma\Delta x\left((\mathcal{E}^+)_{\frac{L}{2}}-(\mathcal{E}^-)_{\frac{L}{2}}\right),\\
&\mathcal{N}_{\frac{L}{2}+1}^i=\mathcal{N}_{\frac{L}{2}-1}^i+2\Delta x\chi_n\mathcal{N}_{\frac{L}{2}}^i\left(\frac{\mathcal{E}^i_{\frac{L}{2}+1}-\mathcal{E}^i_{\frac{L}{2}-1}}{2\Delta x\sqrt{1+\left(\frac{\mathcal{E}^i_{\frac{L}{2}+1}-\mathcal{E}^i_{\frac{L}{2}-1}}{2\Delta x\lambda_E}\right)^2}}\right),\ \mathcal{F}_{x_s+1}^i=\mathcal{F}_{x_s-1}^i,\\
&\mathcal{M}_{x_s+1}^i=\mathcal{M}_{x_s-1}^i-2\Delta x\chi_m\mathcal{M}_{x_s}^i\left(\frac{\mathcal{G}^i_{x_s+1}-\mathcal{G}^i_{x_s-1}}{2\Delta x\sqrt{1+\left(\frac{\mathcal{G}^i_{x_s+1}-\mathcal{G}^i_{x_s-1}}{2\Delta x\lambda_G}\right)^2}}\right),\\
&\mathcal{N}_{x_s-1}^i=\mathcal{N}_{x_s+1}^i-2\Delta x\chi_n\mathcal{N}_{x_s}^i\left(\frac{\mathcal{E}^i_{x_s+1}-\mathcal{E}^i_{x_s-1}}{2\Delta x\sqrt{1+\left(\frac{\mathcal{E}^i_{x_s+1}-\mathcal{E}^i_{x_s-1}}{2\Delta x\lambda_E}\right)^2}}\right),\\
&\mathcal{N}_{x_j}^0=\exp(-40(x_j-1)^2),\ \mathcal{F}_{x_j}^0=\exp(-40x_j^2)r_f,\ \mathcal{M}_{x_j}^0=0.00,\ \mathcal{E}_{x_j}^0=\mathcal{G}_{x_j}^0=1.00,
\end{aligned}
\right\}\quad(5.3.4)
$$

where, the no-flux boundary conditions are discretised by means of the central finite difference [21], $j = -L/2, 2, \ldots, L/2-1$, $i = 0, 1, \ldots, T-1$ and

$$\begin{aligned}(\mathcal{H}_n)_j^i &\approx N(t_i-\tau, x_j),\ (\mathcal{H}_f)_j^i \approx F(t_i-\tau, x_j),\ (\mathcal{H}_G)_j^i \approx G(t_i-\tau, x_j),\\ (\mathcal{H}_m)_j^i &\approx M(t_i-\tau, x_j),\end{aligned} \tag{5.3.5}$$

are denoting the history functions corresponding to n, f, m, G. The system in equation (5.3.4) can further be simplified as

$$\left.\begin{aligned}
&-\tfrac{D_n}{\phi_n^2}\mathcal{N}_{j-1}^{i+1} + \left(\tfrac{1}{\Delta t} + \tfrac{2D_n}{\phi_n^2}\right)\mathcal{N}_j^{i+1} - \tfrac{D_n}{\phi_n^2}\mathcal{N}_{j+1}^{i+1}\\
&\qquad = -\chi_n(D_x^-n_j^i)\frac{(D_x^-\mathcal{E}_j^i)}{\sqrt{1+\left(\frac{D_x^-\mathcal{E}_j^i}{\lambda_E}\right)^2}} - \chi_n\mathcal{N}_j^i\frac{D_x^+(D_x^-\mathcal{E}_j^i)}{\left(1+\left(\frac{D_x^-\mathcal{E}_j^i}{\lambda_E}\right)^2\right)^{3/2}}\\
&\qquad +a_{11}\tfrac{(\mathcal{E}^4)_j^i}{k_E^4+(\mathcal{E}^4)_j^i}\mathcal{N}_j^i(1-\mathcal{N}_j^i/\kappa) + \tfrac{\mathcal{N}_j^i}{\Delta t},\\
&-\tfrac{D_f}{\phi_f^2}\mathcal{F}_{j-1}^{i+1} + \left(\tfrac{1}{\psi_f} + \tfrac{2D_f}{\phi_f^2}\right)\mathcal{F}_j^{i+1} - \tfrac{D_f}{\phi_f^2}\mathcal{F}_{j+1}^{i+1}\\
&\qquad = -a_{21}(\mathcal{H}_G)_j^i(\mathcal{H}_f)_j^i + a_{22}(\mathcal{H}_f)_j^i + \tfrac{\mathcal{F}_j^i}{\psi_f},\\
&-\tfrac{D_m}{\phi_m^2}\mathcal{M}_{j-1}^{i+1} + \left(\tfrac{1}{\psi_m} + \tfrac{2D_m}{\phi_m^2}\right)\mathcal{M}_j^{i+1} - \tfrac{D_m}{\phi_m^2}\mathcal{M}_{j+1}^{i+1}\\
&\qquad = -\chi_m(D_x^-\mathcal{M}_j^i)\frac{(D_x^-\mathcal{G}_j^i)}{\sqrt{1+\left(\frac{D_x^-\mathcal{G}_j^i}{\lambda_G}\right)^2}} - \chi_m\mathcal{M}_j^i\frac{D_x^+(D_x^-\mathcal{G}_j^i)}{\left(1+\left(\frac{D_x^-\mathcal{G}_j^i}{\lambda_G}\right)^2\right)^{3/2}}\\
&\qquad +a_{21}(\mathcal{H}_G)_j^i(\mathcal{H}_f)_j^i + a_{31}\mathcal{M}_j^i + \tfrac{\mathcal{M}_j^i}{\Delta t},\\
&-\tfrac{D_E}{\phi_E^2}\mathcal{E}_{j-1}^{i+1} + \left(\tfrac{1}{\psi_E} + \tfrac{2D_E}{\phi_E^2}\right)\mathcal{E}_j^{i+1} - \tfrac{D_E}{\phi_E^2}\mathcal{E}_{j+1}^{i+1}\\
&\qquad = a_{41}(\mathcal{H}_f)_j^i + Ba_{41}(\mathcal{H}_m)_j^i - a_{43}\mathcal{E}_j^i + \tfrac{\mathcal{E}_j^i}{\psi_E},\\
&-\tfrac{D_G}{\phi_G^2}\mathcal{G}_{j-1}^{i+1} + \left(\tfrac{1}{\psi_G} + \tfrac{2D_G}{\phi_G^2}\right)\mathcal{G}_j^{i+1} - \tfrac{D_G}{\phi_G^2}\mathcal{G}_{j+1}^{i+1}\\
&\qquad = a_{51}(\mathcal{H}_n)_j^i - a_{52}\mathcal{G}_j^i + \tfrac{\mathcal{G}_j^i}{\psi_G},
\end{aligned}\right\} \tag{5.3.6}$$

which can be written as a tridiagonal system given by

$$\left.\begin{aligned}
A_n\mathcal{N}_j^{i+1} &= -\chi_n(D_x^-n_j^i)\frac{(D_x^-\mathcal{E}_j^i)}{\sqrt{1+\left(\frac{D_x^-\mathcal{E}_j^i}{\lambda_E}\right)^2}} - \chi_n\mathcal{N}_j^i\frac{D_x^+(D_x^-\mathcal{E}_j^i)}{\left(1+\left(\frac{D_x^-\mathcal{E}_j^i}{\lambda_E}\right)^2\right)^{3/2}} \\
&\quad +a_{11}\frac{(\mathcal{E}^4)_j^i}{k_E^4+(\mathcal{E}^4)_j^i}\mathcal{N}_j^i(1-\mathcal{N}_j^i/\kappa)+\frac{\mathcal{N}_j^i}{\Delta t}, \\
A_f\mathcal{F}_j^{i+1} &= -a_{21}(\mathcal{H}_G)_j^i(\mathcal{H}_f)_j^i + a_{22}(\mathcal{H}_f)_j^i + \frac{\mathcal{F}_j^i}{\psi_f}, \\
A_m\mathcal{M}_j^{i+1} &= -\chi_m(D_x^-\mathcal{M}_j^i)\frac{(D_x^-\mathcal{G}_j^i)}{\sqrt{1+\left(\frac{D_x^-\mathcal{G}_j^i}{\lambda_G}\right)^2}} - \chi_m\mathcal{M}_j^i\frac{D_x^+(D_x^-\mathcal{G}_j^i)}{\left(1+\left(\frac{D_x^-\mathcal{G}_j^i}{\lambda_G}\right)^2\right)^{3/2}} \\
&\quad +a_{21}(\mathcal{H}_G)_j^i(\mathcal{H}_f)_j^i + a_{31}\mathcal{M}_j^i + \frac{\mathcal{M}_j^i}{\Delta t}, \\
A_E\mathcal{E}_j^{i+1} &= a_{41}(\mathcal{H}_f)_j^i + Ba_{41}(\mathcal{H}_m)_j^i - a_{43}\mathcal{E}_j^i + \frac{\mathcal{E}_j^i}{\psi_E}, \\
A_G\mathcal{G}_j^{i+1} &= a_{51}(\mathcal{H}_n)_j^i - a_{52}\mathcal{G}_j^i + \frac{\mathcal{G}_j^i}{\psi_G},
\end{aligned}\right\} \tag{5.3.7}$$

where,

$$\left.\begin{aligned}
&A_n = \mathrm{Tri}\left(-\tfrac{D_n}{\phi_n^2}, \tfrac{1}{\Delta t}+\tfrac{2D_n}{\phi_n^2}, -\tfrac{D_n}{\phi_n^2}\right),\ A_f = \mathrm{Tri}\left(-\tfrac{D_f}{\phi_f^2}, \tfrac{1}{\psi_f}+\tfrac{2D_f}{\phi_f^2}, -\tfrac{D_f}{\phi_f^2}\right), \\
&A_m = \mathrm{Tri}\left(-\tfrac{D_m}{\phi_m^2}, \tfrac{1}{\psi_m}+\tfrac{2D_m}{\phi_m^2}, -\tfrac{D_m}{\phi_m^2}\right),\ A_E = \mathrm{Tri}\left(-\tfrac{D_E}{\phi_E^2}, \tfrac{1}{\psi_E}+\tfrac{2D_E}{\phi_E^2}, -\tfrac{D_E}{\phi_E^2}\right), \\
&A_G = \mathrm{Tri}\left(-\tfrac{D_G}{\phi_G^2}, \tfrac{1}{\psi_G}+\tfrac{2D_G}{\phi_G^2}, -\tfrac{D_G}{\phi_G^2}\right).
\end{aligned}\right\} \tag{5.3.8}$$

On the interval $[0,\tau]$ the delayed arguments $t_n-\tau$ belong to $[-\tau,0]$, and therefore the delayed variables in equation (5.3.5) are evaluated directly from the history functions

$$n^0(t,x), f^0(t,x), m^0(t,x), G^0(t,x),$$

as

$$\begin{aligned}(\mathcal{H}_n)_j^i &\approx n^0(t_i-\tau,x_j),\ (\mathcal{H}_f)_j^i \approx f^0(t_i-\tau,x_j),\ (\mathcal{H}_m)_j^i \approx m^0(t_i-\tau,x_j),\\ (\mathcal{H}_G)_j^i &\approx G^0(t_i-\tau,x_j),\end{aligned} \tag{5.3.9}$$

and equation (5.3.7) becomes

$$\left.\begin{aligned}
A_n\mathcal{N}_j^{i+1} &= -\chi_n(D_x^-n_j^i)\frac{(D_x^-\mathcal{E}_j^i)}{\sqrt{1+\left(\frac{D_x^-\mathcal{E}_j^i}{\lambda_E}\right)^2}} - \chi_n\mathcal{N}_j^i\frac{D_x^+(D_x^-\mathcal{E}_j^i)}{\left(1+\left(\frac{D_x^-\mathcal{E}_j^i}{\lambda_E}\right)^2\right)^{3/2}}\\
&\quad +a_{11}\frac{(\mathcal{E}^4)_j^i}{k_E^4+(\mathcal{E}^4)_j^i}\mathcal{N}_j^i(1-\mathcal{N}_j^i/\kappa)+\frac{\mathcal{N}_j^i}{\Delta t},\\
A_f\mathcal{F}_j^{i+1} &= -a_{21}G^0(t_i-\tau,x)f^0(t_i-\tau,x)+a_{22}f^0(t_i-\tau,x)+\frac{\mathcal{F}_j^i}{\psi_f},\\
A_m\mathcal{M}_j^{i+1} &= -\chi_m(D_x^-\mathcal{M}_j^i)\frac{(D_x^-\mathcal{G}_j^i)}{\sqrt{1+\left(\frac{D_x^-\mathcal{G}_j^i}{\lambda_G}\right)^2}} - \chi_m\mathcal{M}_j^i\frac{D_x^+(D_x^-\mathcal{G}_j^i)}{\left(1+\left(\frac{D_x^-\mathcal{G}_j^i}{\lambda_G}\right)^2\right)^{3/2}}\\
&\quad +a_{21}G^0(t_i-\tau,x)f^0(t_i-\tau,x)+a_{31}\mathcal{M}_j^i+\frac{\mathcal{M}_j^i}{\Delta t},\\
A_E\mathcal{E}_j^{i+1} &= a_{41}f^0(t_i-\tau,x)+Ba_{41}m^0(t_i-\tau,x)-a_{43}\mathcal{E}_j^i+\frac{\mathcal{E}_j^i}{\psi_E},\\
A_G\mathcal{G}_j^{i+1} &= a_{51}n^0(t_i-\tau,x)-a_{52}\mathcal{G}_j^i+\frac{\mathcal{G}_j^i}{\psi_G}.
\end{aligned}\right\} \tag{5.3.10}$$

Let s be the largest integer such that $\tau_s \le \tau$. By using the system equation (5.3.9) we can compute $\mathcal{N}_j^i, \mathcal{F}_j^i, \mathcal{M}_j^i, \mathcal{E}_j^i, \mathcal{G}_j^i$ for $1 \le i \le s$. Up to this stage, we interpolate the data

$$\begin{aligned}(t_0,\mathcal{N}_j^0),\ (t_1,\mathcal{N}_j^1),\ldots,(t_s,\mathcal{N}_j^s),\ (t_0,\mathcal{F}_j^0),\ (t_1,\mathcal{F}_j^1),\ldots,(t_s,\mathcal{F}_j^s),\\ (t_0,\mathcal{M}_j^0),\ (t_1,\mathcal{M}_j^1),\ldots,(t_s,\mathcal{M}_j^s),\\ (t_0,\mathcal{E}_j^0),\ (t_1,\mathcal{E}_j^1),\ldots,(t_s,\mathcal{E}_j^s),\ (t_0,\mathcal{G}_j^0),\ (t_1,\mathcal{G}_j^1),\ldots,(t_s,\mathcal{G}_j^s),\end{aligned}$$

using an interpolating cubic Hermite spline $\varphi_j(t)$. Then

$$\mathcal{N}_j^i = \varphi_n(t_i, x_j),\ \mathcal{F}_j^i = \varphi_f(t_i, x_j),\ \mathcal{M}_j^i = \varphi_m(t_i, x_j),\ \mathcal{E}_j^i = \varphi_E(t_i, x_j)\ \mathcal{G}_j^i = \varphi_G(t_i, x_j),$$

for all $i = 0, 1, \ldots, s$ and $j = -L/2, 2, \ldots, L/2 - 1$.

For $i = s+1, s+2, \ldots, T-1$, when we move from level i to level $i+1$ we extend the definitions of the cubic Hermite spline $\varphi_j(t)$ to the point

$$(t_i + \Delta t, (\mathcal{H}_n)_j^i, t_i + \Delta t, (\mathcal{H}_f)_j^i, t_i + \Delta t, (\mathcal{H}_m)_j^i, t_i + \Delta t, (\mathcal{H}_G)_j^i).$$

Then the history terms $(\mathcal{H}_n)_j^i, (\mathcal{H}_f)_j^i, (\mathcal{H}_M)_j^i, (\mathcal{H}_G)_j^i$ can be approximated by the functions $(\varphi_n)_j(t_i - \tau), (\varphi_m)_j(t_i - \tau), (\varphi_m)_j(t_i - \tau), (\varphi_G)_j(t_i - \tau)$ for $i \geq s$. This implies that,

$$\begin{aligned} (\mathcal{H}_n)_j^i &\approx (\varphi_n)_j(t_i - \tau),\ (\mathcal{H}_f)_j^i \approx (\varphi_f)_j(t_i - \tau),\ (\mathcal{H}_m)_j^i \approx (\varphi_m)_j(t_i - \tau), \\ (\mathcal{H}_G)_j^i &\approx (\varphi_G)_j(t_i - \tau), \end{aligned} \tag{5.3.11}$$

and equation (5.3.9) becomes

$$\left.\begin{aligned}
A_n\mathcal{N}_j^{i+1} &= -\chi_n(D_x^-n_j^i)\frac{(D_x^-\mathcal{E}_j^i)}{\sqrt{1+\left(\frac{D_x^-\mathcal{E}_j^i}{\lambda_E}\right)^2}} - \chi_n\mathcal{N}_j^i\frac{D_x^+(D_x^-\mathcal{E}_j^i)}{\left(1+\left(\frac{D_x^-\mathcal{E}_j^i}{\lambda_E}\right)^2\right)^{3/2}} \\
&\quad +a_{11}\frac{(\mathcal{E}^4)_j^i}{k_E^4+(\mathcal{E}^4)_j^i}\mathcal{N}_j^i(1-\mathcal{N}_j^i/\kappa)+\frac{\mathcal{N}_j^i}{\Delta t}, \\
A_f\mathcal{F}_j^{i+1} &= -a_{21}(\varphi_G)(t_i-\tau)(\varphi_f)(t_i-\tau)+a_{22}(\varphi_f)(t_i-\tau)+\frac{\mathcal{F}_j^i}{\psi_f}, \\
A_m\mathcal{M}_j^{i+1} &= -\chi_m(D_x^-\mathcal{M}_j^i)\frac{(D_x^-\mathcal{G}_j^i)}{\sqrt{1+\left(\frac{D_x^-\mathcal{G}_j^i}{\lambda_G}\right)^2}} - \chi_m\mathcal{M}_j^i\frac{D_x^+(D_x^-\mathcal{G}_j^i)}{\left(1+\left(\frac{D_x^-\mathcal{G}_j^i}{\lambda_G}\right)^2\right)^{3/2}} \\
&\quad +a_{21}(\varphi_G)(t_i-\tau)(\varphi_f)(t_i-\tau)+a_{31}\mathcal{M}_j^i+\frac{\mathcal{M}_j^i}{\Delta t}, \\
A_E\mathcal{E}_j^{i+1} &= a_{41}(\varphi_f)(t_i-\tau)+Ba_{41}(\varphi_m)(t_i-\tau)-a_{43}\mathcal{E}_j^i+\frac{\mathcal{E}_j^i}{\psi_E}, \\
A_G\mathcal{G}_j^{i+1} &= a_{51}(\varphi_n)(t_i-\tau)-a_{52}\mathcal{G}_j^i+\frac{\mathcal{G}_j^i}{\psi_G},
\end{aligned}\right\} \tag{5.3.12}$$

where,

$$\begin{aligned}
\varphi_n(t_i-\tau) &= [(\mathcal{H}_n)_1^i,(\mathcal{H}_n)_2^i\ldots,(\mathcal{H}_n)_{\frac{L}{2}-1}^i]',\ \varphi_f(t_i-\tau) \\
&= [(\mathcal{H}_f)_{\frac{-L}{2}}^i,(\mathcal{H}_f)_{\frac{-L}{2}+1}^i\ldots,(\mathcal{H}_f)_{x_0-1}^i]', \\
\varphi_m(t_i-\tau) &= [(\mathcal{H}_m)_{\frac{-L}{2}}^i,(\mathcal{H}_m)_{\frac{-L}{2}+1}^i\ldots,(\mathcal{H}_m)_{x_0-1}^i]', \\
\varphi_E(t_i-\tau) &= [\mathcal{E}_{\frac{-L}{2}}^i,\mathcal{E}_{\frac{-L}{2}+1}^i\ldots,\mathcal{E}_{\frac{L}{2}-1}^i]',\ \varphi_G(t_i-\tau) \\
&= [(\mathcal{H}_G)_{\frac{-L}{2}}^i,(\mathcal{H}_G)_{\frac{-L}{2}+1}^i\ldots,(\mathcal{H}_G)_{\frac{L}{2}-1}^i]'.
\end{aligned}$$

Our FOFDM is then consists of equations (5.3.4)-(5.3.12). Rewriting the FOFDM as

a system of equations we have

$$\left.\begin{aligned} A_n\mathcal{N} &= F_n,\\ A_f\mathcal{F} &= F_f,\\ A_m\mathcal{M} &= F_m,\\ A_E\mathcal{E} &= F_E,\\ A_G\mathcal{G} &= F_G, \end{aligned}\right\} \tag{5.3.13}$$

where,

$$\left.\begin{aligned} F_n &= -\chi_n(D_x^-n_j^i)\frac{(D_x^-\mathcal{E}_j^i)}{\sqrt{1+\left(\frac{D_x^-\mathcal{E}_j^i}{\lambda_E}\right)^2}} - \chi_n\mathcal{N}_j^i\frac{D_x^+(D_x^-\mathcal{E}_j^i)}{\left(1+\left(\frac{D_x^-\mathcal{E}_j^i}{\lambda_E}\right)^2\right)^{3/2}}\\ &\quad +a_{11}\frac{(\mathcal{E}^4)_j^i}{k_E^4+(\mathcal{E}^4)_j^i}\mathcal{N}_j^i(1-\mathcal{N}_j^i/\kappa)+\frac{\mathcal{N}_j^i}{\Delta t},\\ F_f &= -a_{21}(\varphi_G)(t_i-\tau)(\varphi_f)(t_i-\tau)+a_{22}(\varphi_f)(t_i-\tau)+\frac{\mathcal{F}_j^i}{\psi_f},\\ F_m &= -\chi_m(D_x^-\mathcal{M}_j^i)\frac{(D_x^-\mathcal{G}_j^i)}{\sqrt{1+\left(\frac{D_x^-\mathcal{G}_j^i}{\lambda_G}\right)^2}} - \chi_m\mathcal{M}_j^i\frac{D_x^+(D_x^-\mathcal{G}_j^i)}{\left(1+\left(\frac{D_x^-\mathcal{G}_j^i}{\lambda_G}\right)^2\right)^{3/2}}\\ &\quad +a_{21}(\varphi_G)(t_i-\tau)(\varphi_f)(t_i-\tau)+a_{31}\mathcal{M}_j^i+\frac{\mathcal{M}_j^i}{\Delta t},\\ F_E &= a_{41}(\varphi_f)(t_i-\tau)+Ba_{41}(\varphi_m)(t_i-\tau)-a_{43}\mathcal{E}_j^i+\frac{\mathcal{E}_j^i}{\psi_E},\\ F_G &= a_{51}(\varphi_n)(t_i-\tau)-a_{52}\mathcal{G}_j^i+\frac{\mathcal{G}_j^i}{\psi_G}. \end{aligned}\right\}$$

Let the functions

$$n(x,t), f(x,t), m(x,t), E(x,t), G(x,t),$$

and their partial derivatives with respect to both t and x be smooth such that they satisfy

$$\begin{aligned}
\left|\frac{\partial^{i+j} n(t,x)}{\partial t^i x^j}\right| &\leq \Upsilon_n, \left|\frac{\partial^{i+j} f(t,x)}{\partial t^i x^j}\right| \leq \Upsilon_f, \\
\left|\frac{\partial^{i+j} m(t,x)}{\partial t^i x^j}\right| &\leq \Upsilon_m, \left|\frac{\partial^{i+j} E(t,x)}{\partial t^i x^j}\right| \leq \Upsilon_E, \\
\left|\frac{\partial^{i+j} G(t,x)}{\partial t^i x^j}\right| &\leq \Upsilon_G, \forall i,j \geq 0,
\end{aligned} \tag{5.3.14}$$

where,

$$\Upsilon_n, \Upsilon_f, \Upsilon_m, \Upsilon_E, \Upsilon_G,$$

are constant that are independent of the time and space step-sizes. Then, we see that the local truncation errors $(\varsigma_n)_j^i, (\varsigma_f)_j^i, (\varsigma_m)_j^i, (\varsigma_E)_j^i, (\varsigma_G)_j^i$ are given by

$$\left.\begin{aligned}
(\varsigma_n)_j^i &= (A_n n)_j^i - (F_n)_j^i = (A_n(n-\mathcal{N}))_j^i, \\
(\varsigma_f)_j^i &= (A_f f)_j^i - (F_f)_j^i = A_f(f-\mathcal{F})_j^i, \\
(\varsigma_m)_j^i &= (A_m m)_j^i - (F_m)_j^i = (A_m(m-\mathcal{M}))_j^i, \\
(\varsigma_E)_j^i &= (A_E E)_j^i - (F_E)_j^i = (A_E(E-\mathcal{E}))_j^i, \\
(\varsigma_G)_j^i &= (A_G G)_j^i - (F_G)_j^i = (A_G(G-\mathcal{G}))_j^i.
\end{aligned}\right\} \tag{5.3.15}$$

Therefore,

$$\left.\begin{array}{l} \max_{i,j}|n_j^i-\mathcal{N}_j^i|\le||A_n^{-1}||\max_{i,j}|(\varsigma_n)_j^i|,\\ \max_{i,j}|f_j^i-\mathcal{F}_j^i|\le||A_f^{-1}||\max_{i,j}|(\varsigma_f)_j^i|,\\ \max_{i,j}|m_j^i-\mathcal{M}_j^i|\le||A_m^{-1}||\max_{i,j}|(\varsigma_m)_j^i|,\\ \max_{i,j}|E_j^i-\mathcal{E}_j^i|\le||A_E^{-1}||\max_{i,j}|(\varsigma_E)_j^i|,\\ \max_{i,j}|G_j^i-\mathcal{G}_j^i|\le||A_G^{-1}||\max_{i,j}|(\varsigma_G)_j^i|, \end{array}\right\} \tag{5.3.16}$$

where,

$$\left.\begin{array}{l} \max_{i,j}|(\varsigma_n)_j^i|\le\frac{(\Delta t)}{2}|n_{tt}(\xi)|-D_n\frac{(\Delta x)^2}{12}|n_{xxxx}(\zeta)|,\ x\in[x_s,L/2],\\ \max_{i,j}|(\varsigma_f)_j^i|\le\frac{(\Delta t)}{2}|f_{tt}(\xi)|-D_f\frac{(\Delta x)^2}{12}|f_{xxxx}(\zeta)|,\ x\in[-\frac{L}{2},x_s],\\ \max_{i,j}|(\varsigma_m)_j^i|\le\frac{(\Delta t)}{2}|m_{tt}(\xi)|-D_m\frac{(\Delta x)^2}{12}|n_{xxxx}(\zeta)|,\ x\in[-\frac{L}{2},x_s],\\ \max_{i,j}|(\varsigma_E)_j^i|\le\frac{(\Delta t)}{2}|E_{tt}(\xi)|-D_E\frac{(\Delta x)^2}{12}|E_{xxxx}(\zeta)|,\ x\in[-\frac{L}{2},\frac{L}{2}],\\ \max_{i,j}|(\varsigma_G)_j^i|\le\frac{(\Delta t)}{2}|G_{tt}(\xi)|-D_G\frac{(\Delta x)^2}{12}|n_{xxxx}(\zeta)|,x\in[-\frac{L}{2},\frac{L}{2}], \end{array}\right\} \tag{5.3.17}$$

for $t_{i-1}\le\xi\le t_{i+1}$ and $x_{j-1}\le\zeta\le x_{j+1}$. In view of inequalities in (5.3.14), we see that

inequalities in (5.3.17) are equivalent to

$$\left.\begin{array}{l} \max_{i,j}|(\varsigma_n)_j^i| \leq \left(\frac{(\Delta t)}{2} - D_n\frac{(\Delta x)^2}{12}\right)\Upsilon_n,\ x \in [x_s, L/2], \\ \max_{i,j}|(\varsigma_f)_j^i| \leq \left(\frac{(\Delta t)}{2} - D_f\frac{(\Delta x)^2}{12}\right)\Upsilon_f,\ x \in [-\frac{L}{2}, x_s], \\ \max_{i,j}|(\varsigma_m)_j^i| \leq \left(\frac{(\Delta t)}{2} - D_m\frac{(\Delta x)^2}{12}\right)\Upsilon_m,\ x \in [-\frac{L}{2}, x_s], \\ \max_{i,j}|(\varsigma_E)_j^i| \leq \left(\frac{(\Delta t)}{2} - D_E\frac{(\Delta x)^2}{12}\right)\Upsilon_E,\ x \in [-\frac{L}{2}, \frac{L}{2}], \\ \max_{i,j}|(\varsigma_G)_j^i| \leq \left(\frac{(\Delta t)}{2} - D_G\frac{(\Delta x)^2}{12}\right)\Upsilon_G, x \in [-\frac{L}{2}, \frac{L}{2}], \end{array}\right\} \quad (5.3.18)$$

for $t_{i-1} \leq \xi \leq t_{i+1}$ and $x_{j-1} \leq \zeta \leq x_{j+1}$. Moreover by [117] we have

$$||A_n^{-1}|| \leq \Xi_n,\ ||A_f^{-1}|| \leq \Xi_f, ||A_m^{-1}|| \leq \Xi_m,\ ||A_E^{-1}|| \leq \Xi_E,\ ||A_G^{-1}|| \leq \Xi_G. \quad (5.3.19)$$

Using (5.3.18) and (5.3.19) in (5.3.16), we obtain the following results.

Theorem 5.3.1. *Let*

$$F_n(x,t), F_f(x,t), F_m(x,t), F_E(x,t), F_G(x,t),$$

be sufficiently smooth functions so that

$$n(x,t), f(x,t), m(x,t), E(x,t), G(x,t) \in C^\infty([-L/2, L/2] \times [0,T]).$$

Let $(\mathcal{N}_j^i, \mathcal{F}_j^i, \mathcal{M}_j^i, \mathcal{E}_j^i, \mathcal{G}_j^i)$, $j = 1, 2, \ldots L, i = 1, 2, \ldots T$ *be the approximate solutions to (5.1.3), obtained using the FOFDM with* $\mathcal{N}_j^0 = n_j^0, \mathcal{F}_j^0 = f_j^0, \mathcal{M}_j^0 = m_j^0, \mathcal{E}_j^0 = E_j^0, \mathcal{G}_j^0 = G_j^0$,. *Then there exists* $\Xi_n, \Xi_f, \Xi_m, \Xi_E, \Xi_G$ *independent of the step sizes* Δt *and* Δx *such*

that

$$\left.\begin{aligned}
&\max_{i,j}|n_j^i - \mathcal{N}_j^i| \leq \Xi_n[\tfrac{(\Delta t)}{2} - D_n\tfrac{(\Delta x)^2}{12}]\Upsilon_n,\\
&\max_{i,j}|f_j^i - \mathcal{F}_j^i| \leq \Xi_f[\tfrac{(\Delta t)}{2} - D_f\tfrac{(\Delta x)^2}{12}]\Upsilon_f,\\
&\max_{i,j}|m_j^i - \mathcal{M}_j^i| \leq \Xi_m[\tfrac{(\Delta t)}{2} - D_m\tfrac{(\Delta x)^2}{12}]\Upsilon_m,\\
&\max_{i,j}|E_j^i - \mathcal{E}_j^i| \leq \Xi_E[\tfrac{(\Delta t)}{2} - D_E\tfrac{(\Delta x)^2}{12}]\Upsilon_E,\\
&\max_{i,j}|G_j^i - \mathcal{G}_j^i| \leq \Xi_G[\tfrac{(\Delta t)}{2} - D_G\tfrac{(\Delta x)^2}{12}]\Upsilon_G,
\end{aligned}\right\} \tag{5.3.20}$$

and this conclude the analysis of our FOFDM.

5.4 Numerical results and discussions

We set $S_x = S_t = 80$ and time $(t) = 25$ or $t = 30$. Then, using the parameter values in Table 5.5.1 ([59]) we first take $L = 5 < T = 20$ and we present our numerical results of the model without delay (5.1.1) in Figure 5.5.1 and Figure 5.5.2, respectively.

For $L = T = 5$ and $t = 25, 30$, we present our numerical results in Figure 5.5.3 ($\tau \equiv 0$), Figure 5.5.4 and for $L = 20 > T = 5$, our numerical results are presented in Figure 5.5.5 ($\tau \equiv 0$) at $t = 25$.

Similarly, for $L = 5 < T = 20$, $t = 25$ and $\tau = 5$, we present our numerical results in Figure 5.5.6 and for $\tau = 20$ we present our results in Figure 5.5.7.

For $L = 5 = T$, $t = 25$ and $\tau = 5$, we present our numerical results in Figure 5.5.8, for $L = 20 = T$ we present our results in Figure 5.5.9, for $t = 25$ and $\tau = 15$ and $L = 20 = T$ we present our results in Figure 5.5.10.

Finally, we present our numerical results for $L = 20 > T = 5$ at $t = 25$ for $\tau = 5, 25$ in Figure 5.5.11 and Figure 5.5.12.

In the figures for the original model in equation (5.1.1), that is Figure 5.5.1 to Figure

5.5.5 we see that the behaviour for the fibroblasts and myfibroblasts are zero almost for entire portion of their compartment, but eventually rise sharply near the end of the compartment in which they are embedded. One notable fact is that fibroblast grows to a very high height than the myfibroblasts. However, for the Transformed epithelial cells we see the oscillations type of behaviour near the preamble membrane when the length (L) of the compartment is lesser than or equal to the time (T) taken for the experiment. However, the oscillation decreases to a sharp peak when L is greater than T. For the excreted molecules, we also see a bigger peaks as compare to the restricted cells for the case when L is lesser, equal to T. However, when we increase L to be bigger than T, we see the excreted molecules grow sharply with slight decrease and increase till their turning point toward the end of the compartment.

For the modified model in equation (5.1.2), that is from Figure 5.5.6 to Figure 5.5.12 we see the following notable features. That is the oscillations behaviour of the Transformed Epithelial cells are prominent for the case of L lesser than T required by this experiment as compare to the behaviour of the vice versa of the length of the compartment to time required by this experiment. However, for the fibroblasts and myfibroblast cells their behaviours remains similar to that of the original model in equation (5.1.1). For the excreted molecules we see that their concentration are inverted in Figure 5.5.6, as compare to their corresponding behaviours in Figure 5.5.1. However, when we increase the delay, we see that the concentration of the Epidermal growth factor smooths out better than its behaviour when there is no delay. Similarly for the concentration of the Transformed growth factor. These behaviours becomes more prominent as we increases the delay around the specified length of the compartment and time.

5.5 Conclusion

In this chapter, we considered a less complicated model simulated in [42] with the aim of shedding more light into the interaction between transformed epithelial cells, fibrob-

lasts and myfibroblasts cells at an early stage of cancer disease. A more advanced model, in which the experiments is carried out in a tumor chamber invasion assay, where a semi-permeable membrane, which allows EGF, TGF$-\beta$ and Matrix Metalloproteinase (MMP) to cross it, coated by extra-cellular matrix (ECM) placed between two chambers, one containing TECs and another containing fibroblasts and myofibroblasts, has been dealt with elsewhere. Thus, we deemed it essential to incorporate some of the crucial transformations ought to take place during the experiment carried out in [63]. Such incorporation of some crucial transformations, led the original model to be transformed to a system of non-linear delay parabolic partial differential equations. We analysed the resulting system of non-linear delay parabolic partial differential equations and determined the global stability conditions for our resulting system. Consequently, we were able to derive a fitted operator finite difference (FOFDM) for solving the modified system in equation (5.1.2). In these experiments we see that the interaction of the two concentrations enhances the growth of the Epidermal growth factor molecules, while maintaining the sensitivity of the TECs to membrane permeability. However, such dynamic is more informative when a delay term is included in the modeling, especially when it comes to the behaviours of the secreted molecules. Thus, our main findings are more vivid, compare to those presented in [42] as well as in [33, 62]. More essentially, the indirect role played by the incorporation of a delay term (τ) in the extended model in equation (5.1.2) through the behaviours of the secreted molecules are more informative than what is presented in [42].

Table 5.5.1: Values of the parameters used in the model (5.3.4) [59]

$D_n = 3.6 \times 10^{-4}$	$\chi_n = 3.6 \times 10^{-8}$	$\lambda_E = 1.00$	$a_{11} = 0.69$
$\kappa = 2.88 \times 10^{3}$	$k_E = 3.32$	$D_f = 6.12 \times 10^{-}5$	$a_{21} = 2.61 \times 10^{-2}$
$a_{22} = 1.58 \times 10^{-2}$	$D_m = 6.12 \times 10^{-4}$	$\chi_m = 3.96 \times 10^{-6}$	$a_{31} = 4.53 \times 10^{-3}$
$\lambda_G = 1.00$	$D_e = 5.98 \times 10^{-1}$	$a_{41} = 1.26$	$a_{43} = 2.89 \times 10^{-2}$
$B = 5.00$	$D_g = 3.6 \times 10^{-1}$	$a_{51} = 2.03 \times 10^{-1}$	$a_{52} = 2.89 \times 10^{-2}$

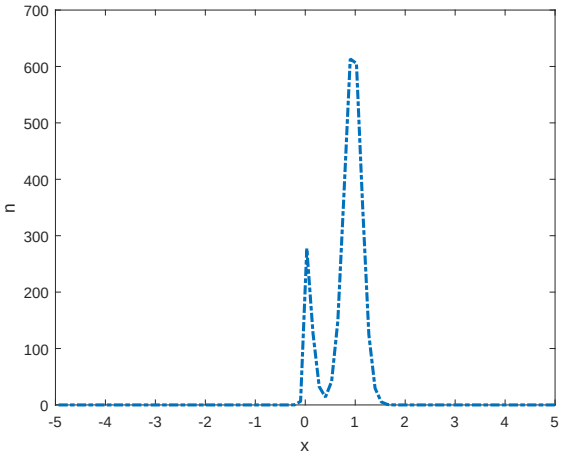

(a) Behaviour of Transformed Epithelial cells (TECs)

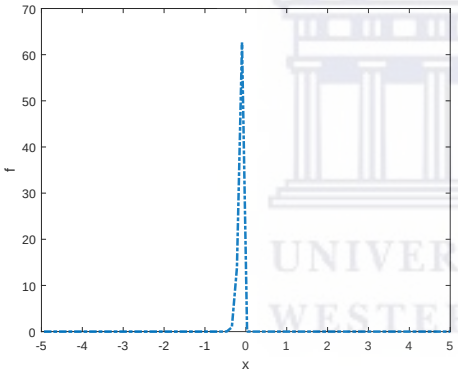

(b) Behaviour of Fibroblasts cells

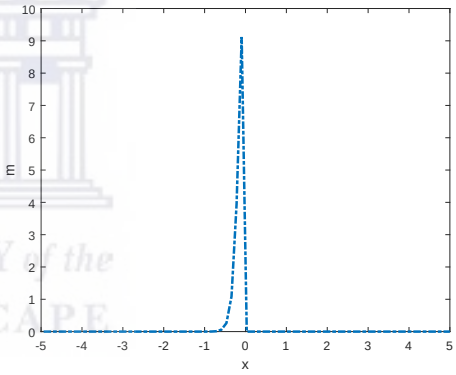

(c) Behaviour of Myfibroblasts cells

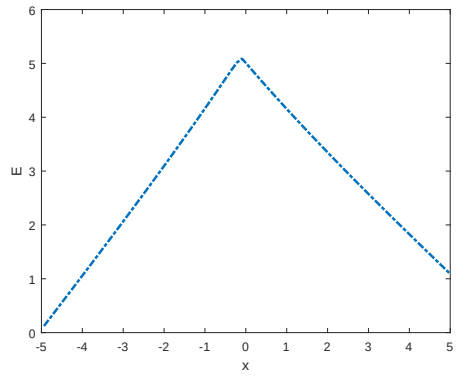

(d) Behaviour of the concentration of Epidermal Growth Factor molecules (EGF)

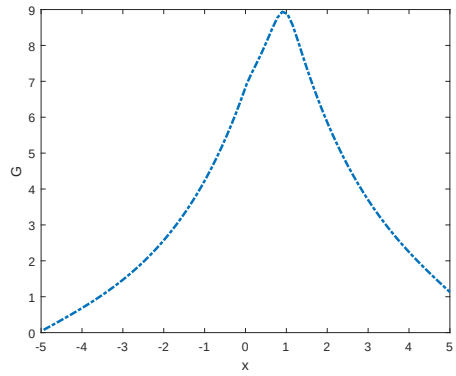

(e) Behaviour of the concentration of Transformed Growth Factor molecules (TGF-β)

Figure 5.5.1: Numerical solution of the system in (5.1.2) without delay at t = 25 for $L < T$.

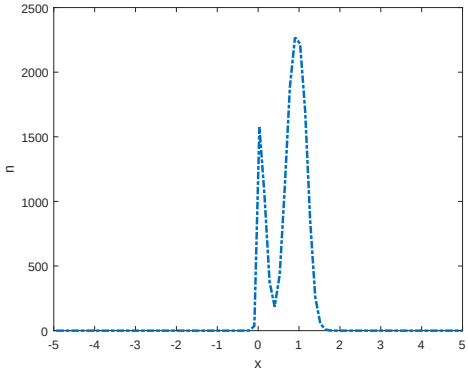

(a) Behaviour of Transformed Epithelial cells (TECs)

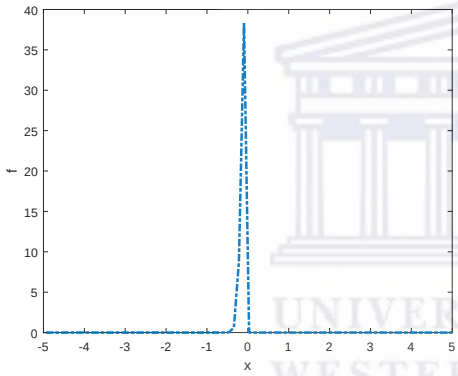

(b) Behaviour of Fibroblasts cells

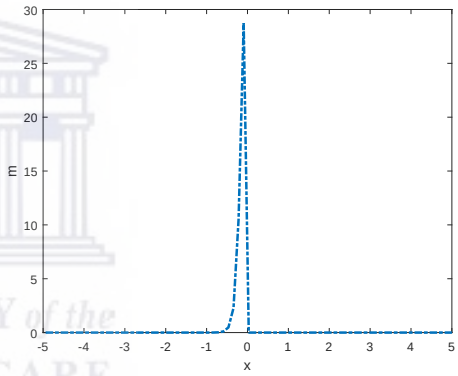

(c) Behaviour of Myfibroblasts cells

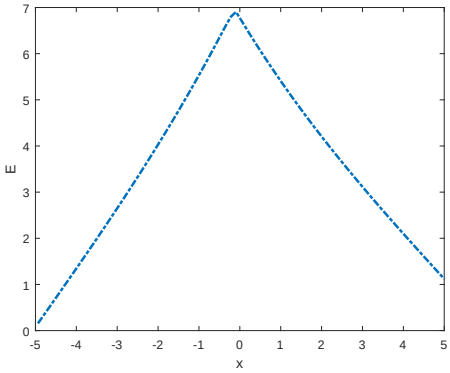

(d) Behaviour of the concentration of Epidermal Growth Factor molecules (EGF)

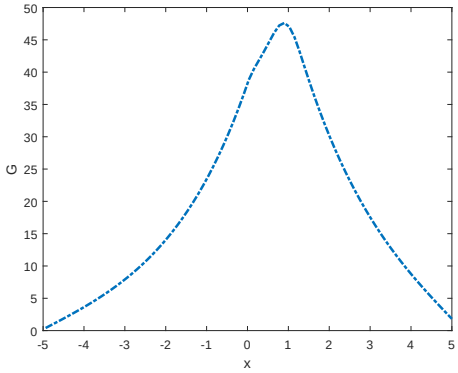

(e) Behaviour of the concentration of Transformed Growth Factor molecules (TGF-β)

Figure 5.5.2: Numerical solution of the system in (5.1.2) without delay at t = 30 for $L < T$.

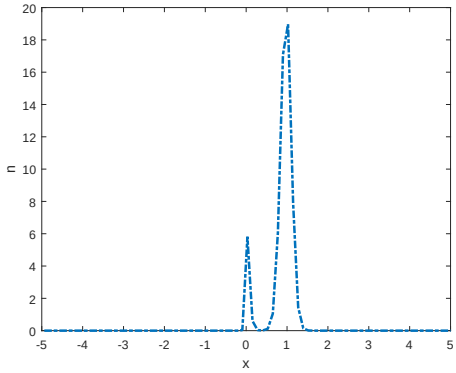

(a) Behaviour of Transformed Epithelial cells (TECs)

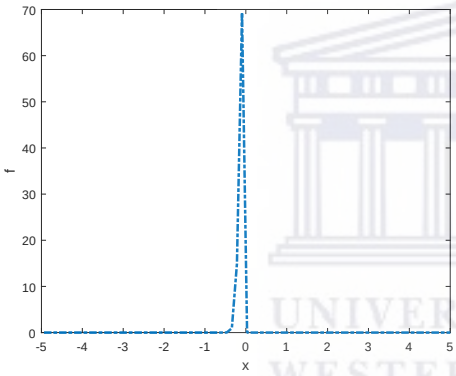

(b) Behaviour of Fibroblasts cells

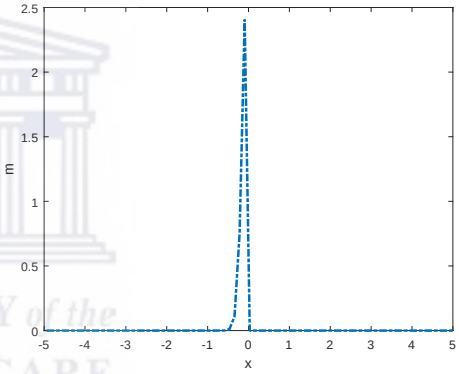

(c) Behaviour of Myfibroblasts cells

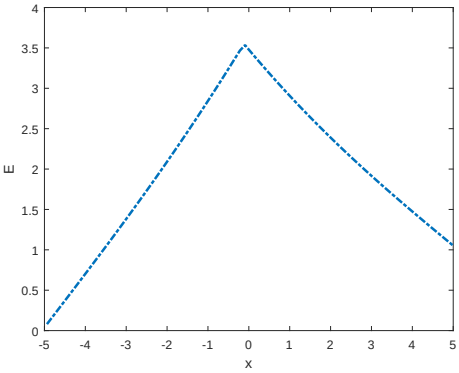

(d) Behaviour of the concentration of Epidermal Growth Factor molecules (EGF)

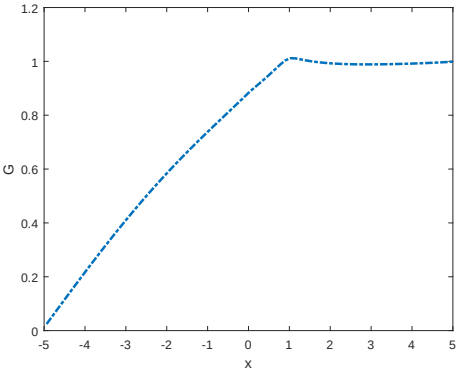

(e) Behaviour of the concentration of Transformed Growth Factor molecules (TGF-β)

Figure 5.5.3: Numerical solution of the system in (5.1.2) without delay at t = 25 for $L = T$.

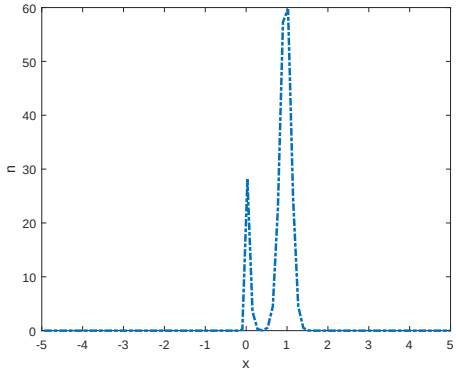

(a) Behaviour of Transformed Epithelial cells (TECs)

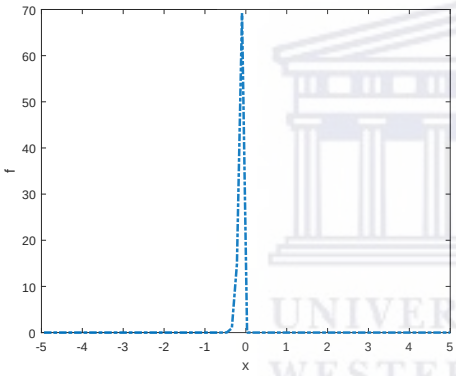

(b) Behaviour of Fibroblasts cells

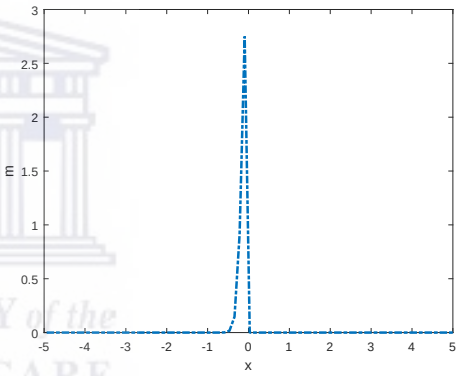

(c) Behaviour of Myfibroblasts cells

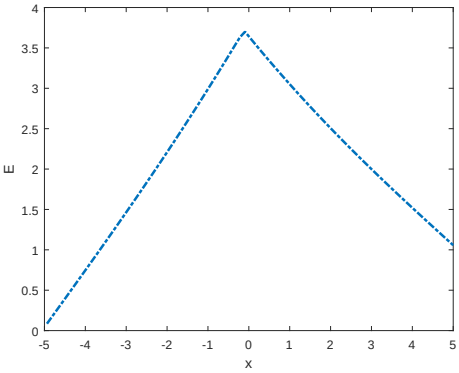

(d) Behaviour of the concentration of Epidermal Growth Factor molecules (EGF)

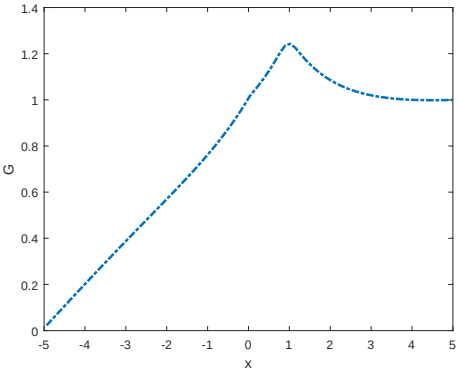

(e) Behaviour of the concentration of Transformed Growth Factor molecules (TGF-β)

Figure 5.5.4: Numerical solution of the system in (5.1.2) without delay at t = 30 for $L = T$.

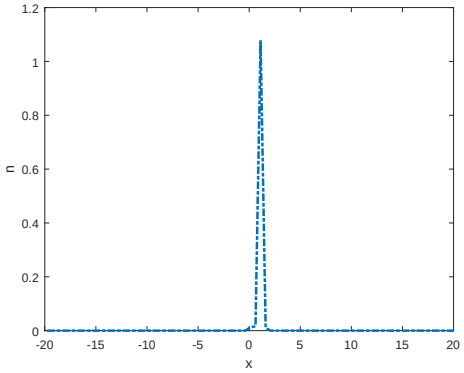

(a) Behaviour of Transformed Epithelial cells (TECs)

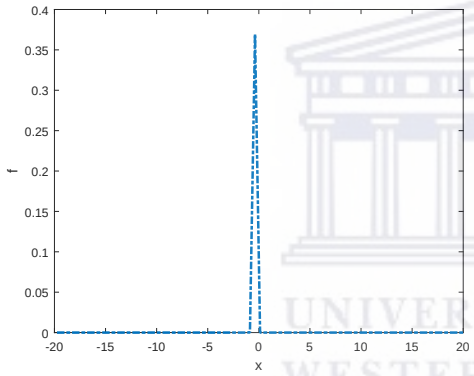

(b) Behaviour of Fibroblasts cells

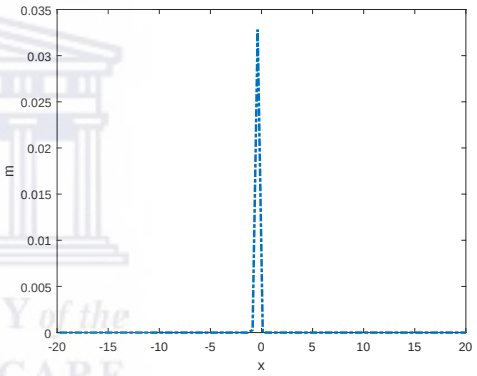

(c) Behaviour of Myfibroblasts cells

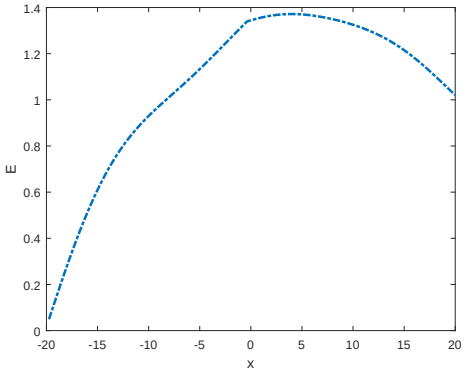

(d) Behaviour of the concentration of Epidermal Growth Factor molecules (EGF)

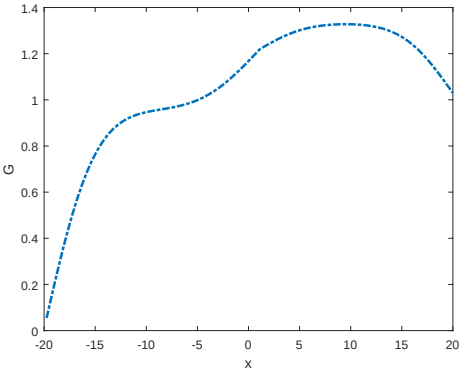

(e) Behaviour of the concentration of Transformed Growth Factor molecules (TGF-β)

Figure 5.5.5: Numerical solution of the system in (5.1.2) without delay at t = 25 for $L > T$.

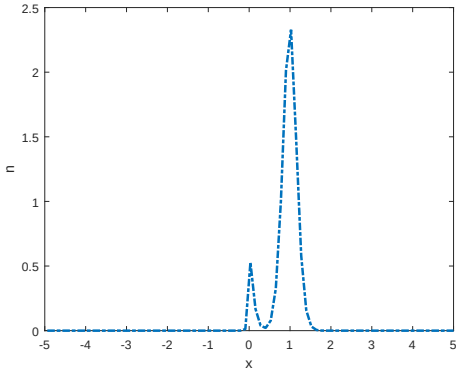

(a) Behaviour of Transformed Epithelial cells (TECs)

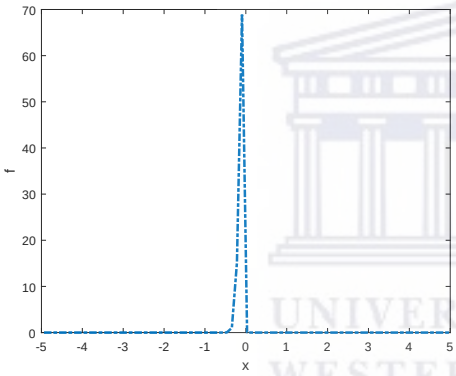

(b) Behaviour of Fibroblasts cells

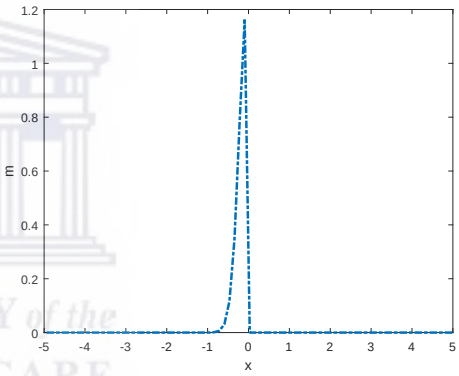

(c) Behaviour of Myfibroblasts cells

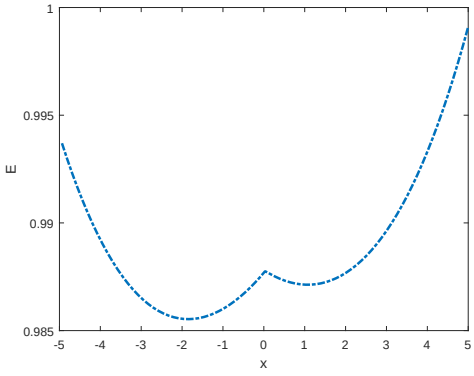

(d) Behaviour of the concentration of Epidermal Growth Factor molecules (EGF)

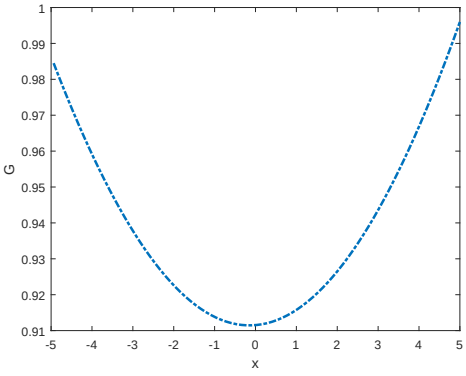

(e) Behaviour of the concentration of Transformed Growth Factor molecules (TGF-β)

Figure 5.5.6: Numerical solution of the system in (5.1.2) with delay=5 days for $L < T$.

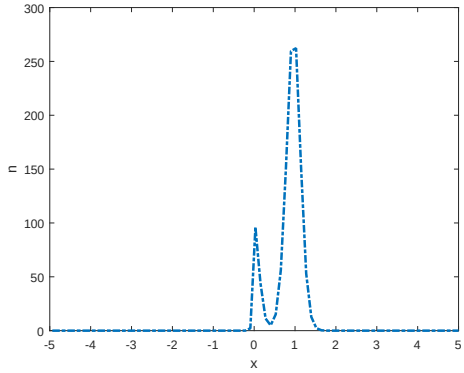

(a) Behaviour of Transformed Epithelial cells (TECs)

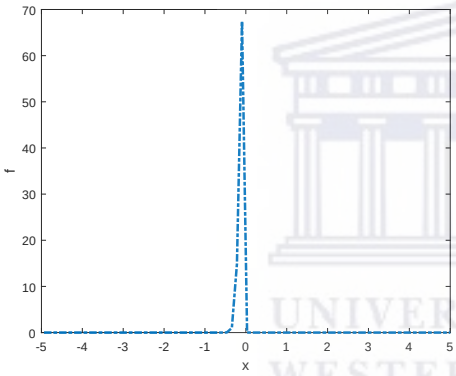

(b) Behaviour of Fibroblasts cells

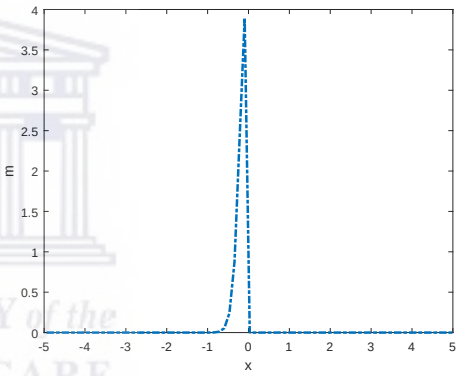

(c) Behaviour of Myfibroblasts cells

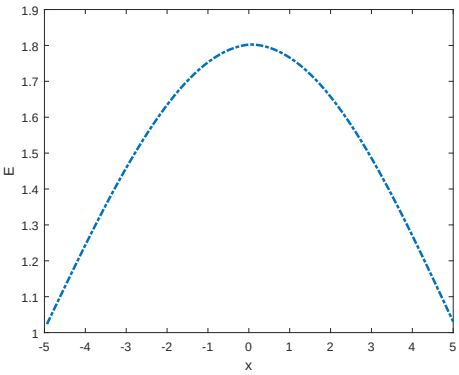

(d) Behaviour of the concentration of Epidermal Growth Factor molecules (EGF)

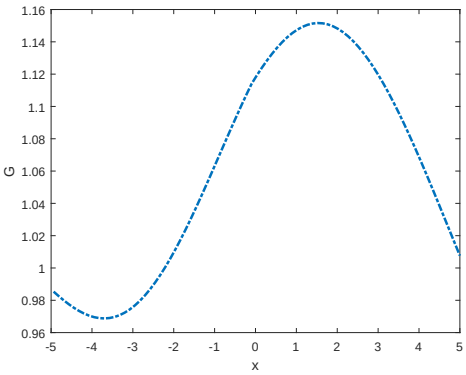

(e) Behaviour of the concentration of Transformed Growth Factor molecules (TGF-β)

Figure 5.5.7: Numerical solution of the system in (5.1.2) with delay=20 days for $L < T$ at t = 25.

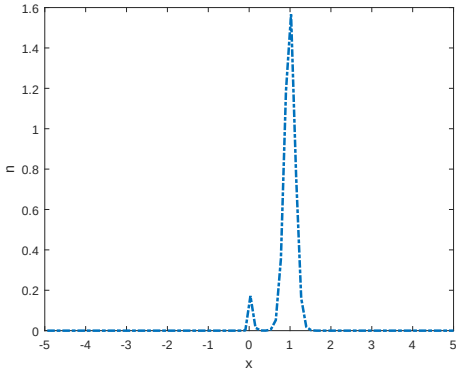

(a) Behaviour of Transformed Epithelial cells (TECs)

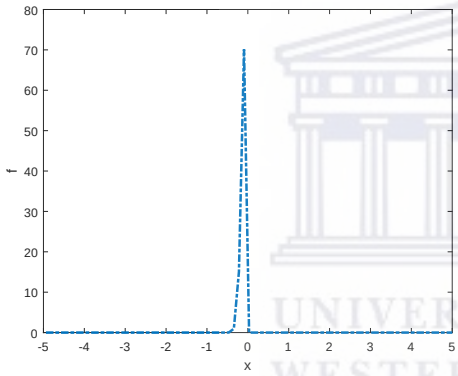

(b) Behaviour of Fibroblasts cells

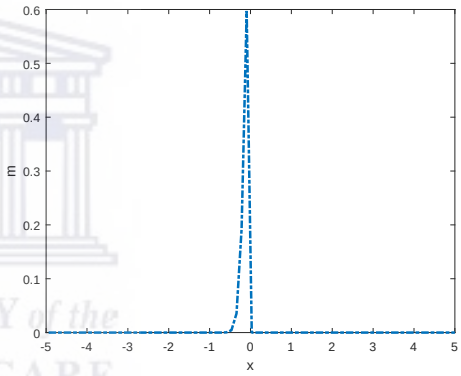

(c) Behaviour of Myfibroblasts cells

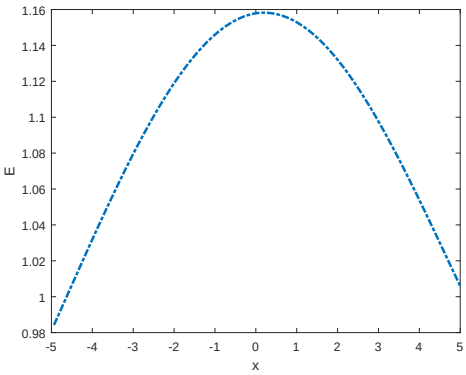

(d) Behaviour of the concentration of Epidermal Growth Factor molecules (EGF)

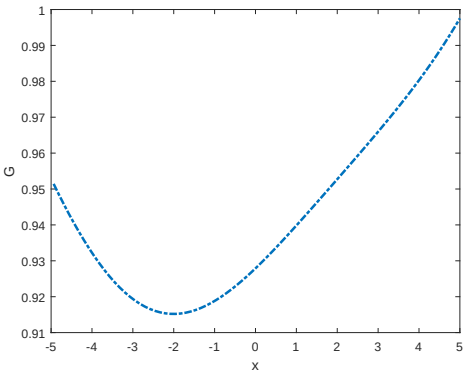

(e) Behaviour of the concentration of Transformed Growth Factor molecules (TGF-β)

Figure 5.5.8: Numerical solution of the system in (5.1.2) with delay=5 days for $L = T$ at $t = 25$.

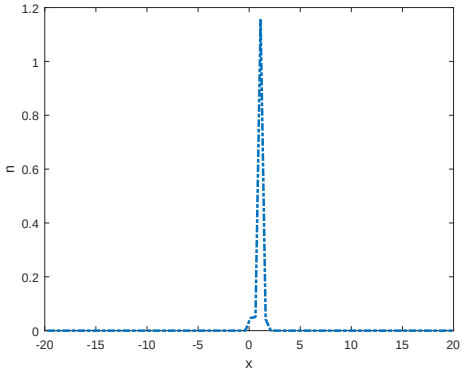

(a) Behaviour of Transformed Epithelial cells (TECs)

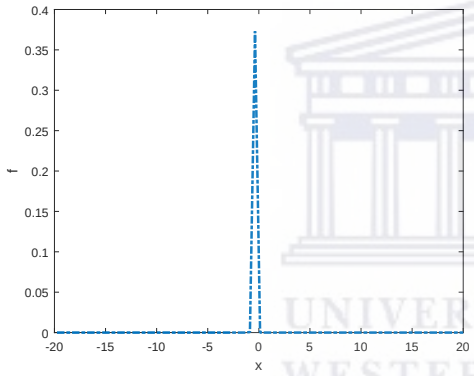

(b) Behaviour of Fibroblasts cells

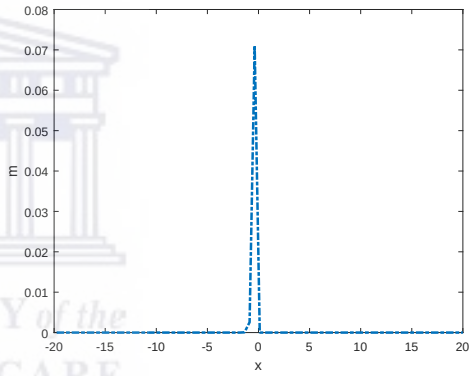

(c) Behaviour of Myfibroblasts cells

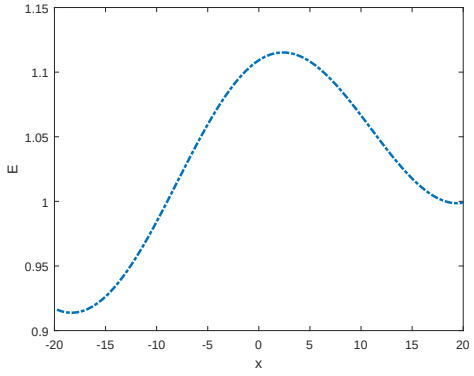

(d) Behaviour of the concentration of Epidermal Growth Factor molecules (EGF)

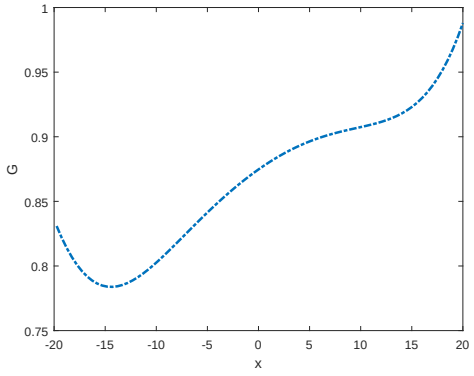

(e) Behaviour of the concentration of Transformed Growth Factor molecules (TGF-β)

Figure 5.5.9: Numerical solution of the system in (5.1.2) with delay=5 days for $L = T$ at $t = 25$.

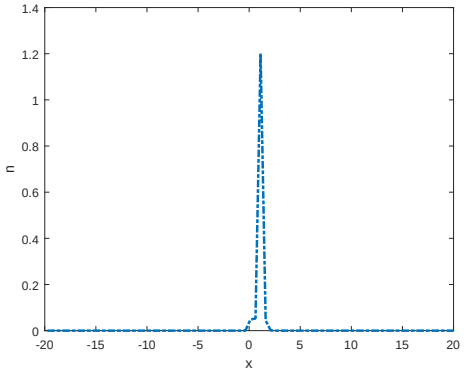

(a) Behaviour of Transformed Epithelial cells (TECs)

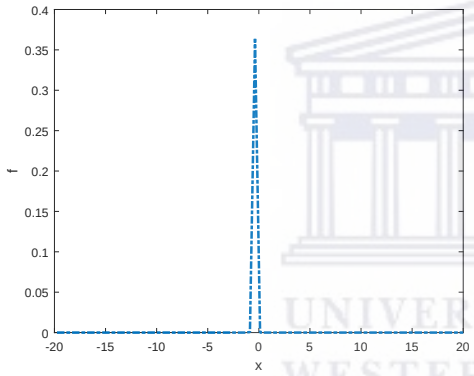

(b) Behaviour of Fibroblasts cells

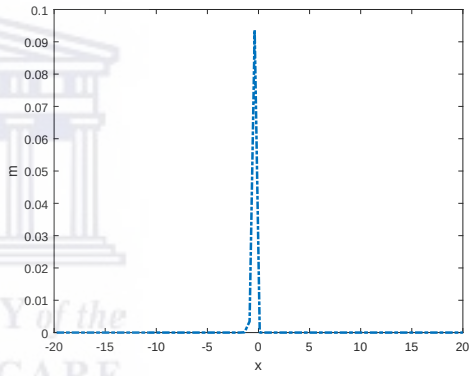

(c) Behaviour of Myfibroblasts cells

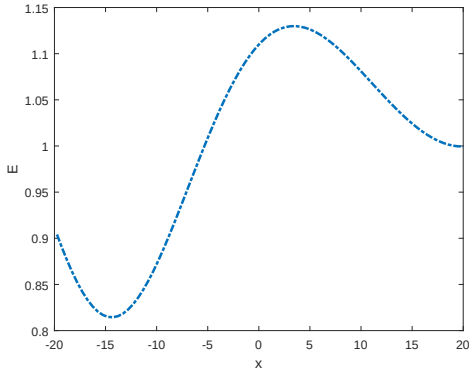

(d) Behaviour of the concentration of Epidermal Growth Factor molecules (EGF)

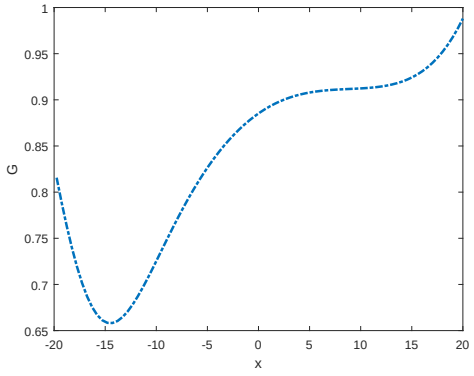

(e) Behaviour of the concentration of Transformed Growth Factor molecules (TGF-β)

Figure 5.5.10: Numerical solution of the system in (5.1.2) with delay=15 days for $L = T$ at $t = 25$.

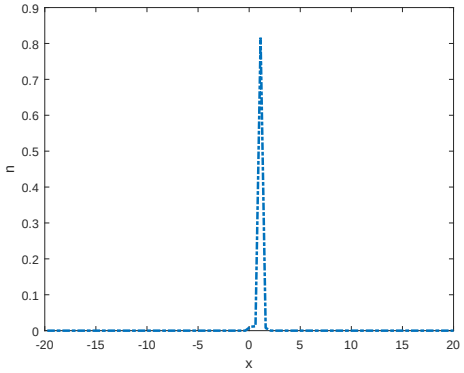

(a) Behaviour of Transformed Epithelial cells (TECs)

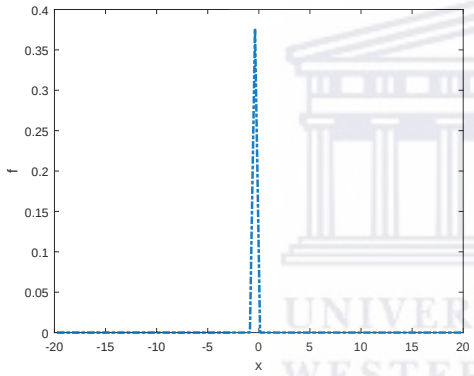

(b) Behaviour of Fibroblasts cells

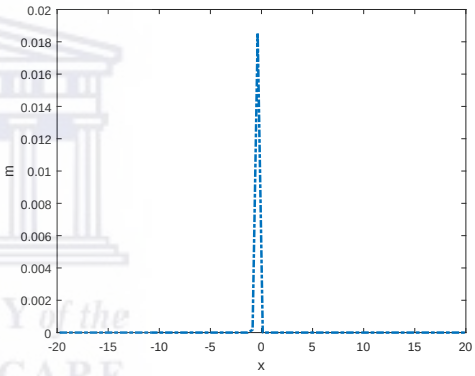

(c) Behaviour of Myfibroblasts cells

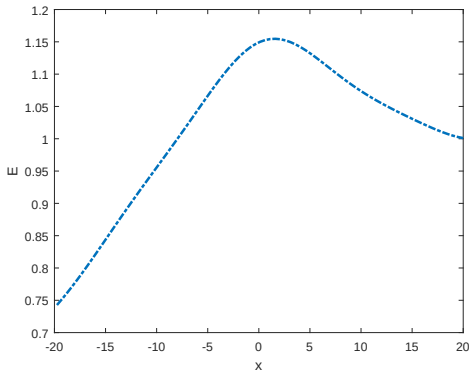

(d) Behaviour of the concentration of Epidermal Growth Factor molecules (EGF)

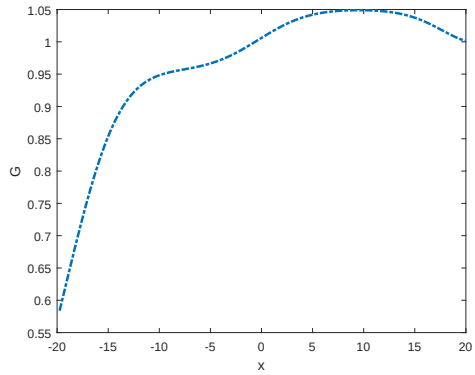

(e) Behaviour of the concentration of Transformed Growth Factor molecules (TGF-β)

Figure 5.5.11: Numerical solution of the system in (5.1.2) with delay=5 days for $L > T$ at $t = 25$.

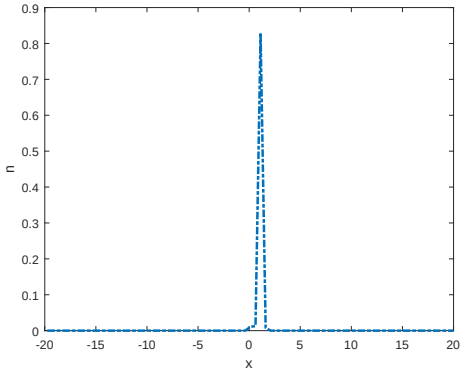

(a) Behaviour of Transformed Epithelial cells (TECs)

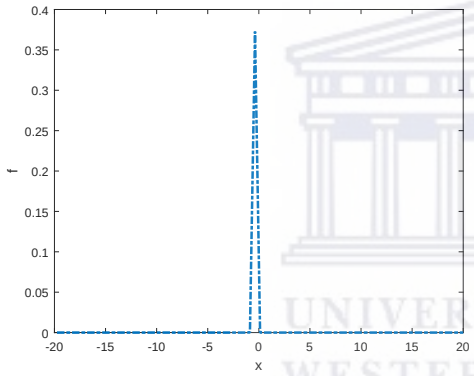

(b) Behaviour of Fibroblasts cells

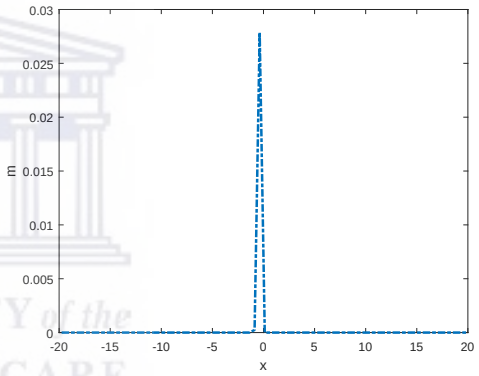

(c) Behaviour of Myfibroblasts cells

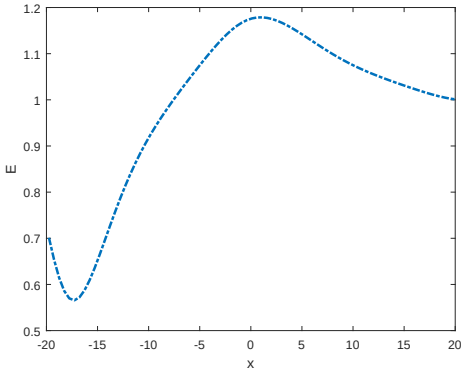

(d) Behaviour of the concentration of Epidermal Growth Factor molecules (EGF)

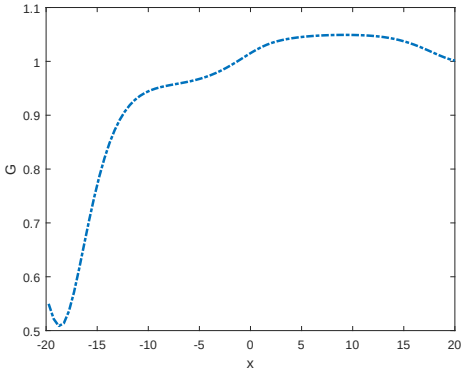

(e) Behaviour of the concentration of Transformed Growth Factor molecules (TGF-β)

Figure 5.5.12: Numerical solution of the system in (5.1.2) with delay=20 days for $L > T$ at $t = 25$.

In view of the previous chapters, we are now at the position for considering a

tumour cells from the cell cycle point of view. Therefore in Chapter 6, we consider the dynamics of tumour cells from the cell cycle point of view.

Chapter 6

A fitted operator method for a mathematical model arising in vascular tumor dynamics

We consider a model for the kinetics of human tumor cells in vitro, differentiated by phases of the cell division cycle and length of time within each phase. Since it is not easy to isolate the effects of cancer treatment on the cell cycle of human cancer lines, during the process of radiotherapy or chemotherapy, therefore, we include the spatial effects of cells in each phase and analyse the extended model. The extended model is not easy to solve analytically, because perturbation by cancer therapy causes the flow cytometric profile to change in relation to one another. Hence, making it difficult for the resulting model to be solved analytically. In [85] it is reported that the non-standard schemes are reliable and propagate sharp fronts accurately, even when the advection, reaction processes are highly dominant and the initial data are not smooth. As a result, we construct a fitted operator finite difference (FOFDM) coupled with non-standard finite difference (NSFDM) to solve the extended model. The FOFDM and NSFDM are analyzed for convergence and are seen that they are unconditionally stable and have the accuracy of $\mathcal{O}(\Delta t + (\Delta x)^2)$, where Δt and Δx denote time and space step-sizes,

respectively. Some numerical results confirming theoretical observations are presented.

6.1 The model

Vascular tumors are a highly diverse group of aberrant growths and they are relatively abundant in the human population, with infantile hemangiomas being the most common tumor in children and cavernous hemangiomas affecting approximately one in every one hundred people see [2] and the references therein. Therefore, in view of our contribution reported in [94, 95, 96, 97, 98] on tumors, we feel that it is essential for us as researchers to understand that genetic differences between people lead to differences in susceptibility. Since tumors develop in different organs and tissues of a body, then this should imply that a genetic heterogeneity among cancer cells, the cellular heterogeneity of the tumor tissue underlie a phenotype heterogeneity of the disease and cancer cells in a tumor are not all identical, but form different clones, defined as sets of cancer cells that share a common genotype [129]. Therefore, in our views, it is also very important to study dynamics for the kinetics of a population of cells differentiated by phases of the cell division cycle such as the ones presented by Jackiewicz et al. [51] as a way toward avoiding incorrect treatment decisions especially, if a biopsy sample is not representative of other parts of the tumor.

On the other hand, it is understood that even in the simplified environment of the laboratory with modern techniques and/or technology, it is not always possible to isolate the effects of cancer treatment on the cell cycle of human cancer cell lines. Therefore, it is important to mentioned some of the work done in the direction of understanding cancer cells from the cells cycle point of view. Thus, we highlight few studies done in this direction. These are for instance Giotti et al. [44] mentioned that cell division is central to the physiology and pathology of all eukaryotic organisms and in [11, 13, 14], have considered the in-vitro model of cancer therapies that target the cellular mechanisms of growth, division and death in all or some stages of the cell cycle. Thus, our first aim in this chapter is to include the spatial distribution of each phase

for the model derived in [11] and presented in [51]. The model in [51] is given as follow,

$$\left.\begin{aligned}
&\tfrac{\partial G_1(x,t)}{\partial t} = 4bM(2x,t) - (k_1+\mu_{G_1})G_1(x,t),\\
&\tfrac{\partial S(x,t)}{\partial t} = \varepsilon\tfrac{\partial^2 S(x,t)}{\partial x^2} - g\tfrac{\partial S(x,t)}{\partial x} - \mu_S S(x,t) + k_1 G_1(x,t) - I(x,t,T_S)),\\
&\tfrac{\partial G_2(x,t)}{\partial t} = I(x,t;T_S) - (k_2+\mu_{G_2})G_2(x,t),\\
&\tfrac{\partial M(x,t)}{\partial t} = k_2 G_2(x,t) - bM(x,t) - \mu_M M(x,t),
\end{aligned}\right\} \quad (6.1.1)$$

where, x,$t \geq 0$, T_S, $G_1(x,t)$, $S(x,t)$, $G_2(x,t)$, $M(x,t)$, μ_{G_1}, μ_S , μ_{G_2} , and μ_M denote the dimensionless relative DNA content, time in hours, time in hours, density of cells in G_1phase, density of cells in DNA synthesis or Sphase, density of cells in G_2phase and metosis or Mphase, death rates in G_1, S, G_2, and M phases, respectively. The parameters k_1 and k_2 denote the transition probabilities of cells from G_1 to Sphase and from G_2 to Mphase, respectively, $b, 0 < \varepsilon <<< 1, g >>> 1$ denote division rate, dispersion coefficient and average growth rate of DNA in the Sphase. The $4bM(2x,t)$ term on the right hand side of the first equation in (6.1.1) arises due to a change of variable in the derivation as cells in an interval $[2x, 2x+2\Delta x]$ are doubled in number and transferred to the interval $[x, x+\Delta x]$ with half the DNA content [51]. The term $I(x,t;T_S)$ denotes cells that have been T_S hours in DNA synthesis and are ready to be transferred to G_2phase, which is also referred to as a delay term and its derivation is explained in [11]. However, $I(x,t;T_S)$ denotes the solution of the diffusion equation

$$\frac{\partial I(x,t;\tau_S)}{\partial \tau_S} + g\frac{\partial I(x,t;\tau_S)}{\partial x} - \epsilon\frac{\partial^2 I(x,t;\tau_S)}{\partial x^2} + \mu_S I(x,t;\tau_S) = 0,\ 0 < x < \infty,\ t > \tau_S > 0,$$

at time $\tau_S = T_S$, where τ_S is the time denoting the time spent by cells in DNA synthesis or Sphase. The analytical solution (with appropriate initial conditions and a zero flux boundary condition) is obtained by using Laplace transform techniques and Green's

functions in [51]. Thus, it reads

$$I(x,t,T_S) = \begin{cases} \int_0^\infty k_1 G_1(y, t-T_S)\gamma(T_S,x,y)dy, \text{ if } t \geq T_S, \\ \\ I(x,t,T_S) = 0, \text{ if } t < T_S, \end{cases} \tag{6.1.2}$$

where $\gamma(T_S, x, y)$ denotes a weight function given by

$$\gamma(T_S,x,y) = \frac{\exp(-\mu_S\tau)}{2\sqrt{\pi\epsilon\tau}}\left(\exp\left(-\frac{((x-g\tau)-y)^2}{4\epsilon\tau}\right)\right)$$

$$-(1+v(\tau,x,y))\exp(-\frac{((x+g\tau)+y)^2}{4\epsilon\tau}), \tag{6.1.3}$$

with

$$v(\tau,x,y) = \frac{x+y}{g\tau}(1+O(\tau^{-1})).$$

In equation (6.1.3) γ denotes a Greens function whereas, ν term arises due to the zero flux boundary condition.

The system (6.1.1) is incomplete without initial and boundary conditions. These conditions, which are chosen according to experimental evidence [51], take the form of

$$\left.\begin{array}{l} G_1(x,0) = \frac{a_0}{\sqrt{2\pi\theta_0^2}}\exp\left(-\frac{(x-1)^2}{2\pi\theta_0^2}\right), \quad 0 < x < \infty, \\ \\ S(x,0) = 0, \;\; G_2(x,0) = 0, \;\; M(x,0) = 0, \;\; 0 < x < \infty, \end{array}\right\} \tag{6.1.4}$$

and the boundary condition

$$\epsilon\frac{\partial S(0,t)}{\partial x} - gS(0,t) = 0, \;\; t > 0. \tag{6.1.5}$$

The initial DNA content of cells in the G_1phase is chosen as a Gaussian distribution

with relative mean DNA content at $x = 1$ equal to a_0, and variance θ_0^2. This variance is chosen sufficiently small so that the extension of $G_1(x, 0)$ into the in-feasible region $x < 0$ is of no significance. In [51] a numerical methods are constructed to solve (6.1.1) supplemented by the initial conditions in equation (6.1.4) and the general boundary conditions of the form of

$$\left.\begin{array}{l} \epsilon\frac{\partial S(0,t)}{\partial x} - gS(0,t) = \alpha, \;\; t > 0, \\ \\ S(L,0) = \beta, \;\; t > 0, \end{array}\right\} \tag{6.1.6}$$

with any real values α and β, where the parameter β was chosen according to the experimental data provided in [12].

We can see that the system in equation (6.1.1) is a semi-system of integro-delayed partial differential equation (IDPDE). Thus, in order to have a complete understanding of the population kinetics of the human tumor cells, it is very important to include the spatial effects of all the cells in each phase, rather only consider the spatial effects of one phase and ignore the other effects of the other three phases. Consequently, mathematical analysis of the extended model is also vital to justify the understanding of the population kinetics of human tumor cells, when one present the experimental results. Therefore, our main aim in this chapter, is to extend the model in equation (6.1.1) to a system of convection-reaction-diffusion equations, investigate the qualitative features of the model with the spatial effects of all the phases and determine the location of the boundary layer. Since, flow cytometry is a technique where the DNA content of individual cells is measured and binned accordingly. The resulting results present clearly the phases which are perturbed and unperturbed by therapy. Thus, perturbation by cancer therapy causes these peaks to change in relation to one another as it can be seen in all the figures presented.

Since, explicit methods such as the finite difference (EFDMs), solve differential equations with low computational cost, within very small stability regions, which in turn implies severe restrictions on meshes sizes, which are required in order to achieve

the desired results, then, implicit finite difference (IFDMs) are more favor to solve differential equations, because of their wider stability regions as compared to the EFDMS [22]. Thus, our second aim in this chapter, is to solve the extended model. Thus, we develop an efficient numerical method for solving the extended model with respect to the qualitative features of the original model.

Thus, extending the IDPDE in equation (6.1.1), we have

$$\left.\begin{aligned}
&\tfrac{\partial G_1(x,t)}{\partial t} = D_{G_1}\tfrac{\partial^2 G_1(x,t)}{\partial x^2} + 4bM(2x,t) - (k_1+\mu_{G_1})G_1(x,t),\\
&\tfrac{\partial S(x,t)}{\partial t} = \epsilon\tfrac{\partial^2 S(x,t)}{\partial x^2} - g\tfrac{\partial S(x,t)}{\partial x} - \mu_S S(x,t) + k_1 G_1(x,t) - I(x,t;T_S),\\
&\tfrac{\partial G_2(x,t)}{\partial t} = D_{G_2}\tfrac{\partial^2 G_2(x,t)}{\partial x^2} + I(x,t;T_S) - (k_2+\mu_{G_2})G_2(x,t),\\
&\tfrac{\partial M(x,t)}{\partial t} = D_M\tfrac{\partial^2 M(x,t)}{\partial x^2} + k_2 G_2(x,t) - bM(x,t) - \mu_M M(x,t),
\end{aligned}\right\} \tag{6.1.7}$$

where, D_{G_1}, D_{G_2}, D_M denote the dispersion coefficient of G_1, G_2 and M cells in each phase, $0 < x < L$ and $t > 0$, subject to the initial data as given in equation (6.1.4) and the boundary conditions are

$$\left.\begin{aligned}
&\tfrac{\partial G_1}{\partial \nu}(0,t) = \tfrac{\partial G_2}{\partial \nu}(0,t) = \tfrac{\partial M}{\partial \nu}(0,t) = \chi_1,\\
&\tfrac{\partial G_1}{\partial \nu}(L,t) = \tfrac{\partial G_2}{\partial \nu}(L,t) = \tfrac{\partial M}{\partial \nu}(L,t) = \chi_2,\\
&\epsilon\tfrac{\partial S(0,t)}{\partial x} - gS(0,t) = \alpha, \;\; t > 0,\\
&S(L,0) = \beta, \;\; t > 0,
\end{aligned}\right\} \tag{6.1.8}$$

where, $\nu, \chi_k, (k = 1, 2)$ denote an outward normal vector, and positive constants, whereas the initial functions $(G_1)_0(x,t), S_0(x,t), (G_2)_0(x,t), M_0(x,t)$ are assumed to

satisfy the compatibility conditions [109],

$$\left.\begin{aligned}
&\tfrac{\partial G_1}{\partial \nu}(0,0) = \tfrac{\partial G_2}{\partial \nu}(0,0) = \tfrac{\partial M}{\partial \nu}(0,0) = \chi_1,\\
&\tfrac{\partial G_1}{\partial \nu}(L,0) = \tfrac{\partial G_2}{\partial \nu}(L,0) = \tfrac{\partial M}{\partial \nu}(L,0) = \chi_2,\\
&\epsilon\tfrac{\partial S(0,0)}{\partial x} - gS(0,0) = \alpha, \;\; t > 0,\\
&S(L,0) = \beta,\\
&\tfrac{\partial G_1(0,0)}{\partial t} = D_{G_1}\tfrac{\partial^2 G_1(0,0)}{\partial x^2} + 4bM(0,0) - (k_1 + \mu_{G_1})G_1(0,0),\\
&\tfrac{\partial S(0,0)}{\partial t} = \epsilon\tfrac{\partial^2 S(0,0)}{\partial x^2} - g\tfrac{\partial S(0,0)}{\partial x} - \mu_S S(0,0) + k_1 G_1(0,0) - I(0,0;0),\\
&\tfrac{\partial G_2(0,0)}{\partial t} = D_{G_2}\tfrac{\partial^2 G_2(0,0)}{\partial x^2} + I(0,0;0) - (k_2 + \mu_{G_2})G_2(0,0),\\
&\tfrac{\partial M(0,0)}{\partial t} = D_M\tfrac{\partial^2 M(0,0)}{\partial x^2} + k_2 G_2(0,0) - bM(0,0) - \mu_M M(0,0),
\end{aligned}\right\} \quad (6.1.9)$$

and

$$\left.\begin{aligned}
&\tfrac{\partial G_1}{\partial \nu}(L,0) = \tfrac{\partial G_2}{\partial \nu}(L,0) = \tfrac{\partial M}{\partial \nu}(L,0) = \chi_1,\\
&\tfrac{\partial G_1}{\partial \nu}(L,0) = \tfrac{\partial G_2}{\partial \nu}(L,0) = \tfrac{\partial M}{\partial \nu}(L,0) = \chi_2,\\
&\epsilon\tfrac{\partial S(L,0)}{\partial x} - gS(L,0) = \alpha, \;\; t > 0,\\
&S(L,0) = \beta,\\
&\tfrac{\partial G_1(L,0)}{\partial t} = D_{G_1}\tfrac{\partial^2 G_1(L,0)}{\partial x^2} + 4bM(L,0) - (k_1 + \mu_{G_1})G_1(L,0),\\
&\tfrac{\partial S(L,0)}{\partial t} = \epsilon\tfrac{\partial^2 S(L,0)}{\partial x^2} - g\tfrac{\partial S(L,0)}{\partial x} - \mu_S S(L,0) + k_1 G_1(L,0) - I(L,0;0),\\
&\tfrac{\partial G_2(L,0)}{\partial t} = D_{G_2}\tfrac{\partial^2 G_2(L,0)}{\partial x^2} + I(L,0;0) - (k_2 + \mu_{G_2})G_2(L,0),\\
&\tfrac{\partial M(L,0)}{\partial t} = D_M\tfrac{\partial^2 M(L,0)}{\partial x^2} + k_2 G_2(L,0) - bM(L,0) - \mu_M M(L,0).
\end{aligned}\right\} \quad (6.1.10)$$

Under the assumptions in (6.1.9)-(6.1.10) the extended model in equation (6.1.7) with the initial and boundary conditions in (6.1.4) and (6.1.8), respectively, has a unique solution [8].

The rest of the chapter is arranged as follow. In section 6.2, we carry out mathematical analysis of the model, whereas in section 6.3, we derive and analyse the numerical method. section 6.4 deals with the implementation of our numerical method, presentation of our numerical results and we conclude the chapter with section 6.5.

6.2 Mathematical analysis of the model

At the equilibria the model in equation (6.1.7) becomes

$$\left.\begin{aligned} &D_{G_1}\tfrac{\partial^2 G_1(x,t)}{\partial x^2} - (k_1+\mu_{G_1})G_1(x,t) = -4bM(2x,t),\\ &\epsilon\tfrac{\partial^2 S(x,t)}{\partial x^2} - g\tfrac{\partial S(x,t)}{\partial x} - \mu_S S(x,t) = I(x,t;T_S) - k_1 G_1(x,t),\\ &D_{G_2}\tfrac{\partial^2 G_2(x,t)}{\partial x^2} - (k_2+\mu_{G_2})G_2(x,t) = I(x,t;T_S),\\ &D_M\tfrac{\partial^2 M(x,t)}{\partial x^2} - (b+\mu_M)M(x,t) = -k_2 G_2(x,t). \end{aligned}\right\} \tag{6.2.1}$$

From the first, third and fourth equations in (6.2.1) we obtain the following solutions for the corresponding homogeneous part

$$\begin{aligned} G_1^*(x) &= c_{g11} + c_{g12}\exp\left(\frac{D_{G_1}}{k_1+\mu_{G_1}}x\right),\\ G_2^*(x) &= c_{g21} + c_{g22}\exp\left(\frac{D_{G_2}}{k_2+\mu_{G_2}}x\right),\\ M^*(x) &= c_{m1} + c_{m2}\exp\left(\frac{D_M}{b+\mu_M}x\right), \end{aligned} \tag{6.2.2}$$

where, $c_{g11}, c_{g12}, c_{g21}, c_{g22}, c_{m1}, c_{m2}$ are non-negative constants. However, for the DNA synthesis or Sphase steady state, we see that the null space is given by

$$S'' - \frac{g}{\epsilon}S' - \frac{\mu_S}{\epsilon}S = 0, \tag{6.2.3}$$

of which the auxiliary equation to the equation (6.2.3) is

$$r^2 - \frac{g}{\epsilon}r - \frac{\mu_S}{\epsilon} = 0, \tag{6.2.4}$$

which implies that the solution to the auxiliary equation in (6.2.4) is

$$r^- = \frac{1}{2}\left(\frac{g}{\epsilon} - \sqrt{\left(\frac{g}{\epsilon}\right)^2 + 4\frac{\mu_S}{\epsilon}}\right), \quad \text{and} \quad r^+ = \frac{1}{2}\left(\frac{g}{\epsilon} + \sqrt{\left(\frac{g}{\epsilon}\right)^2 + 4\frac{\mu_S}{\epsilon}}\right), \tag{6.2.5}$$

which in turn, implies that the solution to the second order differential equation in (6.2.3) is

$$S^* = A\exp(r^- x) + B\exp(r^+ x), \tag{6.2.6}$$

where, from the given general boundary conditions in (6.1.8), we find that

$$A + B = S_0, \text{ and } S_0' = Ar^- + Br^+, \tag{6.2.7}$$

so that

$$\begin{aligned}
\epsilon S_0' + gS_0 &= \alpha, \\
S_0' + \frac{g}{\epsilon}S_0 &= \frac{\alpha}{\epsilon}, \\
Ar^- + Br^+ + \frac{g}{\epsilon}(A+B) &= \frac{\alpha}{\epsilon}, \\
A(r^- + \frac{g}{\epsilon}) + B(r^+ + \frac{g}{\epsilon}) &= \frac{\alpha}{\epsilon}, \\
A &= \frac{\frac{\alpha}{\epsilon} - B(r^+ + \frac{g}{\epsilon})}{(r^- + \frac{g}{\epsilon})}.
\end{aligned} \tag{6.2.8}$$

At $x = L$, the DNA synthesis or Sphase is prescribed as

$$\begin{aligned}
\beta &= A\exp(r^-L) + B\exp(r^+L),\\
\beta &= \frac{\frac{\alpha}{\epsilon} - B(r^+ + \frac{g}{\epsilon})}{(r^- + \frac{g}{\epsilon})}\exp(r^-L) + B\exp(r^+L),\\
\beta(r^- + \frac{g}{\epsilon}) &= \frac{\alpha}{\epsilon} - B(r^+ + \frac{g}{\epsilon})\exp(r^-L) + B\exp(r^+L)(r^- + \frac{g}{\epsilon}),\\
\beta(r^- + \frac{g}{\epsilon}) - \frac{\alpha}{\epsilon} &= \Big(\exp(r^+L)(r^- + \frac{g}{\epsilon}) - (r^+ + \frac{g}{\epsilon})\exp(r^-L)\Big)\,B,\\
B &= \frac{\beta(r^- + \frac{g}{\epsilon}) - \frac{\alpha}{\epsilon}}{\big(\exp(r^+L)(r^- + \frac{g}{\epsilon}) - (r^+ + \frac{g}{\epsilon})\exp(r^-L)\big)}. \qquad (6.2.9)
\end{aligned}$$

Substituting the value of B in (6.2.9) into equation (6.2.8) we obtain

$$A = \frac{\frac{\alpha}{\epsilon}}{(r^- + \frac{g}{\epsilon})} - \frac{(\beta(r^- + \frac{g}{\epsilon}) - \frac{\alpha}{\epsilon})(r^+ + \frac{g}{\epsilon})}{\big(\exp(r^+L)(r^- + \frac{g}{\epsilon}) - (r^+ + \frac{g}{\epsilon})\exp(r^-L)\big)\,(r^- + \frac{g}{\epsilon})}. \qquad (6.2.10)$$

This implies that the solution of the DNA synthesis or Sphase steady state, through the equation in (6.2.6) is

$$\begin{aligned}
S^*(x,\epsilon,g) &= \frac{\frac{\alpha}{\epsilon}}{(r^- + \frac{g}{\epsilon})} - \frac{(\beta(r^- + \frac{g}{\epsilon}) - \frac{\alpha}{\epsilon})(r^+ + \frac{g}{\epsilon})}{\big(\exp(r^+L)(r^- + \frac{g}{\epsilon}) - (r^+ + \frac{g}{\epsilon})\exp(r^-L)\big)\,(r^- + \frac{g}{\epsilon})}\exp(r^-x)\\
&\quad + \frac{\beta(r^- + \frac{g}{\epsilon}) - \frac{\alpha}{\epsilon}}{\big(\exp(r^+L)(r^- + \frac{g}{\epsilon}) - (r^+ + \frac{g}{\epsilon})\exp(r^-L)\big)}\exp(r^+x). \qquad (6.2.11)
\end{aligned}$$

Combining the equation in (6.2.11) with the equilibria in equation (6.2.2), we have the local stability point $\mathcal{E} = (G_1^*, S^*, G_2^*, M^*)$, where,

$$\left.\begin{aligned} G_1^*(x) &= c_{g11} + c_{g12}\exp\left(\frac{D_{G_1}}{k_1+\mu_{G_1}}x\right), \\ S^*(x,\epsilon,g) &= \frac{\frac{\alpha}{\epsilon}}{(r^-+\frac{g}{\epsilon})} - \frac{(\beta(r^-+\frac{g}{\epsilon})-\frac{\alpha}{\epsilon})(r^++\frac{g}{\epsilon})}{\left(\exp(r^+L)(r^-+\frac{g}{\epsilon})-(r^++\frac{g}{\epsilon})\exp(r^-L)\right)(r^-+\frac{g}{\epsilon})}\exp(r^-x) \\ &\quad + \frac{\beta(r^-+\frac{g}{\epsilon})-\frac{\alpha}{\epsilon}}{\left(\exp(r^+L)(r^-+\frac{g}{\epsilon})-(r^++\frac{g}{\epsilon})\exp(r^-L)\right)}\exp(r^+x), \\ G_2^*(x) &= c_{g21} + c_{g22}\exp\left(\frac{D_{G_2}}{k_2+\mu_{G_2}}x\right), \\ M^*(x) &= c_{m1} + c_{m2}\exp\left(\frac{D_M}{b+\mu_M}x\right). \end{aligned}\right\} \quad (6.2.12)$$

These equilibrium point $\mathcal{E}$, enables us to present the behavior of the density of cells in each phase. Moreover, the steady state for the DNA synthesis or Sphase enables us to locate the boundary layer which is a result of perturbation by cancer therapy [51]. Thus, since the singularly perturbation occurs only during the DNA synthesis or Sphase, then it suffices to locate the layer by considering the solution to the steady state of the DNA synthesis or Sphase in equation (6.2.11). Thus, following [105] and the references there in, we see that

$$\begin{aligned} \lim_{x\to 0}\lim_{\epsilon\to 0} S^*(x,\epsilon,g) &= \lim_{\epsilon\to 0}\lim_{x\to 0} S^*(x,\epsilon,g), \\ &\text{and} \\ \lim_{x\to L}\lim_{\epsilon\to 0} S^*(x,\epsilon,g) &\neq \lim_{\epsilon\to 0}\lim_{x\to L} S^*(x,\epsilon,g), \end{aligned} \quad (6.2.13)$$

then, the layer is located on the right-end of the interval, near $x = L$. This implies that, we are now in the position of deriving our numerical method.

6.3 Construction and analysis of the numerical method

In this section, we describe the derivation of the fitted operator finite difference numerical (FOFDM) for solving the G_1phase, G_2phase and metosis or Mphase in equation (6.1.7) and non-standard finite difference (NSFDM) for solving the DNA synthesis or Sphase in equation (6.1.7). We first determine an approximation to the derivatives of the functions $G_1(t,x), G_2(x,t)$ and $M(t,x)$ with respect to the spatial variable x.

Let N_x be a positive integer. Discretize the interval $[0, L]$ through the points

$$x_0 = 0 < x_1 < x_2 < \cdots < x_{N_x} = L,$$

where, the step-size $\Delta x = x_{j+1} - x_j = L/N_x$, $j = 0, 1, \ldots, x_{N_x}$. Let $(\mathcal{G}_1)_j(t), (\mathcal{G}_2)_j(t), \mathcal{M}_j(t)$ denote the numerical approximations of $G_1(t,j), G_2(t,j), M(t,j)$, then we approximate the second order spatial derivative by

$$\begin{aligned}
\frac{\partial G_1}{\partial x^2}(t,x_j) &\approx \frac{(\mathcal{G}_1)_{j+1} - 2(\mathcal{G}_1)_j + (\mathcal{G}_1)_{j-1}}{(\phi_{G_1})_j^2}, \ \frac{\partial G_2}{\partial x^2}(t,x_j) \approx \frac{(\mathcal{G}_2)_{j+1} - 2(\mathcal{G}_2)_j + (\mathcal{G}_2)_{j-1}}{(\phi_{G_2})_j^2}, \\
\frac{\partial M}{\partial x^2}(t,x_j) &\approx \frac{\mathcal{M}_{j+1} - 2\mathcal{M}_j + \mathcal{M}_{j-1}}{\phi_j^2},
\end{aligned} \tag{6.3.1}$$

where,

$$\begin{aligned}
(\phi_{G_1})_j &= \frac{(1 - \exp((\sigma_{G_1})_j \Delta x)}{(\sigma_{G_1})_j}, \ (\phi_{G_2})_j = \frac{(1 - \exp((\sigma_{G_2})_j \Delta x)}{(\sigma_{G_2})_j}, \\
(\phi_M)_j &= \frac{(1 - \exp((\sigma_M)_j \Delta x)}{(\sigma_M)_j},
\end{aligned} \tag{6.3.2}$$

and

$$(\sigma_{G_1})_j = \sqrt{\frac{k_1 + \mu_{G_1}}{D_{G_1}}}, \ (\sigma_{G_2})_j = \sqrt{\frac{k_2 + \mu_{G_2}}{D_{G_2}}}, \ (\sigma_I)_j = \sqrt{\frac{\mu_M + b}{D_M}}.$$

We see that $\phi_{G_1} \to \Delta x$ as $\Delta x \to 0$, $\phi_{G_2} \to \Delta x$ as $\Delta x \to 0$ and $\phi_M \to \Delta x$ as $\Delta x \to 0$.

Let N_t be a positive integer and $\Delta T = T/Nt$ where $0 < t < T$. Discretizing the time interval $[0, T]$ through the points

$$0 = t_0 < t_1 < \cdots < t_{N_t} = T,$$

where,

$$t_{n+1} - t_n = \Delta t,\ n = 0, 1, \ldots, (t_{N_t} - 1).$$

We approximate the time derivative at t_n by

$$\begin{aligned} \frac{d(\mathcal{G}_1)_j(t_n)}{dt} &\approx \frac{(\mathcal{G}_1)_j^{n+1} - (\mathcal{G}_1)_j^n}{\psi_{G_1}}, \ \frac{d(\mathcal{G}_2)_j(t_n)}{dt} \approx \frac{(\mathcal{G}_2)_j^{n+1} - (\mathcal{G}_2)_j^n}{\psi_{G_2}}, \\ \frac{d\mathcal{M}_j(t_n)}{dt} &\approx \frac{\mathcal{M}_j^{n+1} - \mathcal{M}_j^n}{\psi_M}, \end{aligned} \tag{6.3.3}$$

where,

$$\begin{aligned} \psi_{G_1} &= (\exp((k_1 + \mu_{G_1})\Delta t) - 1)/(k_1 + \mu_{G_1}),\ \psi_{G_2} = (\exp((k_2 + \mu_{G_2})\Delta t) - 1)/(k_2 + \mu_{G_2}), \\ \psi_M &= (\exp((b + \mu_M)\Delta t) - 1)/(b + \mu_M), \end{aligned}$$

where we see that $\psi_{G_1} \to \Delta t$ as $\Delta t \to 0$, $\psi_{G_2} \to \Delta t$ as $\Delta t \to 0$ and $\psi_M \to \Delta t$ as $\Delta t \to 0$.

Next we develop the numerical method to solve the DNA synthesis or Sphase in equation (6.1.7). Since the FOFDM and SFDM fail to capture the hyperbolic nature of the advection-diffusion-reaction PDEs, below we follow the development in [85] to derive the NSFDM for the equation modeling the DNA synthesis or Sphase in equation (6.1.7). We proceed as follow. Let $\mathcal{S}_j(t)$ denote the numerical approximations of $S(t, j)$, then using the following sub-equations of the equation modeling the DNA synthesis or

Sphase in equation (6.1.7)

$$\left.\begin{array}{l} \frac{\partial S(x,t)}{\partial t} + g\frac{\partial S(x,t)}{\partial x} = -\mu_S S(x,t), \text{ a PDE,} \\ \\ g\frac{\partial S(x,t)}{\partial x} = \varepsilon\frac{\partial^2 S(x,t)}{\partial x^2}, \text{ an ODE,} \end{array}\right\} \tag{6.3.4}$$

then the exact finite difference schemes for the two sub-equations in equation (6.3.4) are

$$\left.\begin{array}{l} \frac{\mathcal{S}_j^{n+1}-\mathcal{S}_j^n}{(\phi_1)_S(\Delta t)} + g\frac{\mathcal{S}_{j+1}^{n+1}-\mathcal{S}_j^{n+1}}{g(\phi_1)_S(\frac{\Delta x}{g})} = -\mu_S\mathcal{S}_j^n, \text{ a scheme for a PDE} \\ \\ \frac{\mathcal{S}_{j+1}-\mathcal{S}_j}{\Delta x} = \varepsilon\frac{\mathcal{S}_{j+1}-2\mathcal{S}_j+\mathcal{S}_{j-1}}{\frac{\varepsilon\Delta x}{g}(\phi_2)_S(\Delta x)}, \text{ a scheme for an ODE,} \end{array}\right\} \tag{6.3.5}$$

where, $(\phi_1)_S(\Delta t) = (1-\exp(-\mu_S\Delta t))/\mu_S$ and $(\phi_2)_S(\Delta x) = (1-\exp(-\frac{g\Delta x}{\varepsilon}))$. Combining the exact finite difference schemes in equation (6.3.5) and avoid the condition $g\Delta t = \Delta x$, we obtain the NSFDM for the DNA phase as

$$\begin{aligned} \frac{\mathcal{S}_j^{n+1}-\mathcal{S}_j^n}{(\phi_1)_S(\Delta t)} + g\frac{\mathcal{S}_{j+1}^{n+1}-\mathcal{S}_j^{n+1}}{g(\phi_1)_S(\frac{\Delta x}{g})} &= \varepsilon\frac{\mathcal{S}_{j+1}^{n+1}-2\mathcal{S}_j^{n+1}+\mathcal{S}_{j-1}^{n+1}}{\varphi(\Delta x)} - \mu_S\mathcal{S}_j^n \\ &\quad + k_1(\mathcal{G}_1)_j^n - I(x,t;T_S), \end{aligned} \tag{6.3.6}$$

where, $\varphi(\Delta x) = g\phi_S(\frac{\Delta x}{g})\frac{\varepsilon\Delta x}{g}(\phi_2)_S(\Delta x)$. We see that $\phi_S \to \Delta x$ as $\Delta x \to 0$. Similarly for $\varphi(\Delta x)$. The denominator functions in equations (6.3.1), (6.3.3) and (6.3.5) are used explicitly to remove the inherent stiffness in the central finite derivatives parts and can be derived by using the theory of nonstandard finite difference methods, see, e.g., [84, 103, 104] and references therein.

Combining the equation (6.3.1) for the spatial derivatives with the equation (6.3.3) for time derivatives and with equation in (6.3.6), we obtain the system of FOFDM-

NSFDM as

$$\left.\begin{aligned}
&\tfrac{(\mathcal{G}_1)_j^{n+1}-(\mathcal{G}_1)_j^n}{\phi_{G_1}} = D_{G_1}\tfrac{(\mathcal{G}_1)_{j+1}^{n+1}-2(\mathcal{G}_1)_j^{n+1}+(\mathcal{G}_1)_{j-1}^{n+1}}{(\phi_{G_1})_j^2} + 4b\mathcal{M}_{2j}^n - (k_1+\mu_{G_1})(\mathcal{G}_1)_j^n,\\
&\tfrac{\mathcal{S}_j^{n+1}-\mathcal{S}_j^n}{(\phi_1)_S(\Delta t)} + g\tfrac{\mathcal{S}_{j+1}^{n+1}-\mathcal{S}_j^{n+1}}{(\phi_1)_S(\frac{\Delta x}{g})} = \varepsilon\tfrac{\mathcal{S}_{j+1}^{n+1}-2\mathcal{S}_j^{n+1}+\mathcal{S}_{j-1}^{n+1}}{\varphi(\Delta x)} - \mu_S\mathcal{S}_j^n + k_1(\mathcal{G}_1)_j^n - I(x,t;T_S),\\
&\tfrac{(\mathcal{G}_2)_j^{n+1}-(\mathcal{G}_2)_j^n}{\phi_{G_2}} = D_{G_2}\tfrac{(\mathcal{G}_2)_{j+1}^{n+1}-2(\mathcal{G}_2)_j^{n+1}+(\mathcal{G}_2)_{j-1}^{n+1}}{(\phi_{G_2})_j^2} + I(x,t;T_S) - (k_2+\mu_{G_2})(\mathcal{G}_2)_j^n,\\
&\tfrac{\mathcal{M}_j^{n+1}-\mathcal{M}_j^n}{\phi_M} = D_M\tfrac{\mathcal{M}_{j+1}^{n+1}-2\mathcal{M}_j^{n+1}+\mathcal{M}_{j-1}^{n+1}}{(\phi_M)_j^2} + k_2(\mathcal{G}_2)_j^n - (b+\mu_M)\mathcal{M}_j^n,\\
&(\mathcal{G}_1)_1^n = (\mathcal{G}_1)_{-1}^n,\ (\mathcal{G}_2)_1^n = (\mathcal{G}_2)_{-1}^n,\ \mathcal{S}_1^n = \mathcal{S}_{-1}^n,\ \mathcal{M}_1^n = \mathcal{M}_{-1}^n,\\
&(\mathcal{G}_1)_{x_{N_x}}^n = (\mathcal{G}_1)_{x_{N_x-1}}^n,\ (\mathcal{G}_2)_{x_{N_x}}^n = (\mathcal{G}_2)_{x_{N_x-1}}^n,\ \mathcal{S}_{x_{N_x}}^n = \mathcal{S}_{x_{N_x-1}}^n,\\
&\mathcal{M}_{x_{N_x}}^n = \mathcal{M}_{x_{N_x-1}}^n, (\mathcal{G}_1)_j^0 = \tfrac{a_0}{\sqrt{2\pi\theta_0^2}}\exp\left(-\tfrac{(x_j-1)^2}{2\pi\theta_0^2}\right),\ (\mathcal{G}_2)_j^0 = 0,\\
&\mathcal{S}_j^0 = 0,\ \mathcal{M}_j^0 = 0.
\end{aligned}\right\} \quad (6.3.7)$$

The system in equation (6.3.7) can further be simplified as

$$\left.\begin{aligned}
&-\tfrac{D_{G_1}}{(\phi_{G_1})_j^2}(\mathcal{G}_1)_{j-1}^{n+1} + \left(\tfrac{1}{\phi_{G_1}} + \tfrac{2D_{G_1}}{(\phi_T)_j^2}\right)(\mathcal{G}_1)_j^{n+1} - \tfrac{D_{G_1}}{(\phi_{G_1})_j^2}(\mathcal{G}_1)_{j+1}^{n+1}\\
&\qquad = \left(\tfrac{1}{\phi_{G_1}} - (k_1+\mu_{G_1})\right)(\mathcal{G}_1)_j^n + 4b\mathcal{M}_{2j}^n,\\
&-\tfrac{\varepsilon}{\varphi(\Delta x)}\mathcal{S}_{j-1}^{n+1} + \left(\tfrac{1}{(\phi_1)_S(\Delta t)} - \tfrac{g}{(\phi_1)_S(\frac{\Delta x}{g})} + \tfrac{2\varepsilon}{\varphi(\Delta x)}\right)\mathcal{S}_j^{n+1}\\
&+\left(\tfrac{g}{(\phi_1)_S(\frac{\Delta x}{g})} - \tfrac{\varepsilon}{\varphi(\Delta x)}\right)\mathcal{S}_{j+1}^{n+1} = \left(\tfrac{1}{(\phi_1)_S(\Delta t)} - \mu_S\right)\mathcal{S}_j^n + k_1(\mathcal{G}_1)_j^n - I(x,t;T_S),\\
&-\tfrac{D_{G_2}}{(\phi_{G_2})_j^2}(\mathcal{G}_2)_{j-1}^{n+1} + \left(\tfrac{1}{\phi_{G_2}} + \tfrac{D_{G_2}}{(\phi_{G_2})_j^2}\right)(\mathcal{G}_2)_j^{n+1} - \tfrac{D_{G_2}}{(\phi_{G_2})_j^2}(\mathcal{G}_2)_{j+1}^{n+1}\\
&\qquad = \left(\tfrac{1}{\phi_{G_2}} - (k_2+\mu_{G_2})\right)(\mathcal{G}_2)_j^n + I(x,t;T_S),\\
&-\tfrac{D_M}{(\phi_M)_j^2}\mathcal{M}_{j-1}^{n+1} + \left(\tfrac{1}{\phi_M} + \tfrac{D_M}{(\phi_M)_j^2}\right)\mathcal{M}_j^{n+1} - \tfrac{D_M}{(\phi_M)_j^2}\mathcal{M}_{j+1}^{n+1}\\
&\qquad = \left(\tfrac{1}{\phi_M} - (b+\mu_M)\right)\mathcal{M}_j^n + k_2(\mathcal{G}_2)_j^n.
\end{aligned}\right\} \quad (6.3.8)$$

The system in equation (6.3.8) can be written as a tridiagonal system given by

$$\left.\begin{aligned} \mathcal{A}_{G_1}(\mathcal{G}_1) &= \mathcal{F}_{G_1}, \\ \mathcal{A}_S\mathcal{S} &= \mathcal{F}_S, \\ \mathcal{A}_{G_2}(\mathcal{G}_2) &= \mathcal{F}_{G_2}, \\ \mathcal{A}_M\mathcal{M} &= \mathcal{F}_M, \end{aligned}\right\} \tag{6.3.9}$$

where, $j = 1, \ldots, x_{N_x} - 1$, $n = 0, \ldots, t_{N_t} - 1$ and

$$\left.\begin{aligned} \mathcal{A}_{G_1} &= \text{Tri}\left(-\tfrac{D_{G_1}}{(\phi_{G_1})_j^2}, \tfrac{1}{\phi_{G_1}} + \tfrac{2D_{G_1}}{(\phi_T)_j^2}, -\tfrac{D_{G_1}}{(\phi_{G_1})_j^2}\right), \\ \mathcal{A}_S &= \text{Tri}\left(-\tfrac{\varepsilon}{\varphi(\Delta x)}, \tfrac{1}{(\phi_1)_S(\Delta t)} - \tfrac{g}{(\phi_1)_S(\frac{\Delta x}{g})} + \tfrac{2\varepsilon}{\varphi(\Delta x)}, -\tfrac{\varepsilon}{\varphi(\Delta x)}\right), \\ \mathcal{A}_{G_2} &= \text{Tri}\left(-\tfrac{D_{G_2}}{(\phi_{G_2})_j^2}, \tfrac{1}{\phi_{G_2}} + \tfrac{D_{G_2}}{(\phi_{G_2})_j^2}, -\tfrac{D_{G_2}}{(\phi_{G_2})_j^2}\right), \\ \mathcal{A}_M &= \text{Tri}\left(-\tfrac{D_M}{(\phi_M)_j^2}, \tfrac{1}{\phi_M} + \tfrac{D_M}{(\phi_M)_j^2}, -\tfrac{D_M}{(\phi_M)_j^2}\right), \end{aligned}\right\}$$

and

$$\left.\begin{aligned} (\mathcal{F}_{G_1})_j^n &= \left(\tfrac{1}{\phi_{G_1}} - (k_1 + \mu_{G_1})\right)(\mathcal{G}_1)_j^n + 4b\mathcal{M}_{2j}^n, \\ (\mathcal{F}_S)_j^n &= \left(\tfrac{1}{\phi_S(k)} - \mu_S\right)\mathcal{S}_j^n + k_1(\mathcal{G}_1)_j^n - I(x,t;T_S), \\ (\mathcal{F}_{G_2})_j^n &= \left(\tfrac{1}{\phi_{G_2}} - (k_2 + \mu_{G_2})\right)(\mathcal{G}_2)_j^n + I(x,t;T_S), \\ (\mathcal{F}_M)_j^n &= \left(\tfrac{1}{\phi_M} - (b + \mu_M)\right)\mathcal{M}_j^n + k_2(\mathcal{G}_2)_j^n. \end{aligned}\right\}$$

Let the functions

$$G_1(x,t), S(x,t), G_2(x,t), M(x,t),$$

and their partial derivatives with respect to both t and x be smooth such that they satisfy

$$\begin{aligned}\left|\frac{\partial^{i+j}G_1(t,x)}{\partial t^i x^j}\right| &\leq \Upsilon_{G_1}, \left|\frac{\partial^{i+j}S(t,x)}{\partial t^i x^j}\right| \leq \Upsilon_S,\\ \left|\frac{\partial^{i+j}G_2(t,x)}{\partial t^i x^j}\right| &\leq \Upsilon_Z, \left|\frac{\partial^{i+j}M(t,x)}{\partial t^i x^j}\right| \leq \Upsilon_M,\\ &\forall i,j \geq 0,\end{aligned} \tag{6.3.10}$$

where,

$$\Upsilon_{G_1}, \Upsilon_S, \Upsilon_{G_2}, \Upsilon_M,$$

are constant that are independent of the time and space step-sizes. Then, in view of equation (6.3.9), we see that the local truncation errors $((\varsigma_{G_1})_j^n, (\varsigma_S)_j^n, (\varsigma_{G_2})_j^n, (\varsigma_M)_j^n)$ are given by

$$\left.\begin{aligned}(\varsigma_{G_1})_j^n &= (\mathcal{A}_{G_1}G_1)_j^n - (F_{G_1})_j^n = (\mathcal{A}_{G_1}(G_1-\mathcal{G}_1))_j^n,\\ (\varsigma_S)_j^n &= (\mathcal{A}_S S)_j^n - (F_S)_j^n = (\mathcal{A}_S(S-\mathcal{S}))_j^n,\\ (\varsigma_{G_2})_j^n &= (\mathcal{A}_{G_2}\mathcal{G}_2)_j^n - (F_{G_2})_j^n = (\mathcal{A}_{G_2}(G_2-\mathcal{G}_2))_j^n,\\ (\varsigma_S)_j^n &= (\mathcal{A}_M\mathcal{M})_j^n - (F_M)_j^n = (\mathcal{A}_M(M-\mathcal{M}))_j^n.\end{aligned}\right\} \tag{6.3.11}$$

Thus,

$$\left.\begin{array}{l} \max_{1\leq n\leq T,1\leq j\leq L}|(G_1)_j^n-(\mathcal{G}_1)_j^n)|\leq||(\mathcal{A}_{G_1})^{-1}|||(\varsigma_{G_1})_j^n|,\\ \max_{1\leq n\leq T,1\leq j\leq L}|S_j^n-\mathcal{S}_j^n|\leq||(\mathcal{A}_S)^{-1}|||(\varsigma_S)_j^n|,\\ \max_{1\leq n\leq T,1\leq j\leq L}|(G_2)_j^n-(\mathcal{G}_2)_j^n)|\leq||(\mathcal{A}_{G_2})^{-1}|||(\varsigma_{G_2})_j^n|,\\ \max_{1\leq n\leq T,1\leq j\leq L}|M_j^n-\mathcal{M}_j^n|\leq||(\mathcal{A}_M)^{-1}|||(\varsigma_M)_j^n|, \end{array}\right\} \tag{6.3.12}$$

where,

$$\left.\begin{array}{l} \max_{1\leq n-1\leq T,1\leq j\leq L-1}|(\varsigma_{G_1})_j^n|\leq\frac{\Delta t}{2}|(G_1)_{tt}(\zeta)|+D_{G_1}\frac{(\Delta x)^2}{12}|(G_1)_{xxxx}(\xi)|,\\ \max_{1\leq n-1\leq T,1\leq j\leq L-1}|(\varsigma_S)_j^n|\leq\frac{\Delta t}{2}|S_{tt}(\zeta)|+g\frac{\Delta x}{2}|S_{xx}(\xi)|+\varepsilon\frac{(\Delta x)^2}{12}|S_{xxxx}(\xi)|,\\ \max_{1\leq n-1\leq T,1\leq j\leq L-1}|(\varsigma_{G_2})_j^n|\leq\frac{\Delta t}{2}|(G_2)_{tt}(\zeta)|+D_{G_2}\frac{(\Delta x)^2}{12}|(G_2)_{xxxx}(\xi)|,\\ \max_{1\leq n-1\leq T,1\leq j\leq L-1}|(\varsigma_M)_j^n|\leq\frac{\Delta t}{2}|M_{tt}(\zeta)|-D_M\frac{(\Delta x)^2}{12}|M_{xxxx}(\xi)|, \end{array}\right\} \tag{6.3.13}$$

where, $t_{n-1}\leq\zeta\leq t_{n+1}$, $x_{j-1}\leq\xi\leq x_{j+1}$. In view of inequalities in (6.3.10), then the inequalities in (6.3.12) implies that

$$\left.\begin{array}{l} \max_{1\leq n-1\leq T,1\leq j\leq L-1}|(\varsigma_{G_1})_j^n|\leq\left(\frac{\Delta t}{2}+D_{G_1}\frac{(\Delta x)^2}{12}\right)\Upsilon_{G_1},\\ \max_{1\leq n-1\leq T,1\leq j\leq L-1}|(\varsigma_S)_j^n|\leq\left(\frac{\Delta t}{2}+g\frac{\Delta x}{2}+\varepsilon\frac{(\Delta x)^2}{12}\right)\Upsilon_S,\\ \max_{1\leq n-1\leq T,1\leq j\leq L-1}|(\varsigma_{G_2})_j^n|\leq\left(\frac{\Delta t}{2}+D_{G_2}\frac{(\Delta x)^2}{12}\right)\Upsilon_{G_2},\\ \max_{1\leq n-1\leq T,1\leq j\leq L-1}|(\varsigma_M)_j^n|\leq\left(\frac{\Delta t}{2}-D_M\frac{(\Delta x)^2}{12}\right)\Upsilon_M, \end{array}\right\} \tag{6.3.14}$$

where, $t_{n-1} \leq \zeta \leq t_{n+1}$, $x_{j-1} \leq \xi \leq x_{j+1}$ and by [117] we have

$$||(\mathcal{A}_{G_1})^{-1}|| \leq \Xi_{G_1},\ ||(\mathcal{A}_S)^{-1}|| \leq \Xi_S,\ ||(\mathcal{A}_{G_2})^{-1}|| \leq \Xi_{G_2},\ ||(\mathcal{A}_M)^{-1}|| \leq \Xi_M. \quad (6.3.15)$$

Using (6.3.14) and (6.3.15) in (6.3.12), we obtain

$$\left.\begin{array}{l} \max_{1\leq n\leq T,1\leq j\leq L} |(G_1)_j^n - (\mathcal{G}_1)_j^n| \leq \Xi_{G_1}[\frac{\Delta t}{2} + D_{G_1}\frac{(\Delta x)^2}{12}]\Upsilon_{G_1}, \\ \max_{1\leq n\leq T,1\leq j\leq L} |S_j^n - \mathcal{S}_j^n| \leq |\Xi_S|[\frac{\Delta t}{2} + g\frac{\Delta x}{2} + \varepsilon\frac{(\Delta x)^2}{12}]\Upsilon_S, \\ \max_{1\leq n\leq T,1\leq j\leq L} |(G_2)_j^n - (\mathcal{G}_2)_j^n| \leq |\Xi_{G_2}|[\frac{\Delta t}{2} + D_{G_2}\frac{(\Delta x)^2}{12}]\Upsilon_S, \\ \max_{1\leq n\leq T,1\leq j\leq L} |M_j^n - \mathcal{M}_j^n| \leq |\Xi_M|[\frac{\Delta t}{2} - D_M\frac{(\Delta x)^2}{12}]\Upsilon_M. \end{array}\right\}$$

Hence, we obtain the following results.

Theorem 6.3.1. *Let $F_{G_1}(x,t), F_S(x,t), F_{G_2}(x,t), F_M(x,t)$ be sufficiently smooth functions so that $G_1(x,t), S(x,t), G_2(x,t), M(x,t) \in C^\infty([0,L]\times[0,T])$. Let $(\mathcal{G}_1)_j^n, \mathcal{S}_j^n, (\mathcal{G}_2)_j^n, \mathcal{M}_j^n$, $j = 1,2,\ldots L, n = 1,2,\ldots T$ be the approximate solutions to (6.1.7), obtained using the FOFDM-NSFDM with $(\mathcal{G}_1)_j^0 = (G_1)_j^0, \mathcal{S}_j^0 = S_j^0, (\mathcal{G}_2)_j^0 = (G_2)_j^0, \mathcal{M}_j^0 = M_j^0$. Then there exists $\Xi_{G_1}, \Xi_S, \Xi_{G_2}, \Xi_M$ independent of g, ε, the step sizes Δt and Δx such that*

$$\left.\begin{array}{l} \sup_{0<\varepsilon\leq 1, g>>1} \max_{1\leq n\leq T,1\leq j\leq L} |(G_1)_j^n - (\mathcal{G}_1)_j^n| \leq |\Xi_{G_1}|[\frac{\Delta t}{2} + D_{G_1}\frac{(\Delta x)^2}{12}]\Upsilon_{G_1}, \\ \sup_{0<\varepsilon\leq 1, g>>1} \max_{1\leq n\leq T,1\leq j\leq L} |S_j^n - \mathcal{S}_j^n| \leq |\Xi_S|[\frac{\Delta t}{2} + g\frac{\Delta x}{2} + \varepsilon\frac{(\Delta x)^2}{12}]\Upsilon_S, \\ \sup_{0<\varepsilon\leq 1, g>>1} \max_{1\leq n\leq T,1\leq j\leq L} |(G_2)_j^n - (\mathcal{G}_2)_j^n| \leq |\Xi_{G_2}|[\frac{\Delta t}{2} + D_{G_2}\frac{(\Delta x)^2}{12}]\Upsilon_{G_2}, \\ \sup_{0<\varepsilon\leq 1, g>>1} \max_{1\leq n\leq T,1\leq j\leq L} |M_j^n - \mathcal{M}_j^n| \leq |\Xi_M[\frac{\Delta t}{2} - D_M\frac{(\Delta x)^2}{12}]\Upsilon_M. \end{array}\right\}$$

This shows that our FOFDM and NSFDM are unconditionally stable.

6.4 Numerical results and discussions

Setting $D_{G_1} = 10^{-4}, D_{G_2} = 10^{-4}, D_M = 10^{-7}, L = 5, T = 1, x_{N_x} = t_{N_t} = 20$ and , we present our numerical solutions in Figure 6.5.1 (for $\varepsilon = 0.001$), Figure 6.5.2 (for $\varepsilon = 0.01$), Figure 6.5.3 (for $\varepsilon = 0.1$) using the parameter values [11] in Table 6.5.1.

In Figure 6.5.1(a) we see that as time grows the density of cells are increasing within the range of approximately of $x \in (0, 1.5)$, then for the values of $x \in (1.5, 5)$, the profile presents that there are no more cells available for G_1phase.

In Figure 6.5.1(b) we see that as time grows the density of cells form a peak which is increasing within the range of approximately of the values of $x \in (0, 1.5)$, then for the values of $x \in (1.5, 5)$ the density of cells converges to its low positive steady state.

In Figure 6.5.1(c) we see the contrary to the profiles of the two previous profiles. That, as time grows the density of cells grows exponentially for $x \in (0, 1.5)$, till they reach a positive steady state for $x \in (1.5, 5)$. The profile of this phase presents that all cells are well and active for next interactions.

In Figure 6.5.1(d) we see similar development compare to the interactions in the Mphase, that as time grows the density of cells grows exponentially for the values of $x \in (0, 1.5)$, till they reach a positive steady state for $x \in (1.5, 5)$. The profile of this phase presents that all cells are well and active for the next interaction.

The remaining two figures, Figure 6.5.2 and Figure 6.5.3, we have the same profiles as in Figure 6.5.1, for different values of $\varepsilon \in (0, 1)$.

6.5 Conclusion

In this chapter, we extended the model for population kinetics of human tumor in vitro, with the aim to contribute toward the understanding of cells cycle in each phase. This is very essential toward healing cancer as a dreadful disease, since [51] categorically mentioned that even in the simplified environment of the laboratory with modern technology it is not always possible to isolate the effects of cancer treatment on the

cell cycle of human cancer lines. Thus, in view of our numerical results, we see that for the values of $0 < \varepsilon <<< 1$ and $g >>> 1$ our numerical solutions are the same, despite the fact that cells population behave differently in each phase. As time goes, we see that during G_1phase, that the cells grow sharply to a very high height as time increases, but for certain different positions only. During the DNA synthesis or Sphase, we see different peaks for certain different positions only as time increases, unlike for the G_2phase and the metosis Mphase, where we see that the cells grow sharply to their respective uniform equilibria. These growths are due to the equilibria presented in (6.2.12). When we decrease the value for the division rate parameter (b), then the behavior of the metosis or Mphase changes to a linear growth rate, whereas increasing the the division rate (b), changes the growth rate a parabolic growth rate (results not shown). Other changes in the parameter values does not bring new phenomena, except for the fact that $\mu_S \neq 0$, because we believe a small amount cells should be exiting the phase, during this phase too. We also see an important feature in our numerical results that notable interactions takes place at certain positions only in all the phases. This, we believe can contribute quite a great deal toward understanding of cells cycle in each phase, which in turn can be taken up for further cancer research on the cell cycle of human cancer lines. Thus, our approach in this work should serve as a first attempt to incorporate the detailed effects of population kinetics of human tumor. Hence, our future direction is to carry out comparison with the latest reported method(s) in the subsequent recent years chapters.

Table 6.5.1: Values of the parameters used in the model (6.3.7) [11]

$k_1 = 0.8$	$\mu_{G_1} = 0.9$	$\alpha = 2.4$	$g = 30.9$
$\theta_0 = 0.6$	$\mu_S = 0.8$	$\beta = 0.1$	$k_2 = 0.0193$
$\mu_{G_2} = 2.00$	$b = 1.9296$	$\mu_M = 0.01$	$a_0 = 100.0$

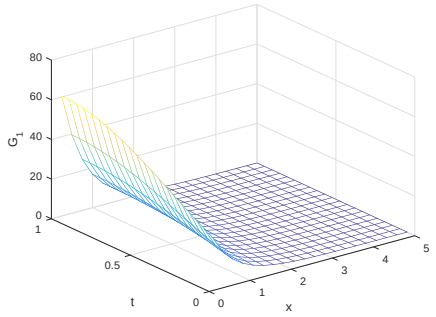

(a) Behaviour of G_1phase

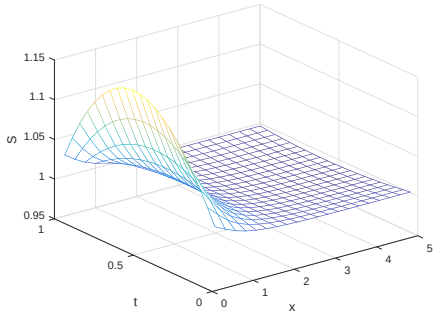

(b) Behaviour of DNA synthesis or Sphase

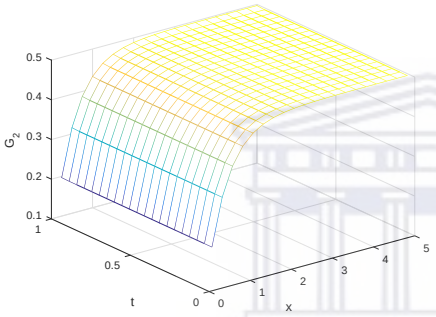

(c) Behaviour of G_2phase

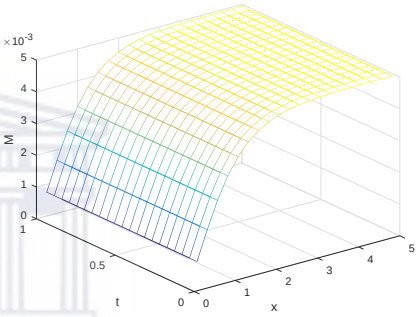

(d) Behaviour of metosis or Mphase

Figure 6.5.1: Numerical solution obtained by using for $\varepsilon = 0.001$.

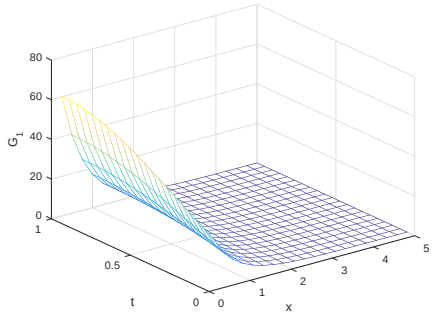

(a) Behaviour of G_1phase

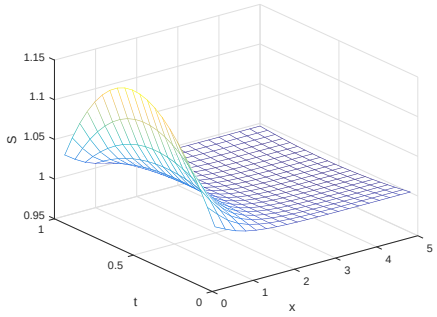

(b) Behaviour of DNA synthesis or Sphase

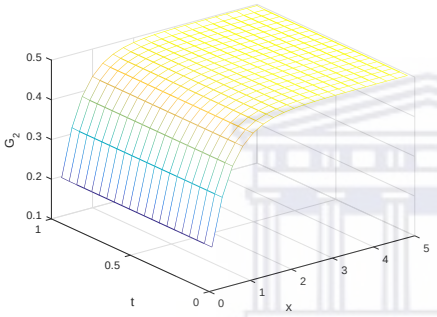

(c) Behaviour of G_2phase

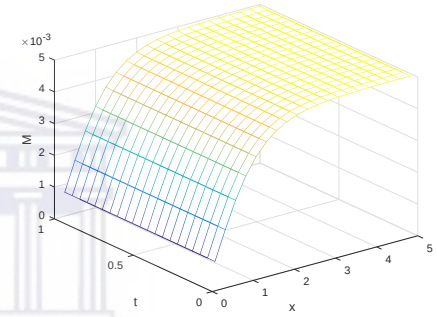

(d) Behaviour of metosis or Mphase

Figure 6.5.2: Numerical solution obtained by using for $\varepsilon = 0.01$.

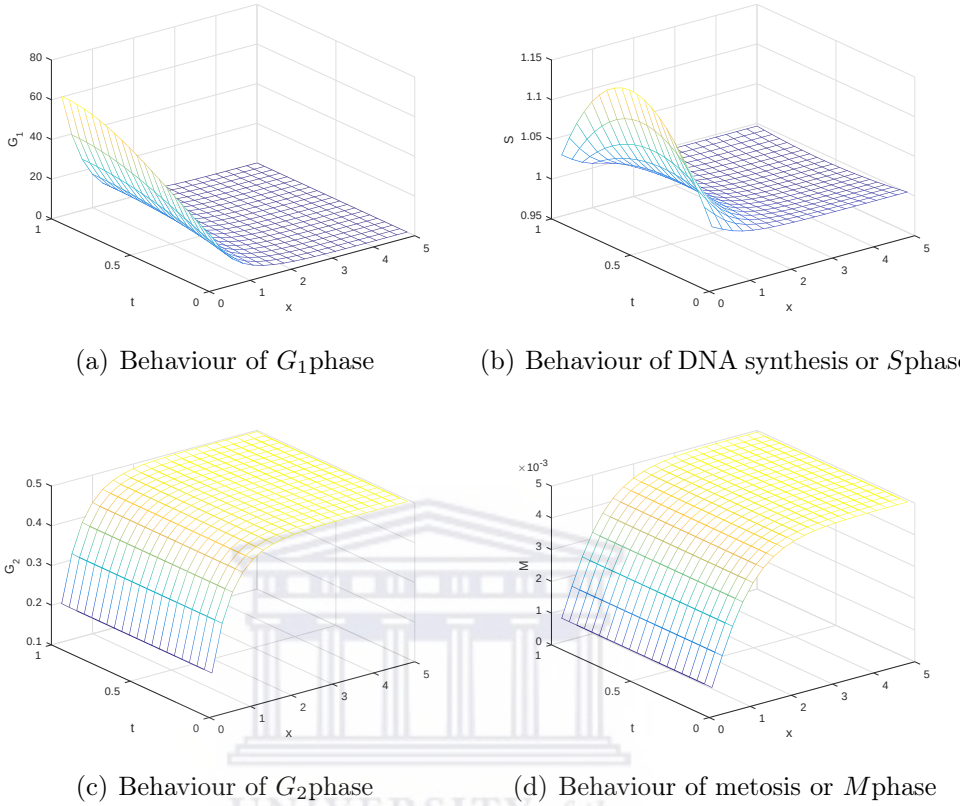

(a) Behaviour of G_1phase (b) Behaviour of DNA synthesis or Sphase

(c) Behaviour of G_2phase (d) Behaviour of metosis or Mphase

Figure 6.5.3: Numerical solution obtained by using for $\varepsilon = 0.1$.

We believe we have covered all essentials of tumour cells in terms of our models considered in the previous chapters as well as in this chapter. Thus, in Chapter 7 we consider some cost-effective, efficient optimization approaches for treating tumour infection.

Chapter 7

Robust numerical solution for a problem arising in angiogenic signalling

Since the process of angiogenesis is controlled by chemical signals, which stimulate both repair of damaged blood vessels and formation of new blood vessels, then other chemical signals known as angiogenesis inhibitors interfere with blood vessels formation. This implies that the stimulating and inhibiting effects of these chemical signals are balanced as blood vessels form only when and where they are needed. Based on this information, an optimal control problem is formulated and the arising model is a system of coupled non-linear equations with adjoint and transversality conditions. Since many of the numerical methods often fail to capture the solution to these type of models, then, in this chapter, we carry out equilibrium analysis of these models before implementing the numerical computations. We analyze and present the numerical estimates as a way of providing more insight into the postvascular dormant state where stimulator and inhibitor come into balance in an optimal manner.

7.1 The model

In [76], Ledzewicz et al. considered two mathematical models for tumour anti-angiogenesis in which one model was originally formulated [48] whereas, the other model is a modification of the model by [38] considered as optimal control problem with the aim of maximizing the tumour reduction achievable with an a priori given amount of angiogenic agents. They argued that depending on the initial conditions, the optimal controls may contain a segment along which the dosage follows a so-called singular control, a time-varying feedback control. Thus, the efficiency of piecewise constant protocols with a small number of switchings is investigated through comparison with the theoretically optimal solutions. It is also shown that these protocols provide generally excellent suboptimal strategies that for many initial conditions come within a fraction of 1% of the theoretically optimal values. When the duration of the dosages are a priori restricted to a daily or semi-daily regimen, still very good approximations of the theoretically optimal solution can be achieved.

Apart from formulating a class of mathematical models for tumor anti-angiogenesis as optimal control problems, Ledzewicz and Cardwell [77] considered the fact on how to schedule an a priori given amount of anti-angiogenic (e.g., vessel disruptive) agents in order to minimize the tumor volume [120, 119], they also analyzed these models for a class of mathematical models that include, based on a model that was developed and biologically validated by Hahnfeldt, Panigrahy, Folkman and Hlatky [48]. Thus, the principal state variables are the primary tumor volume, p, and the carrying capacity of the vasculature, q, where the latter is a measure for the tumor volume sustainable by the vascular network. These dynamics describes the interactions between these variables and the tumor volume p changes according to some growth function dependent on the variable carrying capacity q, where the q-dynamics consists of a balance of stimulatory and inhibitory effects. While significant modeling changes are made in the dynamics for the vascular support of such model, the solutions to the optimal control problem are in fact qualitatively identical.

Thus, let $p, \xi, q, \gamma, u, a, A, b, d, \mu q$ denote the primary tumor volume, tumor growth parameter, endothelial support, anti-angiogenic killing parameter, treatment with an anti-angiogenic agent, a priori set maximum dosage, positive constant, birth rate, death rate, net balance between endothelial cell proliferation and loss to the endothelial cells through natural causes such as death and the parameter $\theta \in [0, 1]$. Then, to reduce the volume (p) of a tumour efficiently results into the maximization of the tumour volume reduction achievable with an apriori amount of angiogenic inhibitors [38, 69, 71, 73, 75]

$$\int_0^T u(t)dt \leq A, \tag{7.1.1}$$

for a free terminal T, minimizes the value $p(T)$ subjects to the dynamics

$$\left.\begin{aligned} \dot{p} &= -\xi p \ln\left(\tfrac{p}{q}\right), \\ \dot{q}_{I_\theta} &= bp^\theta - dp^{\frac{1}{3}}q - q(\mu + \gamma u), \\ \dot{q}_{H_E} &= bq^{\frac{2}{3}} - dq^{\frac{4}{3}} - q(\mu + \gamma u), \\ \dot{q}_{H_1} &= bp - dp^{\frac{2}{3}}q - q(\mu + \gamma u), \\ \dot{y} &= u, \end{aligned}\right\} \tag{7.1.2}$$

with initial conditions $p(0) = p_0 > 0, q(0) = q_0 > 0, y(0) = 0$ [48]. Equation (7.1.1) together with (7.1.2) is an optimal control problem. Therefore, in the next section we determine the Hamiltonian and Lagrange multipliers of the optimal control problem.

7.2 Hamiltonian and Lagrange multipliers

The Pontryagin maximum principle [18, 19, 108] enables us to determine the necessary conditions for optimality of a control u. Thus, for a row-vector $\lambda = (\lambda_1, \lambda_2, \lambda_3)^t \in \mathbb{R}^3$ the Hamiltonian $H := H(\lambda, p, q, u)$ is

$$H = -\lambda_1 \xi p \ln\left(\frac{p}{q}\right) + \lambda_2 \left(S(p, q) - I(p, q) - \mu q - \gamma q u\right) + \lambda_3 u,$$

where, S and I denote endogenous inhibition, stimulation terms. Therefore, the individual Hamiltonians [48] corresponding to equation (7.1.2) are

$$\left.\begin{aligned} H_{I_\theta} &= -\lambda_1 \xi p \ln\left(\tfrac{p}{q}\right) + \lambda_2\left(bp^\theta - dp^{\frac{1}{3}}q - q(\mu+\gamma u)\right) + \lambda_3 u, \\ H_{H_E} &= -\lambda_1 \xi p \ln\left(\tfrac{p}{q}\right) + \lambda_2\left(bq^{\frac{2}{3}} - dq^{\frac{4}{3}} - q(\mu+\gamma u)\right) + \lambda_3 u, \\ H_{H_1} &= -\lambda_1 \xi p \ln\left(\tfrac{p}{q}\right) + \lambda_2\left(bp - dp^{\frac{2}{3}}q - q(\mu+\gamma u)\right) + \lambda_3 u, \end{aligned}\right\} \tag{7.2.1}$$

over all Lebesgue measurable functions $u : [0, T] \to [0, a]$, for which the corresponding trajectory satisfies $y(T) \leq A$ and the transversality conditions are

$$\lambda_1(T) = 1,\ \lambda_2(T) = 0 \text{ and } \lambda_3(T) = \text{constant}. \tag{7.2.2}$$

Let $\bar{x} := (p, q, y)$, then, by Samaee et al. [114], we have

$$\partial_{\bar{x}} f + \lambda^T \left(\partial_{\bar{x}} h - \partial_t \partial_{\dot{x}} h\right) - \dot{\lambda}\partial_{\bar{x}} h = 0, \tag{7.2.3}$$

where,

$$\begin{aligned} f &= u, \\ h &= \begin{pmatrix} \dot{p} + \xi p \ln\left(\tfrac{p}{q}\right), \\ \dot{q}_{I_\theta} - bp^\theta + dp^{\frac{1}{3}}q + q(\mu+\gamma u), \\ \dot{q}_{H_E} - bq^{\frac{2}{3}} + dq^{\frac{4}{3}} + q(\mu+\gamma u), \\ \dot{q}_{H_1} - bp + dp^{\frac{2}{3}}q + q(\mu+\gamma u), \\ \dot{y} - u, \end{pmatrix}, \end{aligned} \tag{7.2.4}$$

obtained through equations in (7.1.2). Applying equation (7.2.3) to model H_1 we obtain

$$\begin{pmatrix} 0 \\ 0 \\ 0 \end{pmatrix} + \lambda \begin{pmatrix} \xi\left(\ln\left(\tfrac{p}{q}\right) + 1\right) \\ dp^{2/3} + (\mu+\gamma u) \\ 0 \end{pmatrix} - \dot{\lambda} \begin{pmatrix} \xi\left(\ln\left(\tfrac{p}{q}\right) + 1\right) \\ dp^{2/3} + (\mu+\gamma u) \\ 0 \end{pmatrix} = \begin{pmatrix} 0 \\ 0 \\ 0 \end{pmatrix}, \tag{7.2.5}$$

which yields

$$\lambda - \dot{\lambda} = 0. \tag{7.2.6}$$

Equation (7.2.6) is also obtained for other two remaining models. Solving equation (7.2.6), we obtain

$$\lambda_{1,2,3}(t) = C\exp(t), \tag{7.2.7}$$

where C, is a constant of integration. Using the transversality conditions we obtain

$$\left.\begin{aligned} \lambda_1(t) &= \exp(t-T), \\ \lambda_2(t) &= 0, \\ \lambda_3(t) &= C. \end{aligned}\right\} \tag{7.2.8}$$

7.3 Equilibrium state

In order to develop the robust numerical methods it is necessary to analyse the equilibrium behaviour of these models. Therefore, in the next subsections we deduce the stability conditions of the models.

7.3.1 Model having I_θ

For this model, we let

$$\left.\begin{aligned} F(p,q,u) &= -\xi p \ln\left(\tfrac{p}{q}\right), \\ G_{I_\theta}(p,q,u) &= bp^\theta - dp^{\frac{1}{3}}q - q\mu, \\ H(p,q,u) &= 0, \end{aligned}\right\} \tag{7.3.1}$$

then

$$\left.\begin{aligned}\frac{\partial F}{\partial p} &= -\xi\left(\ln\left(\frac{p}{q}\right)+p\left(\frac{1}{p}-0\right)\right),\\ &= -\xi\left(\ln\left(\frac{p}{q}\right)+1\right),\\ \frac{\partial F}{\partial q} &= -\xi p\left(0-\frac{1}{q}\right),\\ &= \xi\frac{p}{q},\\ \frac{\partial F}{\partial u} &= 0.\end{aligned}\right\} \tag{7.3.2}$$

We see that $H_p = H_q = H_u = 0$, where the subscripts imply the partial derivatives with respect to a subscript p, q and u in that order. Solving for critical point q^* in equation (7.3.1), we find that

$$\begin{aligned} bp^\theta - dp^{1/3}q - q\mu &= 0,\\ bp^\theta - q\left(dp^{1/3}+\mu\right) &= 0,\\ bp^\theta &= q\left(dp^{1/3}+\mu\right),\\ \frac{bp^\theta}{(dp^{1/3}+\mu)} &= q^*. \end{aligned} \tag{7.3.3}$$

But we know that $q^* \geq p^*$, then this enables us to write

$$\begin{aligned} \frac{bp^\theta}{(dp^{1/3}+\mu)} &\geq p^*,\\ &\Leftrightarrow\ p^*\left(dp^{*1/3}+\mu\right) \geq bp^{*\theta},\\ &\Leftrightarrow\ dp^{*4/3}+p^*\mu - bp^{*\theta} \geq 0,\\ &\Leftrightarrow\ p^*\left(dp^{*1/3}+\mu - bp^{*\theta-1}\right) \geq 0, \end{aligned} \tag{7.3.4}$$

then, $p^* > 0$ as $p^* = 0$ is not admissible. Therefore,

$$dp^{*1/3}+\mu - bp^{*\theta-1} \geq 0, \tag{7.3.5}$$

which we solve and obtain

$$p^* \geq -\frac{(\mu - bp^{\theta-1})^3}{d^3}. \tag{7.3.6}$$

From equation (7.3.2), we obtain the non-zero entries of the Jacobian matrix $J_{I_\theta} := J_{ij}$ for $i = j = 1:3$ as

$$\begin{aligned} J_{1,1} &= -\xi(\ln\left(\frac{p}{q}\right) + 1),\ J_{1,2} = \xi\frac{p}{q},\ J_{2,1} = \theta bp^{\theta-1} - dq/3p^{\frac{2}{3}}, \\ J_{2,2} &= -dp^{\frac{1}{3}} - \mu. \end{aligned} \tag{7.3.7}$$

Using the concept of numeric-analytic dissipativity condition [25], we obtain the characteristic equation

$$\sigma^2 - \text{trace}(\frac{1}{2}(J + J^t))\sigma + \det(\frac{1}{2}(J + J^t)),$$

from $\frac{1}{2}(J + J^t)$. This implies that the model is stable if

$$\left(\xi(\ln\left(\frac{p^*}{q^*}\right) + 1)\right) < 1,\ \left(dp^{*\frac{1}{3}} + \mu\right) < 1,\ \left(\theta bp^{\theta-1} - dq/3p^{\frac{2}{3}}\right) < 1, \tag{7.3.8}$$

which implies that

$$\begin{aligned} \ln\left|\frac{p^*}{q^*}\right| &< \xi \Leftrightarrow \left|\frac{p^*}{q^*}\right| < \exp(-\xi) \text{ and } |p^*| < \left|\left(\frac{\mu}{d}\right)^3\right|, \\ p^{\theta-1} &< \frac{dq^*}{3\theta bp^{\frac{1}{3}}}. \end{aligned} \tag{7.3.9}$$

7.3.2 Adjoint for the model having I_θ

Since the Hamiltonian $H = H(\lambda, p, q, u)$, where the λ's are constants multipliers then

$$\left.\begin{aligned} \frac{dH_{I_\theta}}{dt} &= \frac{\partial H_{I_\theta}}{\partial \lambda}\frac{d\lambda}{dt} + \frac{\partial H_{I_\theta}}{\partial p}\frac{dp}{dt} + \frac{\partial H_{I_\theta}}{\partial q}\frac{dq}{dt} + \frac{\partial H_{I_\theta}}{\partial u}\frac{du}{dt}, \\ \frac{dH_{I_\theta}}{dt} &= \frac{\partial H_{I_\theta}}{\partial p}\frac{dp}{dt} + \frac{\partial H_{I_\theta}}{\partial q}\frac{dq}{dt}, \end{aligned}\right\} \tag{7.3.10}$$

because $d\lambda/dt = 0$ and by the stationary condition we have $\partial H_{I_\theta}/\partial u = 0$. Therefore, for the equilibrium equation in (7.3.10) becomes

$$\begin{aligned} \frac{\partial H_{I_\theta}}{\partial p}\frac{dp}{dt} + \frac{\partial H_{I_\theta}}{\partial q}\frac{dq}{dt} &= 0, \\ &\Leftrightarrow \quad \frac{\partial H_{I_\theta}}{\partial p}\frac{dp}{dt} = -\frac{\partial H_{I_\theta}}{\partial q}\frac{dq}{dt}, \\ &\Leftrightarrow \quad \frac{\partial H_{I_\theta}}{\partial p}\frac{dp}{dt} = 0, \\ &\Leftrightarrow \quad -\frac{\partial H_{I_\theta}}{\partial q}\frac{dq}{dt} = 0. \end{aligned} \tag{7.3.11}$$

Using equation (7.3.11) we find the corresponding critical points by linearizing the Jacobian matrices as follow

$$\begin{aligned} 0 &= \frac{\partial H_{I_\theta}}{\partial p}\frac{dp}{dt}, \\ &= \left(-\lambda_1\xi\left(\ln\left(\frac{p}{q}\right)+1\right) + \lambda_2\left(b\theta p^{\theta-1} - \frac{dq}{3p^{2/3}}\right)\right)\left(-\xi p\ln\left(\frac{p}{q}\right)\right), \end{aligned} \tag{7.3.12}$$

and

$$\begin{aligned} 0 &= -\frac{\partial H_{I_\theta}}{\partial q}\frac{dq}{dt}, \\ &= \left(\xi\lambda_1\frac{p}{q} - \lambda_2\left(dp^{1/3}+\mu\right)\right)\left(bp^\theta - dp^{1/3}q - q\mu\right). \end{aligned} \tag{7.3.13}$$

Solving for the critical point q^* in (7.3.13) we find

$$q_1^* = \frac{\xi\lambda_1 p}{\lambda_2 d p^{1/3} + \mu} \text{ and } q_2^* = \frac{\xi\lambda_1 p^\theta}{d p^{1/3} + \mu}. \tag{7.3.14}$$

The Jacobian matrix is

$$\mathrm{J}_{I_\theta} = \begin{bmatrix} \left(\frac{\partial H_{I_\theta}}{\partial p}\right)_p & \left(\frac{\partial H_{I_\theta}}{\partial p}\right)_q & \left(\frac{\partial H_{I_\theta}}{\partial p}\right)_u \\ \left(\frac{\partial H_{I_\theta}}{\partial q}\right)_p & \left(\frac{\partial H_{I_\theta}}{\partial q}\right)_q & \left(\frac{\partial H_{I_\theta}}{\partial q}\right)_u \\ \left(\frac{\partial H_{I_\theta}}{\partial u}\right)_p & \left(\frac{\partial H_{I_\theta}}{\partial u}\right)_q & \left(\frac{\partial H_{I_\theta}}{\partial u}\right)_u \end{bmatrix},$$

$$= \begin{bmatrix} -\frac{\lambda_1\xi}{p} + \lambda_2 b\theta(\theta-1)p^{\theta-2} + \frac{2dq}{9p^{\frac{1}{3}}} & \frac{\lambda_1\xi}{q} - \frac{\lambda_2 d}{3p^{\frac{2}{2}}} & 0 \\ \frac{\lambda_1\xi}{q} - \frac{\lambda_2 d}{3p^{\frac{2}{3}}} & -\frac{\lambda_1 p}{q^2} & 0 \\ 0 & 0 & 0 \end{bmatrix}.$$

Therefore, the adjoint is stable if and if and the eigenvalues are

$$\left|-\frac{\lambda_1\xi}{p^*} + \lambda_2 b\theta(\theta-1)p^{*\theta-2} + \frac{dq^*}{2p^{*\frac{1}{3}}}\right| < 0, \left|\frac{\lambda_1 p^*}{q^{*2}}\right| < 0, \left|\frac{\lambda_1\xi}{q} - \frac{\lambda_2 d}{3p^{\frac{2}{2}}}\right| < 0,$$

which implies that

$$\begin{aligned} \left|\exp(t-T)\frac{\xi}{p^*} + \frac{dq^*}{2p^{*\frac{1}{3}}}\right| &< 1, \left|\exp(t-T)\frac{p^*}{q^{*2}}\right| < 1, \left|\exp(t-T)\frac{\xi}{q}\right| < 1, \\ \Rightarrow \exp(t-T)\frac{\xi}{p^*} &< -\frac{dq^*}{2p^{*\frac{1}{3}}}, \text{ and } \xi < 1. \end{aligned}$$

7.3.3 Model having H_e

Applying the same procedures as in the above section we have,

$$\left.\begin{aligned} F(p,q,u) &= -\xi p \ln\left(\tfrac{p}{q}\right), \\ G_E(p,q,u) &= bq^{\frac{2}{3}} - dq^{\frac{4}{3}} - q(\mu+\gamma u), \\ H(p,q,u) &= 0, \end{aligned}\right\}$$

then

$$\begin{aligned} \frac{\partial F}{\partial p} &= -\xi \frac{\partial}{\partial p}\left(\ln\left(\frac{p}{q}\right) + p\left(\frac{1}{p} - 0\right)\right), \\ &= -\xi\left(\ln\left(\frac{p}{q}\right) + 1\right), \\ \frac{\partial F}{\partial q} &= -\xi p\left(0 - \frac{1}{q}\right), \\ &= \xi\frac{p}{q}, \\ \frac{\partial F}{\partial u} &= 0, \end{aligned} \tag{7.3.15}$$

and we also see that $H_p = H_q = H_u = 0$, where the subscripts denote the partial derivatives with respect to p, q and u, respectively.

Then from the second equation in (7.3.15) we see that

$$q\left(bq^{-1/3} - dq^{1/3} - \mu\right) = 0, \tag{7.3.16}$$

which implies that $bq^{-1/3} - dq^{1/3} - \mu = 0$, as $q^* \neq 0$. This implies that

$$\begin{aligned} q_1^* &= \frac{1}{2}\frac{\left(-\mu + \sqrt{\mu^2+4bd}\right)b + \frac{-\mu+\sqrt{\mu^2+4bd}\mu^2}{d} - b\mu}{d^2} \text{ and} \\ q_2^* &= -\frac{1}{2}\frac{\left(\mu - \sqrt{\mu^2+4bd}\right)b - \frac{\mu+\sqrt{\mu^2+4bd}\mu^2}{d} - b\mu}{d^2}, \end{aligned} \tag{7.3.17}$$

because $u^* = 0$. Take $q^* \geq p^*$ and the non-zero entries of the Jacobian matrix $J_E := J_{ij}$ where $i = 1:3$ and $j = 1:3$ are

$$\begin{aligned} J_{1,1} &= -\xi\left(\ln\left(\frac{p}{q}\right)+1\right), \\ J_{1,2} &= \xi\frac{p}{q},\ J_{2,2} = 2bq^{\frac{1}{3}}/3 - 4dq^{\frac{1}{3}}/3 - \mu, \end{aligned} \tag{7.3.18}$$

which implies that the model is stable if and only if

$$\begin{aligned} |\xi| &< 1,\ |2b/3q^{*\frac{1}{3}} - 4dq^{*\frac{1}{3}}/3 - \mu| < 1, \\ \Rightarrow 2b/3q^{*\frac{1}{3}} &< 4dq^{*\frac{1}{3}}/3 + \mu. \end{aligned}$$

7.3.4 Adjoint for the model having H_e

Let $H = H(\lambda, p, q, u)$, then

$$\left.\begin{aligned} \frac{dH_{H_E}}{dt} &= \frac{\partial H_{H_E}}{\partial \lambda}\frac{d\lambda}{dt} + \frac{\partial H_{H_E}}{\partial p}\frac{dp}{dt} + \frac{\partial H_{H_E}}{\partial q}\frac{dq}{dt} + \frac{\partial H_{H_E}}{\partial u}\frac{du}{dt}, \\ \frac{dH_{H_E}}{dt} &= \frac{\partial H_{H_E}}{\partial p}\frac{dp}{dt} + \frac{\partial H_{H_E}}{\partial q}\frac{dq}{dt}, \end{aligned}\right\}$$

as $d\lambda/dt = 0$ and by the stationary condition we see that $\partial H/\partial u = 0$. Thus, for the equilibrium we have

$$\begin{aligned} \frac{\partial H_{H_E}}{\partial p}\frac{dp}{dt} + \frac{\partial H_{H_E}}{\partial q}\frac{dq}{dt} &= 0, \\ \Leftrightarrow\ \frac{\partial H_{H_E}}{\partial p}\frac{dp}{dt} &= -\frac{\partial H_{H_E}}{\partial q}\frac{dq}{dt}, \\ \Leftrightarrow\ \frac{\partial H_{H_E}}{\partial p}\frac{dp}{dt} &= 0, \\ \Leftrightarrow\ -\frac{\partial H_{H_E}}{\partial q}\frac{dq}{dt} &= 0. \end{aligned} \tag{7.3.19}$$

In view of equation (7.3.19) we have

$$0 = \frac{\partial H_{H_E}}{\partial p}\frac{dp}{dt} = \lambda_1 \xi^2 p \ln\left(\frac{p}{q}\right)\left(\ln\left(\frac{p}{q}\right) + \frac{p}{q}\right),$$

$$\Leftrightarrow \quad p^* \leq q^* \quad \text{or} \quad q^* = p^* \exp(\frac{p^*}{q^*}), \tag{7.3.20}$$

and from

$$\begin{aligned} 0 &= -\frac{\partial H_{H_E}}{\partial q}\frac{dq}{dt}, \\ &= -\left(\frac{\lambda_1 \xi p}{q} + \lambda_2\left(\frac{2b}{3q^{\frac{1}{3}}} - \frac{4dq^{\frac{1}{3}}}{3} - \mu\right)\right)\left(bq^{2/3} - dq^{4/3} - q\mu\right), \end{aligned}$$

which implies that

$$p^* = \frac{q^*\lambda_2\left(\frac{2b}{3q^{*\frac{1}{3}}} - \frac{4dq^{*\frac{1}{3}}}{3} - \mu\right)}{\lambda_1 \xi} \text{ and } q^* = \frac{b^3}{(dq^{*1/3} + \mu)^3}.$$

The corresponding Jacobian matrix $J_{H_E} := J_{ij}$ for $i = j = 1:3$ is

$$\begin{aligned} \mathrm{J}_{H_E} &= \begin{bmatrix} \left(\frac{\partial H}{\partial p}\right)_p & \left(\frac{\partial H}{\partial p}\right)_q & \left(\frac{\partial H}{\partial p}\right)_u \\ \left(\frac{\partial H}{\partial q}\right)_p & \left(\frac{\partial H}{\partial q}\right)_q & \left(\frac{\partial H}{\partial q}\right)_u \\ \left(\frac{\partial H}{\partial u}\right)_p & \left(\frac{\partial H}{\partial u}\right)_q & \left(\frac{\partial H}{\partial u}\right)_u \end{bmatrix}, \\ &= \begin{bmatrix} -\lambda_1\xi\left(\frac{1}{p} + \frac{1}{p}\right) & \lambda_1\xi\left(\frac{1}{q} + \frac{p}{q^2}\right) & 0 \\ \left(\frac{\partial H}{\partial q}\right)_p & \left(\frac{\partial H}{\partial q}\right)_q & \left(\frac{\partial H}{\partial q}\right)_u \\ \left(\frac{\partial H}{\partial u}\right)_p & \left(\frac{\partial H}{\partial u}\right)_q & \left(\frac{\partial H}{\partial u}\right)_u \end{bmatrix}, \end{aligned} \tag{7.3.21}$$

where, the non-zero entries are

$$\begin{aligned} J_{1,1} &= -\lambda_1\xi\left(\frac{1}{p^*}+\frac{1}{q^*}\right)\ J_{1,2}=\lambda_1\xi\left(\frac{1}{q^*}+\frac{p^*}{q^{*2}}\right),\ J_{2,1}=\frac{\lambda_1\xi}{q^*}, \\ J_{2,2} &= -\left(\frac{\lambda_1\xi p^*}{q^{*2}}+\lambda_2\left(\frac{2b-4d}{9q^{*\frac{2}{3}}}\right)\right). \end{aligned}$$

Therefore, the adjoint of this model is stable if

$$\left|-\exp(t-T)\xi\left(\frac{1}{p^*}+\frac{1}{q^*}\right)\right|<1,\ \xi<1,\ \frac{1}{q^*}<-\frac{p^*}{q^{*2}}.$$

7.3.5 Model having H_1

We let

$$\left.\begin{aligned} &F(p,q,u)=-\xi p\ln\left(\tfrac{p}{q}\right), \\ &G_{H_1}(p,q,u)=bp-dp^{\frac{2}{3}}q-q\mu, \\ &H(p,q,u)=0, \end{aligned}\right\} \tag{7.3.22}$$

so that

$$\begin{aligned} \frac{\partial F}{\partial p} &= -\xi\frac{\partial}{\partial p}\left(\ln\left(\frac{p}{q}\right)+p\left(\frac{1}{p}-0\right)\right), \\ &= -\xi\left(\ln\left(\frac{p}{q}\right)+1\right), \\ \frac{\partial F}{\partial q} &= -\xi p\left(0-\frac{1}{q}\right), \\ &= \xi\frac{p}{q}, \\ \frac{\partial F}{\partial u} &= 0, \end{aligned} \tag{7.3.23}$$

where, see that $H_p = H_q = H_u = 0$. The subscripts imply the partial derivatives with respect to p, q and u, respectively. Therefore,

$$\left.\begin{aligned} \frac{\partial G_{H_1}}{\partial p} &= \frac{\partial}{\partial p}\left(bp - dp^{\frac{2}{3}}q - q\mu\right), \\ &= b - 2dq/3p^{(1/3)}, \\ \frac{\partial G_{H_1}}{\partial q} &= \frac{\partial}{\partial q}\left(bp - dp^{\frac{2}{3}}q - q\mu)\right), \\ &= -\left(dp^{\frac{2}{3}} + \mu\right), \\ \frac{\partial G_{H_1}}{\partial u} &= \frac{\partial}{\partial u}\left(bp - dp^{\frac{2}{3}}q - q\mu\right), \\ &= 0, \end{aligned}\right\} \tag{7.3.24}$$

and the Jacobian matrix $J_{H_1} := J_{ij}$ for $i = j = 1:3$ is

$$J_{H_1} = \begin{bmatrix} \frac{\partial F}{\partial p} & \frac{\partial F}{\partial q} & \frac{\partial F}{\partial u} \\ \frac{\partial G_{H_1}}{\partial p} & \frac{\partial G_{H_1}}{\partial q} & \frac{\partial G_{H_1}}{\partial u} \\ \frac{\partial H}{\partial p} & \frac{\partial H}{\partial q} & \frac{\partial H}{\partial u} \end{bmatrix}, \tag{7.3.25}$$

where, the non-zero entries are

$$\begin{aligned} J_{1,1} &= -\xi\left(\ln\left(\frac{p}{q}\right) + 1\right) J_{1,2} = \xi\frac{p}{q},\ J_{2,1} = b - 2dq/3p^{(1/3)}, \\ J_{2,2} &= -\left(dp^{\frac{2}{3}} + \mu\right). \end{aligned}$$

In view of equation (7.3.22), we see that,

$$\left.\begin{aligned} 0 &= -\xi p \ln\left(\tfrac{p}{q}\right), \\ 0 &= bp - dp^{\frac{2}{3}}q - q(\mu + \gamma u). \end{aligned}\right\} \tag{7.3.26}$$

The first equation in (7.3.26) requires that $-\xi p = 0$ or $\ln(p/q) = 0$. However, based on the construction of this model, neither $\xi \neq 0$ nor $p \neq 0$, then the only choice is

$$\ln\left(\frac{p}{q}\right) = 0,$$
$$\Rightarrow \exp\left(\ln(\frac{p}{q})\right) = 1 \Leftrightarrow p = q. \tag{7.3.27}$$

However, further basic requirement on this model is such that $\ln(p/q)$ should be a decreasing function and this is only possible if $q^* \geq p^*$. Solving for q in the second equation in (7.3.26) we obtain

$$q^* = \frac{bp^*}{dp^{*2/3} - \mu}, \text{ as } u^* = 0. \tag{7.3.28}$$

But $q^* \geq p^*$, then in view of equation (7.3.28), we see that

$$\frac{bp^*}{dp^{*2/3} - \mu} \geq p^* \Leftrightarrow p^*\left(dp^{*2/3} - \mu\right) \geq bp^*,$$
$$\Leftrightarrow dp^{*5/3} - \mu p^* \geq bp^*,$$
$$\Leftrightarrow dp^{*5/3} - \mu p^* - bp^* \geq 0,$$
$$\Leftrightarrow dp^{*5/3} \geq p^*(\mu + b),$$
$$\Leftrightarrow p^{*2/3} \geq (\mu + b)/d,$$
$$\Leftrightarrow p^* \geq ((\mu + b)/d)^{3/2}, \tag{7.3.29}$$

which enables us to rewrite equation (7.3.28) as

$$\begin{aligned} q^* &= \frac{b\left(\mu+b\right)/d)^{3/2}}{d\left(\left(\mu+b\right)/d\right)-\mu}, \\ &= \frac{b\left(\mu+b\right)^{3/2}}{d^{3/2}(\left(\mu+b\right)-\mu)}, \\ &= \frac{(\mu+b))^{3/2}}{d^{3/2}}. \end{aligned} \tag{7.3.30}$$

Hence, the model is stable if and only if

$$\xi < 1, \left| d\frac{(\mu+b)^{3/2}}{d^{3/2}} \right| < 1, \frac{dq}{3p^{(1/3)}} < \frac{b}{2}. \tag{7.3.31}$$

7.3.6 Adjoint for the model having H_1

For this model we have

$$\left.\begin{aligned} \frac{dH}{dt} &= \frac{\partial H_{H_1}}{\partial \lambda}\frac{d\lambda}{dt} + \frac{\partial H_{H_1}}{\partial p}\frac{dp}{dt} + \frac{\partial H_{H_1}}{\partial q}\frac{dq}{dt} + \frac{\partial H_{H_1}}{\partial u}\frac{du}{dt}, \\ \frac{dH_{H_1}}{dt} &= \frac{\partial H}{\partial p}\frac{dp}{dt} + \frac{\partial H_{H_1}}{\partial q}\frac{dq}{dt}. \end{aligned}\right\}$$

as $d\lambda/dt = 0$ and by the stationary condition we see that $(\partial H/\partial u) = 0$. Thus, for the equilibrium point equation (7.3.32) becomes

$$\begin{aligned} \frac{\partial H_{H_1}}{\partial p}\frac{dp}{dt} + \frac{\partial H_{H_1}}{\partial q}\frac{dq}{dt} &= 0, \\ \Leftrightarrow \quad \frac{\partial H_{H_1}}{\partial p}\frac{dp}{dt} &= -\frac{\partial H_{H_1}}{\partial q}\frac{dq}{dt}, \\ \Leftrightarrow \quad \frac{\partial H_{H_1}}{\partial p}\frac{dp}{dt} &= 0, \\ \Leftrightarrow \quad -\frac{\partial H_{H_1}}{\partial q}\frac{dq}{dt} &= 0. \end{aligned} \tag{7.3.32}$$

Using equation (7.3.32) we have,

$$\left.\begin{array}{l} \frac{\partial H_{H_1}}{\partial p} = -\lambda_1 \xi \left(\ln\left(\frac{p}{q}\right) + 1\right), \\ \frac{\partial H_{H_1}}{\partial q} = \xi \lambda_1 \frac{p}{q}. \end{array}\right\} \tag{7.3.33}$$

In view of equation (7.3.32) we see that

$$0 = -\frac{\partial H}{\partial q}\frac{dq}{dt} = \xi\lambda_1 \frac{p}{q}\left(bp - dp^{2/3}q + q\mu\right), \tag{7.3.34}$$

which implies that

$$p^* = (-\frac{\mu}{d})^{3/2}. \tag{7.3.35}$$

Whereas

$$\begin{aligned} 0 &= \frac{\partial H_{H_1}}{\partial p}\frac{dp}{dt}, \\ &= -\lambda_1 \xi^2 \left(\ln\left(\frac{p}{q}\right)+1\right)^2, \end{aligned} \tag{7.3.36}$$

which implies that $p^*/q^* = 0$, which is possible if $p^* = 0$ and $q^* \neq 0$. The Jacobian matrix is

$$\mathrm{J}_{H_1} = \begin{bmatrix} \left(H_p p_{\lambda_1}\lambda_{1t} + H_p p_{\lambda_2}\lambda_{2t}\right)_p & \left(H_p p_{\lambda_1}\lambda_{1t} + H_p p_{\lambda_2}\lambda_{2t}\right)_q & \left(H_p p_{\lambda_1}\lambda_{1t} + H_p p_{\lambda_2}\lambda_{2t}\right)_u \\ \left(H_q q_{\lambda_1}\lambda_{1t} + H_q q_{\lambda_2}\lambda_{2t}\right)_q & \left(H_q q_{\lambda_1}\lambda_{1t} + H_q q_{\lambda_2}\lambda_{2t}\right)_q & \left(H_q q_{\lambda_1}\lambda_{1t} + H_q q_{\lambda_2}\lambda_{2t}\right)_u \\ \left(\frac{\partial H}{\partial u}\right)_p & \left(\frac{\partial H}{\partial u}\right)_q & \left(\frac{\partial H}{\partial u}\right)_u \end{bmatrix}, \tag{7.3.37}$$

in which we see that

$$\left(\frac{\partial H_{H_1}}{\partial u}\right)_p = \left(\frac{\partial H_{H_1}}{\partial u}\right)_q = \left(\frac{\partial H_{H_1}}{\partial u}\right)_u = 0,$$

and

$$p_{\lambda_1} = p_{\lambda_2} = q_{\lambda_1} = q_{\lambda_2} = 0.$$

Thus, the adjoint of this model is unconditional stable.

7.4 Singular controls for the models

Since the Hamiltonian (H) is linear in u, then minimizing the control requires that $u = 0$ or $u = a$ [18]. This is known as the bang controls. In view of equations in (7.2.1), we obtain the switching function (Φ) as

$$\Phi(t) = \lambda_3 - \lambda_2(t)\gamma q(t), \tag{7.4.1}$$

such that the singular control is [18]

$$u^{\sin}(t) = \begin{cases} 0 & \text{if} \quad \Phi(t) > 0, \\ a & \text{if} \quad \Phi(t) < 0, \end{cases}$$

where, for the three models we have the optimal singular arcs

$$\left.\begin{array}{l} u^{\sin}_{I_\theta} = \frac{1}{\gamma}\left[\theta\xi\left(\ln\left(\frac{p}{q}\right) - 1\right) + \frac{1}{3}\xi\frac{d}{b}p^{\frac{1}{3}-\theta}q - \left(dp^{\frac{1}{3}} + \mu\right) + b\frac{p^\theta}{q} + \xi\right] [75], \\ u^{\sin}_{H_E} = \frac{1}{\gamma}\left(\frac{b-dq^{2/3}}{q^{1/3}} + 2\xi\frac{b+dq^{2/3}}{b-dq^{2/3}} - \mu\right) [74], \\ u^{\sin}_{H_1} = \frac{1}{\gamma}\left(\xi\ln\left(\frac{p}{q}\right) + b\frac{p}{q} + \frac{2}{3}\xi\frac{d}{b}\frac{q}{p^{1/3}} - \left(\mu + dp^{2/3}\right)\right) [70]. \end{array}\right\} \quad (7.4.2)$$

7.5 Numerical method

Not withstanding the associated optimal synthesis of the models considered in this chapter, but it is evident from the stability structures of the continuous models that reliable numerical method should be developed. Thus, in order to accomplish the development of a robust numerical method for optimal problems arising as a result of angiogenic signalling, we believe we first have to consider the existing numerical methods for these types of models. However, in this chapter, we consider only one type of the numerical method for the models. Thus, we sub-divide the interval [0,T] into equal pieces with specific points of interest

$$0 = t_0, t_1, t_2, \cdots, t_{N+1} = T,$$

where N is a positive integer denoting the number of sub-intervals. Since the total-enumeration methods or linear programming techniques can be used to solve optimal control problems such the one in [15], because such methods fail to capture the associated optimality, adjoint equation and the transversality condition. Therefore the

only applicable methods are Runge-Kutta or adaptive schemes and the boundary value problems such as shooting method [21, 26]. Hence, following the Forward-backward sweep method [78] then the optimal control problem is implemented as we have shown here below.

7.5.1 Forward-backward sweep method (FBSM) for model having I_θ

Set the $flag = -1$, then define the step-size $h = 1/N$, and initialize the controls, states and the adjoints with their initial conditions, we have

$$u_{I_\theta}^{\sin} = 1/\gamma(\theta\xi(\log(p_1/q_1) - 1) + 1/3\xi d/bp_1^{1/3-\theta}q_1 - (dp_1^{1/3} + \mu) + bp_1^{\theta}/q_1 + \xi);$$

and *Step:.* WHILE ($flag < 0$) do the following steps.
Step 1a. oldu= u; oldp= p; oldq= q; oldy= y; oldlambda1=λ_1;
oldlambda2= λ_2; oldlambda3= λ_3;

Step 2a

FOR $i = 1, 2, \cdots, N$ set

$$
\begin{aligned}
k_{11} &= -\xi p_i \log(p_i/q_i); \\
k_{12} &= bp_i^{\theta} - dp_i^{1/3} q_i - \mu q_i - \gamma q_i u_i; \\
k_{13} &= u_i; \\
k_{21} &= -\xi(p_i + h_2 k_{11}) \log\left((p_i + h_2 k_{11})/(q_i + h_2 k_{12})\right); \\
k_{22} &= b(p_i^{\theta} + h_2 k_{11}) - d(p_i^{(1/3)} + h_2 k_{11}) q_i - \mu(q_i + h_2 k_{12}) \\
&\quad -\gamma(q_i + h_2 k_{12}) 0.5(u_i + u_{i+1}); \\
k_{23} &= 0.5(u_i + u_{i+1}); \\
k_{31} &= -\xi(p_i + h_2 k_{21}) \log\left((p_i + h_2 k_{21})/(q_i + h_2 k_{22})\right); \\
k_{32} &= b(p_i^{\theta} + h_2 k_{21}) - d(p_i^{(1/3)} + h_2 k_{21}) q_i - \mu(q_i + h_2 k_{22}) \\
&\quad -\gamma(q_i + h_2 k_{22}) 0.5(u_i + u_{i+1}); \\
k_{33} &= 0.5(u_i + u_{i+1}); \\
k_{41} &= -\xi(p_i + h_2 k_{31}) \log\left((p_i + h_2 k_{31})/(q_i + h_2 k_{32})\right); \\
k_{42} &= b(p_i^{\theta} + h_2 k_{31}) - d(p_i^{1/3} + h_2 k_{31}) q_i - \mu(q_i + h_2 k_{32}) \\
&\quad -\gamma(q_i + h_2 k_{32}) 0.5(u_i + u_{i+1}); \\
k_{43} &= u_{i+1}; \\
p_{i+1} &= p_i + (h/6)(k_{11} + 2k_{21} + 2k_{31} + k_{41}); \\
q_{i+1} &= q_i + (h/6)(k_{12} + 2k_{22} + 2k_{32} + k_{42}); \\
y_{i+1} &= y_i + (h/6)(k_{13} + 2k_{23} + 2k_{33} + k_{43});
\end{aligned}
$$

STOP

Step 3a

FOR $i = 1, 2, \cdots, N$ and $j = N + 1 - i$ set

$$
\begin{aligned}
k_{11} &= \lambda_{1j}\xi \log(p_j/q_j) + \lambda_{1j}\xi - \lambda_{2j}\left(b\theta p_j^{\theta-1} - dq_j/3p_j^{2/3}\right); \\
k_{12} &= -\xi\lambda_{1j}p_j/q_j + \lambda_{2j}(dp_j^{1/3} + \mu + \gamma 0.5(u_j + u_{j-1})); \\
k_{13} &= C; \\
k_{12} &= (\lambda_{1j} - h_2k_{11}\xi \log\left(0.5(p_j + p_{j-1})/(0.5(q_j + q_{j-1}))\right)) + (\lambda_{1j} - h_2k_{11})\xi \\
&\quad -(\lambda_{2j} - h_2k_{12})\left(b\theta((0.5(p_j + p_{j-1}))^{\theta-1}\right) \\
&\quad -(\lambda_{2j} - h_2k_{12})\left(d(0.5(q_j + q_{j-1}))/3(0.5(p_j + p_{j-1}))^{2/3})\right); \\
k_{22} &= -\xi(\lambda_{1j} - h_2k_{11})0.5(p_j + p_{j-1})/0.5(q_j + q_{j-1}) \\
&\quad +(\lambda_{2j} - h_2k_{12})\left(d(0.5(p_j + p_{j-1}))^{1/3} + \mu + \gamma 0.5(u_j + u_{j-1})\right); \\
k_{23} &= C; \\
k_{31} &= (\lambda_{1j} - h_2k_{21})\xi \log\left(0.5(p_j + p_{j-1})/0.5(q_j + q_{j-1})\right) + (\lambda_{1j} - h_2k_{21})\xi \\
&\quad -(\lambda_{2j} - h_2k_{22})\left(b\theta(0.5(p_j + p_{j-1}))^{\theta-1}\right) \\
&\quad -(\lambda_{2j} - h_2k_{22})\left(d(0.5(q_j + q_{j-1}))/3((0.5(p_j + p_{j-1}))^{2/3})\right); \\
k_{32} &= -\xi(\lambda_{1j} - h_2k_{21})0.5(p_j + p_{j-1})/0.5(q_j + q_{j-1}) \\
&\quad +(\lambda_{2j} - h_2k_{22})(d(0.5(p_j + p_{j-1}))^{1/3} + \mu + \gamma 0.5(u_j + u_{j-1})); \\
k_{33} &= C; \\
k_{41} &= (\lambda_{1j} - h_2k_{31})\xi \log\left(0.5p_{j-1}/0.5q_{j-1}\right) + (\lambda_{1j} - h_2k_{31})\xi \\
&\quad -(\lambda_{2j} - h_2k_{32})\left(b\theta(0.5p_{j-1})^{\theta-1}\right) \\
&\quad -(\lambda_{2j} - h_2k_{32})\left(d0.5q_{j-1}/3(0.5p_{j-1})^{2/3}\right); \\
k_{42} &= -\xi(\lambda_{1j} - h_2k_{31})0.5p_{j-1}/0.5q_{j-1} \\
&\quad +(\lambda_{2j} - h_2k_{32})(d(0.5p_{j-1})^{1/3} + \mu + \gamma 0.5u_{j-1}); \\
k_{43} &= C; \\
\lambda_{1j-1} &= \lambda_{1j} - (h/6)(k_{11} + 2k_{21} + 2k_{31} + k_{41}); \\
\lambda_{2j-1} &= \lambda_{2j} - (h/6)(k_{12} + 2k_{22} + 2k_{32} + k_{42}); \\
\lambda_{3j-1} &= \lambda_{3j} - (h/6)(k_{13} + 2k_{23} + 2k_{33} + k_{43});
\end{aligned}
$$

7.6 Stability analysis of FBSM

Basically the FBSM first solves the state equation with a forward in time Runge-Kutta method, then solves the costate equation backwards in time with the Runge-Kutta method and then updates the control. Then, stability analysis should follow the procedures carried out when one determine the condition of the Runge-Kutta method. Since we have impose the numeric-analytic dissipativity condition [25] to the models eigenvalues, then FBSM is A-stable.

7.7 Numerical result and discussions

Based on the initial conditions $p_0 = 8.00, q_0 = 4.00, u_0 = 0.1$, parameter values $\xi = 0.084, b = 5.85, d = 0.00873, \mu = 0.02; \gamma = 0.01, \theta = 0.1, \delta = 0.1$ ([73]), we implemented the Forward-backward sweep method (FBSM) for the systems in (7.1.2) and (7.2.1) as shown up for the case of model having I_θ, where the numerical approximations are presented in Figure 7.8.1 and for the remaining two models the results are presented in Figure 7.8.2 and Figure 7.8.3. Our aim in this chapter is to present the numerical solutions of the three models, we have considered. Thus, we see that the control (u) and angiogenesis (q) increases monotonically but remain bounded, except for the model having H_1. We also see that the tumour volume (p) decreases and increases eventually. This is due to the ever growing agiogenesis system of the tumor. Such phenomena is also evident for model having H_1. The above-mentioned behaviours remain the same, when we perturb the initial values and for an increased values of T.

7.8 Conclusion

In view of the problem description, Hamiltonian and Lagrange multipliers, we were able to deduce the multipliers for these models. We have also established the stability conditions for each model which in turn guaranteed the stability of the Forward-backward

sweep method. In doing so, we believe that this can enable us to attain most features of each model which can give deeper insight of the properties of the models. Since the authors in [70, 74, 75] were mainly interested in attaining the singular arc of the models, it is important to combine the defining element and all the syntheses of optimally controlled trajectories qualitatively and quantitative with the associated solution to a problem. Therefore, this chapter should be viewed as a first attempt to combine singular arc with their associated solutions of the optimal problems. Hence, our future research direction is to extend the chapter to higher dimensional space, with the inclusion of the spatial effects.

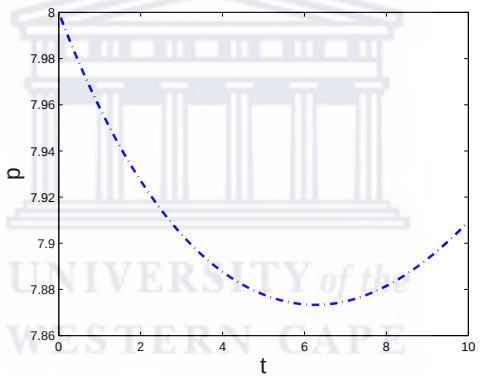

(a) Behaviour of tumor volume

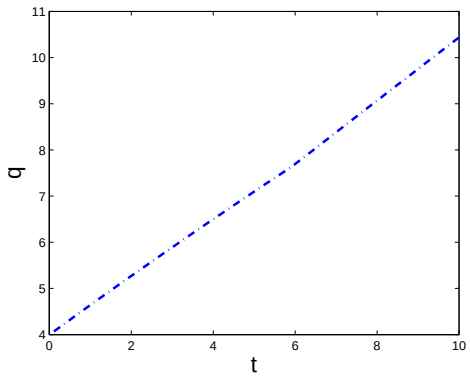

(b) Behaviour of angiogenesis for tumor growth

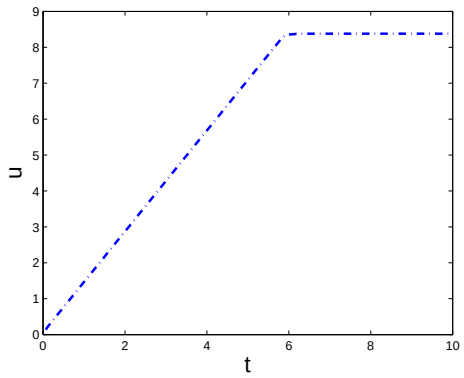

(c) Behaviour of control on tumor volume growth

Figure 7.8.1: Numerical approximation of the model having I_θ.

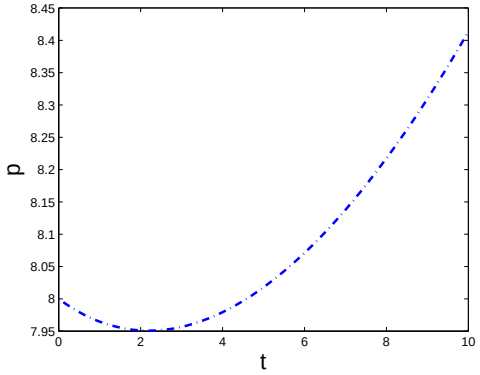

(a) Behaviour of tumor volume

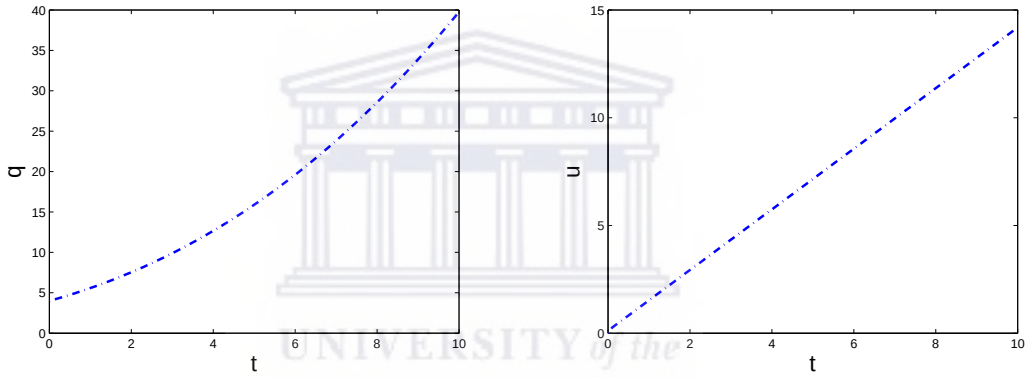

(b) Behaviuor of angiogenesis for tumor growth (c) Behaviour of control on tumor volume growth

Figure 7.8.2: Numerical approximation of the model having H_e.

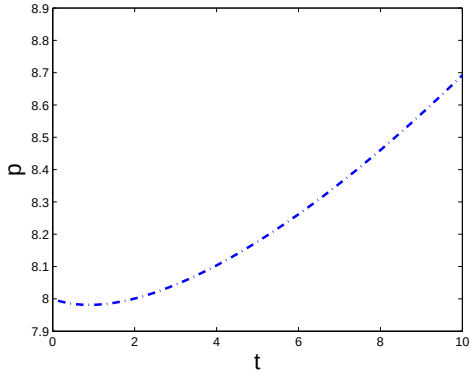

(a) Behaviuor of Tumor volume

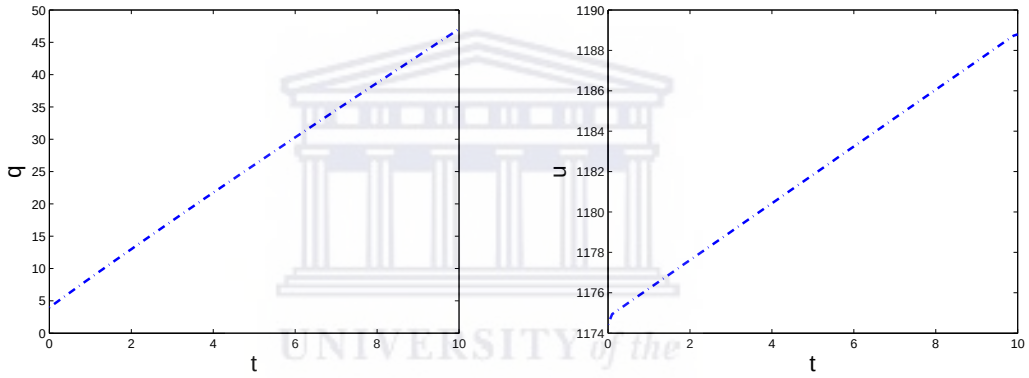

(b) Behaviour of angiogenesis for tumor growth (c) Behaviour of control on tumor volume growth

Figure 7.8.3: Numerical approximation of the model having H_1.

In view of the previous chapters and this chapter, we are now at the stage to conclude the thesis. Thus, in Chapter 8, we conclude the thesis and provide the scope for future research.

Chapter 8

Concluding remarks and scope for further research

In this thesis, we considered different classes of system of differential equations (DEs) models having biological applications. These biological models include a system of mixed of (first and second) order of system differential equations, system of first order delay differential equations (DDEs), system of parabolic differential equations (PDEs), system of delay integro-differential equations (DIDEs) and system of optimal control problems (OCPs). For each class of models, we have analysed the model. Due to the similarity of most of these models, a suitable numerical methods have been designed and analyzed. Based on our analysis of the models, we have not seen any numerical methods in the literature for the presented hypothesis arising from our mathematical analysis. Therefore, our quantitative work is a new contribution to both analytic and numerical world for these problems. Moreover, these numerical methods are very robust.

In Chapter 2, we considered the systems of semi-parabolic differential equations modeling the dynamics of chemotherapy application of spatial tumor-host interaction. Based on the previous experiments on the models, we realized that mathematical rigor has not been explored, therefore, our emphasis in that chapter is on the qualitative

features of the models presented. Consequently, the fitted numerical method that we have designed and analyzed is of relatively low order, but our emphasis is mainly on our hypothesis deduced from qualitative features of the models. This is despite the fact that the fitted numerical method captured the qualitative features as we have hypothesized. Currently, we are busy investigating on how how we can improve the order of convergence of the method. Our future plans for these problems include the construction of direct higher order numerical methods.

In Chapter 3, we have extended a system of first order delay differential equations (DDEs) to a system of delay parabolic partial differential equations (DPPDEs), modeling biological stoichiometry of tumour dynamics. Based on the work done on the dynamics of the models, we have based our straight forward analysis with respect to the process of vascularizations. Thus, a fitted numerical method is designed and analyzed. Even-though, the fitted numerical method is of low order, it has captured our hypothesis as we have presented them. Hence, we are exploring ways of extending our work to high dimensional space.

Once, again in Chapter 4, we extended a system of delay differential equations (DDEs), to a system of delay parabolic partial differential equations (DPPDEs) modeling the HIV related cancer-immune system dynamics. Our aim was to dispose the features of extended model with respect to original model. Thus, to do so, we designed and analysed a fitted numerical method. Our hypothesis are clearly presented from our numerical estimate. Hence, currently, we are busy working on a numerical methods that possesses high rate of convergence.

Chapter 5, dealt with the scrutiny of the system of parabolic partial differential equations (PPDEs), modeling the dynamics of tumour cells within its micro-environment. To this end, we designed a fitted numerical method to present our numerical aspirations with respect to the effects of the micro-environment. Thus, we currently working on the implementation of the models into high dimensions.

In view of the model considered in Chapter 6, we have extended the model in order to have a clear view of each phase emphasized by the model. Thus, our mathematical

analysis enabled us to design a suitable fitted operator numerical method. Hence, we believe our numerical method were able to present each phase by its own merits. Currently, we are busy exploring ways on how to improve the rate of convergence of our method.

Lastly, but not least, in Chapter 7, we have combined the optimal control problems in one system of optimal control problems. Our aim was to present their qualitative features so that one is able to develop a reliable numerical method. However, due to the high rate of convergence of the forward-backward sweep numerical method, we decided to adopt the method and implement it for each system considered. As expected, the forward-backward sweep numerical method captured the desirable numerical results. Therefore, we are currently considering a direct method for solving the models considered.

Finally, it should be noted that almost all the numerical methods that we have developed for different problems in this thesis are comparable with (and in some cases better than) the well-known solvers, like MATLAB's ode23s and dde23.

As far as the **scope for further research is concerned**, we would like to mention the following

- Some of the methods developed in this thesis can further be extended in the optimal control set up.
- Theoretical analysis of the numerical methods in certain cases can be improved further.
- We also aim to extend the models in higher dimensions which will be quite challenging to solve numerically and would therefore require extensive analysis.

Bibliography

[1] M. Abundo and C. Rossi, Numerical simulation of a stochastic model for cancerous cells submitted to chemotherapy, *Journal of Mathematical Biology* **27** (1989) 81-90.

[2] C.N. Amaya, D.C. Mitchell and B.A. Bryan, Rho kinase proteins display aberrant up regulation in vascular tumors and contribute to vascular tumor growth, *BMC Cancer* **17** (2017) 485.

[3] J.L. Albritton and J.S. Miller, 3D bioprinting: improving in vitro models of metastasis with heterogeneous tumor micro-environments, *Disease Model Mechanism* **10(1)** (2017) 3-14.

[4] A.R.A. Anderson, A hybrid mathematical model of solid tumor invasion: the importance of cell adhesion, *IMA Journal of Applied Mathematics* **22** (2005) 163-186.

[5] A.R.A. Anderson and M.A.J. Chaplain, Continuous and discrete mathematical models of tumor-induced angiogenesis, *Bulletin of Mathematical Biology* **60** (1998) 857-899.

[6] A.R.A. Anderson, A. Weaver, P. Cummings and V. Quaranta, Tumor morphology and phenotypic evolution driven by selective pressure from the microenvironment, *Cell* **127** (2006) 905-915.

[7] E. De Angelis and L. Preziosi, Advection-diffusion models for solid tumor evolution in vivo and related free boundary problem, *Mathematical Models Methods Application of Science* **10** (2000) 379-408.

[8] A.R. Ansari, S.A. Bakr and G.I. Shishkin, A parameter-robust finite difference method for singularly perturbed parabolic partial differential equations, *Journal of Computational and Applied Mathematics* **205** (2007), 552-566.

[9] S. Aznavoorian, M.L. Stracke, H. Krutzsch, E. Schiffmann and L.A. Liotta, Signal transduction for chemotaxis and haptotaxis by matrix molecules in tumor cells, *Journal of Cellular Biology* **110** (1990) 1427-1438.

[10] H.T. Banks, J.E. Banks, E. John, R. Bommarco, A.N. Laubmeier, N.J. Myers, M. Rundlöf and K. Tillman, Modeling bumble bee population dynamics with delay differential equations, *Ecological Modelling* **351** (2017) 14-23.

[11] B. Basse, B.C. Baguley, E.S. Marshall and W.R. Joseph, A mathematical model for analysis of the cell cycle in cell lines derived from human tumours, *Journal of Mathematical Biology* **47** (2003) 295-312.

[12] B. Basse, B.C. Baguley, E.S. Marshall, G.C. Wake and D.J.N. Wall, Modelling cell population growth with applications to cancer therapy in human tumor cell lines, *Progress In Biophysics And Molecular Biology* **85** (2004) 353-368.

[13] B. Basse and P. Ubezio, A generalised age and phase structured model of human tumour cell populations both unperturbed and exposed to a range of cancer therapies, *Bulletin Mathematical Biology* **69(5)** (2007) 1673-1690.

[14] B. Basse, G.C. Wake, D.J.N. Wall and B. van Brunt, On a cell growth model for plankton, *Mathematical Medicine and Biology, A Journal of the IMA* **21** (2004) 49-61.

[15] J.T. Betts, *Practical method for optimal control using nonlinear programming*, SIAM, Philadelphia, 2001.

[16] M. Bodnar, U. Foryś and Z. Szymańska, A model of AIDS-related tumor with time delay, *Proceedings of the Fourteenth National Conference on Application of Mathematics in Biology and Medicine* (2008) 12-17.

[17] M. Bodnar, U. Foryś and Z. Szymańska, Model of AIDS-related tumor with time delay, *Applied Mathematics* **36** (2009) 263-278.

[18] B. Bonnard and M. Chyba, *Singular trajectories and their role in control theory*, Springer Verlag, 2003.

[19] A. Bressan and B. Piccoli, Introduction to the mathematical theory of control, *American Institute of Mathematical Sciences* (2007) 159-184.

[20] R.J. Buchsbaum and S.Y. Oh, Breast cancer-associated fibroblasts: Where we are and where we need to go, *Cancers* **8** (2016) 19.

[21] R.L. Burden and J.D. Faires, *Numerical Analysis* Brooks/Cole, USA, 2011.

[22] J.C. Butcher, Implicit Runge-Kutta processes, *Mathematics of Computation*, **18(85)** (1964) 50-64.

[23] H.S. Carslaw and J.C. Jaeger, *Conduction of Heat in Solids*, Oxford University Press, London (1956).

[24] M. Chen, M. Fan and Y. Kuang, Global dynamics in a stoichiometric food chain model with two limiting nutrients, *Mathematical Biosciences* **289** (2017) 9-19.

[25] J.H.E. Cartwright and O. Piro, The Dynamics of Runge-Kutta Methods, *International Journal of Bifurcation and Chaos* **2** (1192) 427-449.

[26] W. Cheney and D. Kincaid, *Numerical mathematics and computing*, Thomson, Belmont, California, 2004.

[27] J. Cheng and L. Weiner, Tumours and their micro-environments: tilling the soil Commentary re: A.M. Scott et al., A Phase I dose-escalation study of sibrotuzumab in patients with advanced or metastatic fibroblast activation protein-positive cancer, *Cancer Research* **9(5)** (2003) 1590-1595.

[28] M. Cherif, Stoichiometry and population growth in osmotrophs and non-osmotrophs, *John Wiley & Sons, Ltd*, **DOI 10.1002/9780470015902** (2016) a0026353.

[29] C. Cherubini, A. Gizzi, M. Bertolaso, V. Tambone, and S. Filippi, A Bistable Field Model of Cancer Dynamics, *Communications in Computational Physics* **11(1)** (2012) 1-18.

[30] K.L. Cooke and P. van den Driessche, On zeros of some transcendental equations, *Funkcialaj Ekvacioj* **27** (1986) 77-90.

[31] V. Cristini, X. Li, J.S. Lowengrub and S.M. Wise, Nonlinear simulations of solid tumor growth using a mixture model: invasion and branching, *Journal of Mathematical Biology* **58(4-5)** (2008) 723-763.

[32] R.V. Culshaw and S. Ruan, A delay-differential equation model of HIV infection of CD4+ T-Cells, *Mathematical Bioscience* **165** (2000) 27-39.

[33] B. Dalal, P. Keown and A. Greenberg, Immunocytochemical localization of secreted transforming growth factor-beta 1 to the advancing edges of primary tumours and to lymph node metastases of human mammary carcinoma, *American Journal of Pathology* **143(2)** (1993) 381-389.

[34] P.J. Delves, D.J. Martin, D.R. Burton and I.M. Roitt, *Roitt's Essential Immunology*, Blackwell Science, Oxford, 2006.

[35] A.L. Dontchev and W.W. Hager, The Euler approximation in state constrained optimal control, *Mathematics of Computation* **70(233)** 173-203.

[36] R.D. Driver, *Ordinary and Delay Differential Equations*, Springer-Verlag, New York, 1977.

[37] J.J. Elser, Y. Kuang and J.D. Nagy, Biological stoichiometry: An ecological perspective on tumor dynamics, *BioScience* **53(11)** (2003) 1112-1120.

[38] A. Ergun, K. Camphausen and L.M. Wein, Optimal scheduling of radiotherapy and angiogenic inhibitors, *Bulletin of Mathematical Biology* **65** (2003) 407-424.

[39] S.O. Fatunla, *Numerical Methods for IVPs in Ordinary Differential Equations*, Academic Press, Harcourt Brace Jovanovich Publishers, New York, 1988.

[40] U. Foryś, N.Z. Bielczyk, K. Piskaa, M. Pomecka and J. Poleszczuk, Impact of Time Delay in Perceptual Decision-Making: Neuronal Population Modeling Approach, *Hindawi Complexity* **2017** (2017) 14.

[41] U. Foryś and J. Poleszczuk, A delay-differential equation model of HIV related cancer-immune system dynamics, *Mathematical Biosciences and Engineering* **8(2)** (2011) 627-641.

[42] A. Friedman and Y. Kim, Tumor Cells Proliferation and migration under the influence of their micro-environment, *Mathematical Biosciences and Engineering* **8(2)** (2011) 371-383.

[43] P. Gerlee and A.R.A. Anderson, An evolutionary hybrid cellular automaton model of solid tumor growth, *Journal of Theoretical Biology* **246** (2007) 583-603.

[44] B. Giotti, A. Joshi, and T.C. Freeman, Meta-analysis reveals conserved cell cycle transcriptional network across multiple human cell types, *BMC Genomics* **18** (2017) 30.

[45] K. Goebel and N.D. Merner, A monograph proposing the use of canine mammary tumours as a model for the study of hereditary breast cancer susceptibility genes in humans, *Veterinary Medicine and Science* **3(2)** (2017) 51-62.

[46] J. Golab, M. Jacóbisiak and W. Lasek, Immunologia, *Wydawnictwo Naukowe PWN* (2002) 337-355.

[47] S.A. Gourley, Y. Kuang and J.D. Nagy, Dynamics of a delay differential equation model of hepatitis B virus infection, *Journal of Biological Dynamics* **2(2)** (2008) 140-153.

[48] P. Hahnfeldt, D. Panigrahy, J. Folkman and L. Hlatky, Tumor development under angiogenic signaling: a dynamical theory of tumor growth, treatment response, and postvascular dormancy, *Cancer Research* **59** (1999) 4770-4775.

[49] P. Hinow, P. Gerlee, L.J. McCawley, V. Quaranta, M. Ciobanu, S. Wang, J.M. Graham, B.P. Ayati, K.R. Swanson, J. Claridge, M. Loveless and A.R.A. Anderson, A spatial model of tumor-host interaction: application of chemotherapy, *Mathematical Biosciences and Engineering* **6(3)** (2009) 521-546.

[50] Catholic Encyclopedia with Wikisource reference, History of medicine 1913.

[51] Z. Jackiewicz, B. Zubik-Kowal and B. Basse, Finite-difference and Pseudo-spectral methods for the numerical Simulations of in vitro human tumour cell population kinetics, *Mathematical Biosciences and Engineering* **6(3)** (2009) 561-572.

[52] A. Jafarian, M. Mokhtarpour and D. Baleanu, Artificial neural network approach for a class of fractional ordinary differential equation, *Neural Computing and Applications* **28(4)** (2017) 765-773.

[53] R.K. Jain, Normalizing tumor vasculature with anti-angiogenic therapy: a new paradigm for combination therapy, *Nature Medicine* **7** (2001) 987-989.

[54] R.K. Jain and L.L. Munn, Vascular normalization as a rationale for combining chemotherapy with antiangiogenic agents, *Principles of Practical Oncology* **21** (2007) 1-7.

[55] A. Jemal, R. Siegel and E. Ward E, Cancer statistics, *A Cancer Journal for Clinicians* **58** (2008) 71-96.

[56] R.E. Kalman, Contribution to the theory of optimal control, *Buletin Sociedad Matematica Mexicana* **5(1)** (1960) 102-119.

[57] R.S. Kerbel, Inhibition of tumor angiogenesis as a strategy to circumvent acquired resistance to anti-cancer therapeutic agents, *BioEssays* **13(1)** (1991) 31-36.

[58] H. Khan, A. Szeghegyi and J. K. Tar, Fixed point transformation-based adaptive optimal control using nonlinear programming, *Proceedings of the 2017 IEEE 30th Jubilee Neumann Colloquium* (2017) 35-40.

[59] Y. Kim and A. Friedman, Interaction of tumor with its micro-environment: A mathematical model, *Bulletin of Mathematical Biology* **72** (2010) 1029-1068.

[60] Y. Kim, H. Jeon and H. Othmer, The Role of the Tumor Microenvironment in Glioblastoma: A Mathematical Model, *IEEE Transactions on Biomedical Engineering* **64(3)** (2016) 519-527.

[61] Y. Kim, M.A. Stolarsk and H.G. Othmer, The role of the micro-environment in tumor growth and invasion, *Progress in Biophysics and Molecular Biology* **106(2)** (2011) 353-379.

[62] Y. Kim, J. Wallace, F. Li, M. Ostrowski and A. Friedman, Transformed epithelial cells and fibroblasts/myofibroblasts interaction in breast tumor: A mathematical model and experiments, *Journal of mathematical biology* **61** (2009) 401-21.

[63] Y. Kim, J. Wallace, F. Li, M. Ostrowski and A. Friedman, Transformed epithelial cells and fibroblasts/myofibroblasts interaction in breast tumor: A mathematical model and experiments, *Journal of Mathematical Biology* **61(3)** (2010) 401-421.

[64] D. Kirschner and J.C. Panetta, Modelling immunotherapy of the tumor-immune interaction, *Journal of Mathematical Biology* **37** (1998) 235-252.

[65] R.S. Kerbel, A cancer therapy resistant to resistance, *Nature* **390** (1997) 335-336.

[66] M. Kolev and B. Zubik-Kowal, Numerical solutions for a model of tissue invasion and migration of tumor cells, *Computational and Mathematical Methods in Medicine* **2011** (2011).

[67] V.A. Kuznetsov, I.A. Makalkin, M.A. Taylor and A.S. Perelson, Non-linear dynamics of immunogenic tumors: Parameter estimation and global bifurcation analysis, *Bulletin of Mathematical Biology* **56** (1994) 295-321.

[68] U. Ledzewicz and H. Schättler, The influence of PK/PD on the structure of optimal controls in cancer chemotherapy models, *Mathematical Biosciences and Engineering* **2** (2005) 561-578.

[69] U. Ledzewicz and H. Schättler, A synthesis of optimal controls for a model of tumor growth a under angiogenic inhibitors, *Proceedings of the 44th IEEE Conference on Decision and Control* **2005** (2005) 1582277.

[70] U. Ledzewicz and H. Schättler, *Anti-angiogenic therapy in cancer treatment as an optimal control problem*, *Society for Industrial and Applied Mathematics* **46(3)** (2007) 1052-1079.

[71] U. Ledzewicz and H. Schättler, Anti-angiogenic therapy in cancer treatment as an optimal a control problem, *SIAM Journal on Control and Optimization* **46** (2007) 1052-1079.

[72] U. Ledzewicz and H. Schättler, Analysis of a mathematical model for tumor anti-angiogenesis, *an Optimal Control Applications and Methods* **29** (2008) 41-57.

[73] U. Ledzewicz and H. Schättler, Optimal and suboptimal protocols for a class of mathematical a models of tumor anti-angiogenesis, *Journal of Theoretical Biology* **252** (2008) 295-312.

[74] U. Ledzewicz, J. Munden and H. Schȧttler, Bang-bang controls for anti-angiogenesis under logistics growth of the tumor, *International Journal of Pure and Applied Mathematics* **9(4)** (2008) 511-516.

[75] U. Ledzewicz, J. Munden, and H. Schättler, Scheduling of angiogenic inhibitors for Gomapertzian and logistic tumor growth models, *Discrete and Continuous Dynamical Systems, Series B* **12** (2009) 415-438.

[76] U. Ledzewicz, J. Marriott, H. Maurer and H. Schättler, Realizable protocols for optimal administration of drugs in mathematical models for anti-angiogenic treatment, *Mathematical Medicine and Biology* **27(2)** (2009) 157-179.

[77] U. Ledzewicz and B. Cardwell, Robustness of optimal controls for a class of mathematical models for tumor anti-angiogenesis, *Mathematical Biosciences and engineering* **8(2)** (2011) 355-369.

[78] S. Lenhart and J.T. Workman, *Optimal control applied to biological models*, Chapman & Hall/CRC, 2007.

[79] G.M. Lieberman, *Second Order Parabolic Equations*, World Scientific, New Jersey, 2005.

[80] H.J. Lin and J. Lin, Seed-in-soil: Pancreatic cancer influenced by tumor microenvironment, *Cancers* **9** (2017) 93.

[81] J. Lou, T. Ruggeri and C. Tebaldi, Modelling cancer in HIV-1 infected individuals: Equilibria, cycles and chaotic behaviour, *Mathematical Biosciences and Engineering* **3** (2006) 313-324.

[82] J. Lou and T. Ruggeri, A time delay model about AIDS-related cancer: Equilibria, cycles and chaotic behaviour, *Ricerche di Matematica* **56** (2007) 195-208.

[83] J.B. McCarthy, M.L. Basara, S.L. Palm, D.F. Sas, and L.T. Furcht, The role of cell adhesion proteins-laminin and fibronectin in the movement of malignant and metastatic cells, *Cancer Metastasis Reviews* **4(2)** (1985) 125-152.

[84] R.E. Mickens, *Nonstandard Finite Difference Models of Differential Equations*, World Scientific, Singapore, 1994.

[85] R.E. Mickens, *Applications of Nonstandard Finite Difference Schemes*, World Scientific, Singapore, 2000.

[86] I.A. Minigalieva, B.A. Katsnelson, V.G. Panov, A.N. Varaksin, V.B. Gurvich, L.I. Privalova, M.P. Sutunkova, and S.V. Klinova, Experimental study and mathematical modeling of toxic metals combined action as a scientific foundation for occupational and environmental health risk assessment, *Toxicology Reports* **4** (2017) 194-201.

[87] J.D. Murray, *Mathematical Biology II: Spatial Models and Biomedical Applications*, Springer, Berlin, 2003.

[88] P. W. Nelson, *Mathematical models in immunology and HIV pathogenesis*, Department of Applied Mathematics, University of Washington, Seattle WA, 1998.

[89] P.W. Nelson, J.D. Murray and A.S. Perelson, Delay model for the dynamics in HIV infection, *Mathematical Bioscience* **163** (2000) 201-215.

[90] "II Neoplasms", World Health Organization. Retrieved 19 June 2014.

[91] E.S. Norris, J.R. King and H.M. Byrne, Modeling the response of spatially structured tumors to chemotherapy: Drug kinetics, *Mathematical and Computer Modelling* **43** (2006) 820-837.

[92] G. Nunnari, J.A. Smith and R. Daniel, HIV-1 Tat and AIDS-associated cancer: targeting the cellular anti-cancer barrier? *Journal of Experimental & Clinical Cancer Research* **27(1)** (2008) 3.

[93] A. Okubo and S.A. Levin, *Diffusion and Ecological Problems: Modern Perspectives*, Springer, New York, 2001.

[94] K.M. Owolabi, K.C. Patidar and A. Shikongo, Mathematical analysis and numerical simulation of a tumor-host model with chemotherapy application, *Communications in Mathematical Biology and Neuroscience* **2018** (2018).

[95] K.M. Owolabi, K.C. Patidar and A. Shikongo, Efficient numerical method for a model arising in biological stoichiometry of tumour dynamics, *Discrete and Continuous Dynamical Systems Series S* **12(3)** (2019) 591-613.

[96] K.M. Owolabi, K.C. Patidar and A. Shikongo, A fitted numerical method for a model arising in HIV related cancer-immune system dynamics, *Communications in Mathematical Biology and Neuroscience* **2019** (2019).

[97] K.M. Owolabi, K.C. Patidar and A. Shikongo, Numerical solution for a problem arising in angiogenic signaling, *AIMS Mathematics* **4(1)** (2019) 43-63.

[98] K.M. Owolabi, K.C. Patidar and A. Shikongo, A fitted operator method for tumour cells dynamics in their micro-environment, *Communications in Mathematical Biology and Neuroscience* **2019** (2019).

[99] J.C. Panetta, A mathematical model of breast and ovarian cancer treated with paclitaxel, *Mathematical Biosciences* **146** (1997) 89-113.

[100] C.V. Pao, *Nonlinear Parabolic and Elliptic Equations*, Plenum, New York, 1996.

[101] C.V. Pao, Dynamics of nonlinear parabolic system with time delays, *Journal of Mathematical Analysis and Applications* **198** (1996) 751-779.

[102] C.V. Pao, Convergence of solutions of reaction-diffusion systems with time delays, *Nonlinear Analysis* **48** (2002) 349-362.

[103] K.C. Patidar, On the use of non-standard finite difference methods, *Journal of Difference Equations and Applications* **11** (2005) 735-758.

[104] K.C. Patidar, Nonstandard finite difference methods: recent trends and further developments, *Journal of Difference Equations and Applications* **22(6)** (2016) 817-849.

[105] K.C. Patidar and A. Shikongo, The Application of Asymptotic Analysis for Developing Reliable Numerical Method for a Model Singular Perturbation Problem, *Journal of Numerical Analysis, Industrial and Applied Mathematics* **2(3-4)** (2007) 193-207.

[106] A. Pazy, *Semigroups of linear operators and applications to partial differential equations*, Springer-Verlag, New York, 1983.

[107] A.S. Perelson and P.W. Nelson, Mathematical models of HIV-1 dynamics in vivo, *SIAM Review* **41** (1999) 3-44.

[108] L.S. Pontryagin, V.G. Boltyanskii, R.V. Gamkrelidze and E.F. Mishchenko, *The mathematical theory of optimal processes*, MacMillan, New York, 1964.

[109] M.H. Protter and H.F. Weinberger, *Maximum Principles in Differential Eqquations*, Prentice Hall, Englewood Cliffs, New Jork, 1967.

[110] K.A. Rejniak and L.J. McCawley, Current trends in mathematical modeling of tumor-micro-environment interactions: a survey of tools and applications, *Experimental Biology and Medicine* **235(4)** (2010) 411-23.

[111] A. Resclgnow and C. Delisi, Immune Surveillance and Neoplasia-II a two-stage Mathematical Model, *Bulletin of Mathematical Biology* **39(2)** (1977) 133-296.

[112] F.A. Rihan and and N.F. Rihan, Dynamics of Cancer-Immune System with External Treatment and Optimal Control, *Journal of Cancer Science and Therapy* **DOI** (2016) 8-10.

[113] L. Rong, M.A. Gilchrist, Z. Feng and A.S. Perelson, Modelling within-host HIV-1 dynamics and the evolution of drug resistance: Trade-offs between viral enzyme

function and drug susceptibility, *Journal of Theoretical Biology* **247** (2007) 804-818.

[114] S.S. Samaee, O. Yazdanpanah and D.D. Ganji, New approaches to identification of the Lagrange multiplier in the variational iteration method, *Journal of the Brazilian Society of Mechanical Sciences and Engineering* **37(3)** (2015) 937-944.

[115] K. Schmitt, *Delay and Functional Differential Equations and Their Applications*, Academic Press, New York and London (1972).

[116] H. Schättler and U. Ledzewic, *Optimal control for mathematical models of cancer therapies*, Springer, USA, 2010.

[117] P.N. Shivakumar and K. Ji, Upper and lower bounds for inverse elements of finite and infinite tridiagonal matrices, *Linear Algebra and its Applications* **247** (1996) 297-316.

[118] H. Smith, *An Introduction to Delay Differential Equations with Sciences Applications*, Springer, New York, 2011.

[119] A. Swierniak, Direct and indirect control of cancer populations, *Bulletin of the Polish Academy of Sciences, Technical Sciences* **56** (2008) 367-378.

[120] A. Swierniak, Comparison of six models of antiangiogenic therapy, *Applied Mathematics* **36** (2009) 333-348.

[121] A. Świerniak, U. Ledzewicz and H. Schättler, Optimal control for a class of compartmental models in cancer chemotherapy, *International Journal of Applied Mathematics and Computer Science* **13** (2003) 357-368.

[122] N.H. Tuan, V. Van Au, V.A. Khoa and D. Lesnic, Identification of the population density of a species model with nonlocal diffusion and nonlinear reaction, *IOP Publishing Ltd Inverse Problems* **33(5)** (2017) 055019.

[123] L.N. Trefethen, *Finite Difference and Spectral Methods for Ordinary and Partial Differential Equations*, Upson Hall Cornell University Ithaca, New York, 1996.

[124] J.R. Usher and D. Henderson, Some drug-resistant models for cancer chemotherapy Part 1: Cycle-non-specific drugs, *Mathematical Medicine and Biology* **13** (1996) 99-126.

[125] V. Vavourakis, P.A. Wijeratne, R. Shipley, M. Loizidou, T. Stylianopoulos and D.J. Hawkes, A Validated Multiscale In-Silico Model for Mechano-sensitive tumor Angiogenesis and Growth, *Plos Computational Biology* **0** (2017) 1005259.

[126] Y. Wang, P. Pivonka, P.R. Buenzli, D.W. Smith and C.R. Dunstan, Computational modeling of interactions between multiple myeloma and the bone microenvironment, *Plos One* **6(11)** (2011) e27494.

[127] T. Wedeking, S. Löchte, C.P. Richter, M. Bhagawati, J. Piehler and C. You, Single cell GFP-trap reveals stoichiometry and dynamics of cytosolic protein complexes, *Nano Letters*, **15(5)** (2015) 3610-3615.

[128] J. Wu, *Theory and Applications of Partial Functional Differential Equations*, Springer, New York, 1996.

[129] R.A. Weinberg, *The Biology of Cancer*, W.W. Norton & Company, New York, 2013.

[130] Q.X. Ye and Z.Y. Li, *Introduction to Reaction-Diffusion Equations*, Science Press, Beijing, China, 1990.